AD NUMBER
AD863422
LIMITATION CHANGES
TO: **Approved for public release; distribution is unlimited.**
FROM: **Distribution authorized to U.S. Gov't. agencies only; Administrative/Operational Use; 17 SEP 1969. Other requests shall be referred to Naval Ordnance Laboratory, White Oak, MD 20910.**
AUTHORITY
USNOL ltr dtd 29 Aug 1974

NOLTR 69-164

STATIC STABILITY AND AXIAL FORCE COEFFICIENTS FOR THE 0.125 SCALE MODEL MARK 82 LOW DRAG BOMB WITH CLOSED SNAKEYE I FINS AT SUBSONIC AND TRANSONIC SPEEDS

By
V. L. Schemerhorn

17 SEPTEMBER 1969

NOL

UNITED STATES NAVAL ORDNANCE LABORATORY, WHITE OAK, MARYLAND.

20910

NOLTR 69-164

179

NOLTR 69-164

STATIC STABILITY AND AXIAL FORCE COEFFICIENTS FOR THE 0.125 SCALE MODEL MARK 82 LOW DRAG BOMB WITH CLOSED SNAKEYE I FINS AT SUBSONIC AND TRANSONIC SPEEDS

Prepared by:
V. L. Schermerhorn

ABSTRACT: Static stability and axial force coefficients are presented as a function of angle of attack for the Mk 82 Low Drag Bomb with Snakeye Fins in the closed position. These data were obtained for a Mach number range from 0.6 to 1.1; an angle-of-attack range from -6 to +20 degrees; and, a roll-angle range from 0 to 225 degrees in the NOL Supersonic Tunnel No. 1, using a subsonic nozzle.

U. S. NAVAL ORDNANCE LABORATORY
WHITE OAK, MARYLAND

NOLTR 69-164 17 September 1969

STATIC STABILITY AND AXIAL FORCE COEFFICIENTS FOR THE 0.125 SCALE MODEL MARK 82 LOW DRAG BOMB WITH CLOSED SNAKEYE I FINS AT SUBSONIC AND TRANSONIC SPEEDS

The purpose of the test was to furnish static stability and drag data. These tests were conducted at the request of NWL under task number NOL-795/NWL.

GEORGE G. BALL
Captain, USN
Commander

L. H. SCHINDEL
By direction

CONTENTS

ILLUSTRATIONS

TABLES

INTRODUCTION

This report gives the results of static wind-tunnel tests on the Navy Mk 82 Low Drag Bomb using the Snakeye I Fins, in the unretarded mode (closed position) as stabilizers.

LIST OF SYMBOLS

A	reference area, $\pi\ d^2/4$
C_A	axial force coefficient, F_A/qA
C_{A_o}	axial force coefficient at zero angle of attack
C_{A_f}	axial force coefficient, with base drag removed
C_ℓ	rolling moment coefficient, M_X/qAd
C_m	pitching moment coefficient, My/qAd
C_{m_α}	static stability index
C_N	normal force coefficient, F_N/qA
C_{n_α}	normal force coefficient derivative
C_n	yawing moment coefficient, M_Z/qAd
C_y	side force coefficient, F_y/qA
c.g.	moment reference center (6.025 inches from model base)
d	maximum body diameter
F_A	axial force
F_N	normal force
Fy	side force
M	Mach number
M_X	rolling moment
My	pitching moment

M_Z	yawing moment
P_b	base pressure
P_s	free-stream static pressure
P_o	stagnation pressure
q	dynamic pressure, $\rho V^2/2$
Re	Reynolds' number/ft
V	free-stream velocity
x,y,z	body axes
α	angle of attack
β	fin opening angle
ρ	free-stream density
ϕ	roll angle

MODEL, DATA ACQUISITION AND DATA REDUCTION

Model

A 0.125-scale model of the Mk 82 Bomb with Snakeye I fins in the closed position (unretarded mode) was tested; a sketch of the model configuration is shown on Figure 1. The scaled model was 11.180 inches long and had a maximum body diameter of 1.347 inches. To accommodate the sting balance, half of the inner shaft and 1.30 inches of the tail fin length, at the rear of the model, between the panel stiffeners, was removed. A sketch of the full-scale bomb is presented on Figure 2, for comparison purposes.

Balance

The NOL 6-14 balance, an internal strain-gage axial balance, was used to obtain the experimental data, which was collected and stored in digital form on magnetic tape.

Test Conditions

The model was tested at an angle-of-attack range from -6 to +20 degrees; for roll angles of 0, 1.33 (a case where the model moved), 6, 12, 18, 22.5, 45, 90, 180, 186, 202.5 and 225 degrees; and at Mach numbers ranging from 0.6 to 1.1. These tests were conducted in the NOL Supersonic Tunnel Number 1, using the subsonic nozzle. Observations of the flow field, made while the test was being conducted, indicated that a shock reflection on the tail of the model occurred at M = 1.1. As a consequence of this condition, no further tests at this Mach number were conducted. For the remainder of the test program, a free-stream Mach Number of 1.05 was selected as an upper limit value.

Data Reduction

The experimental data were reduced to aerodynamic coefficients, using a center-of-gravity position 6.025 inches ahead of the fin base as a moment reference center. Figures 3 to 166 are plots of the various coefficients as a function of angle of attack. For these figures, the angle of attack has been corrected for elastic deflection of the sting balance due to aerodynamic loading. Since an internal strain-gage balance was used here, no correction has been applied to the data for base pressure even though the base pressure was measured and is included here on Figure 167, as a function of Mach number and for zero angle of attack.

Correction to the axial force coefficient, for base pressure, could be made by means of the following expression:

$$C_{A_f} = C_A + A_b (P_b - P_s)/qA,$$

wherein $A_b = 0.3207$ in.^{2} (inner shaft area). This expression would yield a maximum change in axial force coefficient, $C_{A_f} - C_A = 0.015$ since the difference $(P_b - P_s)$ is very small (see Fig. 167).

As a definition of roll-angle orientation it has been assumed that when the juncture of two fin panels was in the vertical plane, the roll was zero. During this investigation, tests were conducted at roll angles of 0, 6, 12, 18, 22.5, and 45 degrees to see if any significant (induced) rolling moment would be imparted to the model by the fin-panel stiffeners. Tests also were conducted at roll angles of 90, 180, 186, 202.5 and 225 degrees to determine the effect on the coefficients due to the fin misalinement.

Table 1 is a listing of the average tunnel conditions which were used in the data reduction program. It should be understood that these conditions vary to some small degree since they are dependent upon the barometric pressure and temperature of the day. For reference purposes, the actual Mach number associated with each individual run is listed on the appropriate data figure.

RESULTS

Normal force and pitching moment coefficients, as functions of angle of attack, are presented on Figures 3 through 84. Side force, yawing moment, rolling moment and axial force coefficients are similarly presented on Figures 85 through 166. For an angle of attack near 15 degrees, and at a Mach number of 0.75 and greater, the fins were noted to vibrate. This action is reflected in all of the data, but is most visible in the pitching moment results obtained for this region of the tests (see Fig. 4). When vibration occurs, the fins would hit the balance (Fig. 4 at 16 degrees). For the remainder of the figures (Fig. 5 to 166), data is only presented up to the point where vibration starts. As a high balance sensitivity was needed to measure the small axial force loads, the balance was sensitive to tunnel and model vibrations. This accounts for the scatter seen in the axial force data (Figs. 84 to 166)

The static margin, in calibers, $C_{m_\alpha}/C_{N_\alpha}$, obtained at zero $\pm 1^\circ$ and 7 $\pm 1^\circ$ degrees angle of attack, and plotted as a function of Mach number, is given on Figure 168. The axial force at zero angle of attack versus Mach number is shown on Figure 169.

CONCLUSIONS

The bomb has essentially neutral static stability in the angle-of-attack range from -4 to +4 degrees. An increase in stability in the region of -4 to +4 degrees angle of attack could probably be obtained by increasing the fin span. No significant induced rolling moments, which could be attributed to the fin panel stiffeners, were ascertained. Comparison of the data at 0, 90 and 180 degrees indicates that the trim angle noted in the figures is due to fin misalinement.

Table 1

WIND TUNNEL TEST CONDITIONS

Average Supply Temperature = 22 Degrees Centigrade

Average Mach Number M	Average Supply Pressure P_o--mm Hg	Reynolds Number/ft (Re/ft.)x 10^{-6}
0.6	745	3.40
0.7	742	3.80
0.75	741	3.90
0.8	740	4.00
0.85	739	4.15
0.9	738	4.25
0.95	738	4.35
0.99	738	4.40
1.05	737	4.50
1.10	737	4.55

FIG. 1 MK 82 LOW-DRAG BOMB WITH SNAKEYE FINS (0.125 SCALE MODEL WITH FINS CLOSED (UNRETARDED MODE))

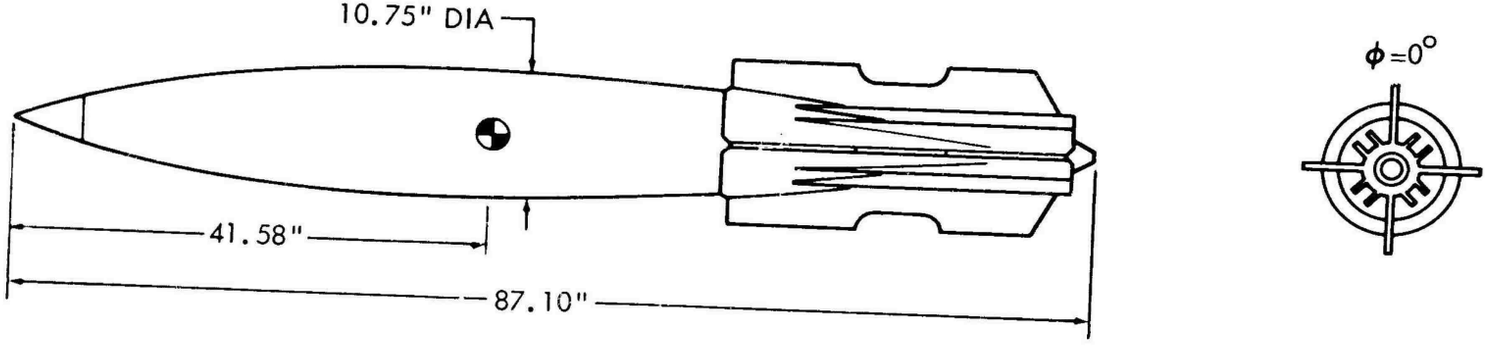

FIG. 2 MK 82 LOW DRAG BOMB WITH SNAKEYE I FINS (FULL SCALE WITH FINS CLOSED (UNRETARDED MODE))

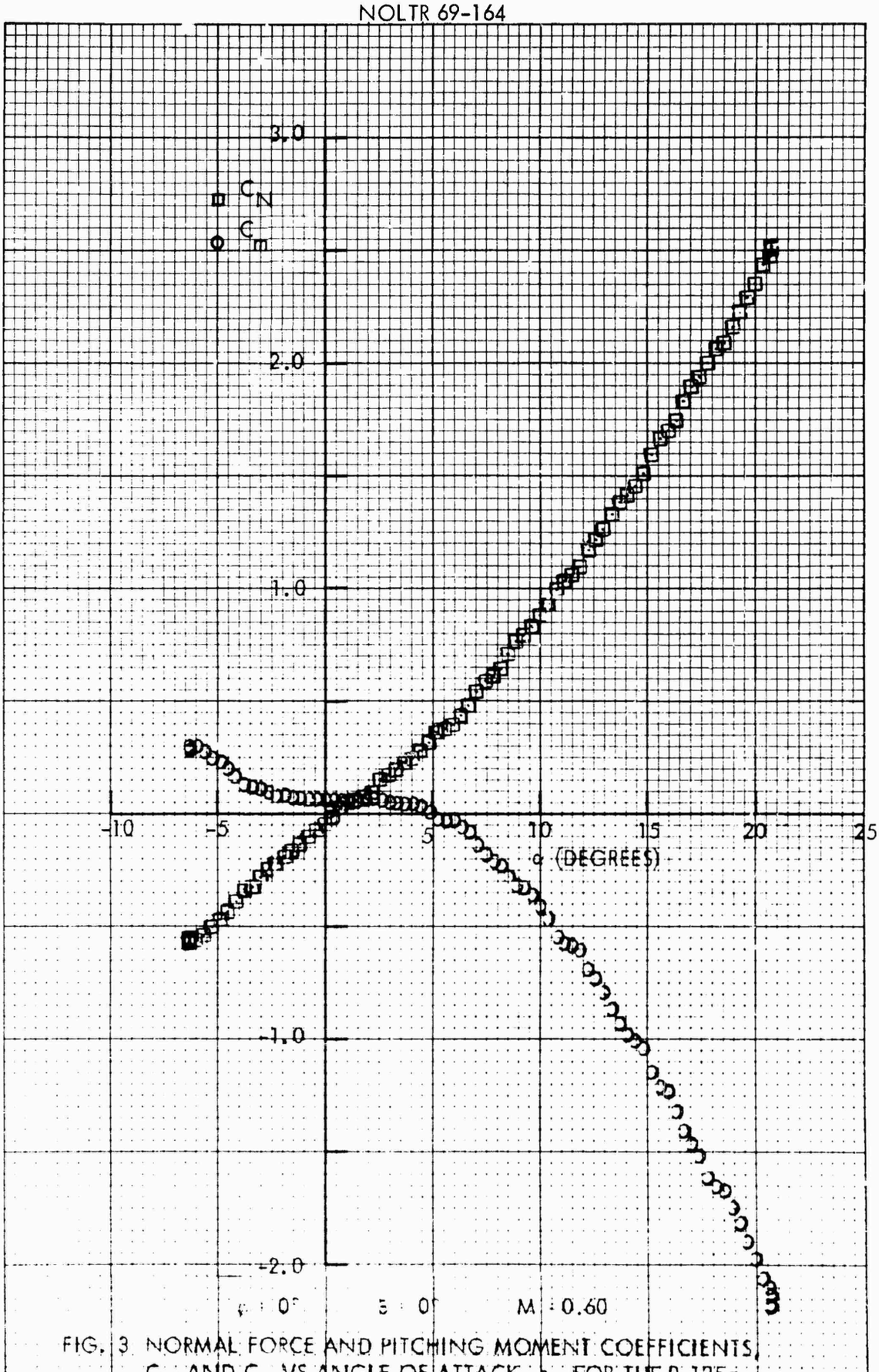

FIG. 3 NORMAL FORCE AND PITCHING MOMENT COEFFICIENTS, C_N AND C_m VS ANGLE OF ATTACK, α, FOR THE 0.125-SCALE MK 82-SNAKEYE BOMB WITH FINS CLOSED

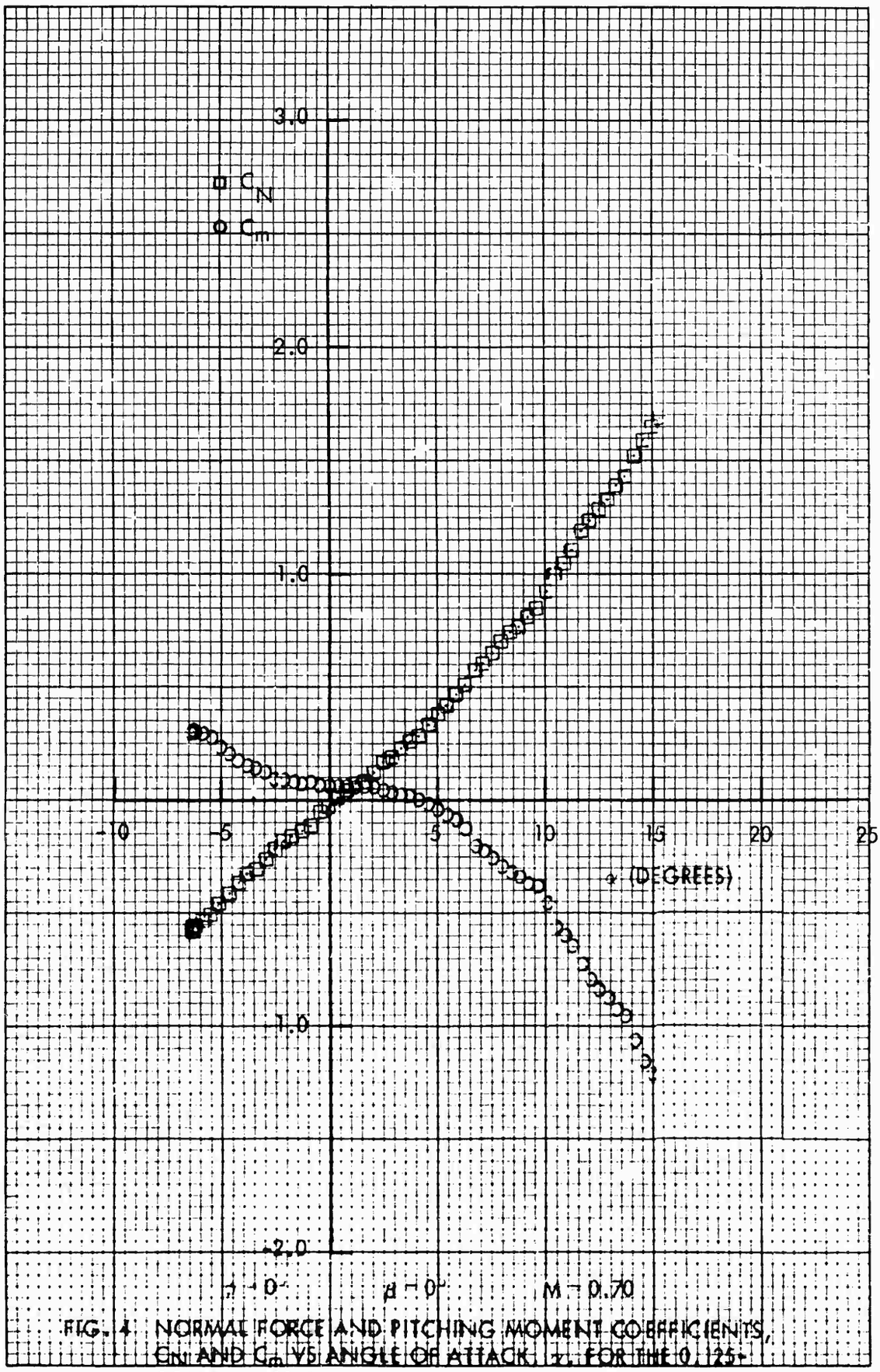

FIG. 4 NORMAL FORCE AND PITCHING MOMENT COEFFICIENTS, C_N AND C_m VS ANGLE OF ATTACK, α, FOR THE 0.125-SCALE MK 82-SNAKEYE BOMB WITH FINS CLOSED

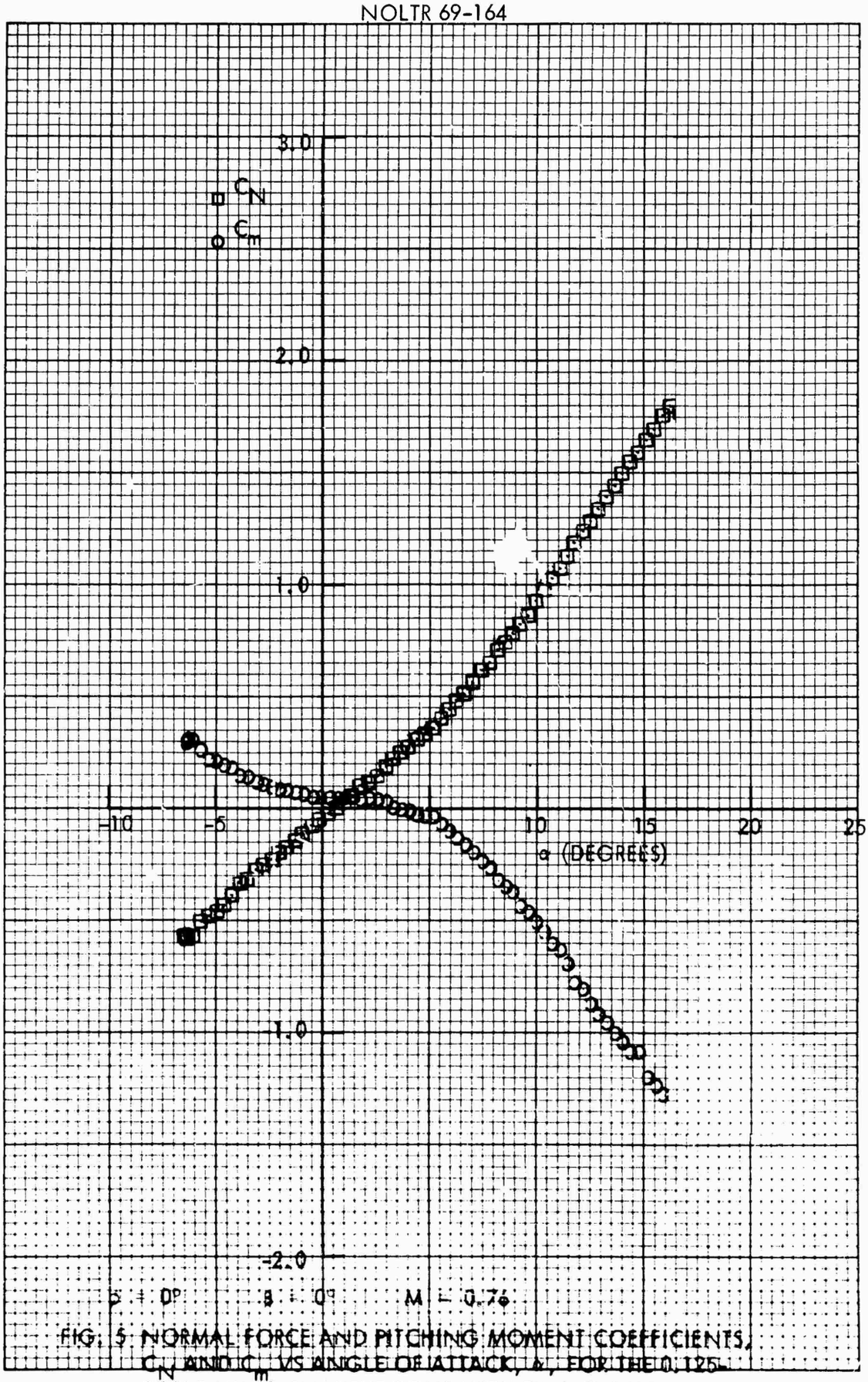

FIG. 5 NORMAL FORCE AND PITCHING MOMENT COEFFICIENTS, C_N AND C_m VS ANGLE OF ATTACK, α, FOR THE 0.125-SCALE MK 82-SNAKEYE BOMB WITH FINS CLOSED

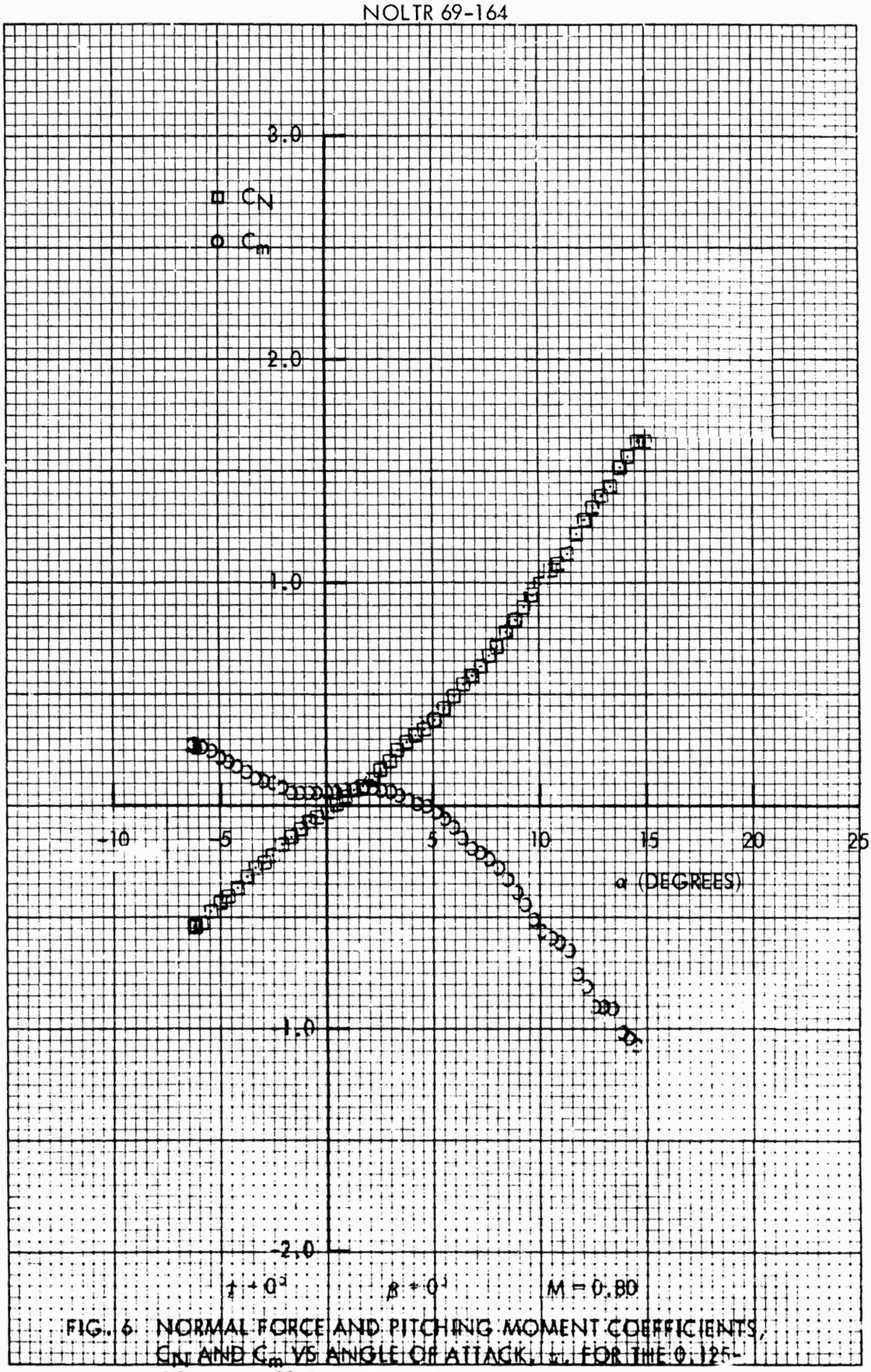

FIG. 6 NORMAL FORCE AND PITCHING MOMENT COEFFICIENTS, C_N AND C_m VS ANGLE OF ATTACK, α, FOR THE 0.125-SCALE MK 82-SNAKEYE BOMB WITH FINS CLOSED

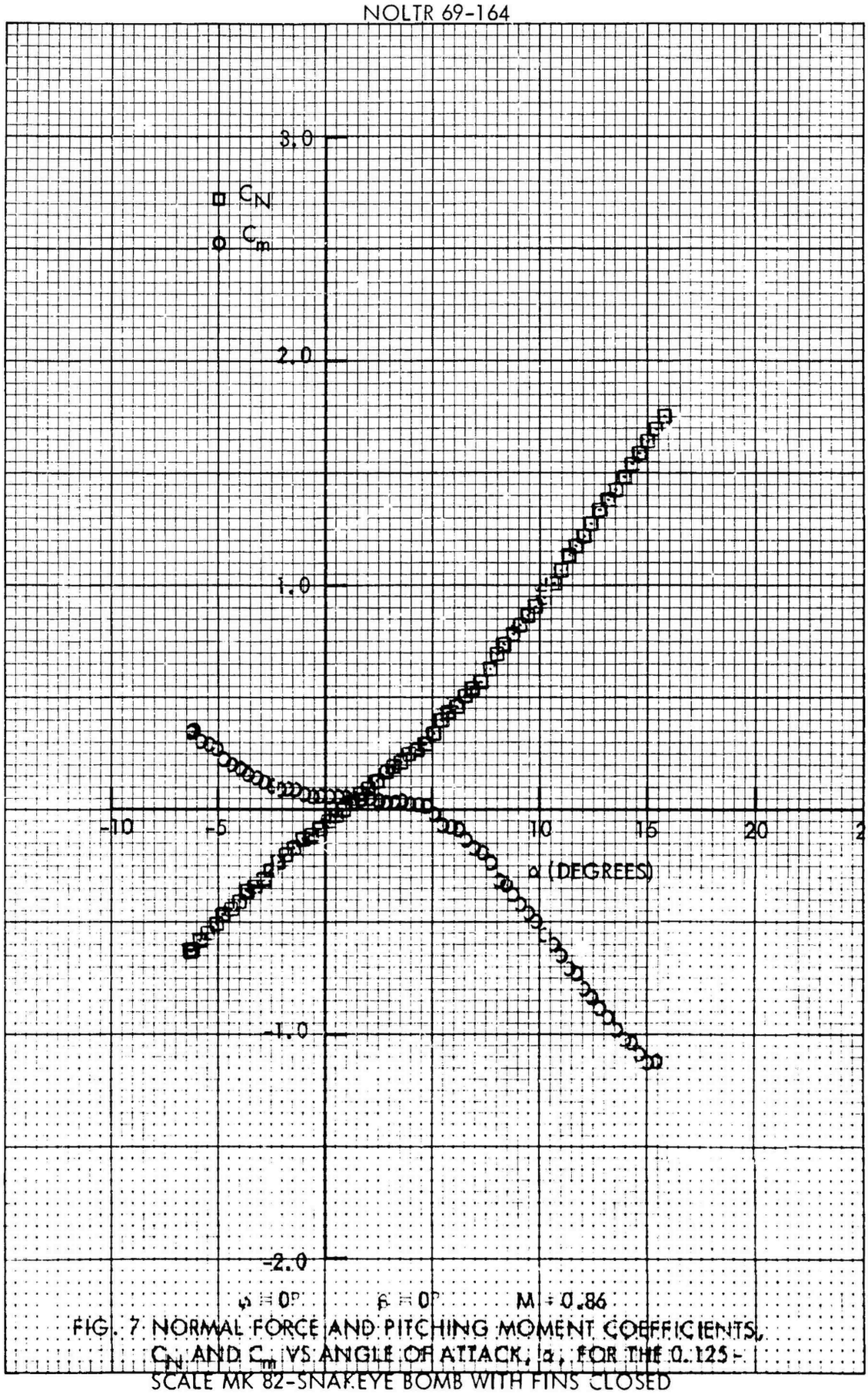

FIG. 7 NORMAL FORCE AND PITCHING MOMENT COEFFICIENTS, C_N AND C_m VS ANGLE OF ATTACK, α, FOR THE 0.125-SCALE MK 82-SNAKEYE BOMB WITH FINS CLOSED

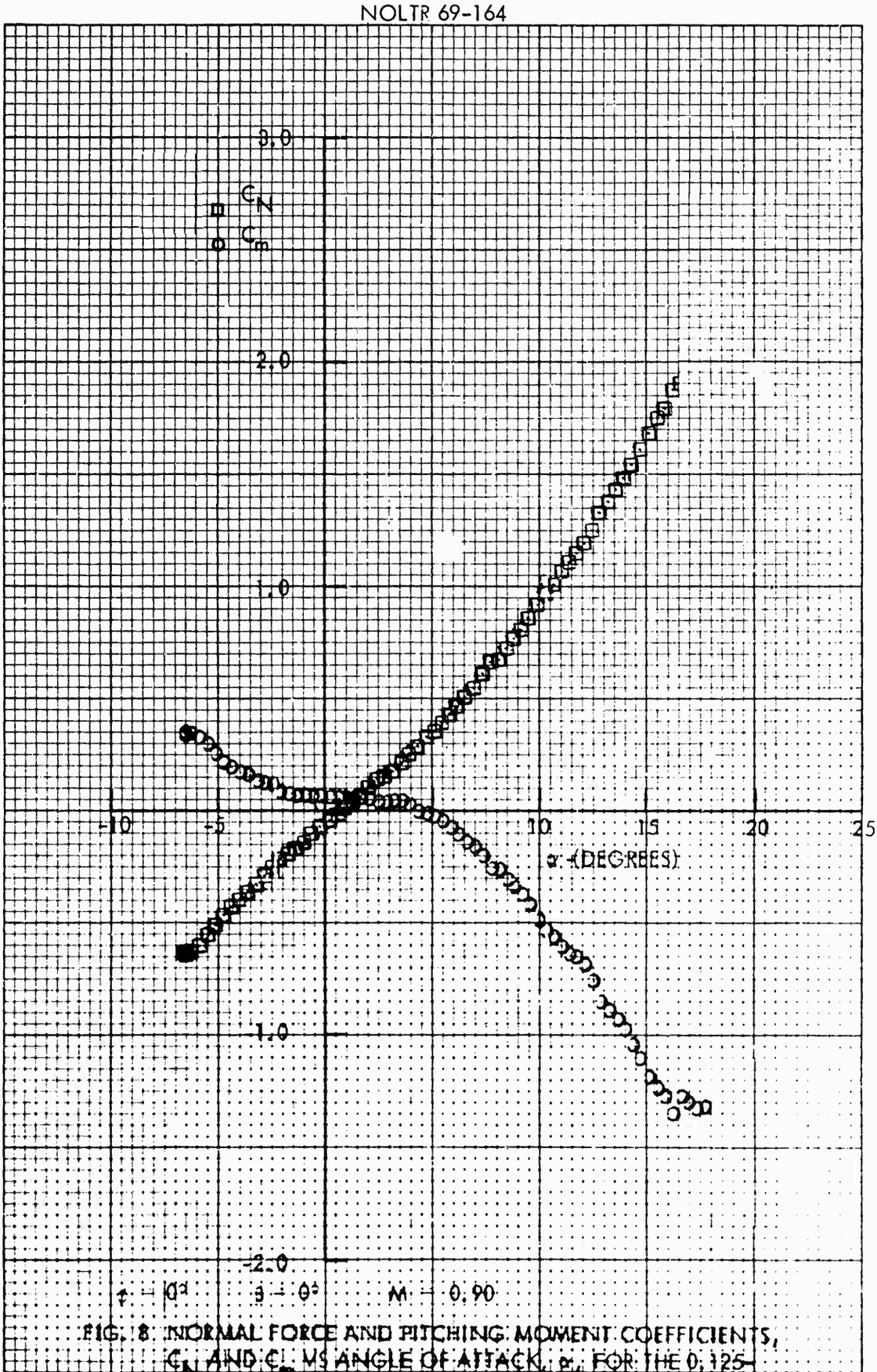

FIG. 8. NORMAL FORCE AND PITCHING MOMENT COEFFICIENTS, C_N AND C_m VS ANGLE OF ATTACK, α, FOR THE 0.125-SCALE MK 82-SNAKEYE BOMB WITH FINS CLOSED

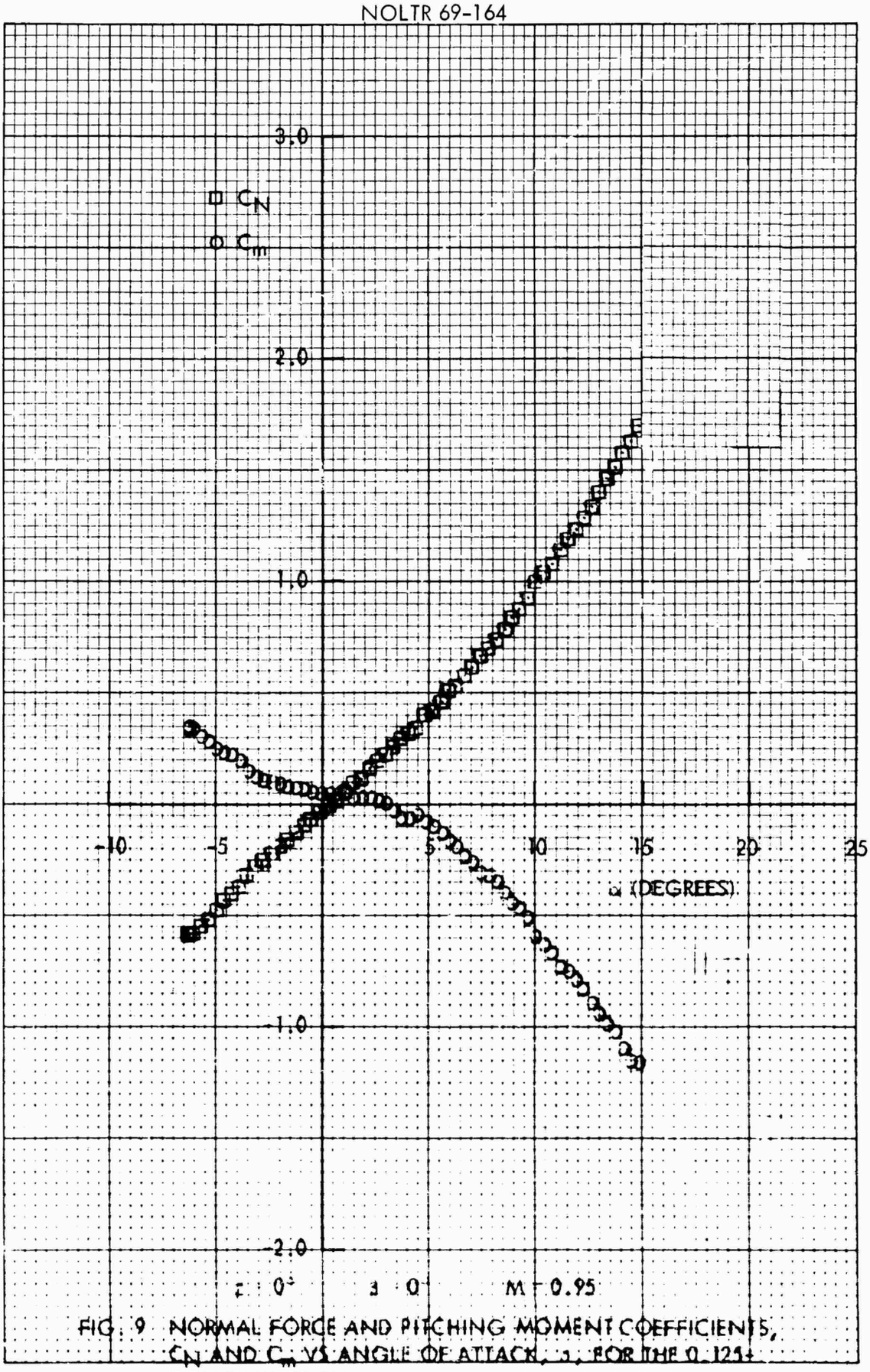

FIG. 9 NORMAL FORCE AND PITCHING MOMENT COEFFICIENTS, C_N AND C_m VS ANGLE OF ATTACK, α, FOR THE 0.125+ SCALE MK 82-SNAKEYE BOMB WITH FINS CLOSED

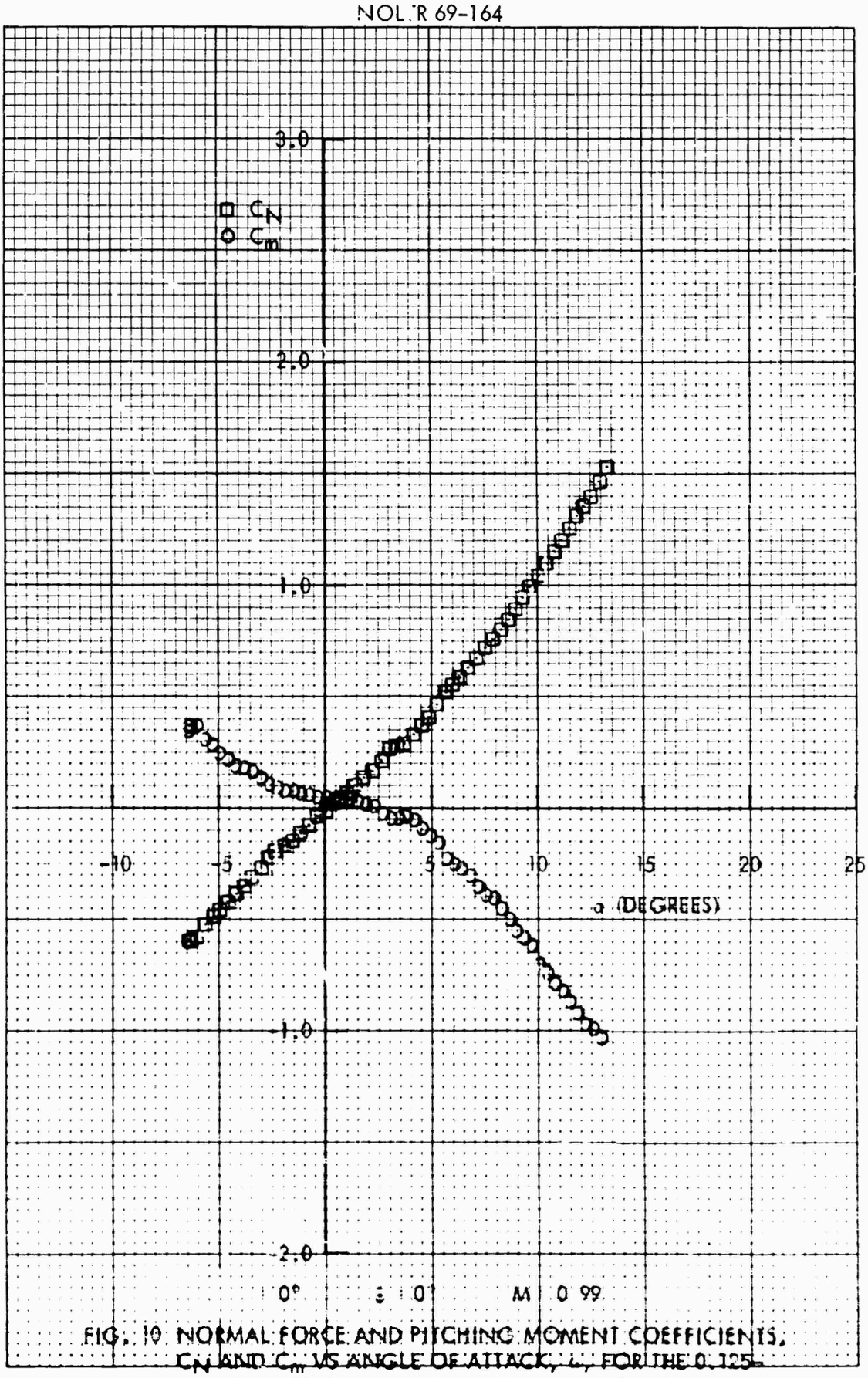

FIG. 10 NORMAL FORCE AND PITCHING MOMENT COEFFICIENTS, C_N AND C_m VS ANGLE OF ATTACK, α, FOR THE 0.125-SCALE MK 82-SNAKEYE BOMB WITH FINS CLOSED

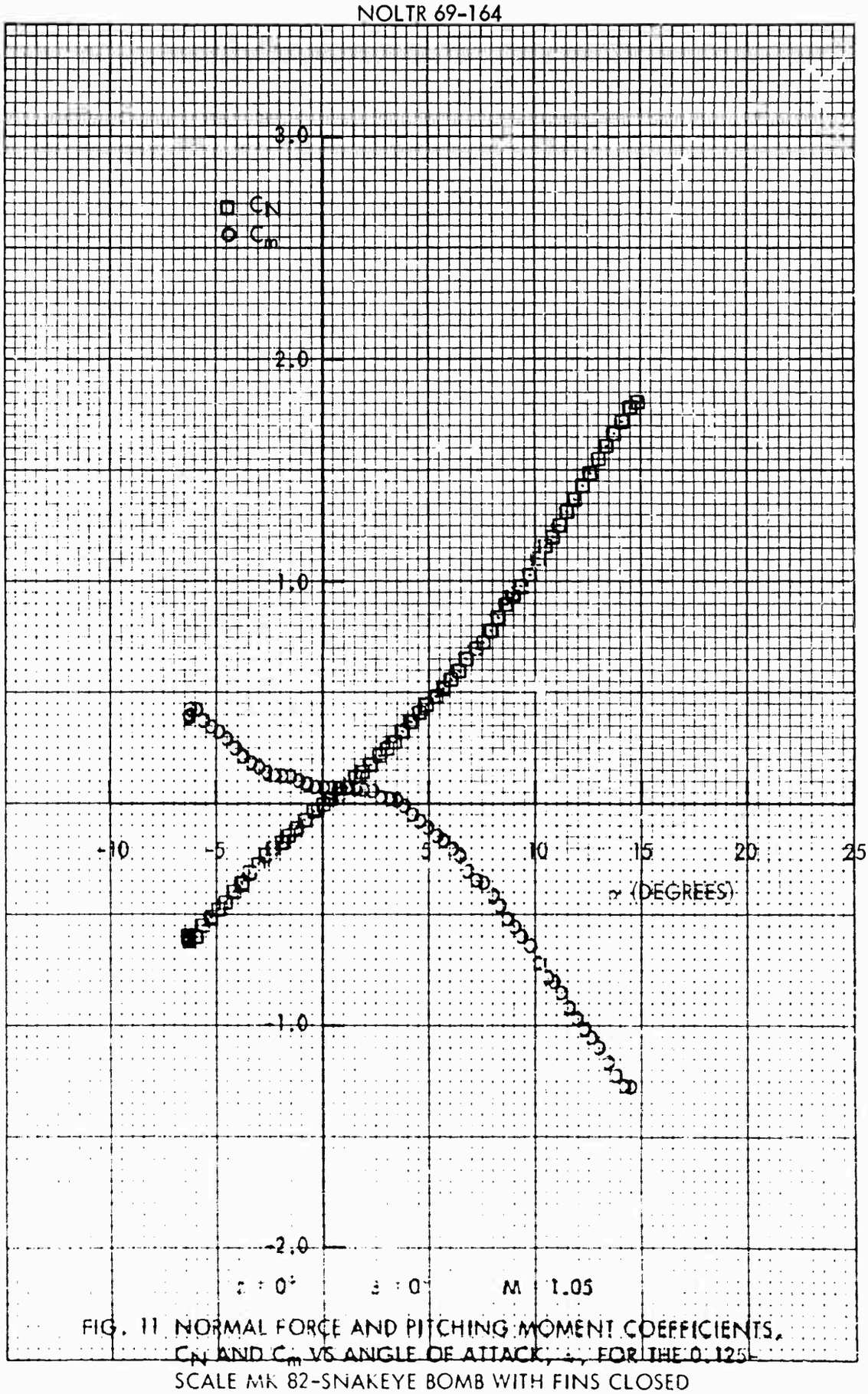

FIG. 11 NORMAL FORCE AND PITCHING MOMENT COEFFICIENTS, C_N AND C_m VS ANGLE OF ATTACK, α, FOR THE 0.125-SCALE MK 82-SNAKEYE BOMB WITH FINS CLOSED

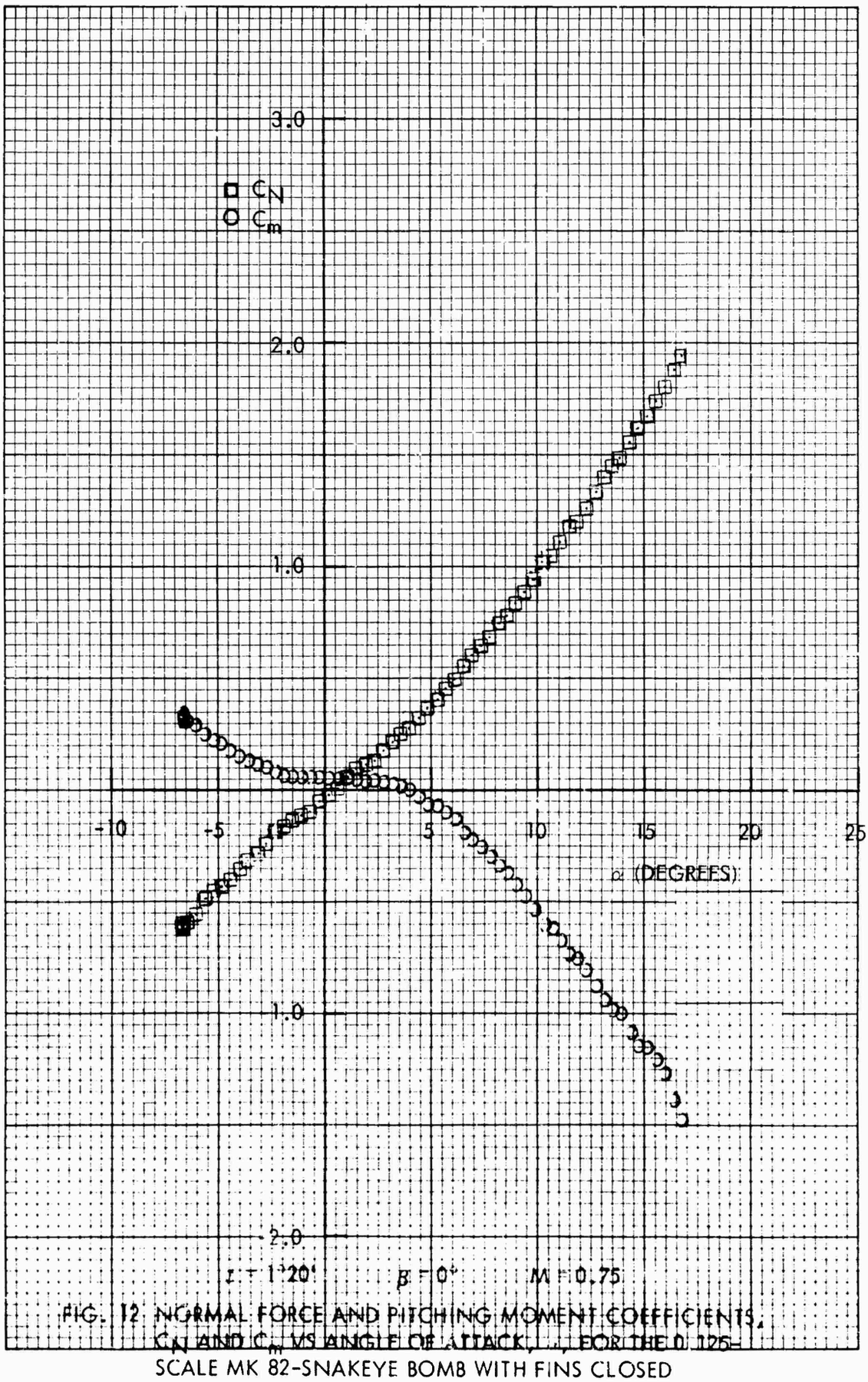

FIG. 12 NORMAL FORCE AND PITCHING MOMENT COEFFICIENTS, C_N AND C_m VS ANGLE OF ATTACK, α, FOR THE 0.125-SCALE MK 82-SNAKEYE BOMB WITH FINS CLOSED

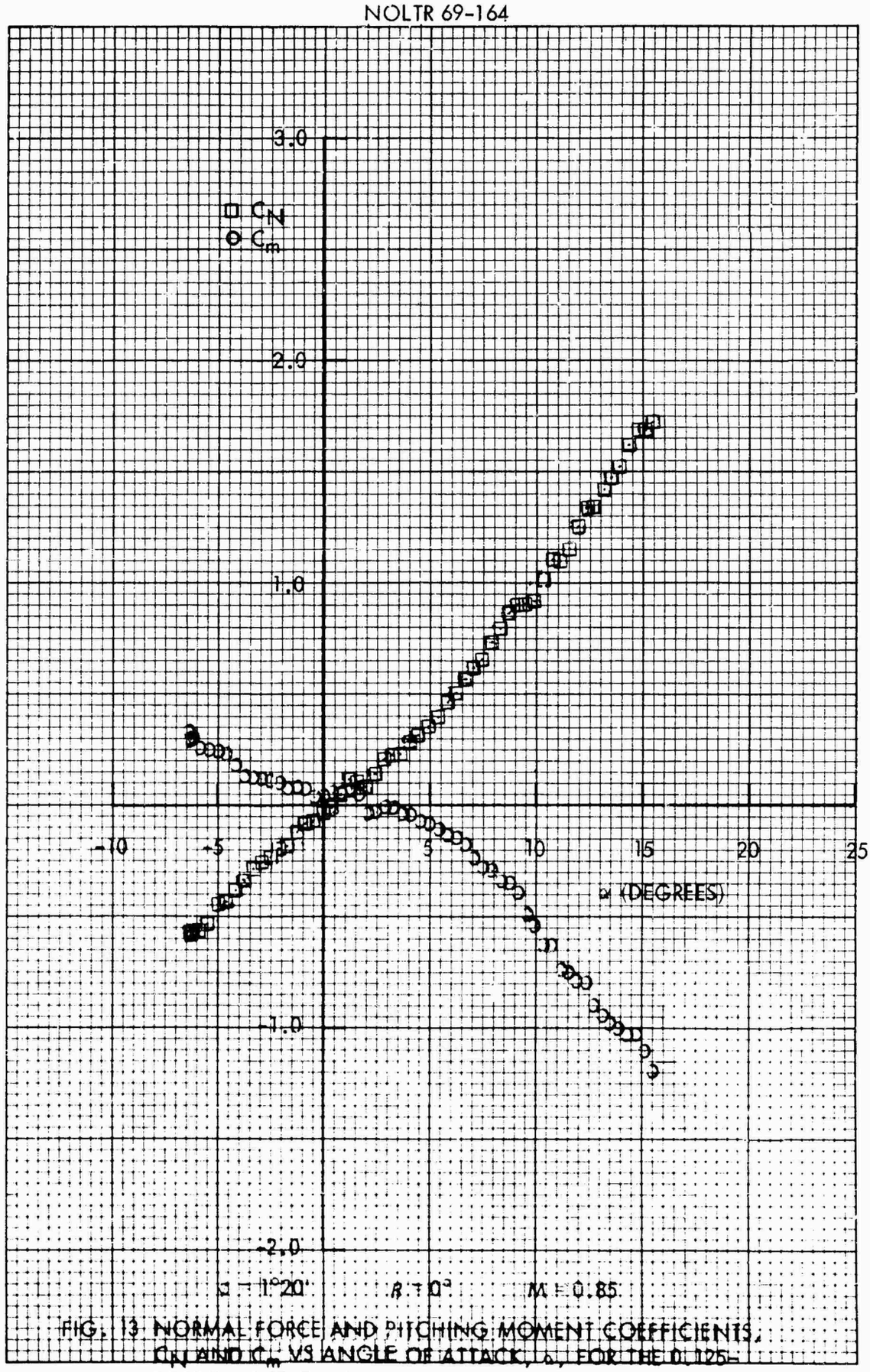

FIG. 13 NORMAL FORCE AND PITCHING MOMENT COEFFICIENTS, C_N AND C_m VS ANGLE OF ATTACK, α, FOR THE 0.125-SCALE MK 82-SNAKEYE BOMB WITH FINS CLOSED

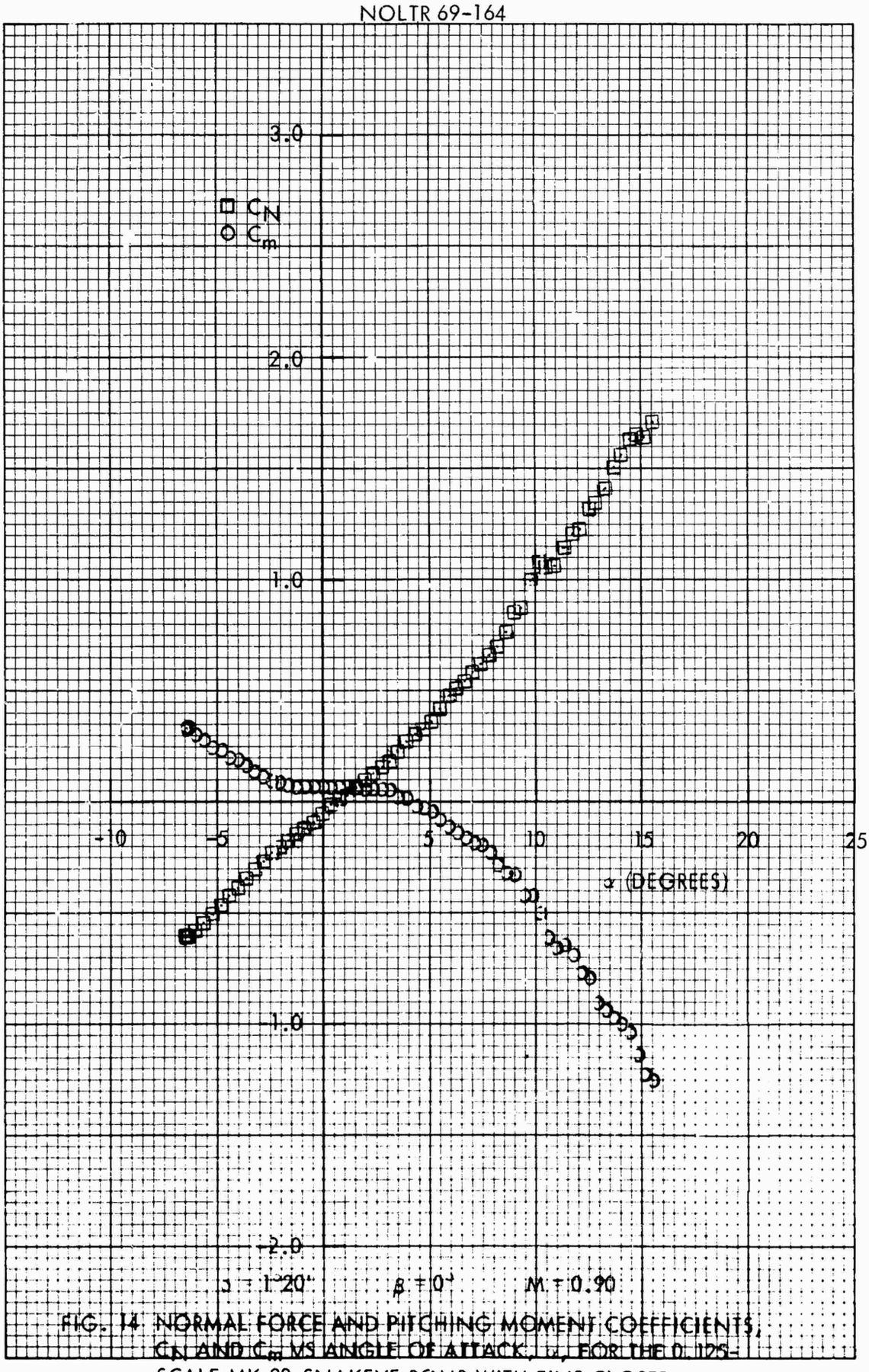

FIG. 14 NORMAL FORCE AND PITCHING MOMENT COEFFICIENTS, C_N AND C_m VS ANGLE OF ATTACK, α, FOR THE 0.125-SCALE MK 82-SNAKEYE BOMB WITH FINS CLOSED

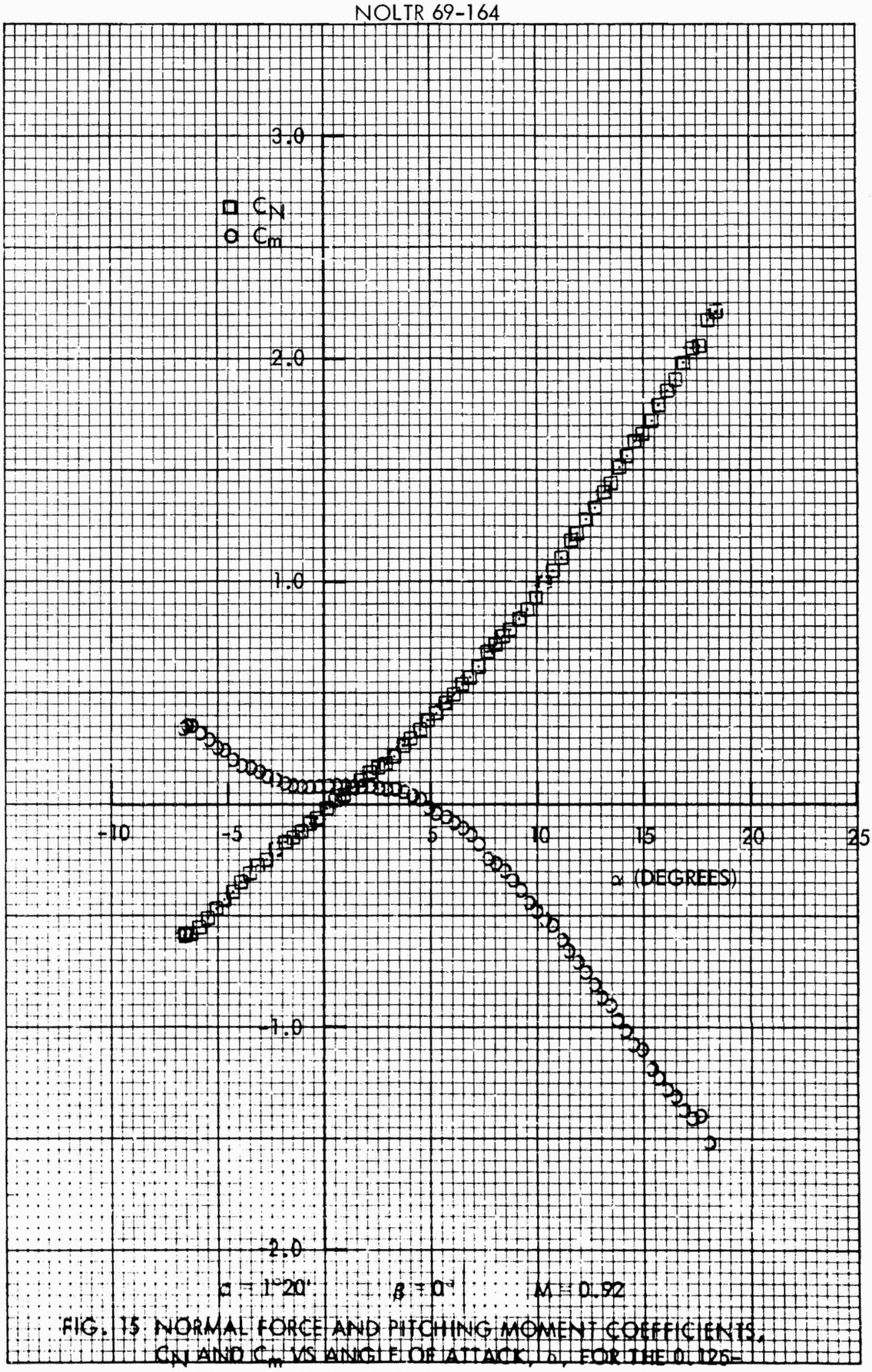

FIG. 15 NORMAL FORCE AND PITCHING MOMENT COEFFICIENTS, C_N AND C_m VS ANGLE OF ATTACK, α, FOR THE 0.125-SCALE MK 82-SNAKEYE BOMB WITH FINS CLOSED

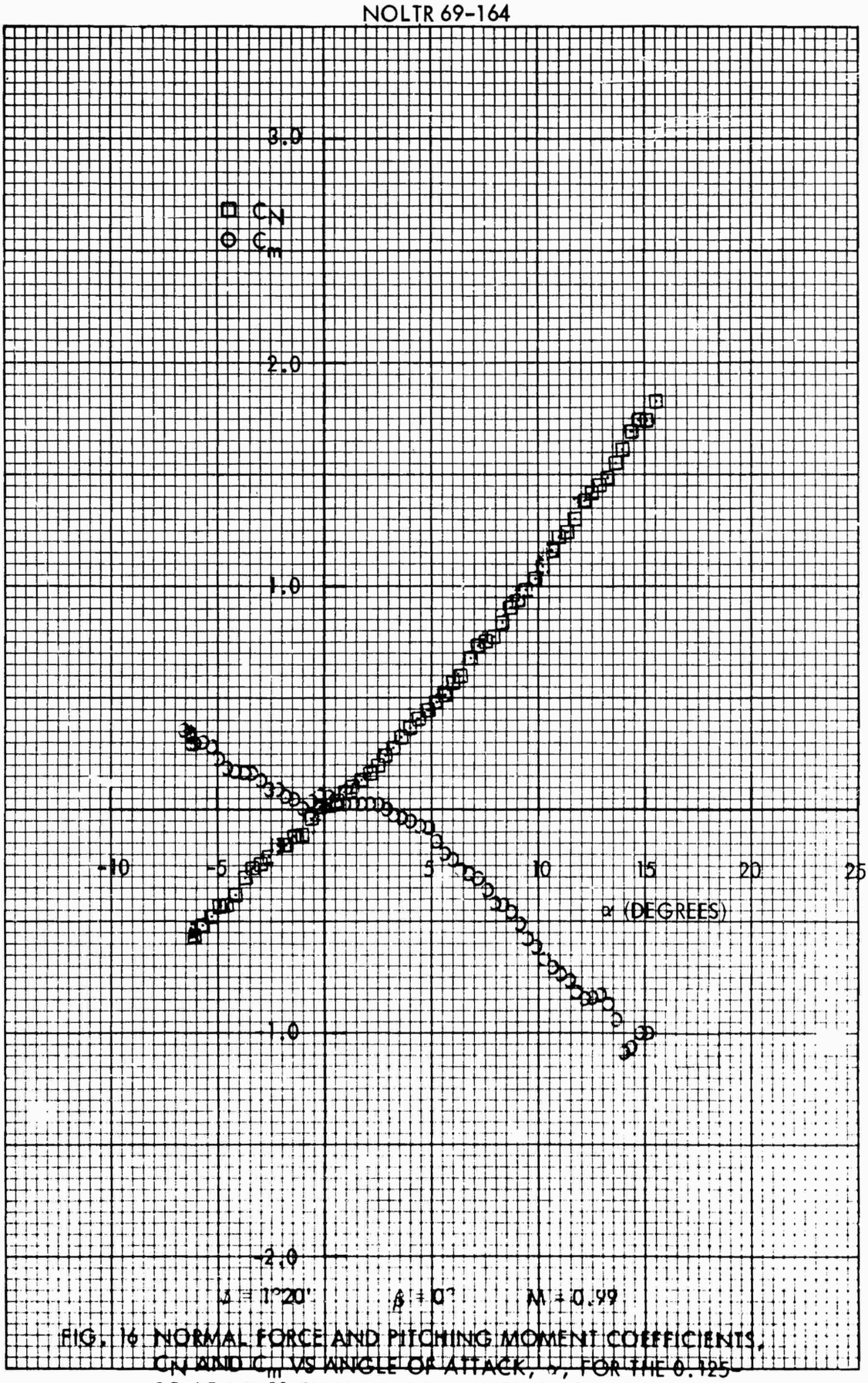

FIG. 16 NORMAL FORCE AND PITCHING MOMENT COEFFICIENTS, C_N AND C_m VS ANGLE OF ATTACK, α, FOR THE 0.125-SCALE MK 82-SNAKEYE BOMB WITH FINS CLOSED

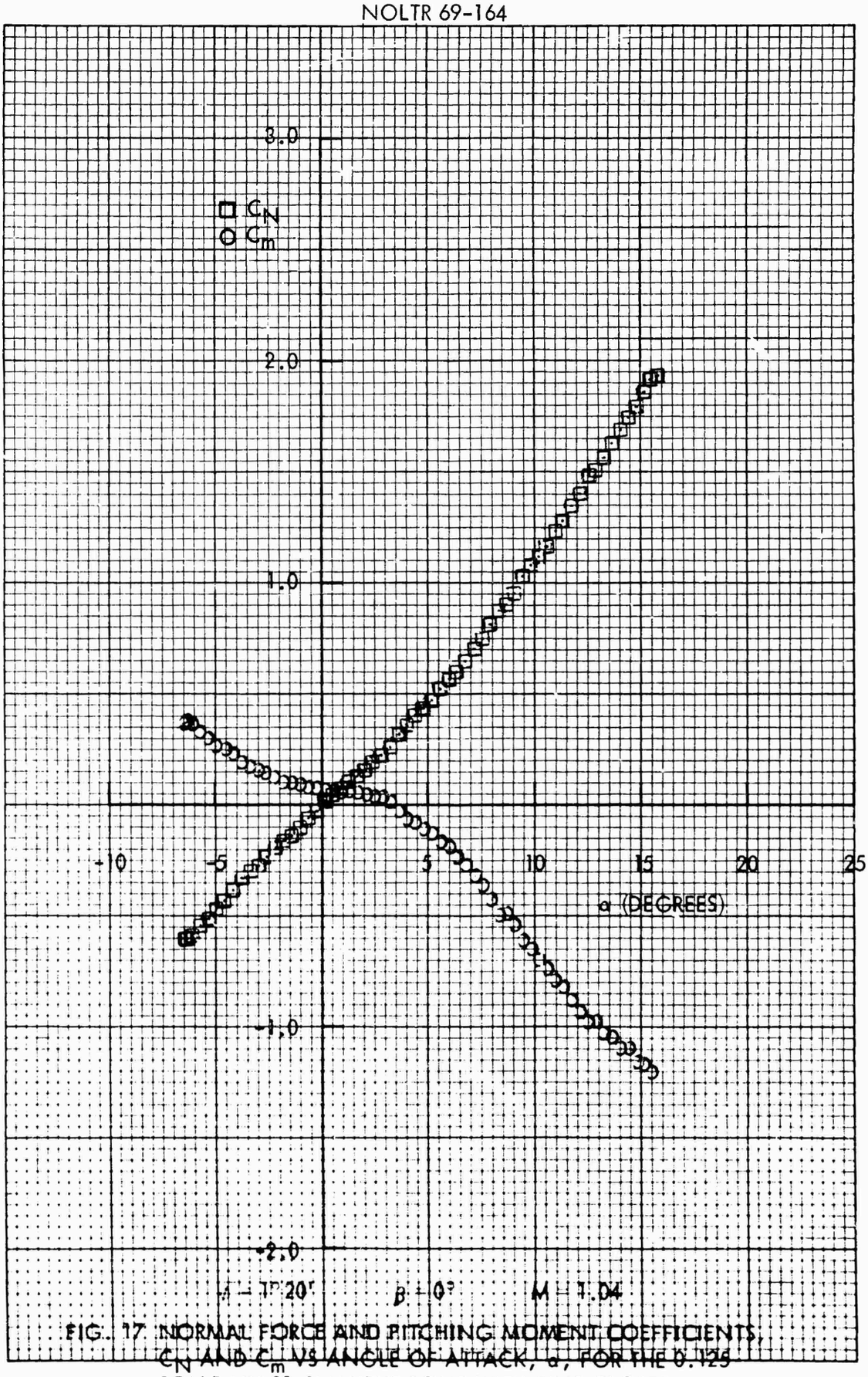

FIG. 17 NORMAL FORCE AND PITCHING MOMENT COEFFICIENTS, C_N AND C_m VS ANGLE OF ATTACK, α, FOR THE 0.125-SCALE MK 82-SNAKEYE BOMB WITH FINS CLOSED

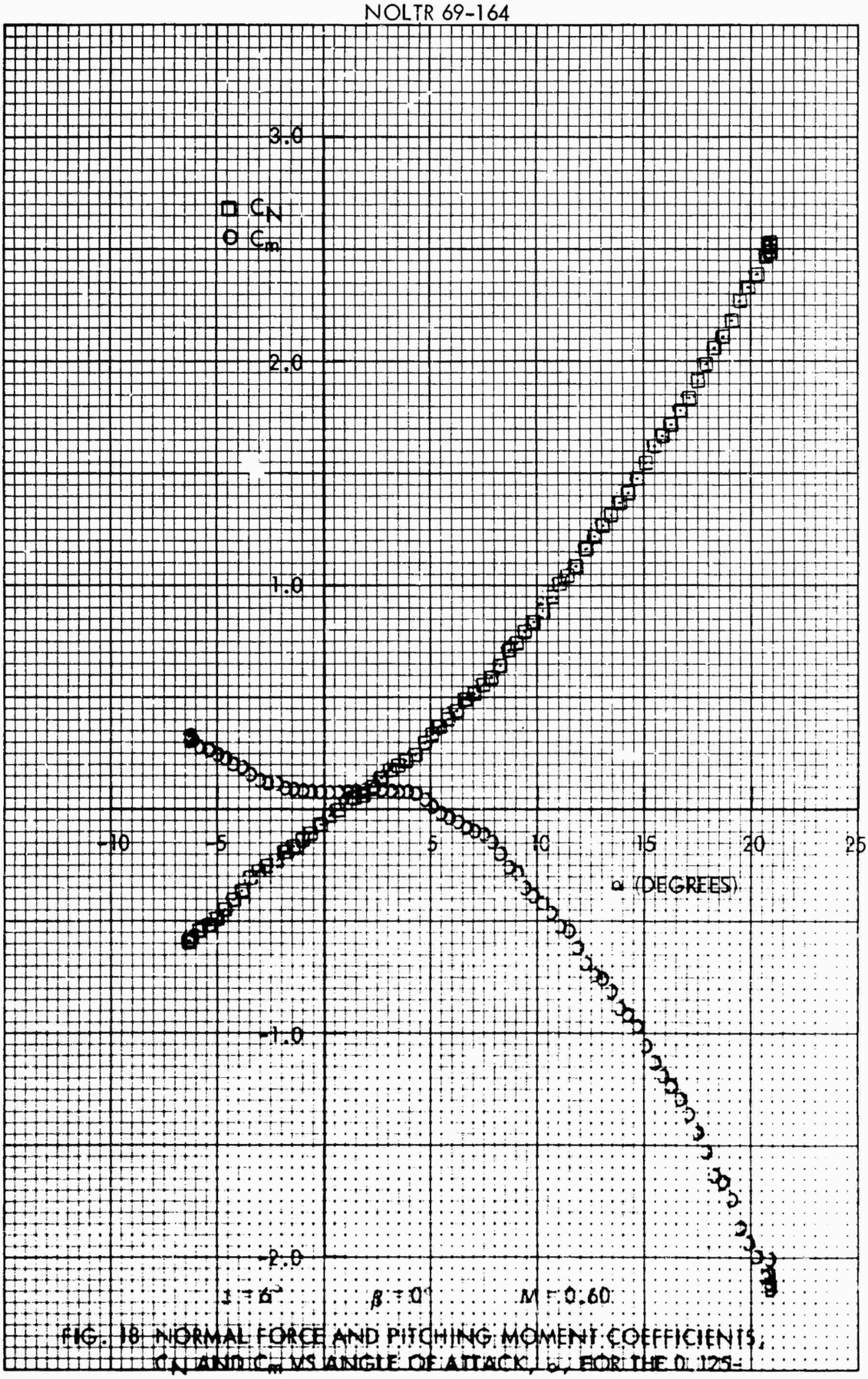

FIG. 18 NORMAL FORCE AND PITCHING MOMENT COEFFICIENTS, C_N AND C_m VS ANGLE OF ATTACK, α, FOR THE 0.125-SCALE MK 82-SNAKEYE BOMB WITH FINS CLOSED

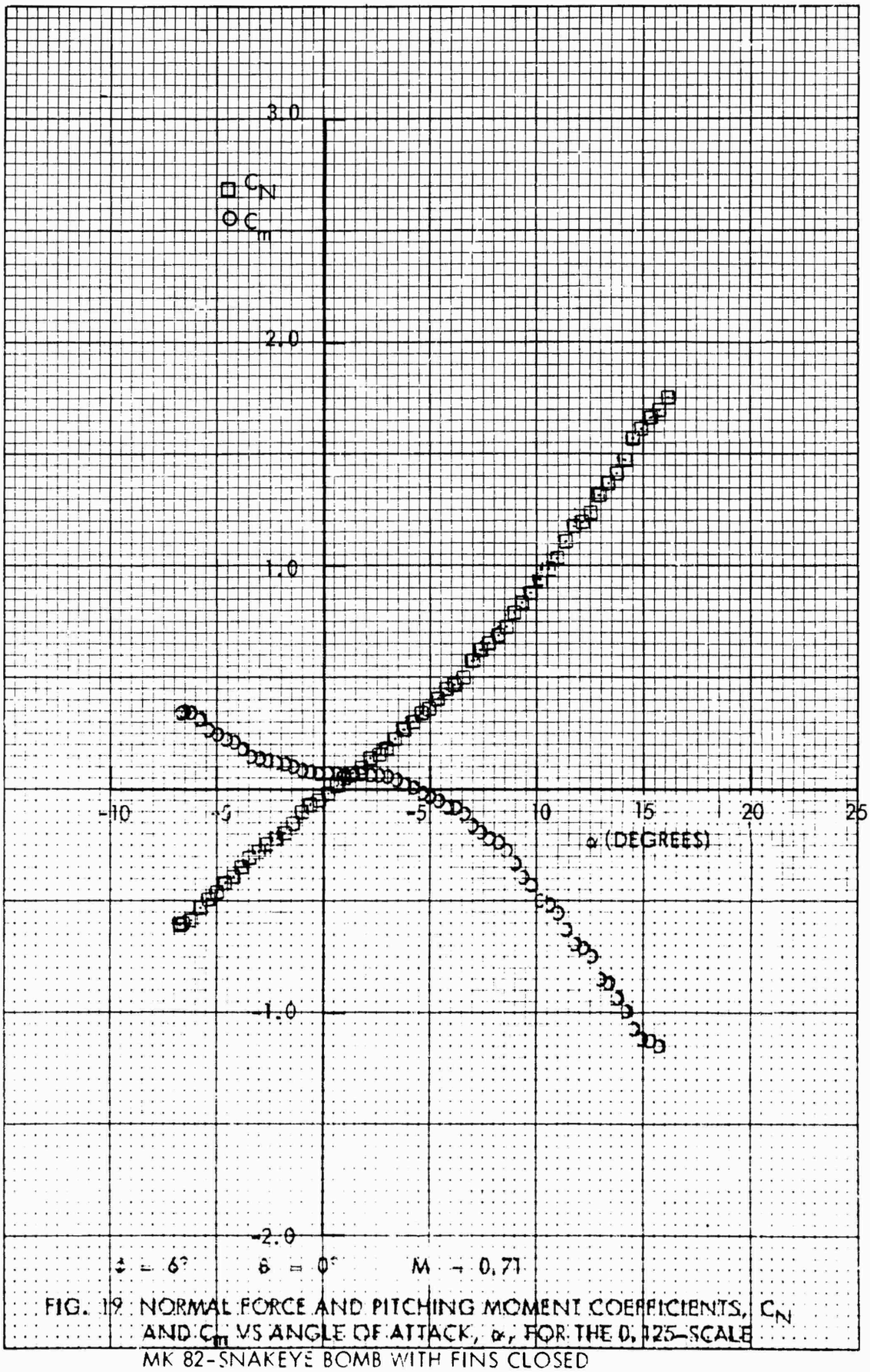

FIG. 19 NORMAL FORCE AND PITCHING MOMENT COEFFICIENTS, C_N AND C_m VS ANGLE OF ATTACK, α, FOR THE 0.125-SCALE MK 82-SNAKEYE BOMB WITH FINS CLOSED

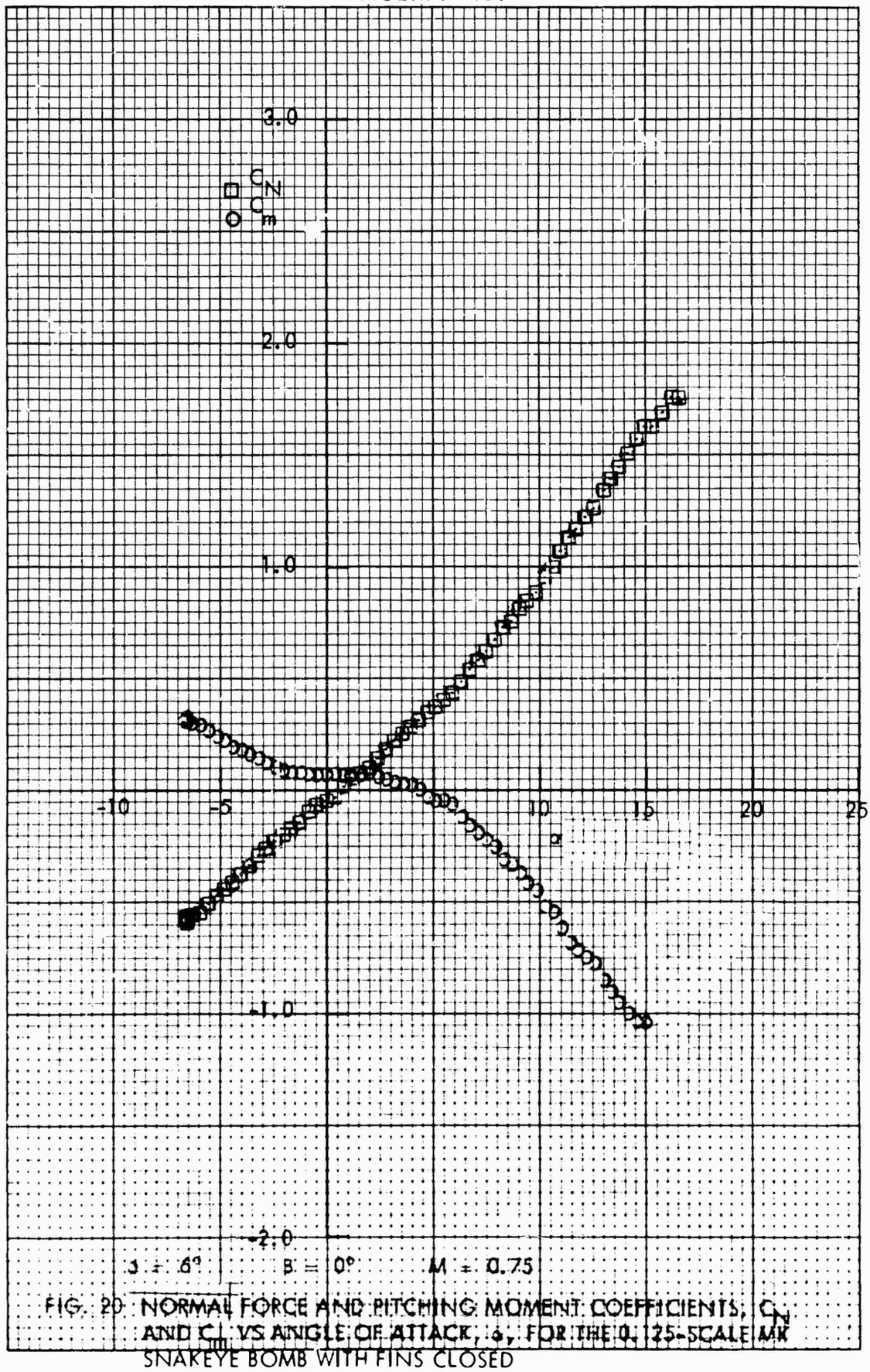

FIG. 20 NORMAL FORCE AND PITCHING MOMENT COEFFICIENTS, C_N AND C_m VS ANGLE OF ATTACK, α, FOR THE 0.125-SCALE MK SNAKEYE BOMB WITH FINS CLOSED

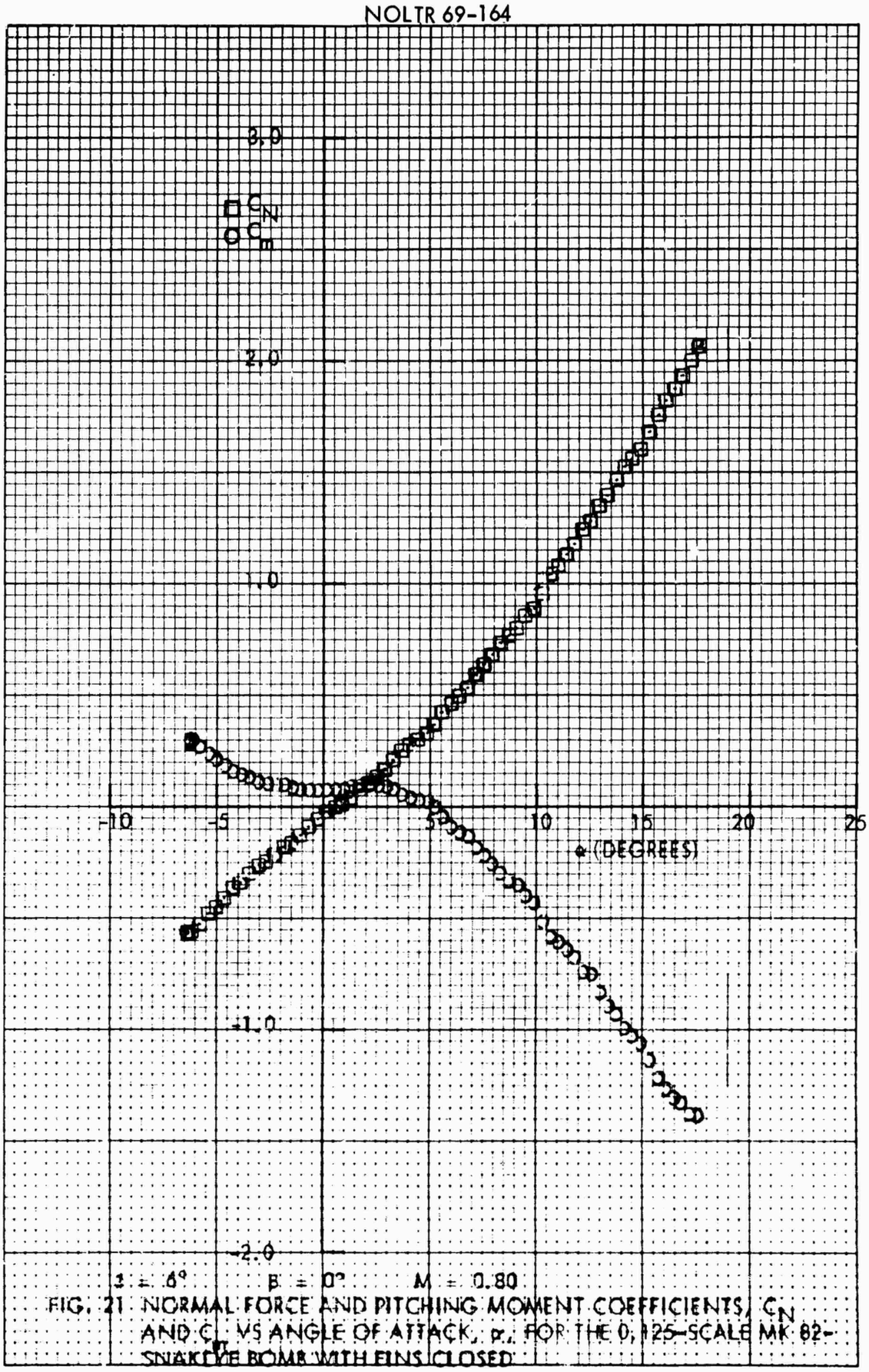

δ = 6° β = 0° M = 0.80

FIG. 21 NORMAL FORCE AND PITCHING MOMENT COEFFICIENTS, C_N AND C_m VS ANGLE OF ATTACK, α, FOR THE 0.125-SCALE MK 82-SNAKEYE BOMB WITH FINS CLOSED

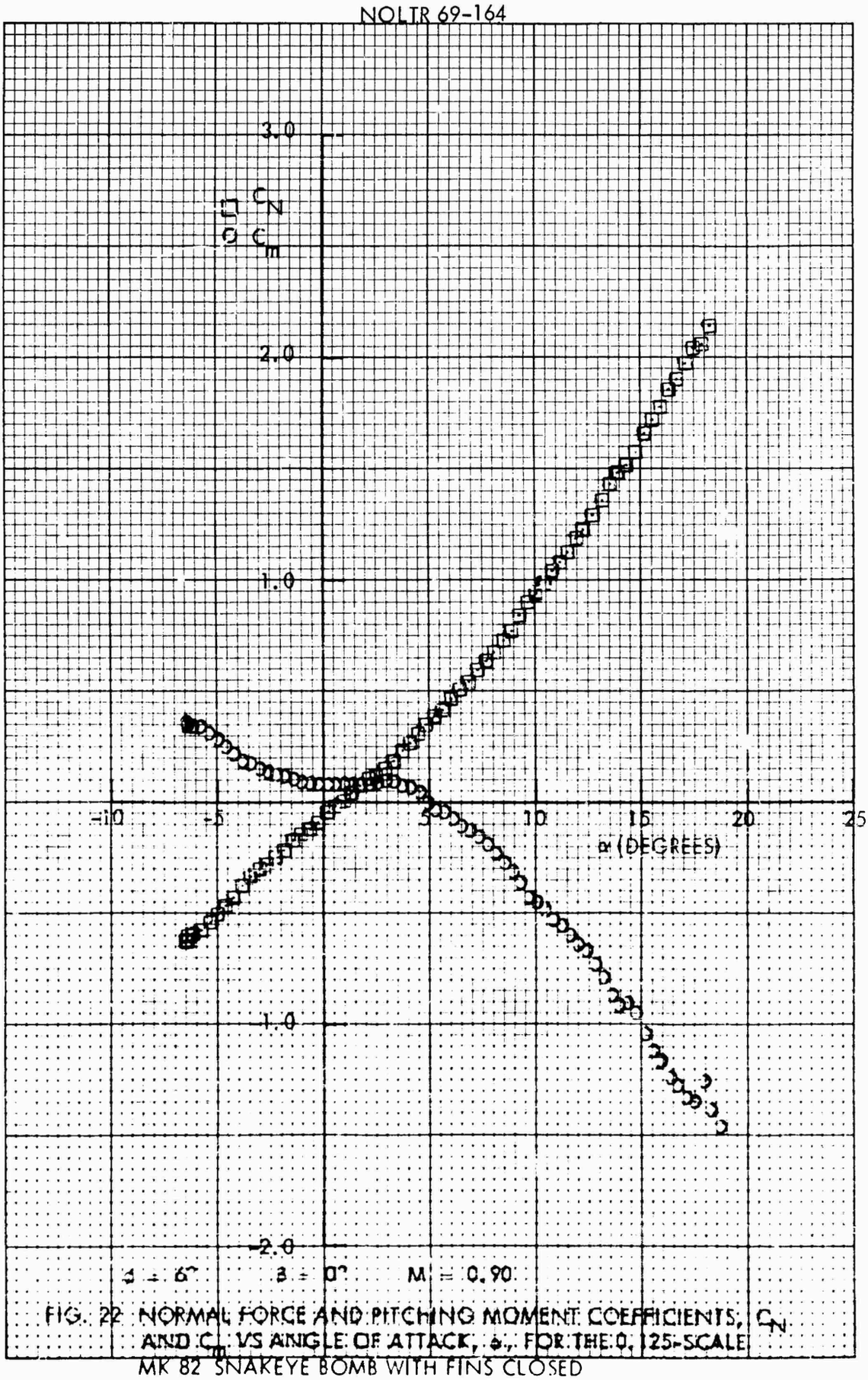

FIG. 22 NORMAL FORCE AND PITCHING MOMENT COEFFICIENTS, C_N AND C_m VS ANGLE OF ATTACK, α, FOR THE 0.125-SCALE MK 82 SNAKEYE BOMB WITH FINS CLOSED

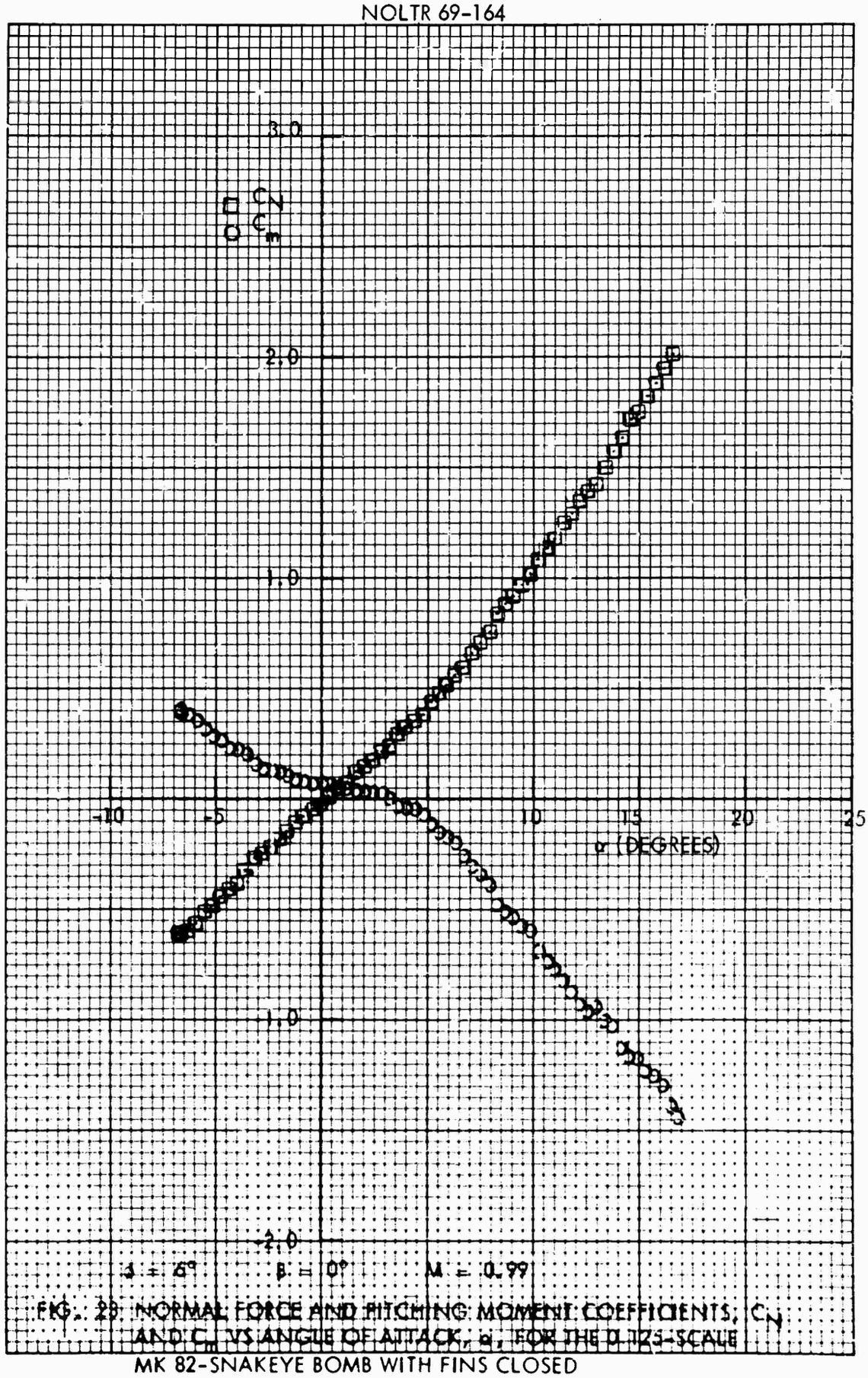

FIG. 29. NORMAL FORCE AND PITCHING MOMENT COEFFICIENTS, C_N AND C_m VS ANGLE OF ATTACK, α, FOR THE 0.175-SCALE MK 82-SNAKEYE BOMB WITH FINS CLOSED

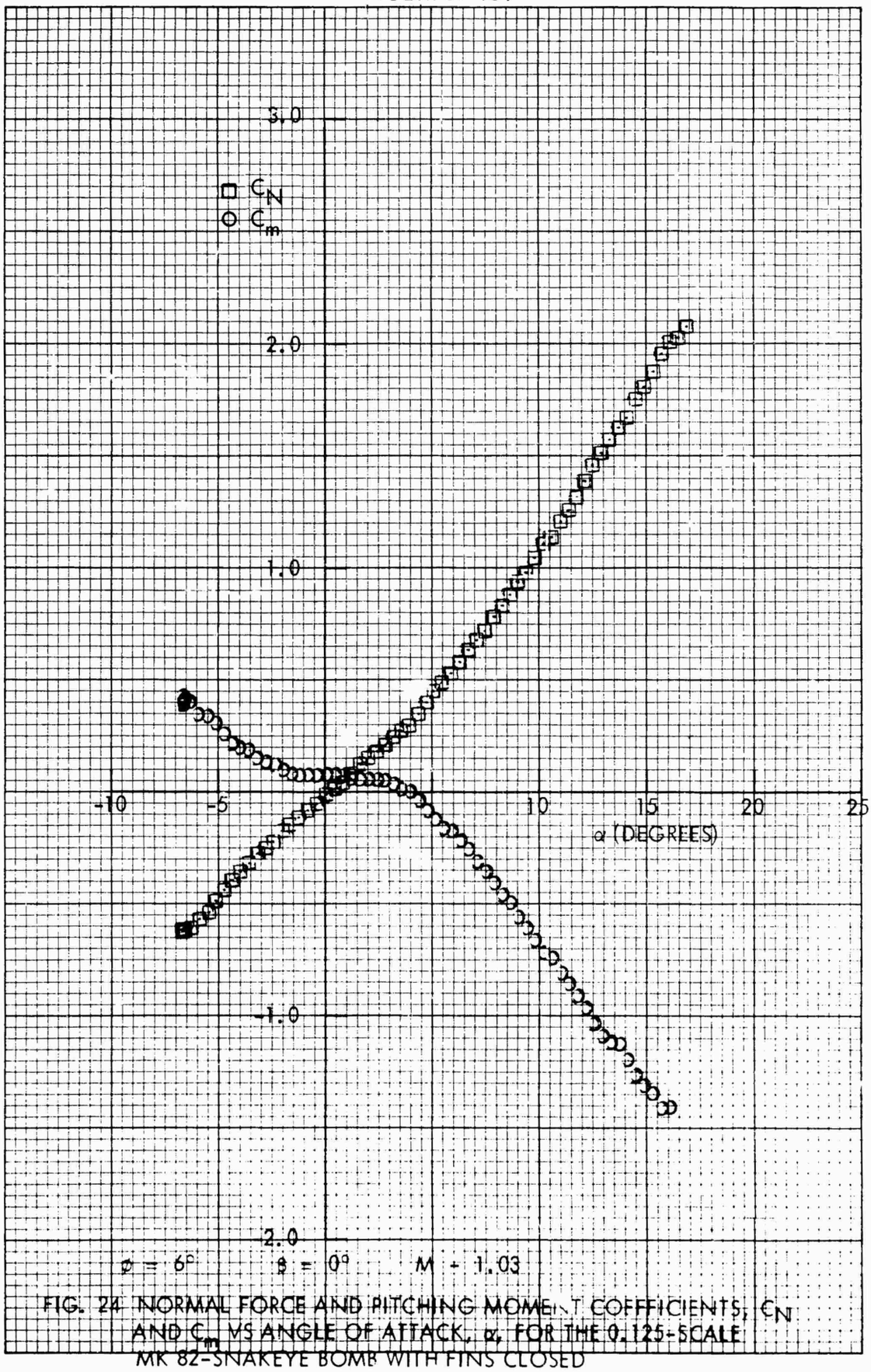

FIG. 24 NORMAL FORCE AND PITCHING MOMENT COFFFICIENTS, C_N AND C_m VS ANGLE OF ATTACK, α, FOR THE 0.125-SCALE MK 82-SNAKEYE BOMB WITH FINS CLOSED

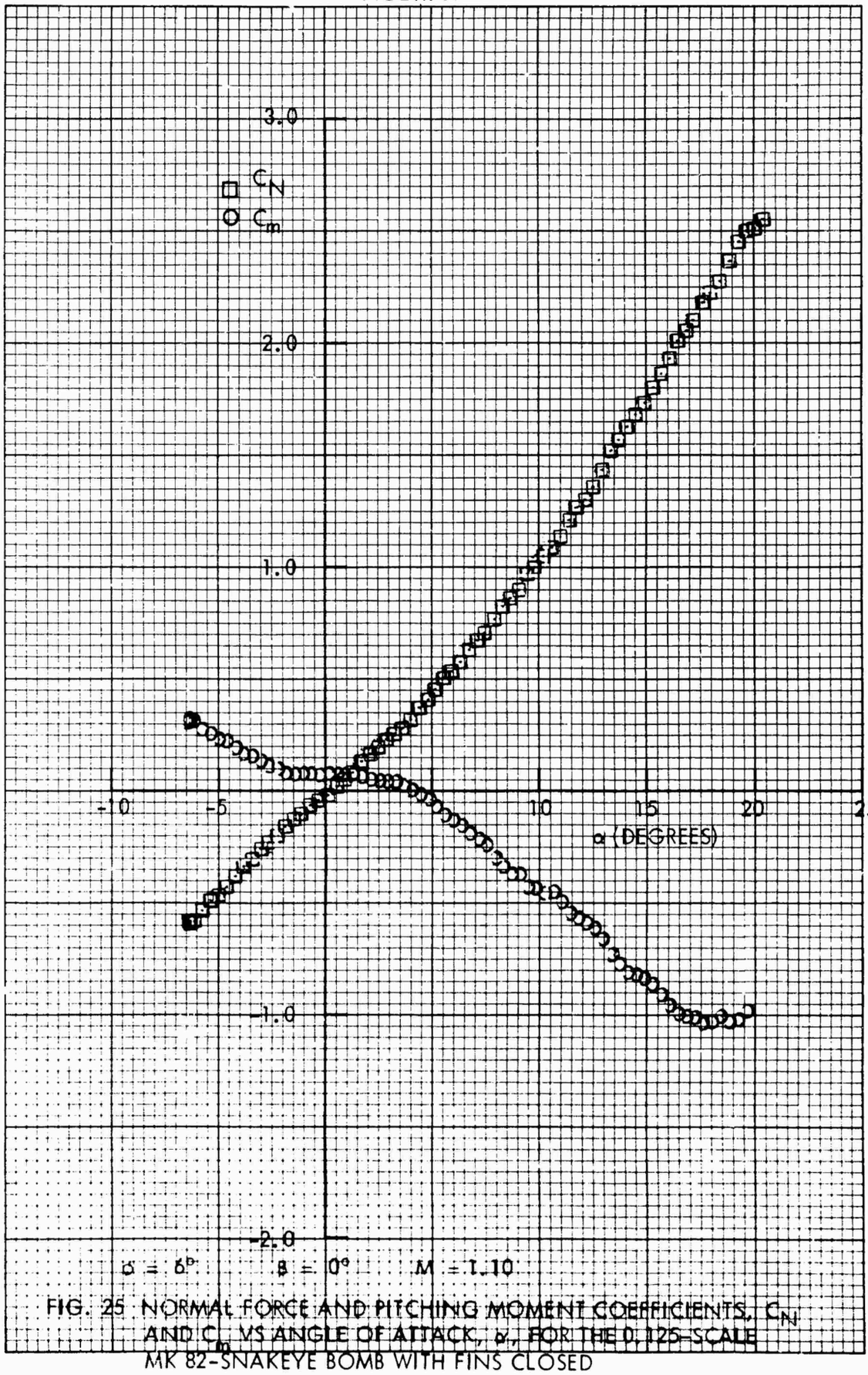

FIG. 25 NORMAL FORCE AND PITCHING MOMENT COEFFICIENTS, C_N AND C_m VS ANGLE OF ATTACK, α, FOR THE 0.125-SCALE MK 82-SNAKEYE BOMB WITH FINS CLOSED

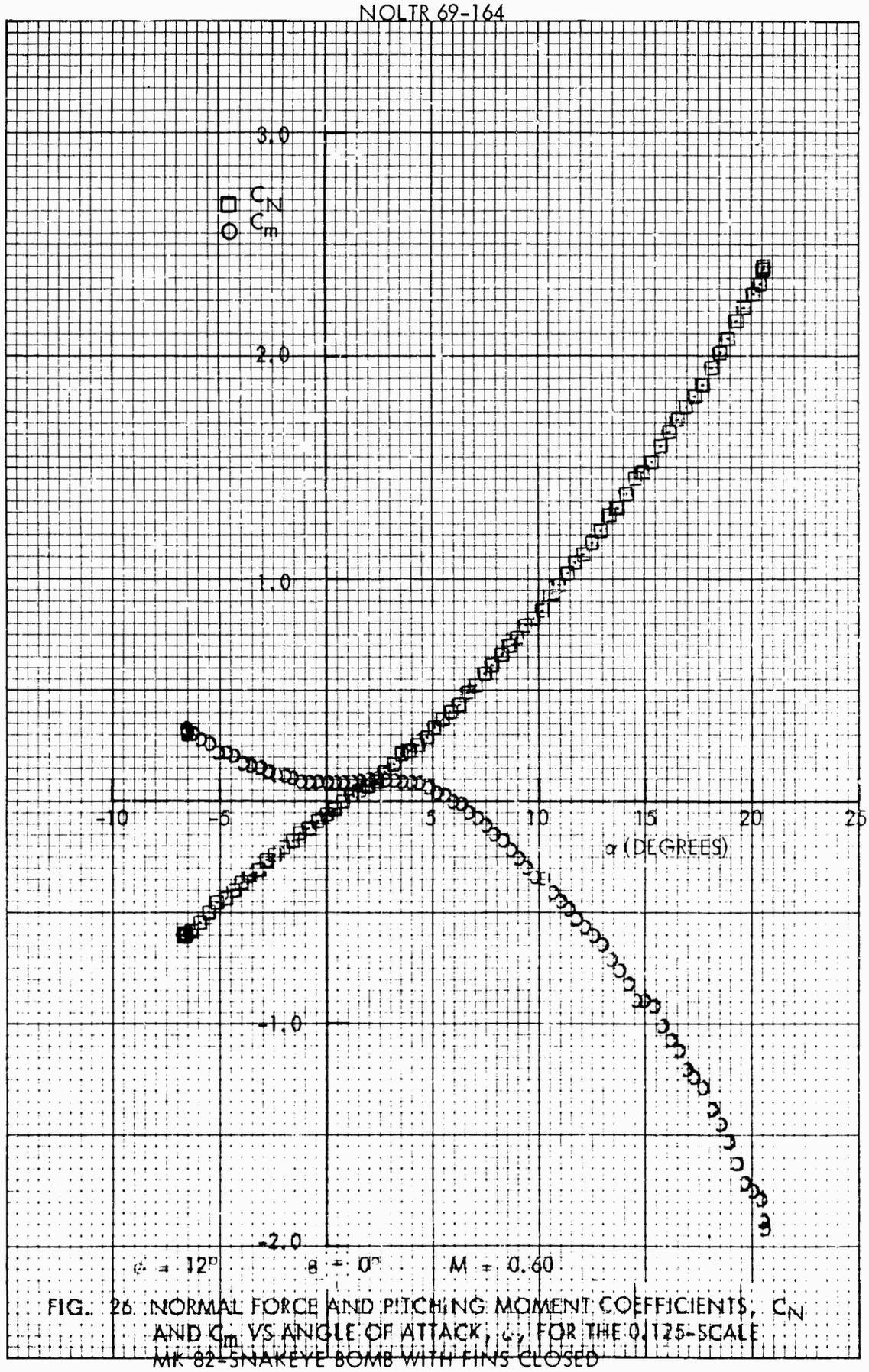

FIG. 26 NORMAL FORCE AND PITCHING MOMENT COEFFICIENTS, C_N AND C_m VS ANGLE OF ATTACK, α, FOR THE 0.125-SCALE MK 82-5 SNAKEYE BOMB WITH FINS CLOSED

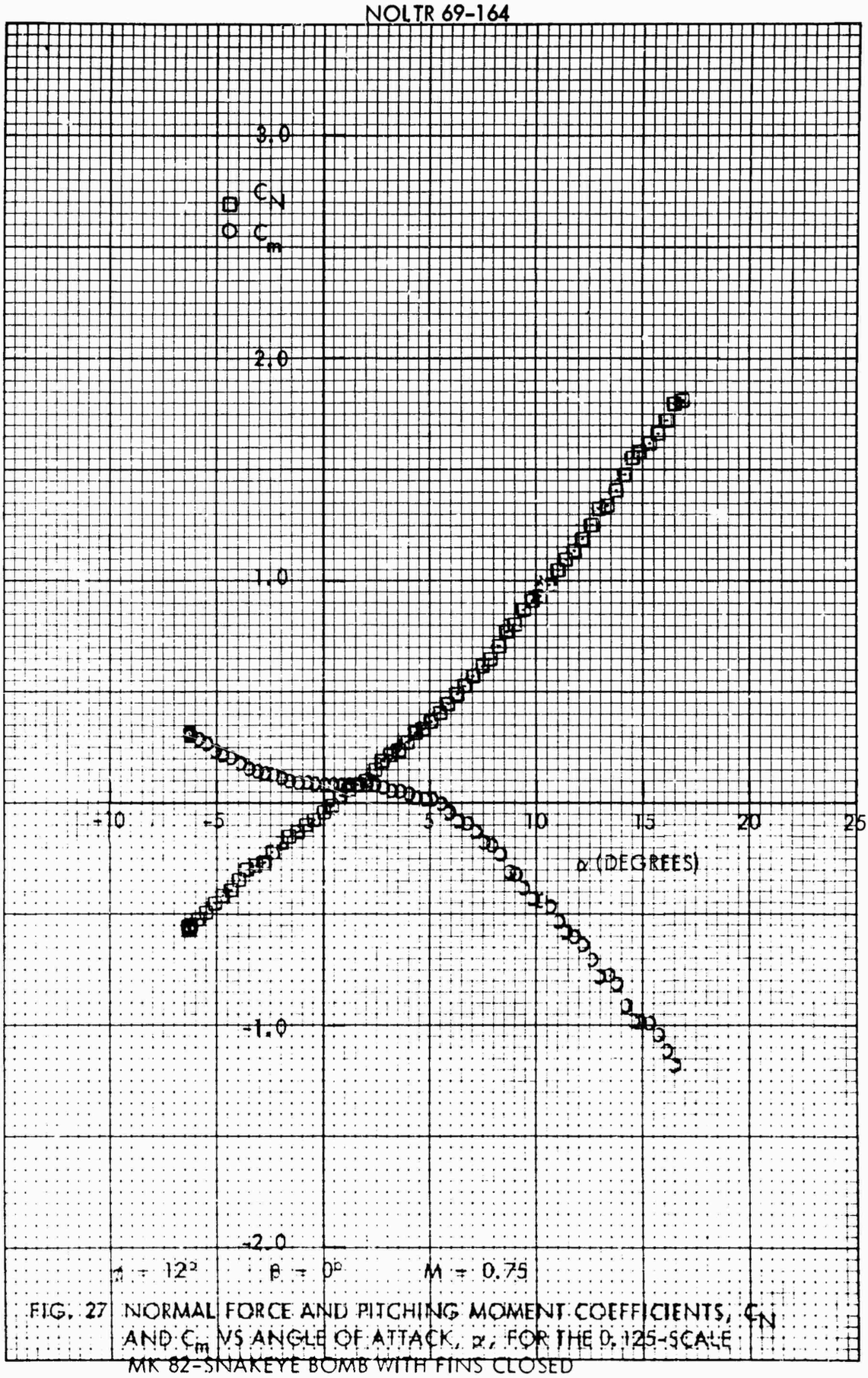

FIG. 27 NORMAL FORCE AND PITCHING MOMENT COEFFICIENTS, C_N AND C_m VS ANGLE OF ATTACK, α, FOR THE 0.125-SCALE MK 82-SNAKEYE BOMB WITH FINS CLOSED

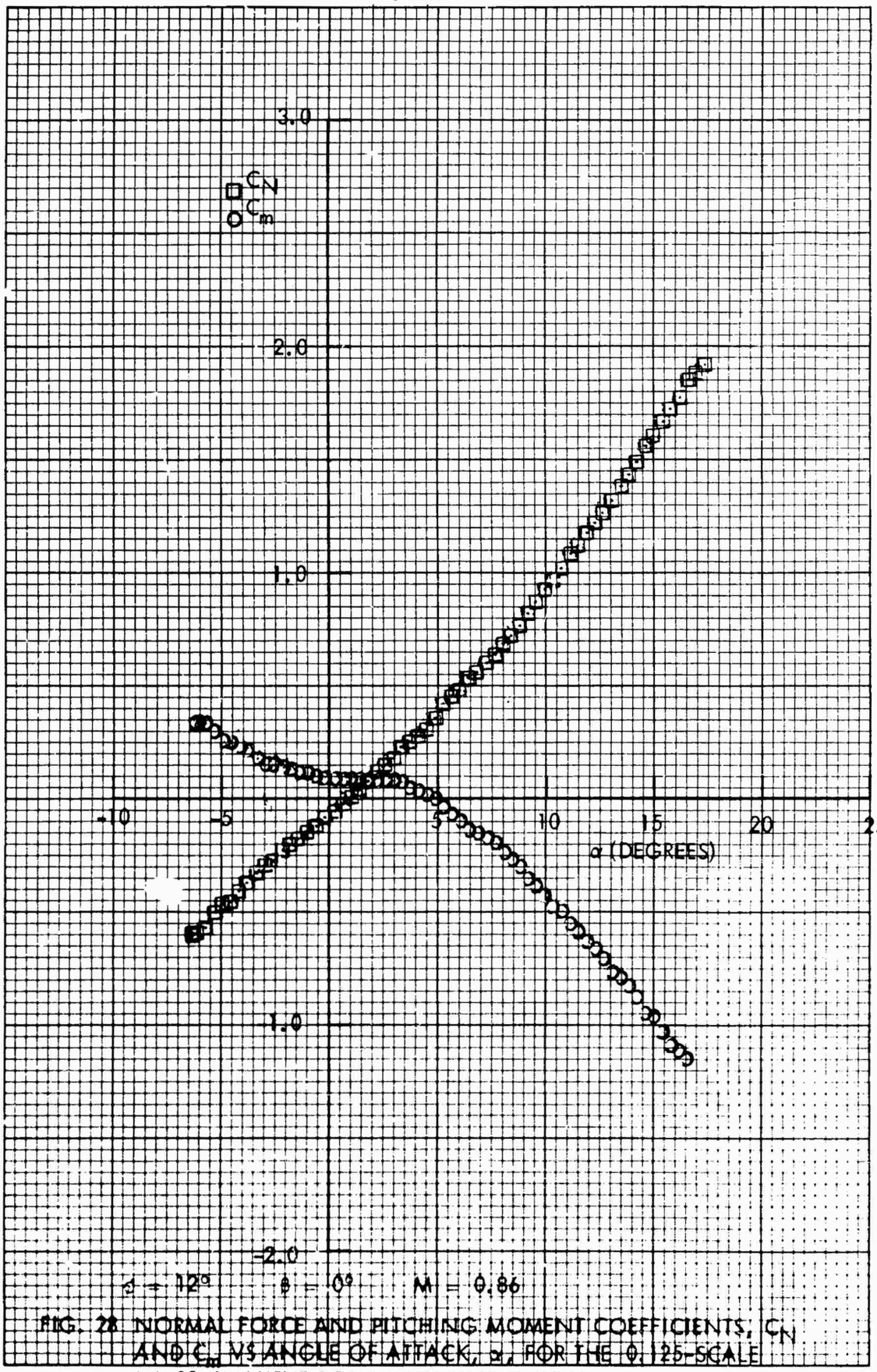

FIG. 28 NORMAL FORCE AND PITCHING MOMENT COEFFICIENTS, C_N AND C_m VS ANGLE OF ATTACK, α, FOR THE 0.125-SCALE MK 82-SNAKEYE BOMB WITH FINS CLOSED

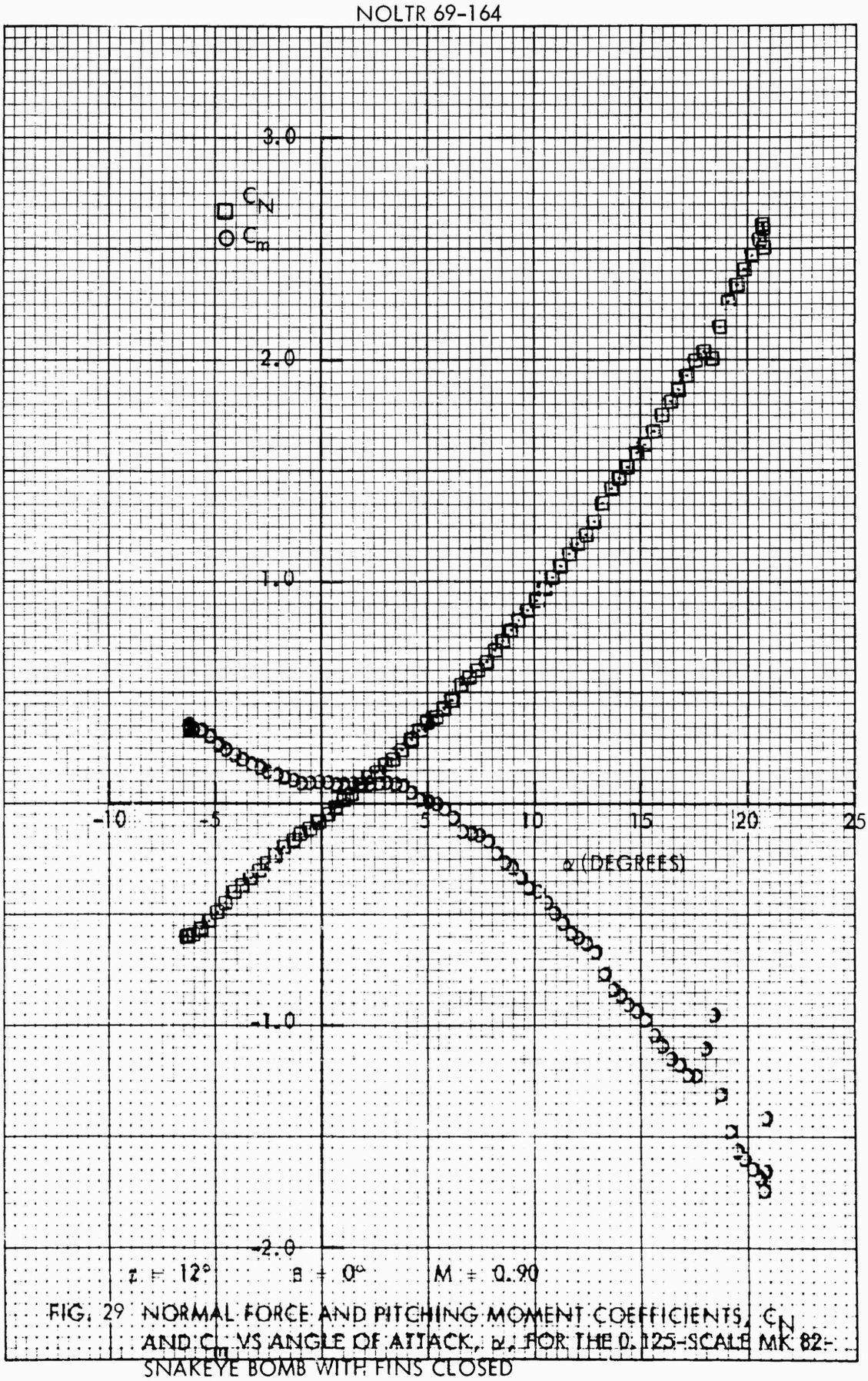

FIG. 29 NORMAL FORCE AND PITCHING MOMENT COEFFICIENTS, C_N AND C_m VS ANGLE OF ATTACK, α, FOR THE 0.125-SCALE MK 82-SNAKEYE BOMB WITH FINS CLOSED

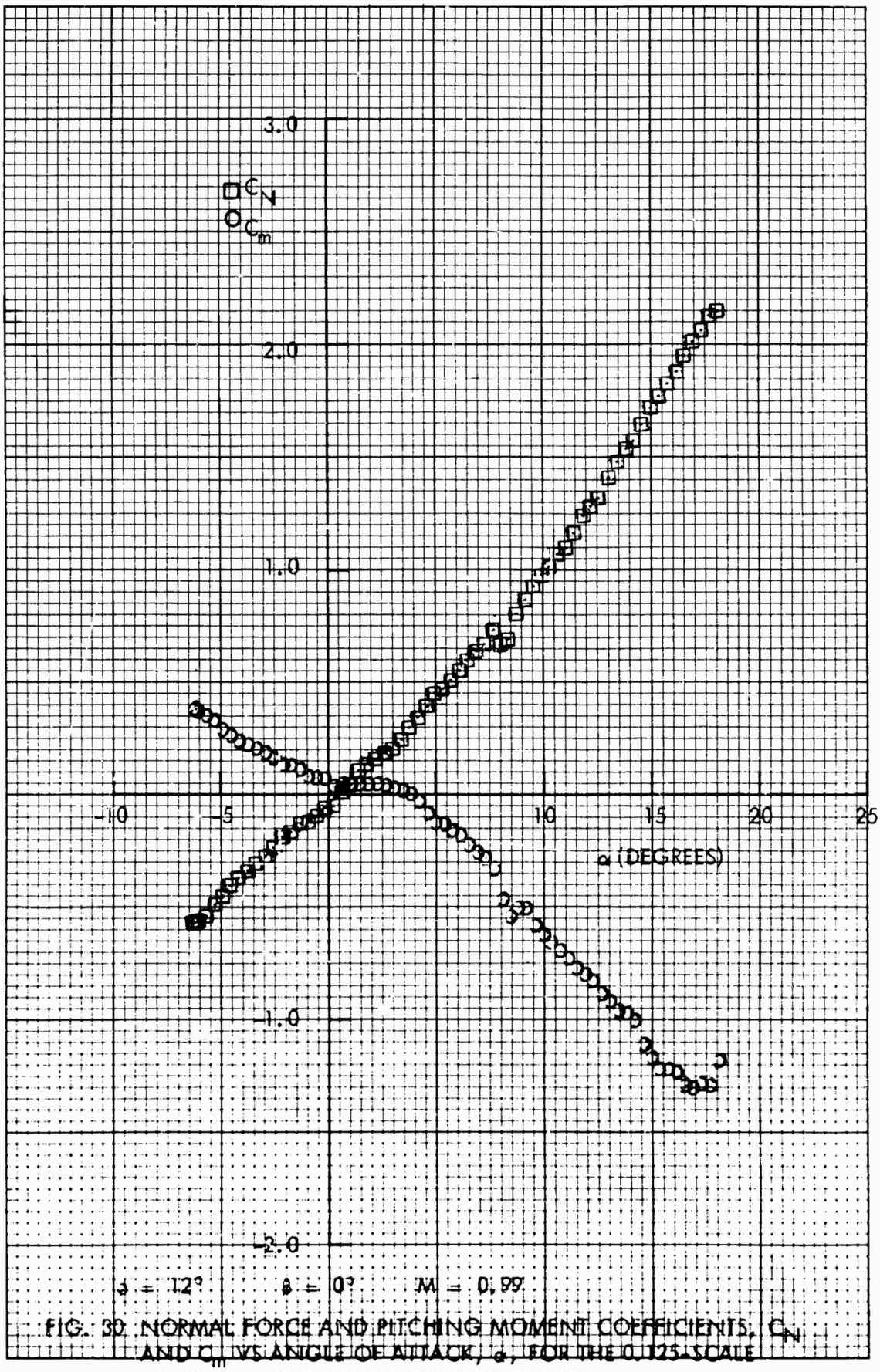

FIG. 30 NORMAL FORCE AND PITCHING MOMENT COEFFICIENTS, C_N AND C_m VS ANGLE OF ATTACK, α, FOR THE 0.125-SCALE MK 82-SNAKEYE BOMB WITH FINS CLOSED

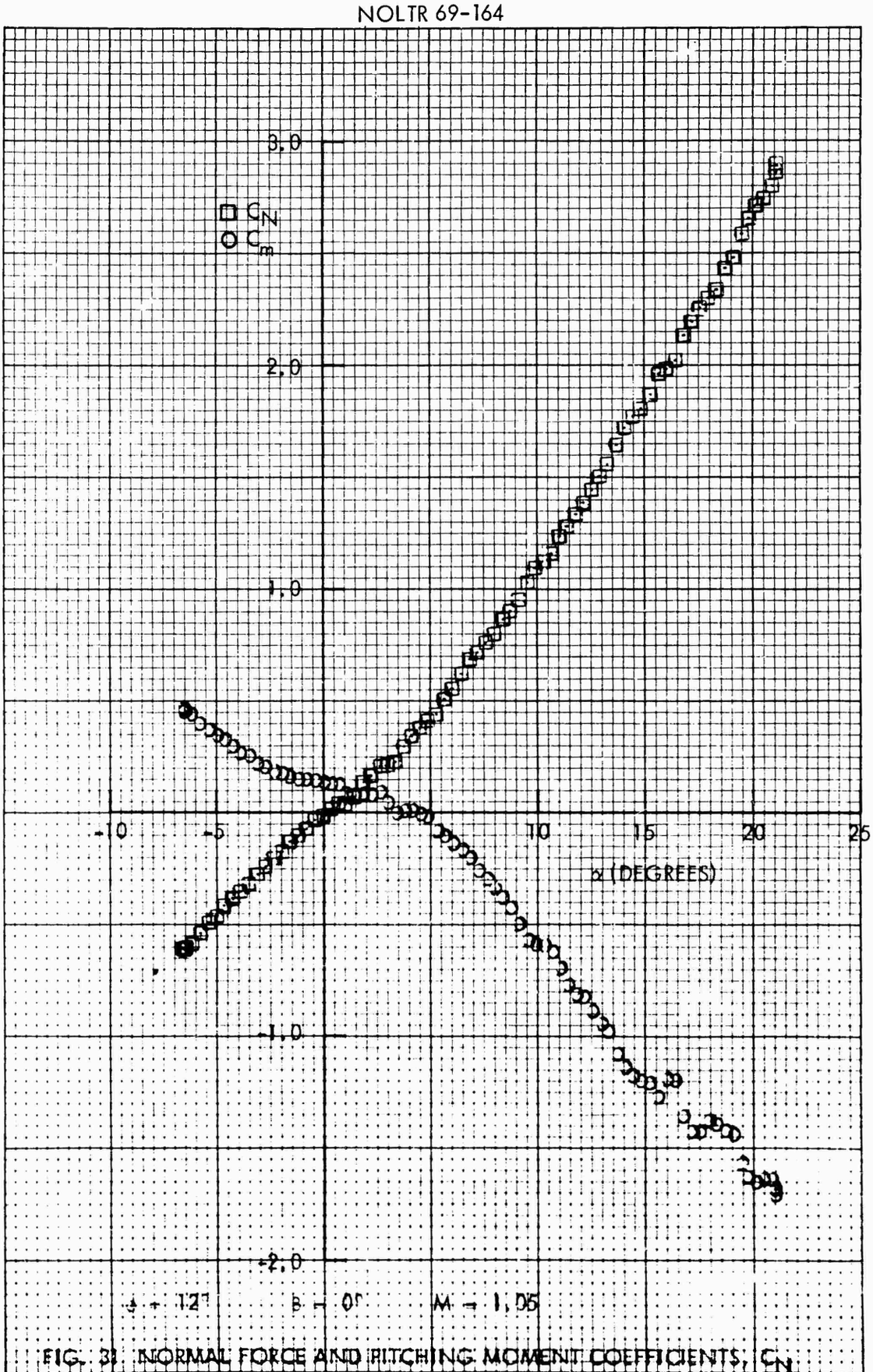

FIG. 31 NORMAL FORCE AND PITCHING MOMENT COEFFICIENTS, C_N AND C_m VS ANGLE OF ATTACK, α, FOR THE 0.125-SCALE MK 82-SNAKEYE BOMB WITH FINS CLOSED

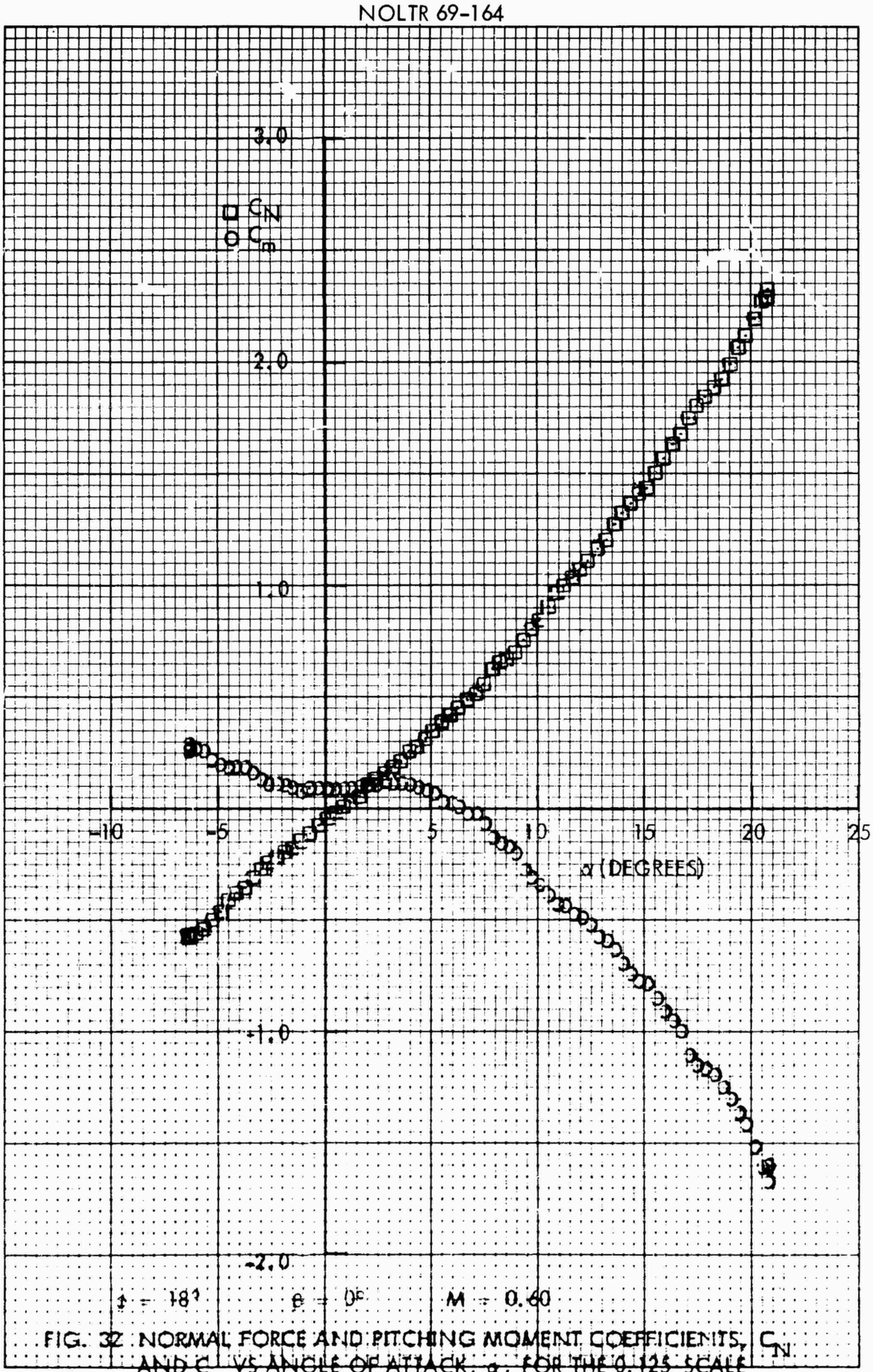

FIG. 32 NORMAL FORCE AND PITCHING MOMENT COEFFICIENTS, C_N AND C_m VS ANGLE OF ATTACK, α, FOR THE 0.125 SCALE MK 82-SNAKEYE BOMB WITH FINS CLOSED

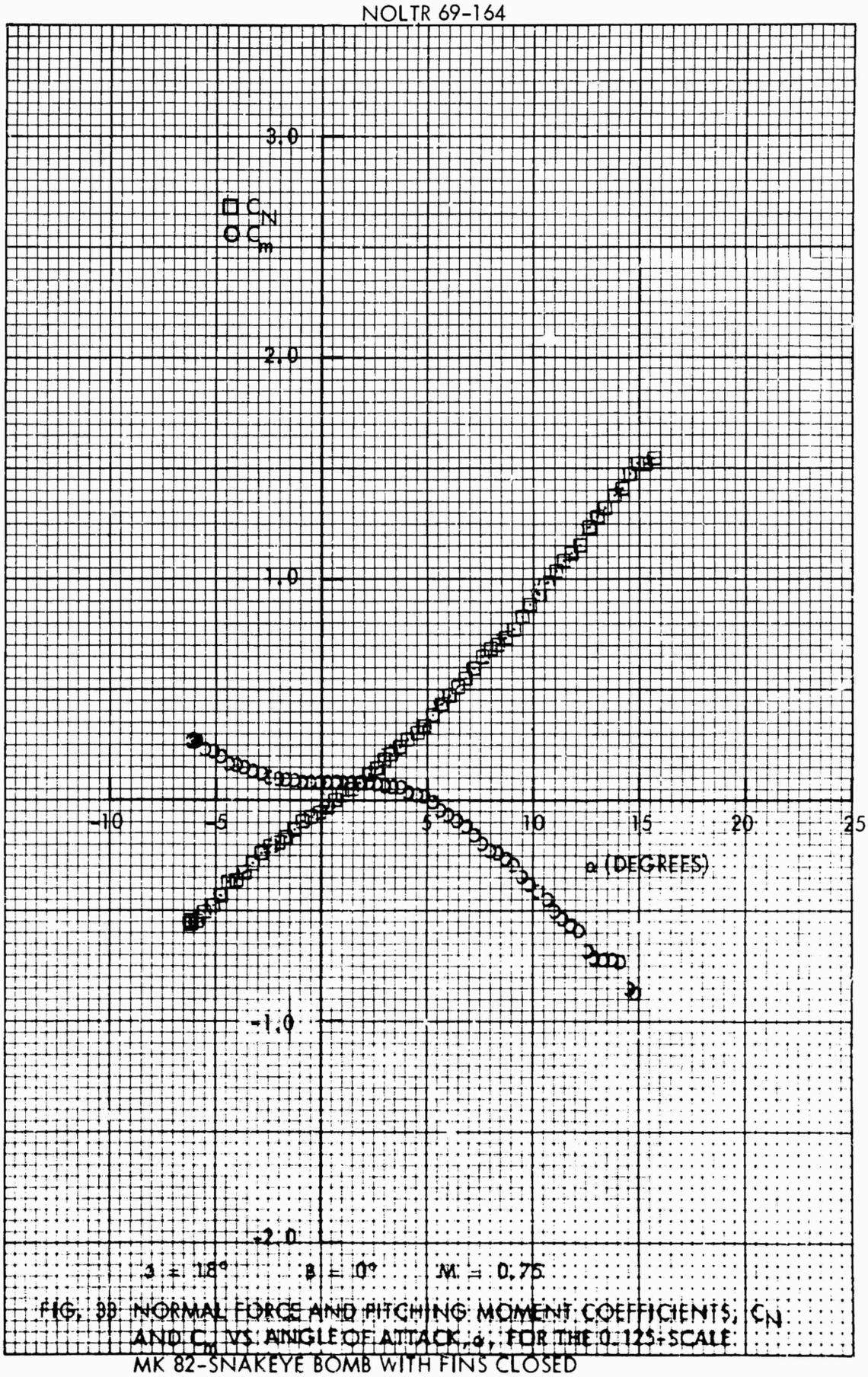

FIG. 38 NORMAL FORCE AND PITCHING MOMENT COEFFICIENTS, C_N AND C_m VS. ANGLE OF ATTACK, α, FOR THE 0.125-SCALE MK 82-SNAKEYE BOMB WITH FINS CLOSED

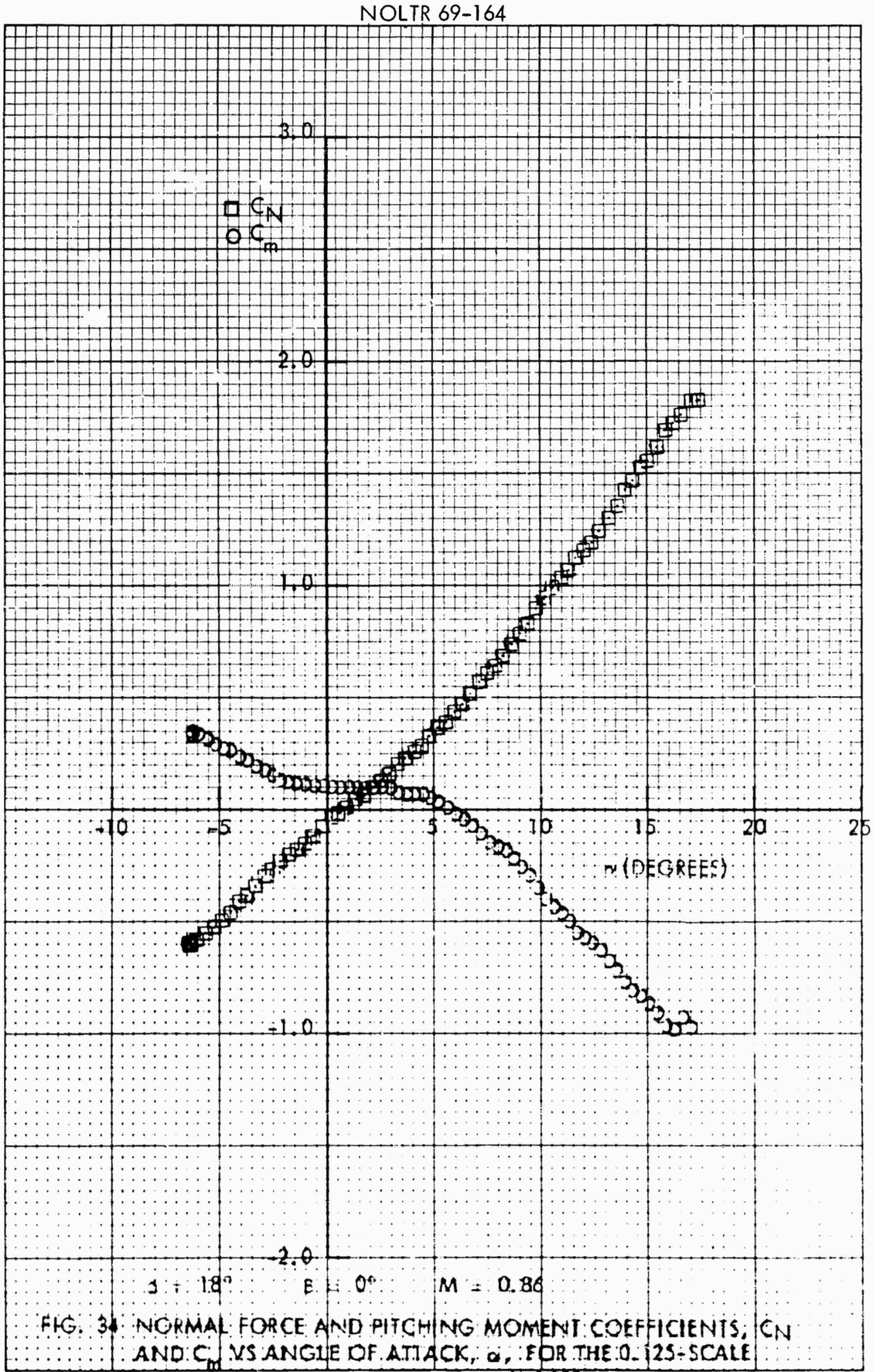

FIG. 34 NORMAL FORCE AND PITCHING MOMENT COEFFICIENTS, C_N AND C_m VS ANGLE OF ATTACK, α, FOR THE 0.125-SCALE MK 82-SNAKEYE BOMB WITH FINS CLOSED

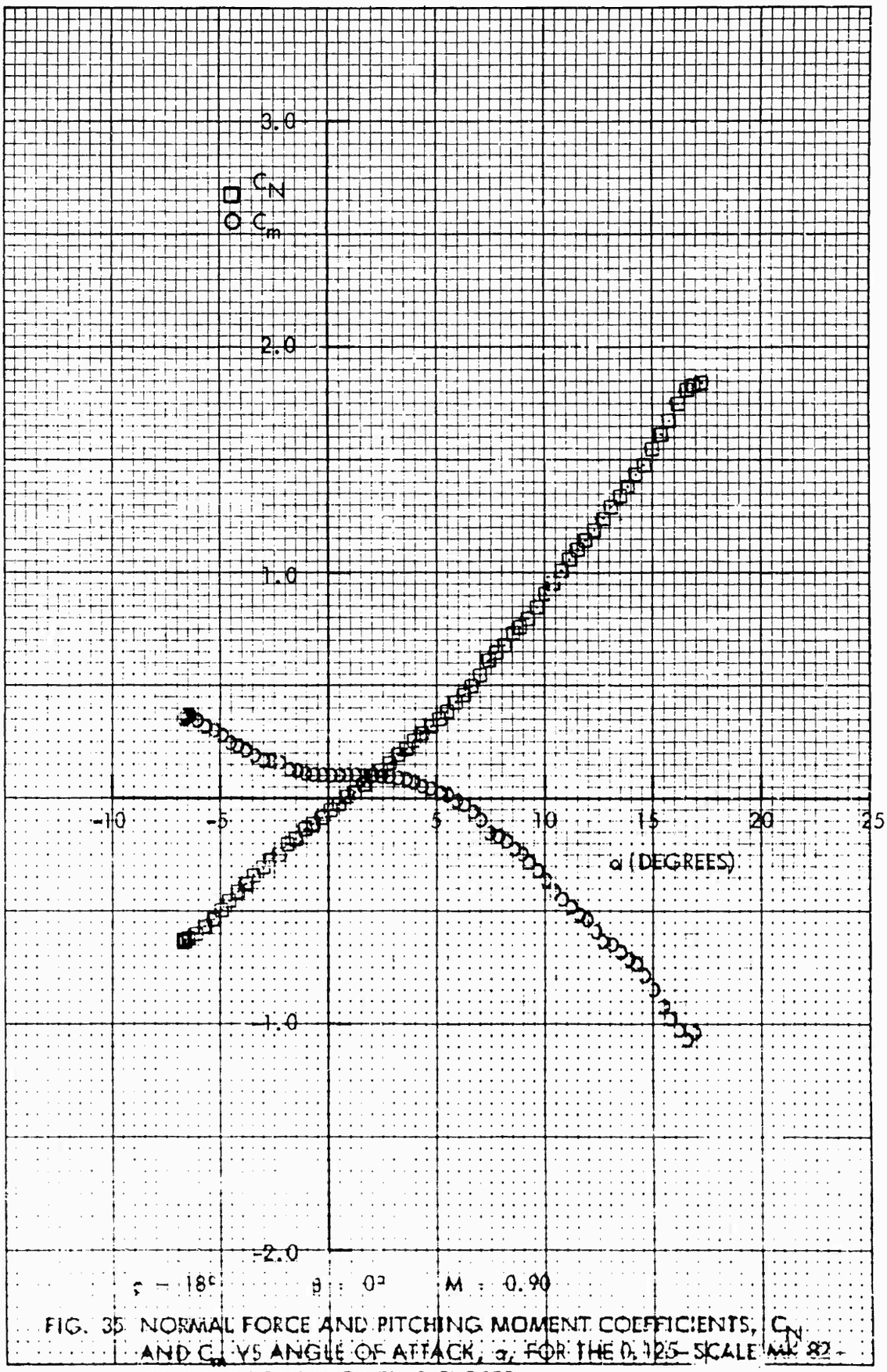

FIG. 35 NORMAL FORCE AND PITCHING MOMENT COEFFICIENTS, C_N AND C_m VS ANGLE OF ATTACK, α, FOR THE 0.125-SCALE MK 82 SNAKEYE BOMB WITH FINS CLOSED

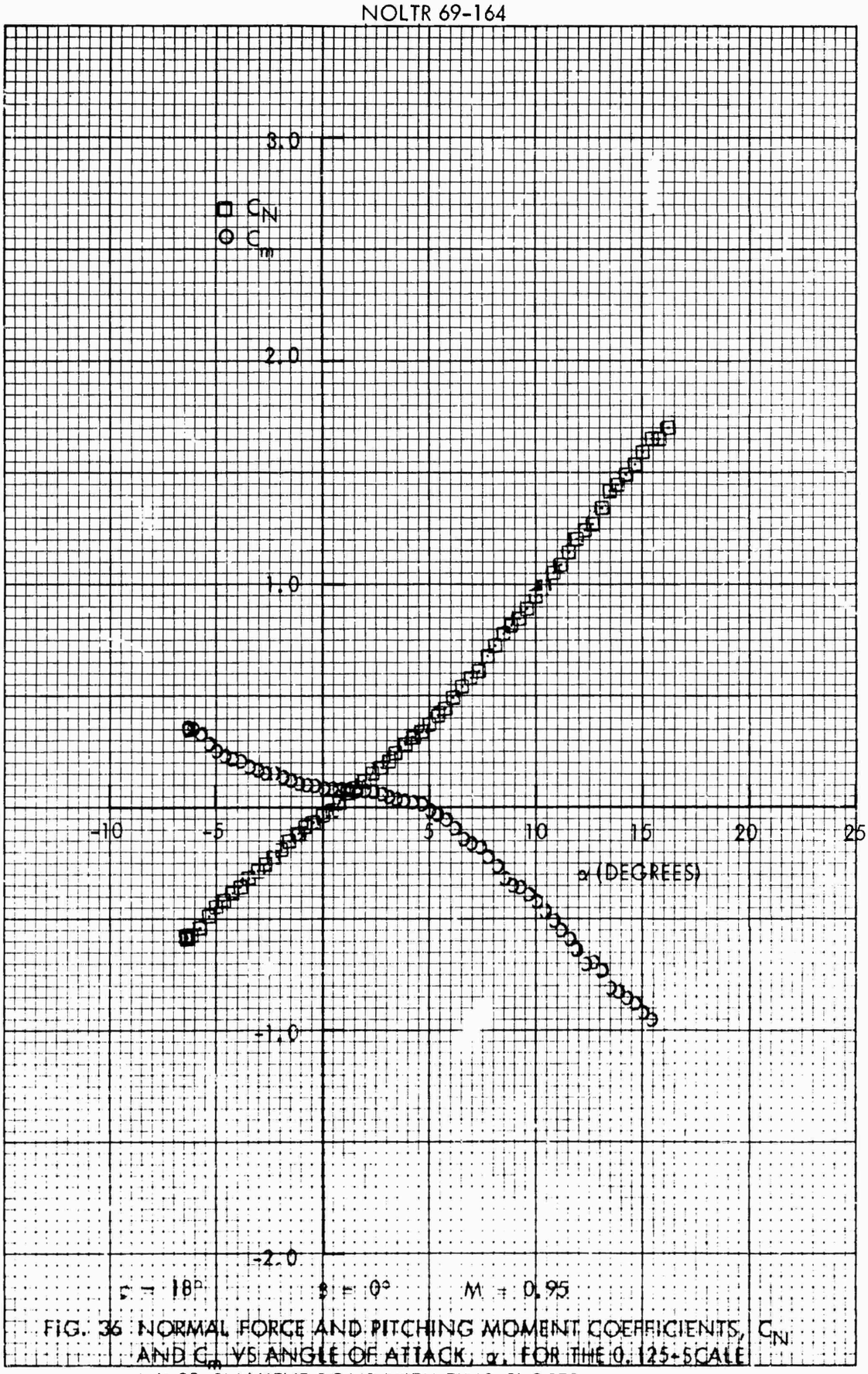

FIG. 36 NORMAL FORCE AND PITCHING MOMENT COEFFICIENTS, C_N AND C_m VS ANGLE OF ATTACK, α, FOR THE 0.125-SCALE MK 82-SNAKEYE BOMB WITH FINS CLOSED

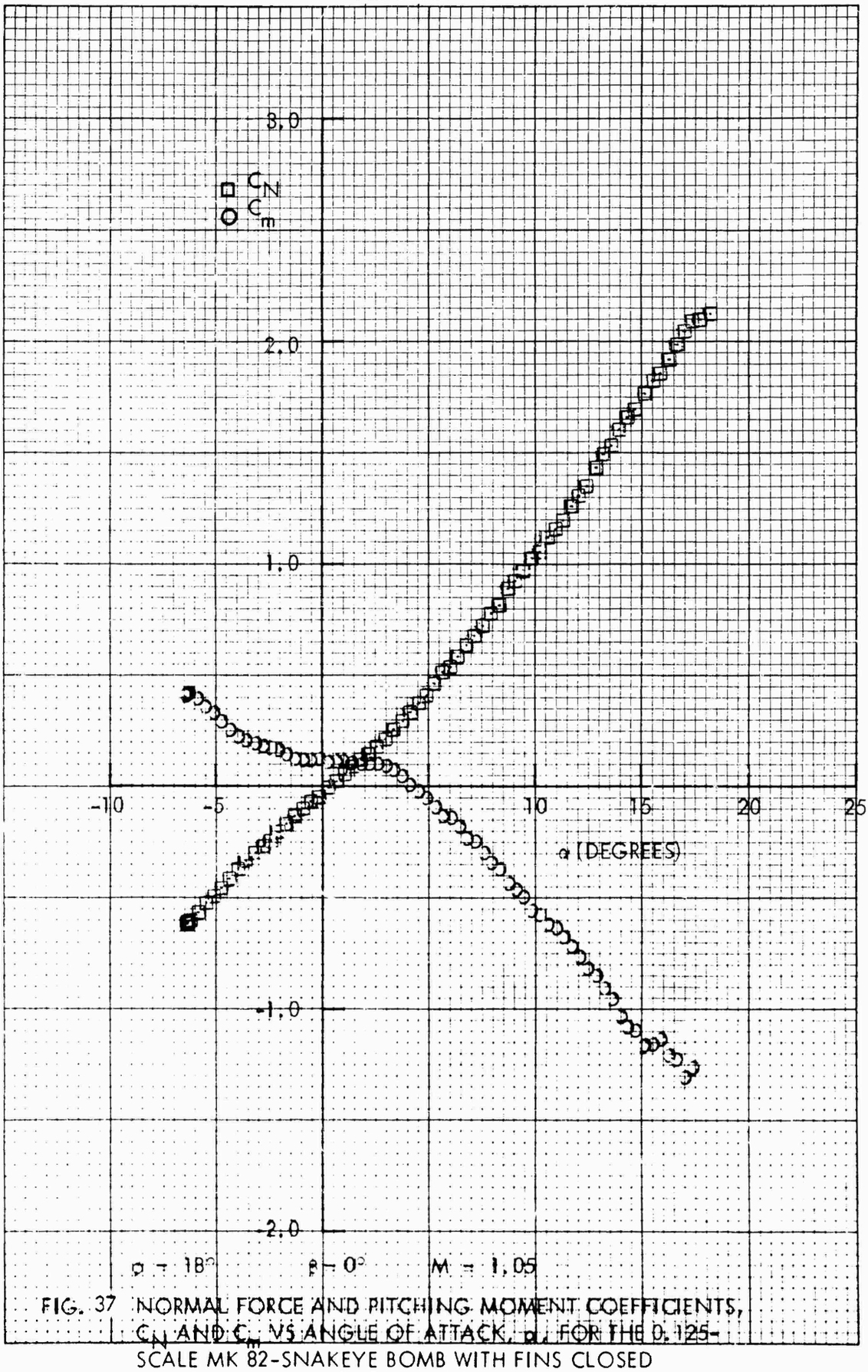

FIG. 37 NORMAL FORCE AND PITCHING MOMENT COEFFICIENTS, C_N AND C_m VS ANGLE OF ATTACK, α, FOR THE 0.125-SCALE MK 82-SNAKEYE BOMB WITH FINS CLOSED

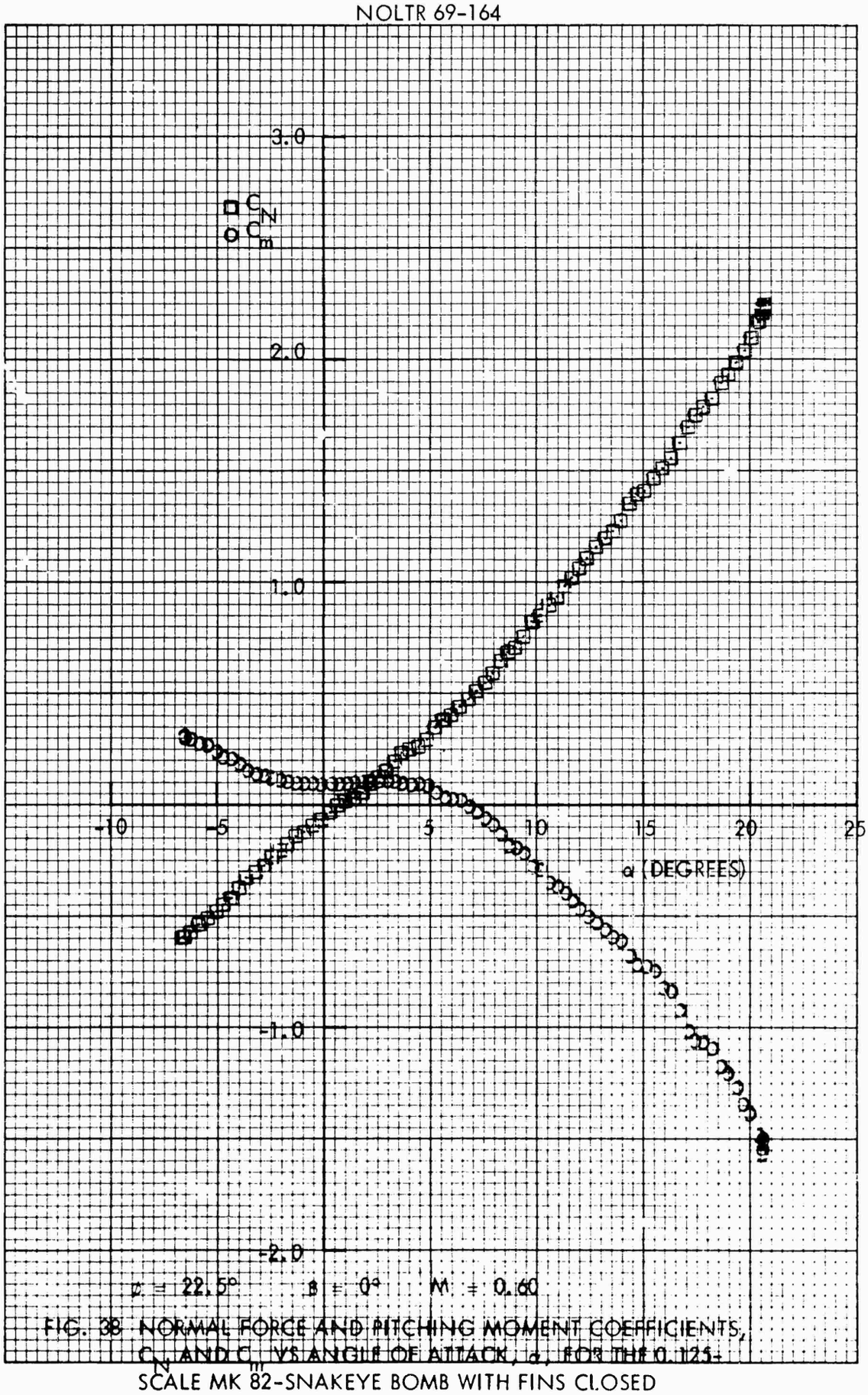

FIG. 38 NORMAL FORCE AND PITCHING MOMENT COEFFICIENTS, C_N AND C_m VS ANGLE OF ATTACK, α, FOR THE 0.125-SCALE MK 82-SNAKEYE BOMB WITH FINS CLOSED

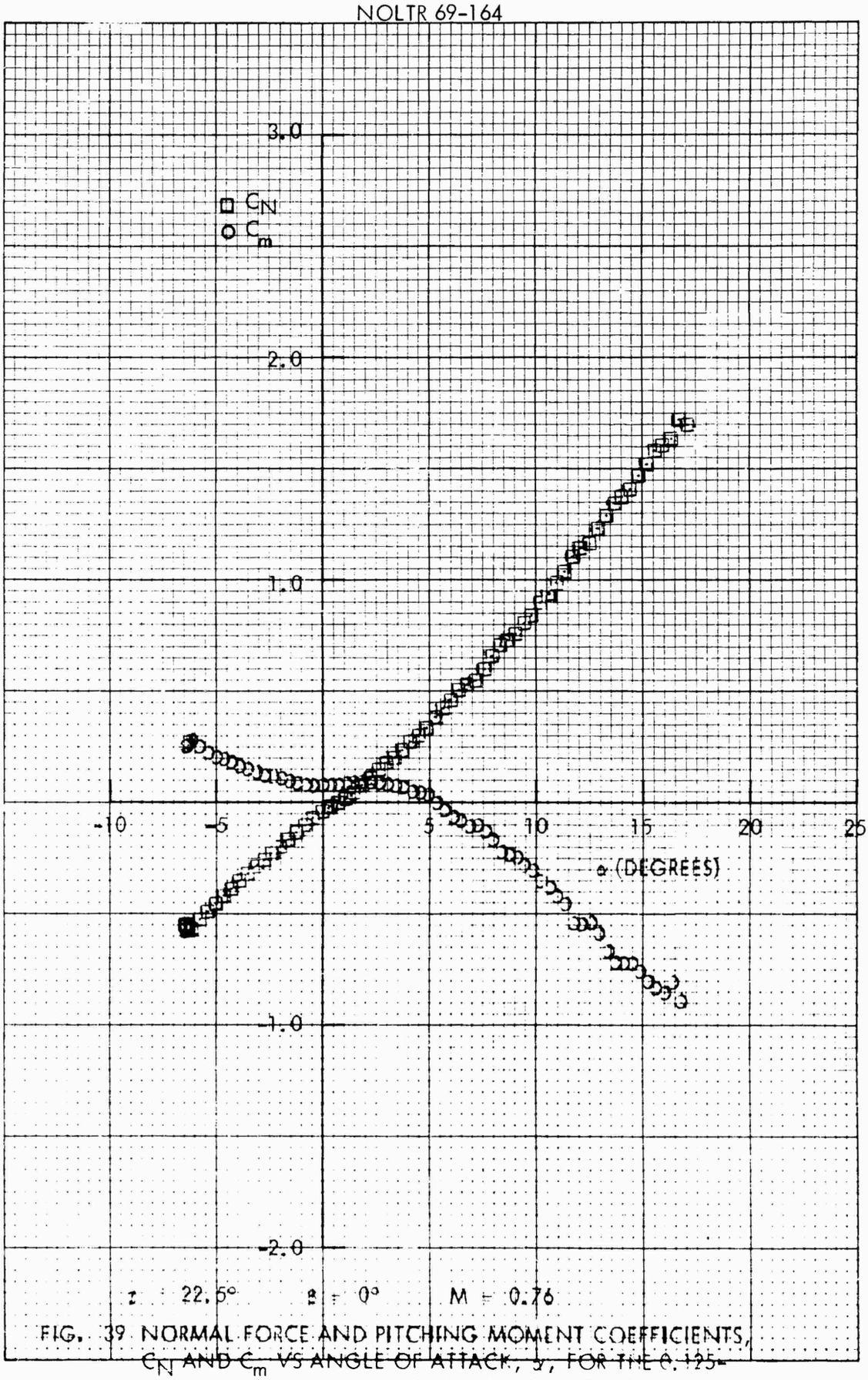

FIG. 39 NORMAL FORCE AND PITCHING MOMENT COEFFICIENTS, C_N AND C_m VS ANGLE OF ATTACK, α, FOR THE 0.125-SCALE MK 82-SNAKEYE BOMB WITH FINS CLOSED

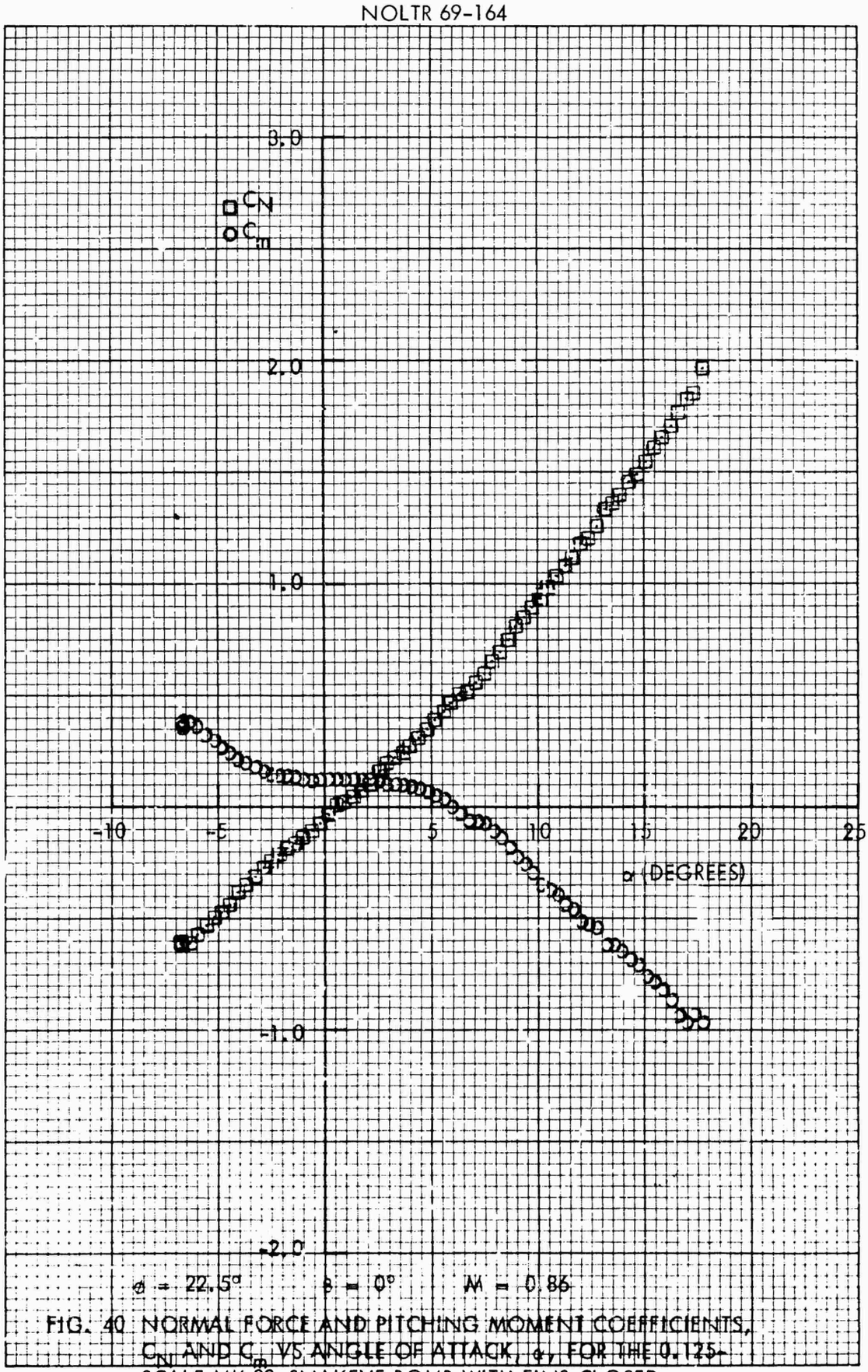

FIG. 40 NORMAL FORCE AND PITCHING MOMENT COEFFICIENTS, C_N AND C_m VS ANGLE OF ATTACK, α, FOR THE 0.125-SCALE MK 82-SNAKEYE BOMB WITH FINS CLOSED

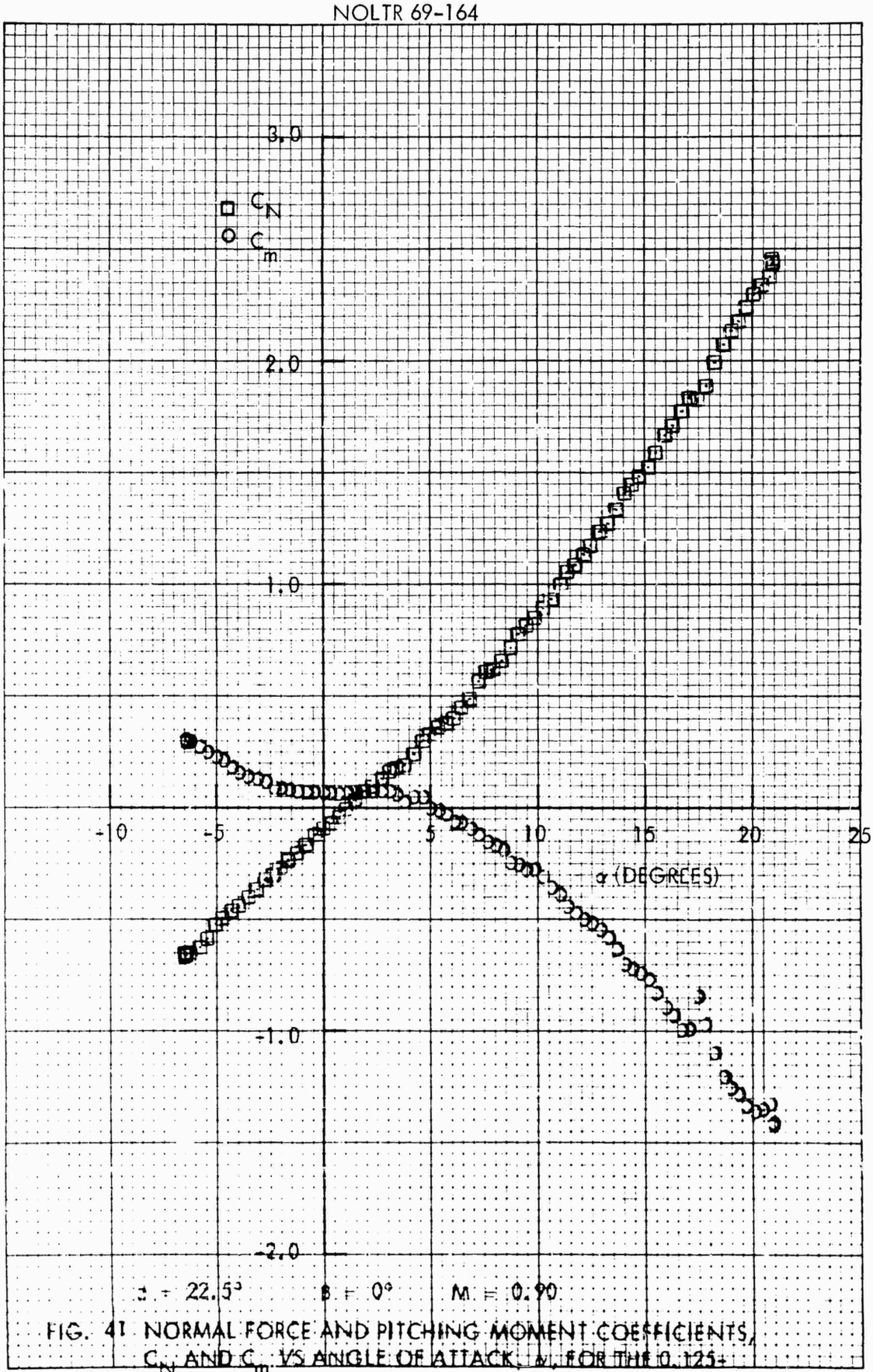

FIG. 41 NORMAL FORCE AND PITCHING MOMENT COEFFICIENTS, C_N AND C_m VS ANGLE OF ATTACK, α, FOR THE 0.125-SCALE MK 82-SNAKEYE BOMB WITH FINS CLOSED

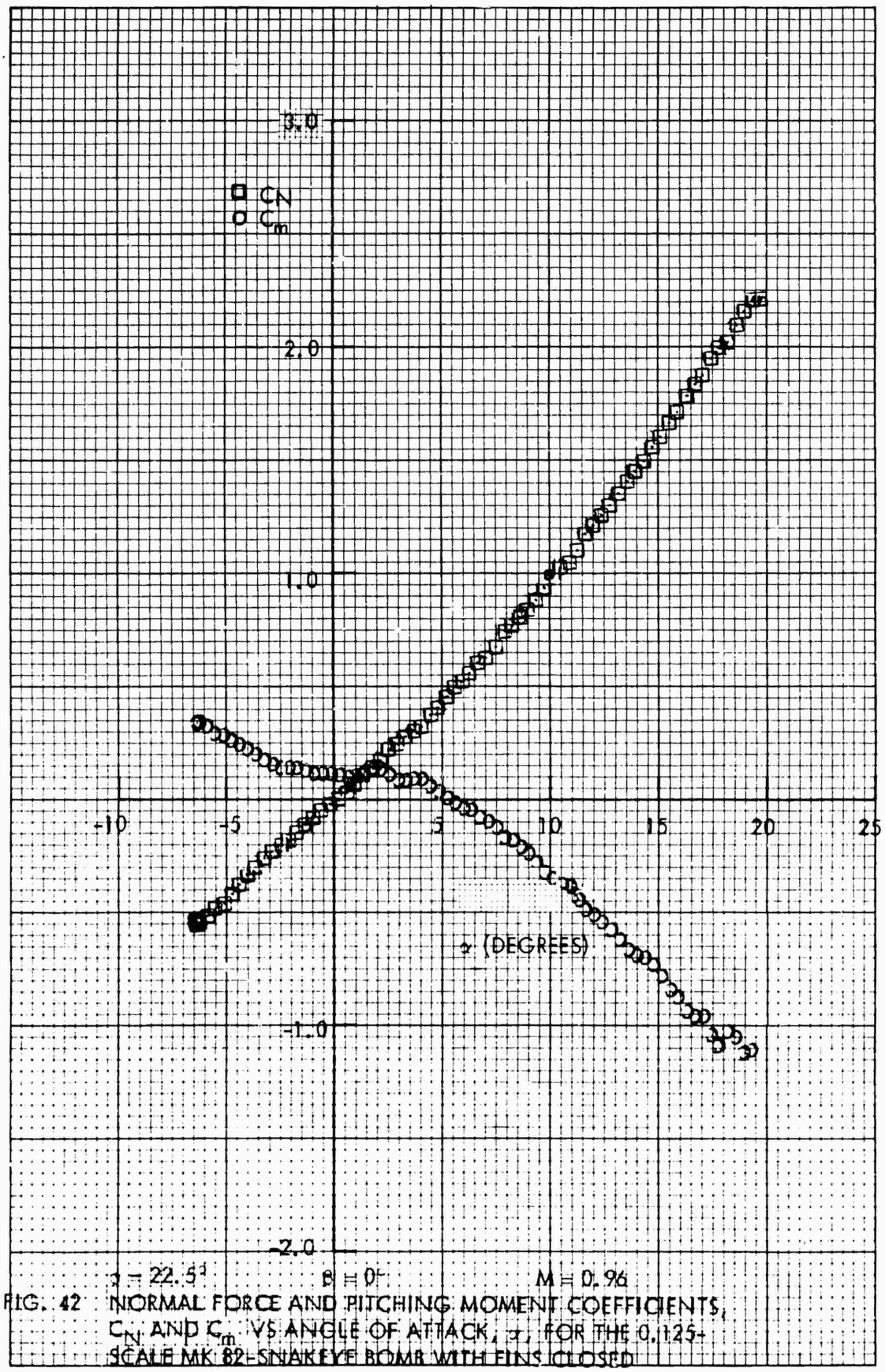

FIG. 42 NORMAL FORCE AND PITCHING MOMENT COEFFICIENTS, C_N AND C_m VS ANGLE OF ATTACK, α, FOR THE 0.125-SCALE MK 82-SNAKEYE BOMB WITH FINS CLOSED

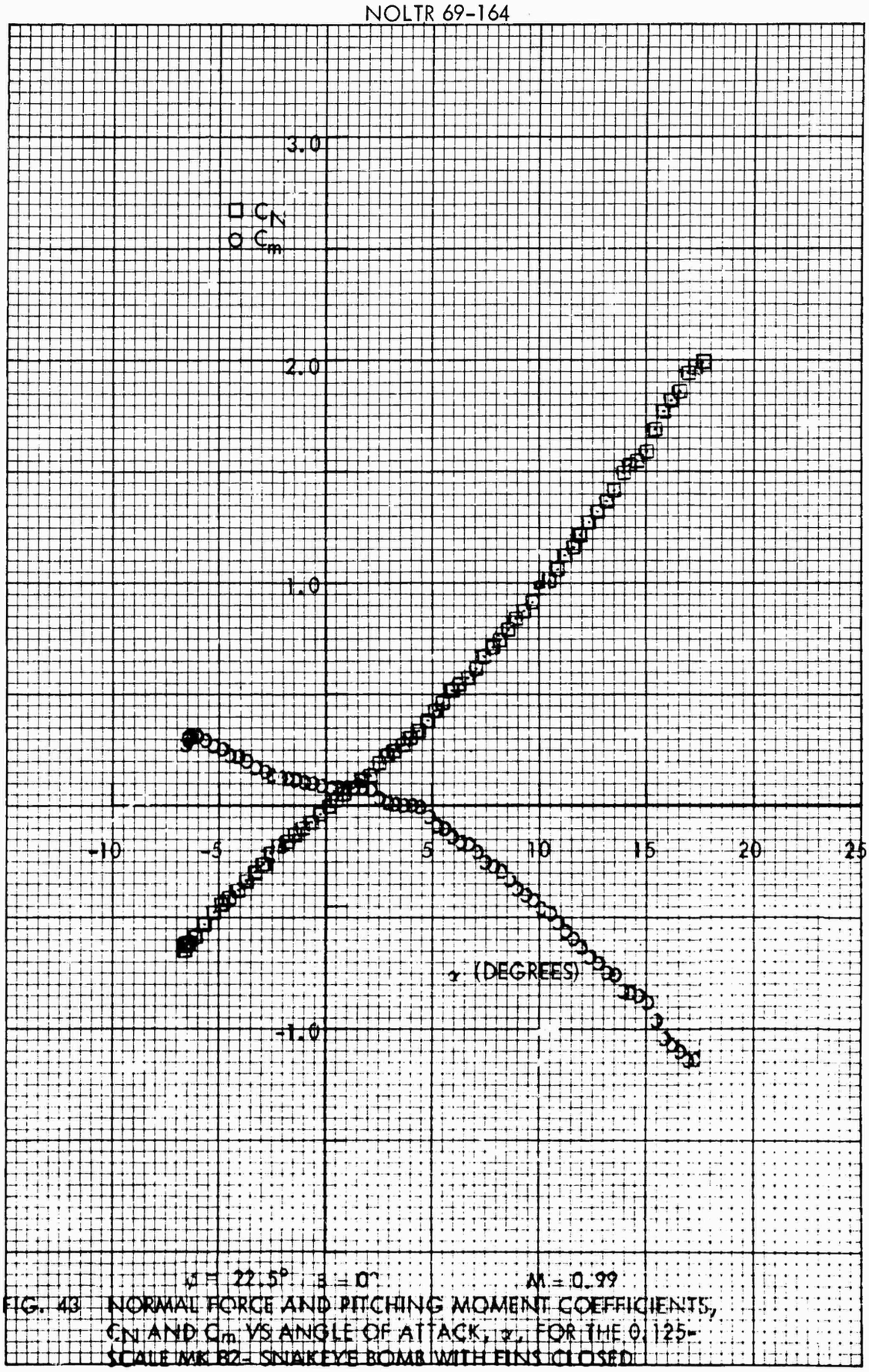

ϕ = 22.5° , β = 0° M = 0.99

FIG. 43 NORMAL FORCE AND PITCHING MOMENT COEFFICIENTS, C_N AND C_m VS ANGLE OF ATTACK, α, FOR THE 0.125-SCALE MK 82 SNAKEYE BOMB WITH FINS CLOSED

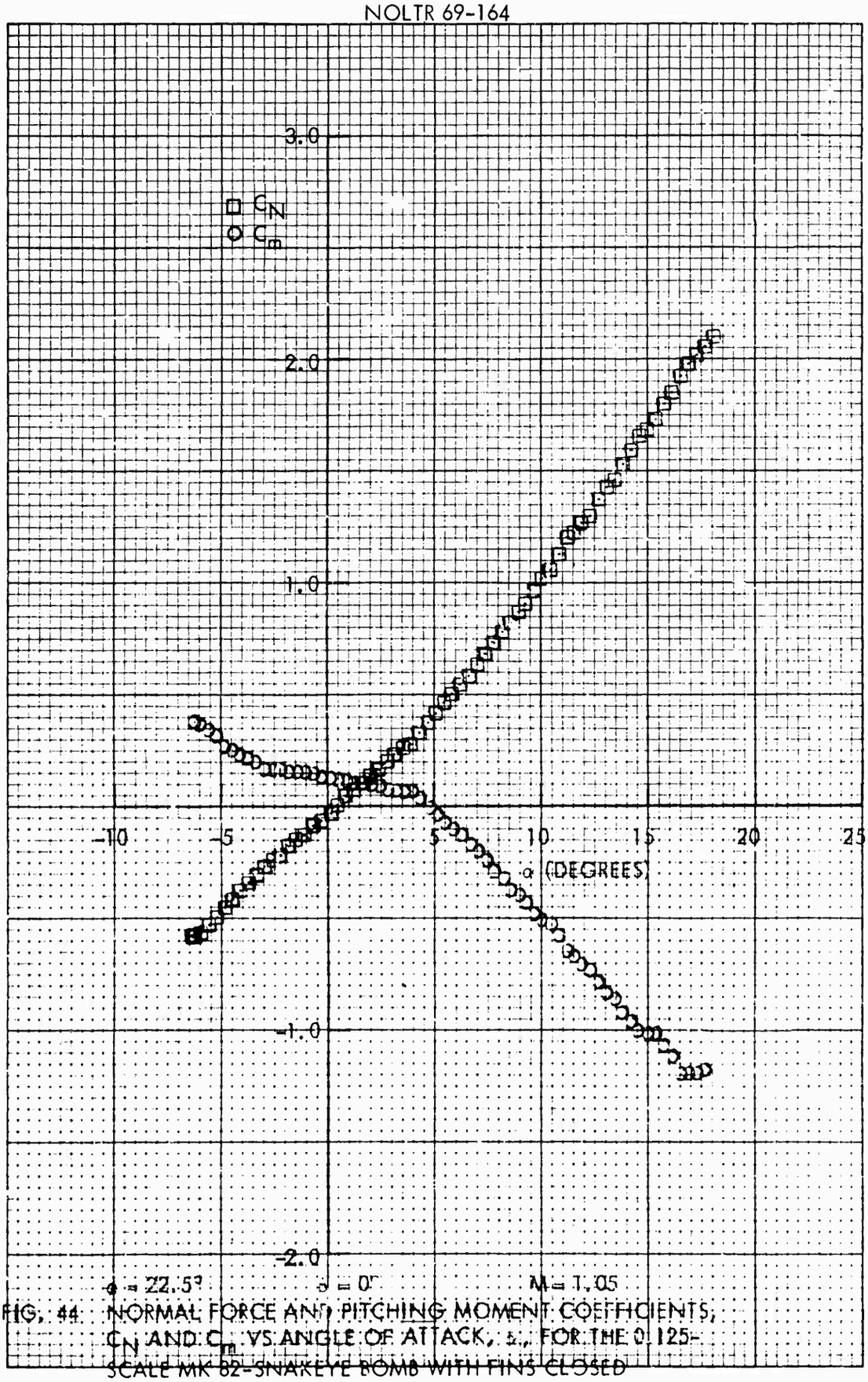

FIG. 44 NORMAL FORCE AND PITCHING MOMENT COEFFICIENTS, C_N AND C_m VS ANGLE OF ATTACK, α, FOR THE 0.125-SCALE MK 82-SNAKEYE BOMB WITH FINS CLOSED

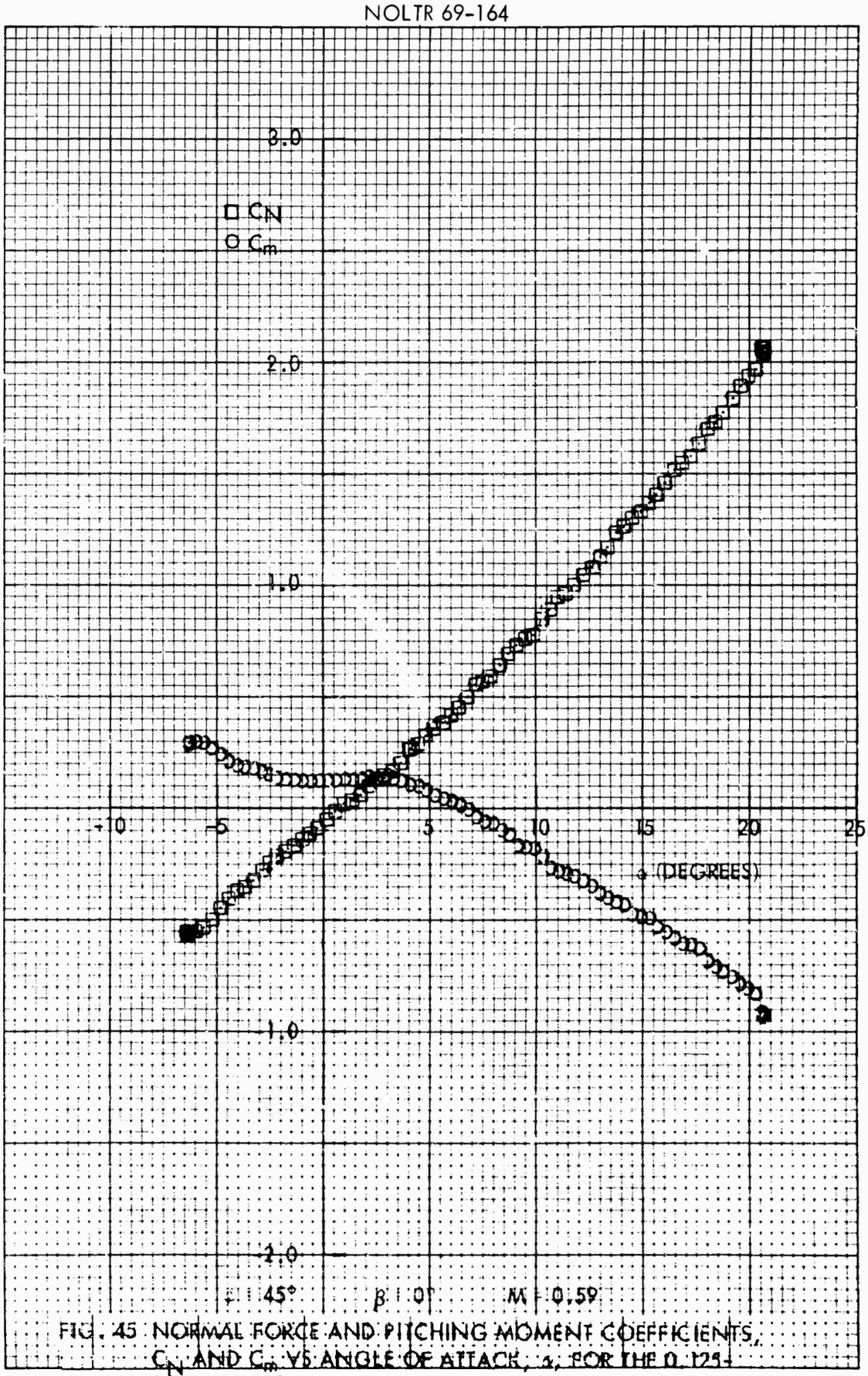

FIG. 45 NORMAL FORCE AND PITCHING MOMENT COEFFICIENTS, C_N AND C_m VS ANGLE OF ATTACK, α, FOR THE 0.125-SCALE MK 82-SNAKEYE BOMB WITH FINS CLOSED

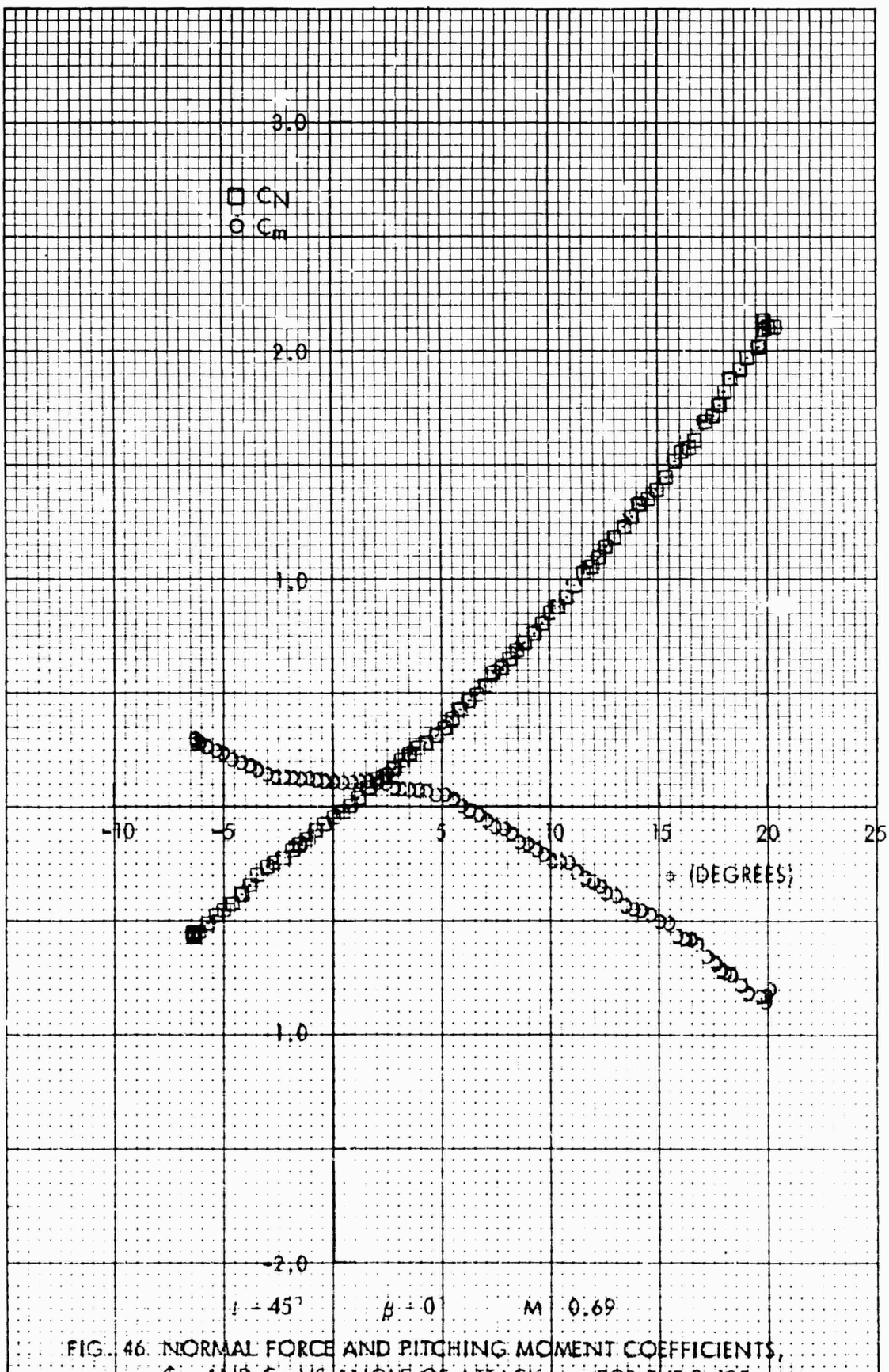

FIG. 46 NORMAL FORCE AND PITCHING MOMENT COEFFICIENTS, C_N AND C_m VS ANGLE OF ATTACK, α, FOR THE 0.125-SCALE MK 82-SNAKEYE BOMB WITH FINS CLOSED

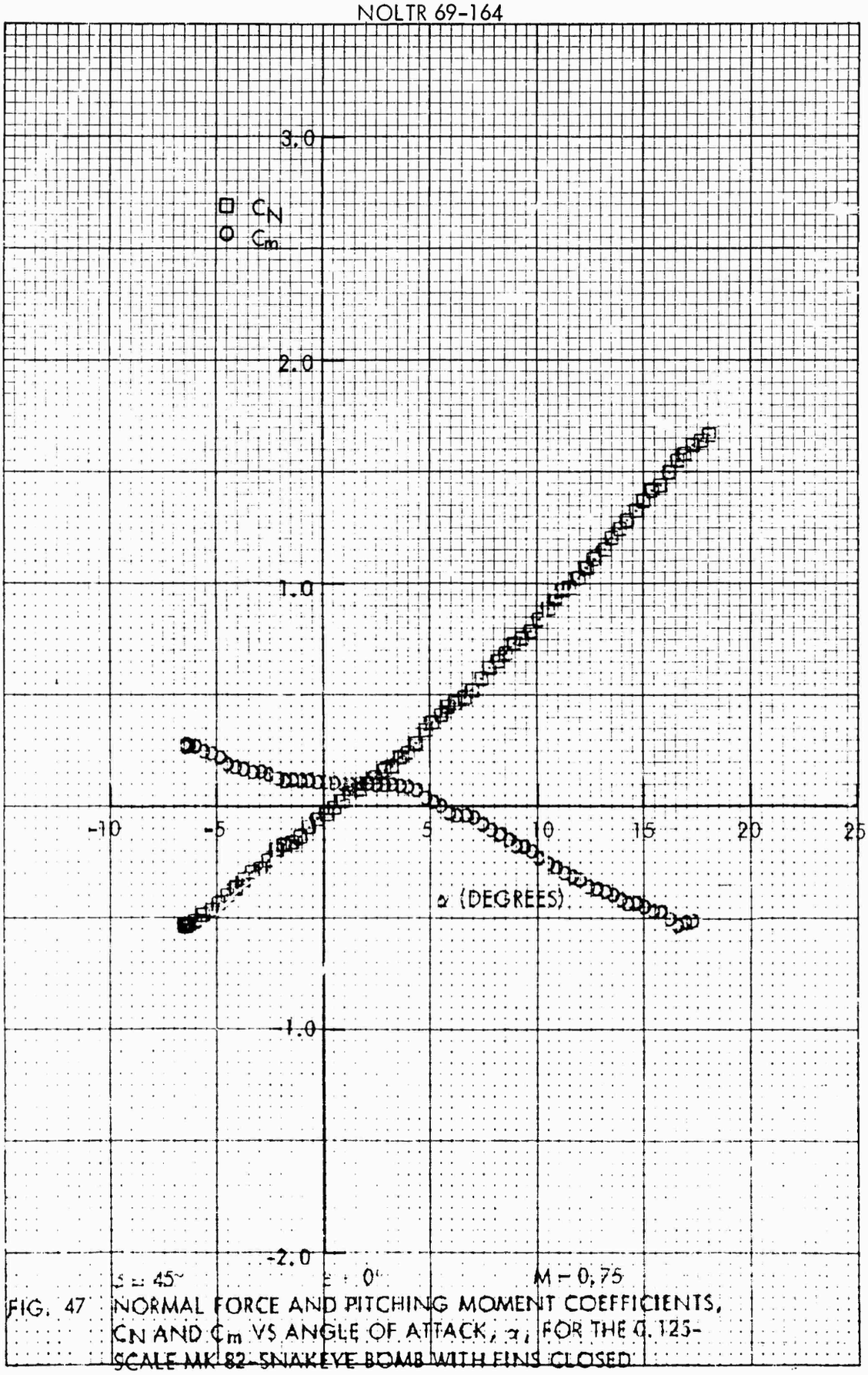

FIG. 47 NORMAL FORCE AND PITCHING MOMENT COEFFICIENTS, C_N AND C_m VS ANGLE OF ATTACK, α, FOR THE 0.125-SCALE MK 82-SNAKEYE BOMB WITH FINS CLOSED

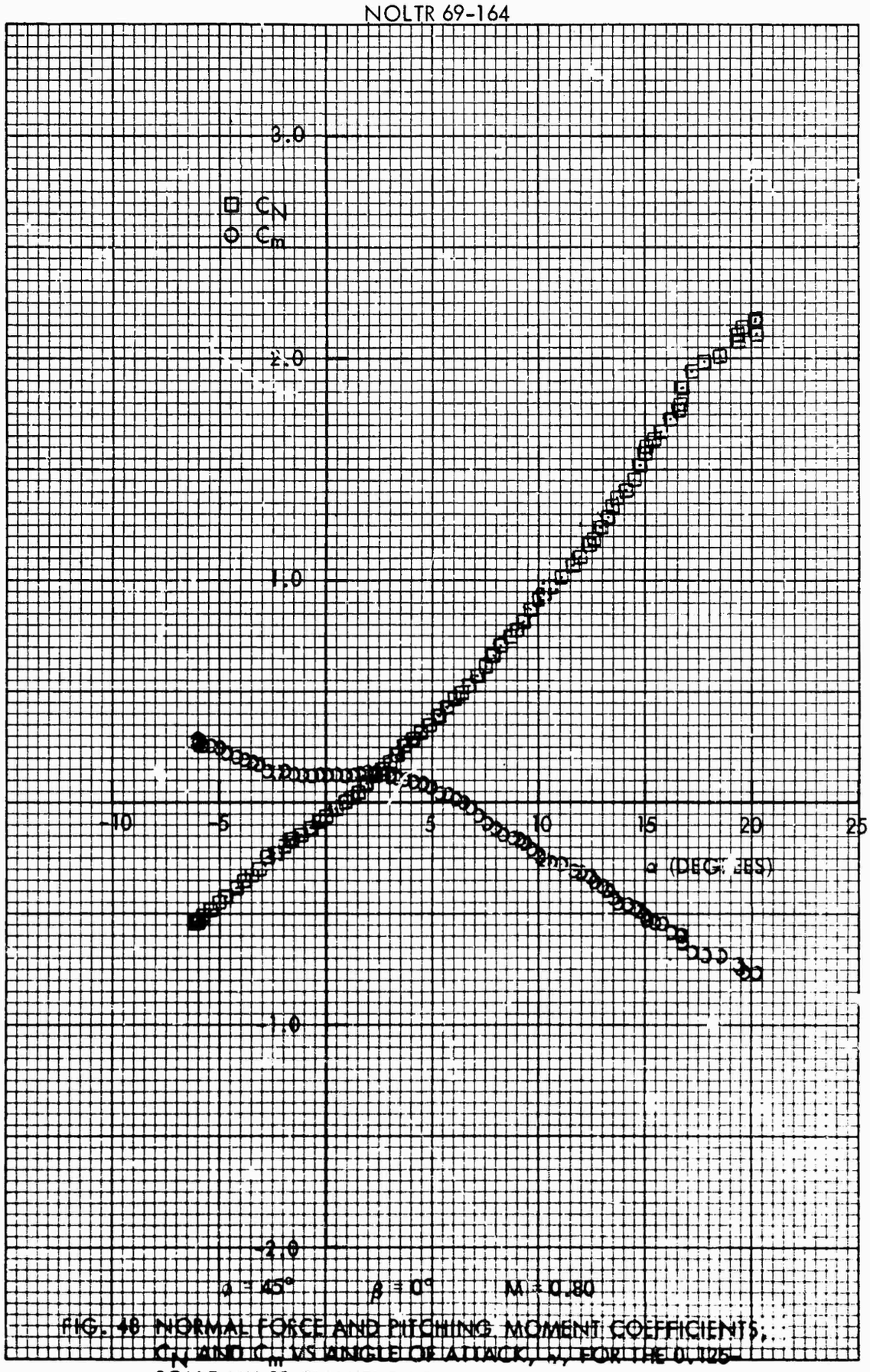

FIG. 48 NORMAL FORCE AND PITCHING MOMENT COEFFICIENTS, C_N AND C_m VS ANGLE OF ATTACK, α, FOR THE 0.125-SCALE MK 82-SNAKEYE BOMB WITH FINS CLOSED

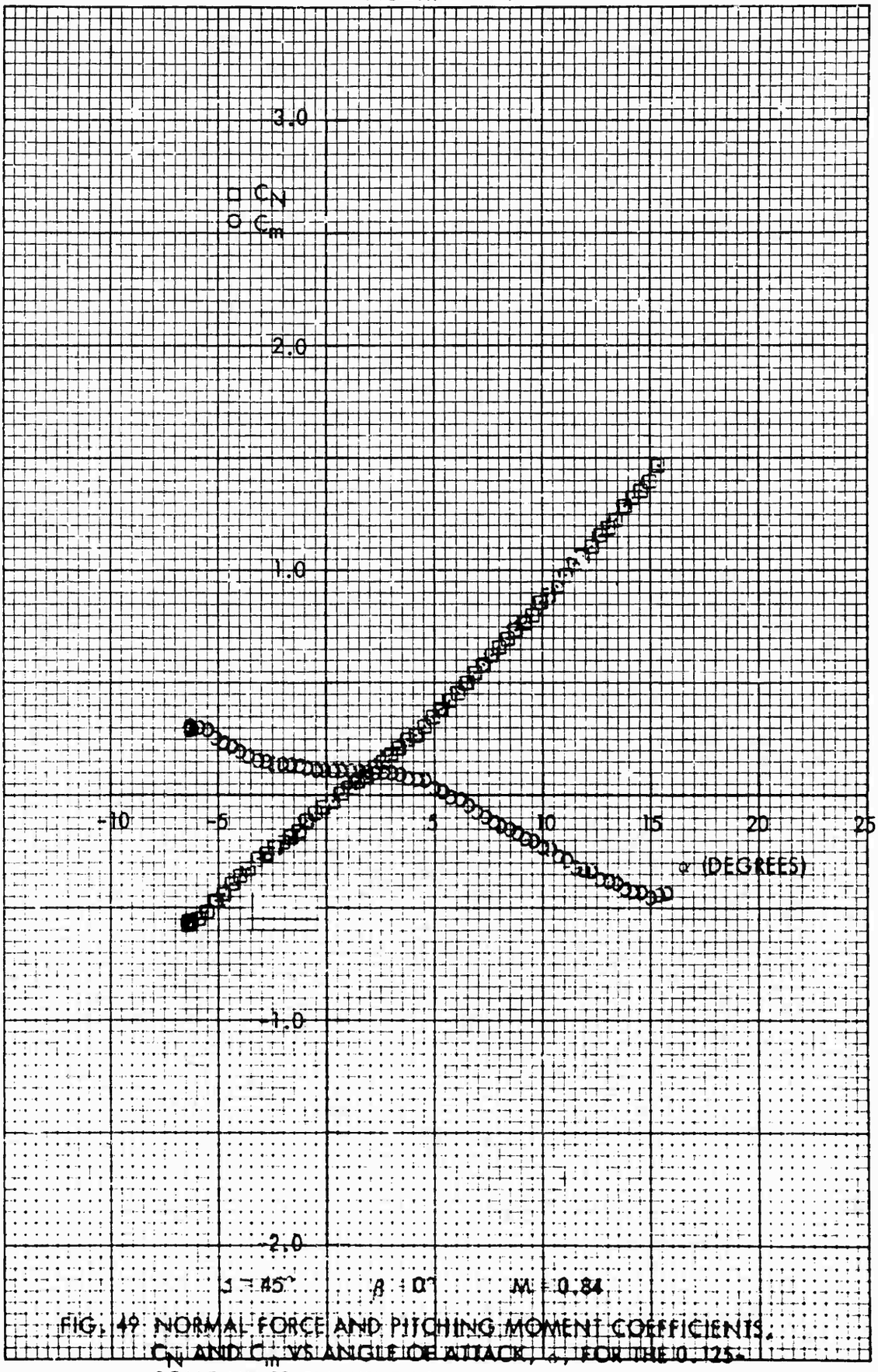

FIG. 49 NORMAL FORCE AND PITCHING MOMENT COEFFICIENTS, C_N AND C_m VS ANGLE OF ATTACK, α, FOR THE 0.125-SCALE MK 82-SNAKEYE BOMB WITH FINS CLOSED

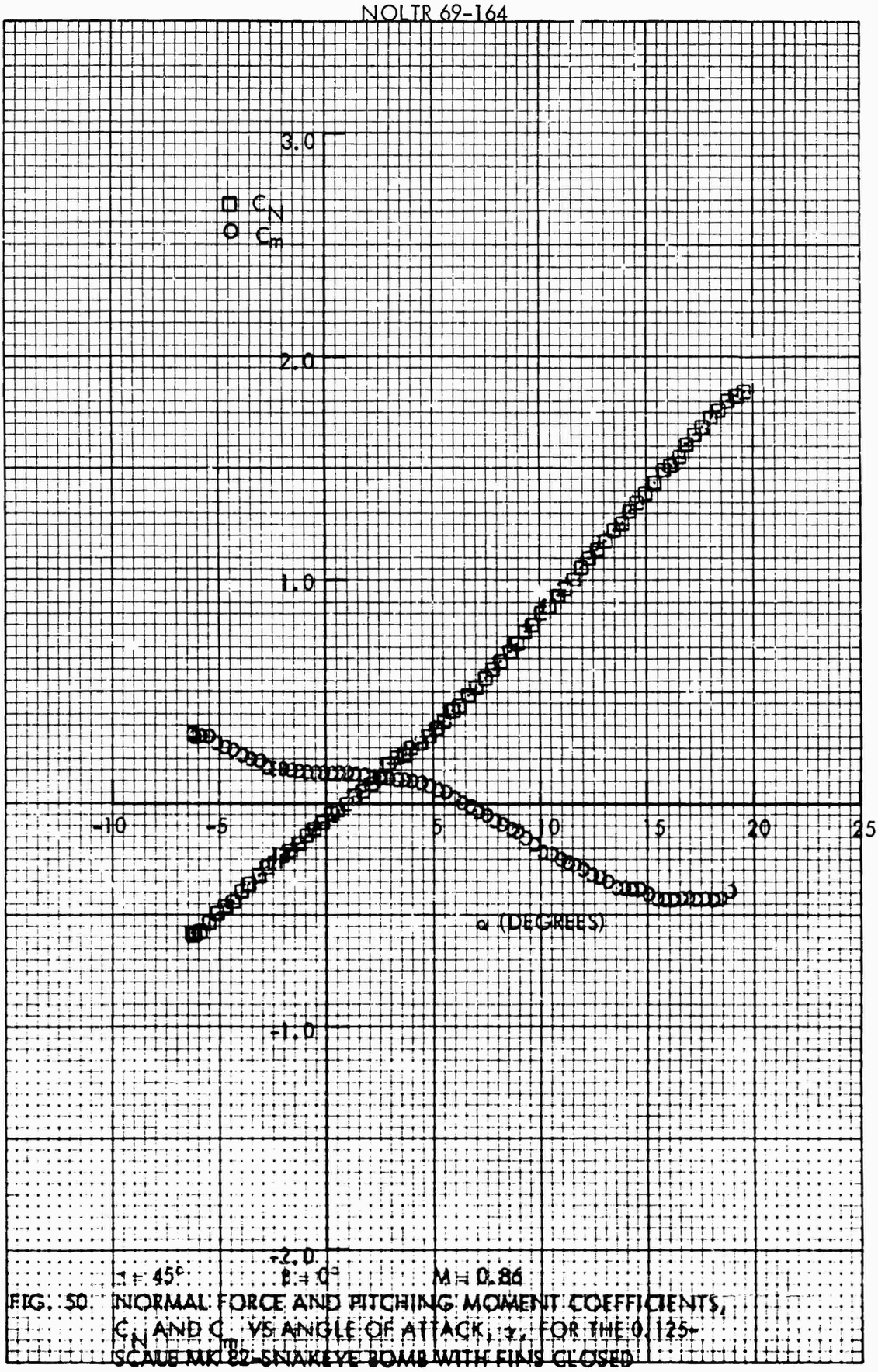

FIG. 50 NORMAL FORCE AND PITCHING MOMENT COEFFICIENTS, C_N AND C_m VS ANGLE OF ATTACK, α, FOR THE 0.125-SCALE MK 82-SNAKEYE BOMB WITH FINS CLOSED

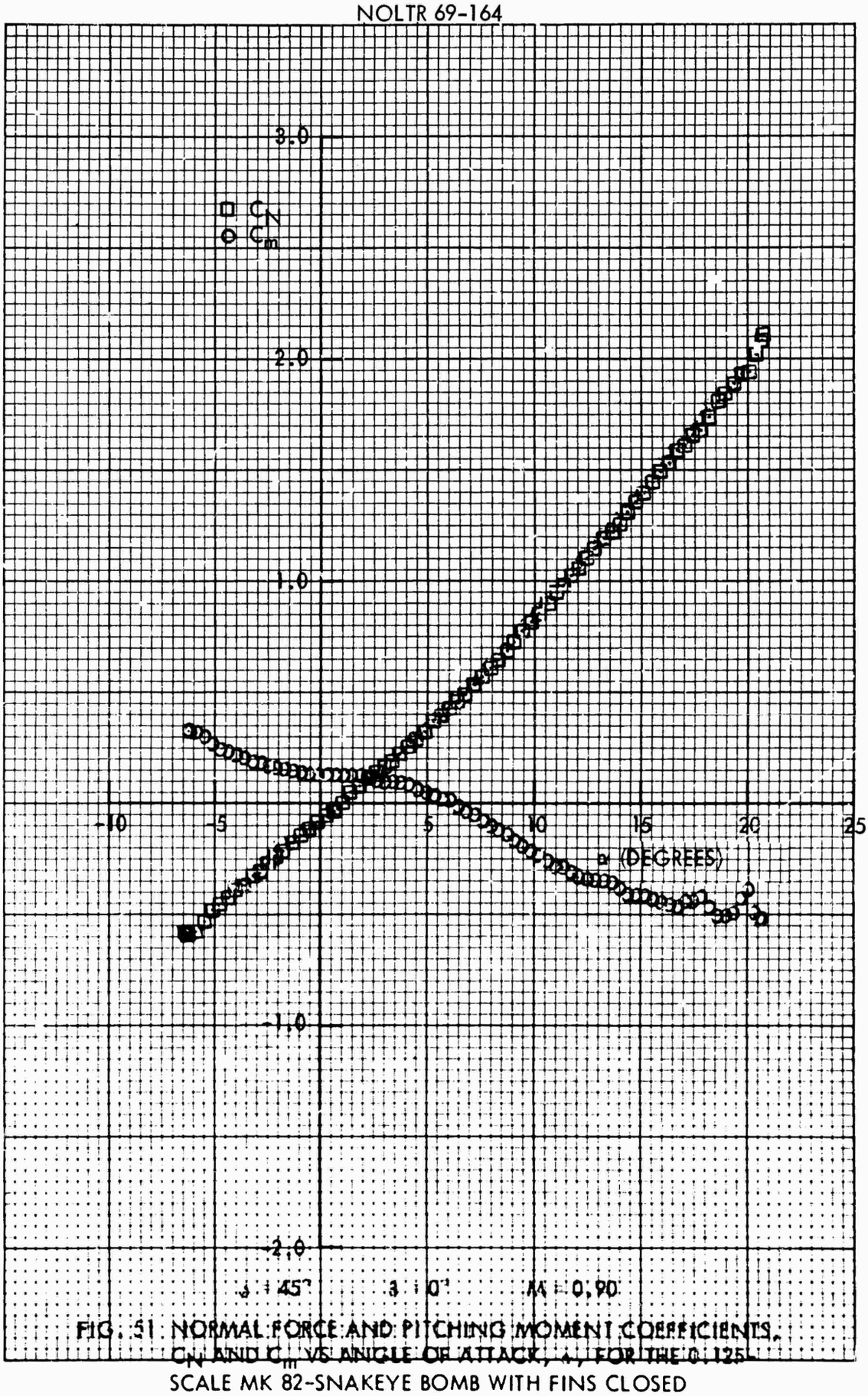

FIG. 51 NORMAL FORCE AND PITCHING MOMENT COEFFICIENTS, C_N AND C_m VS ANGLE OF ATTACK, α, FOR THE 0.125-SCALE MK 82-SNAKEYE BOMB WITH FINS CLOSED

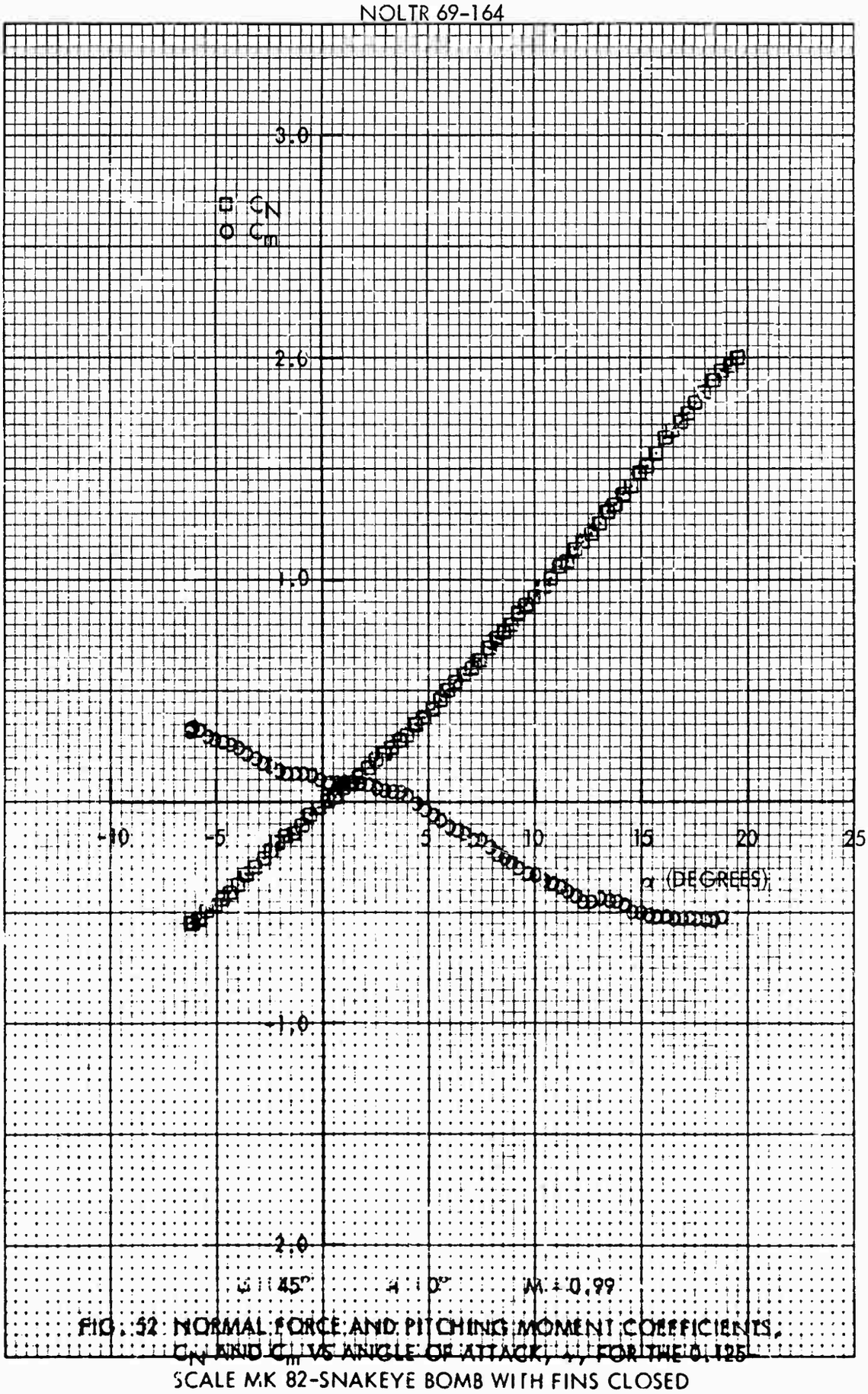

FIG. 52 NORMAL FORCE AND PITCHING MOMENT COEFFICIENTS, C_N AND C_m VS ANGLE OF ATTACK, α, FOR THE 0.125 SCALE MK 82-SNAKEYE BOMB WITH FINS CLOSED

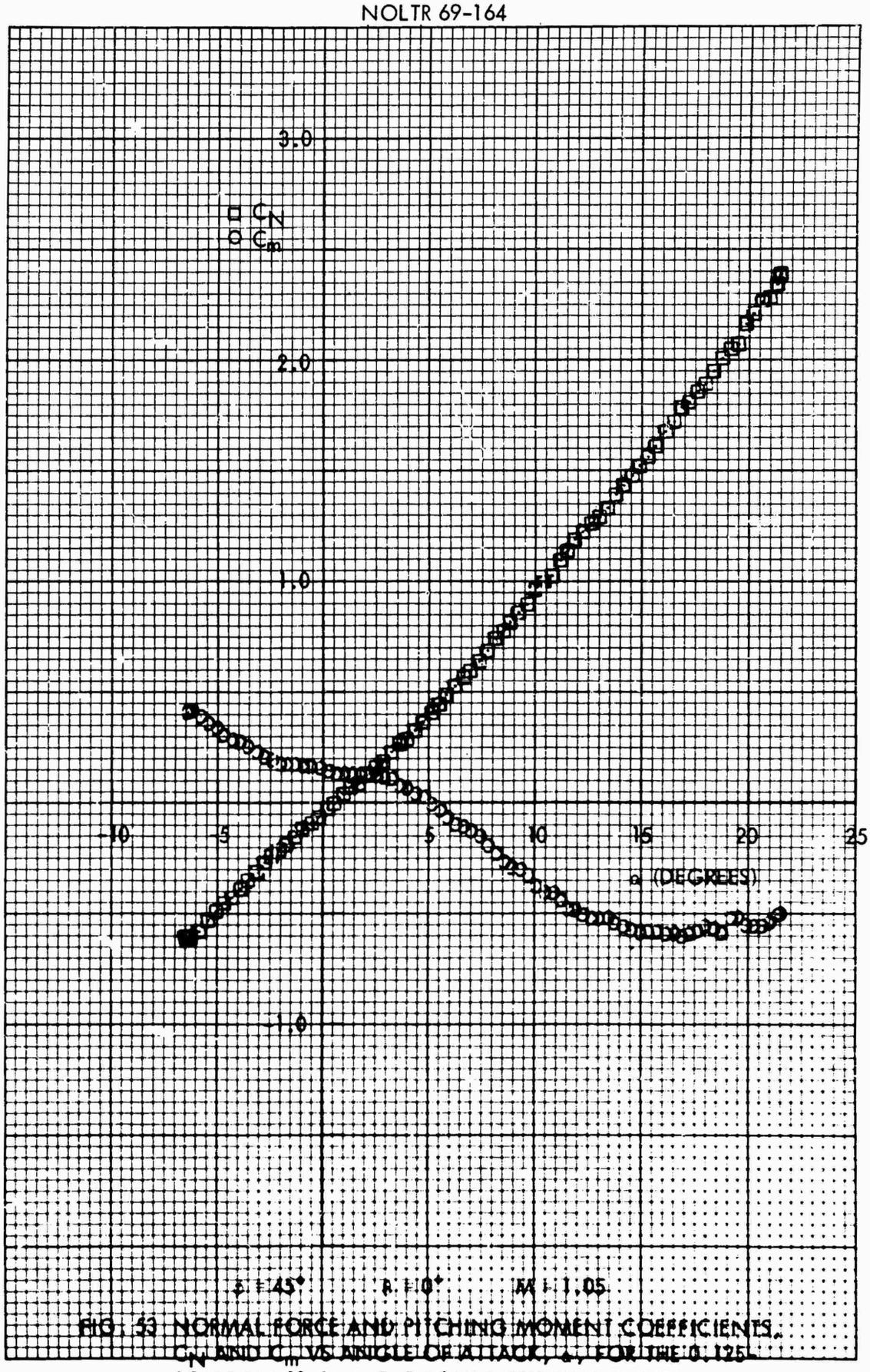

FIG. 53 NORMAL FORCE AND PITCHING MOMENT COEFFICIENTS, C_N AND C_m VS ANGLE OF ATTACK, α, FOR THE 0.125-SCALE MK 82-SNAKEYE BOMB WITH FINS CLOSED

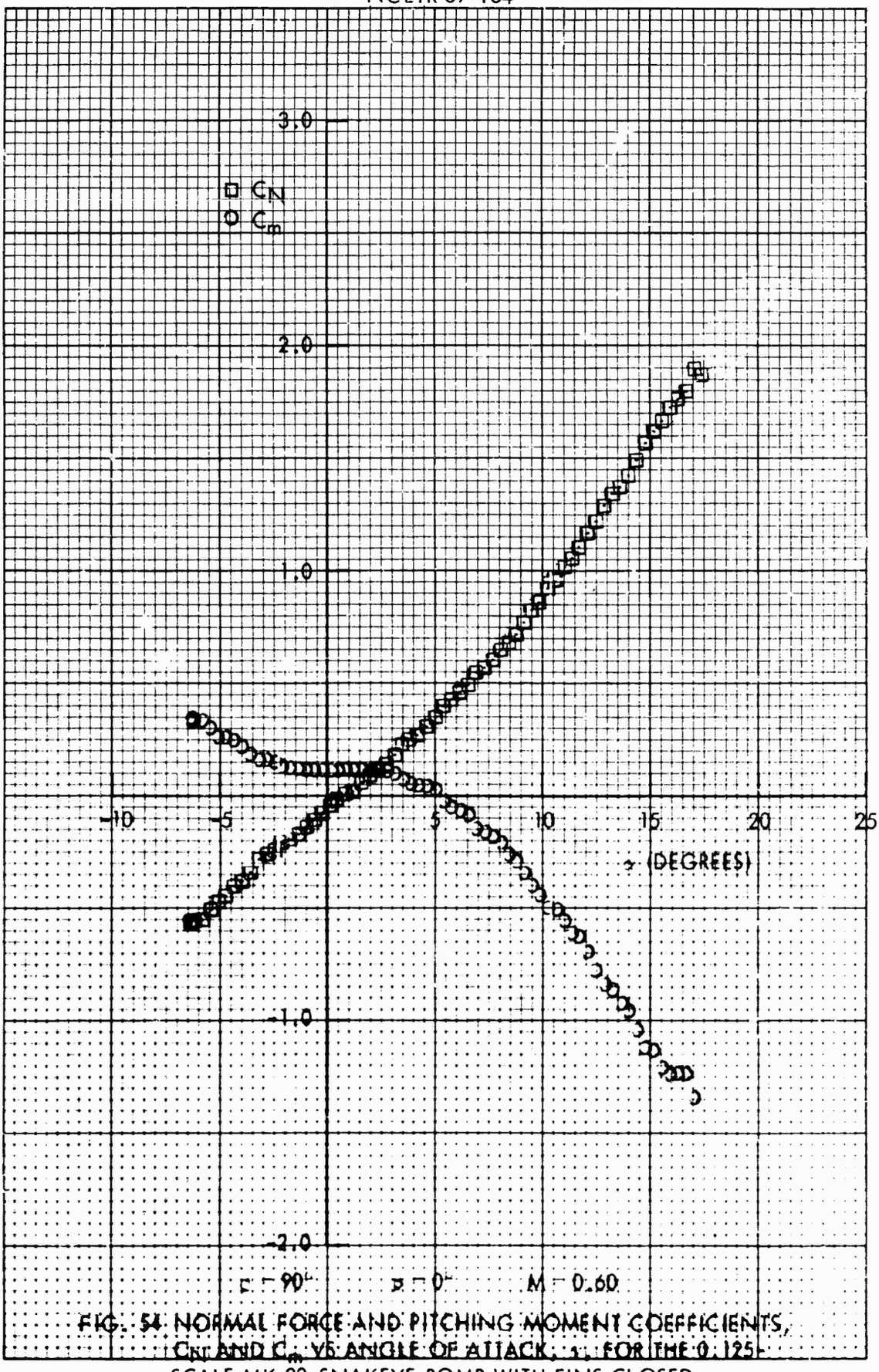

FIG. 54 NORMAL FORCE AND PITCHING MOMENT COEFFICIENTS, C_N AND C_m VS ANGLE OF ATTACK, α, FOR THE 0.125-SCALE MK 82-SNAKEYE BOMB WITH FINS CLOSED

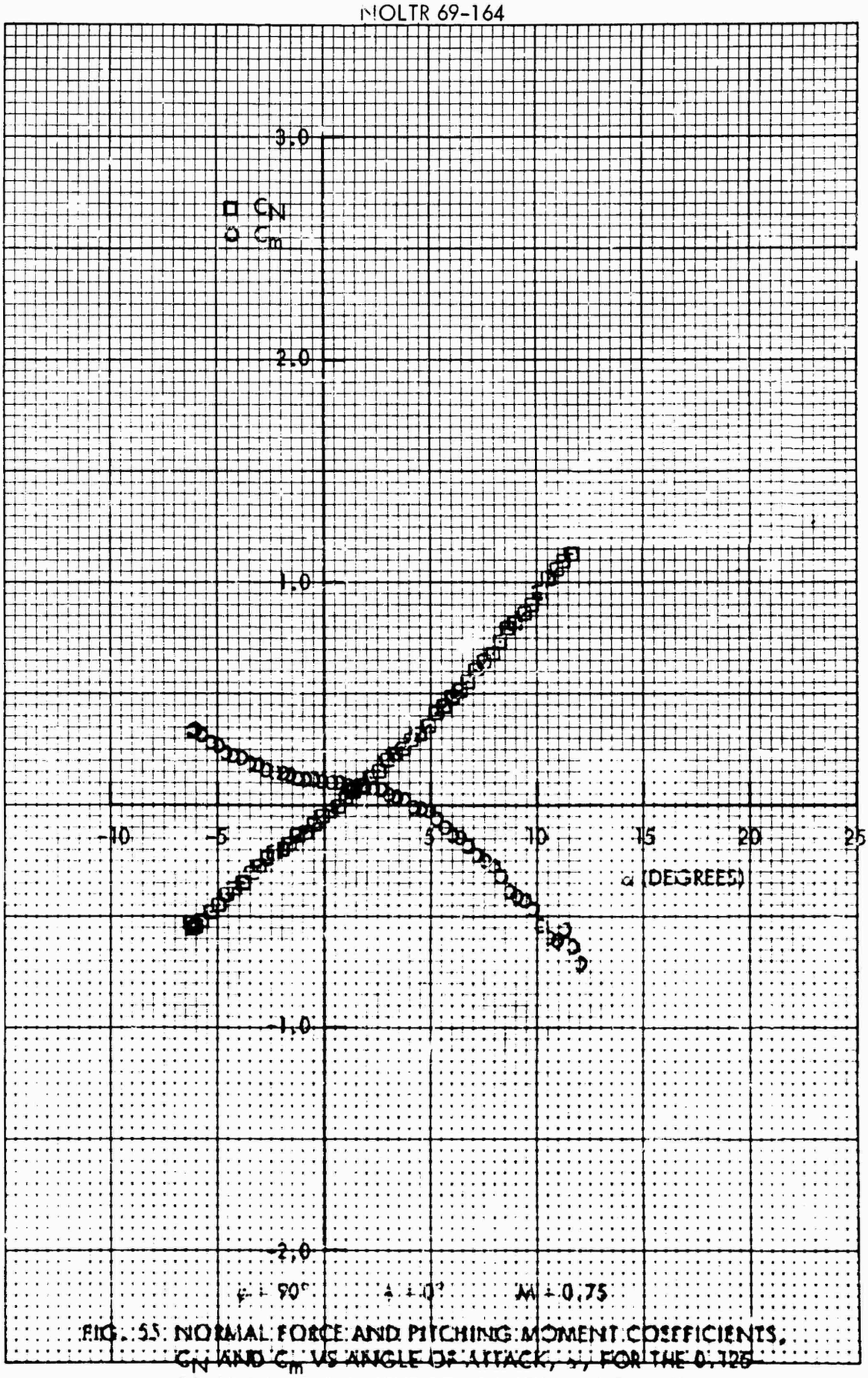

FIG. 55 NORMAL FORCE AND PITCHING MOMENT COEFFICIENTS, C_N AND C_m VS ANGLE OF ATTACK, α, FOR THE 0.125 SCALE MK 82-SNAKEYE BOMB WITH FINS CLOSED

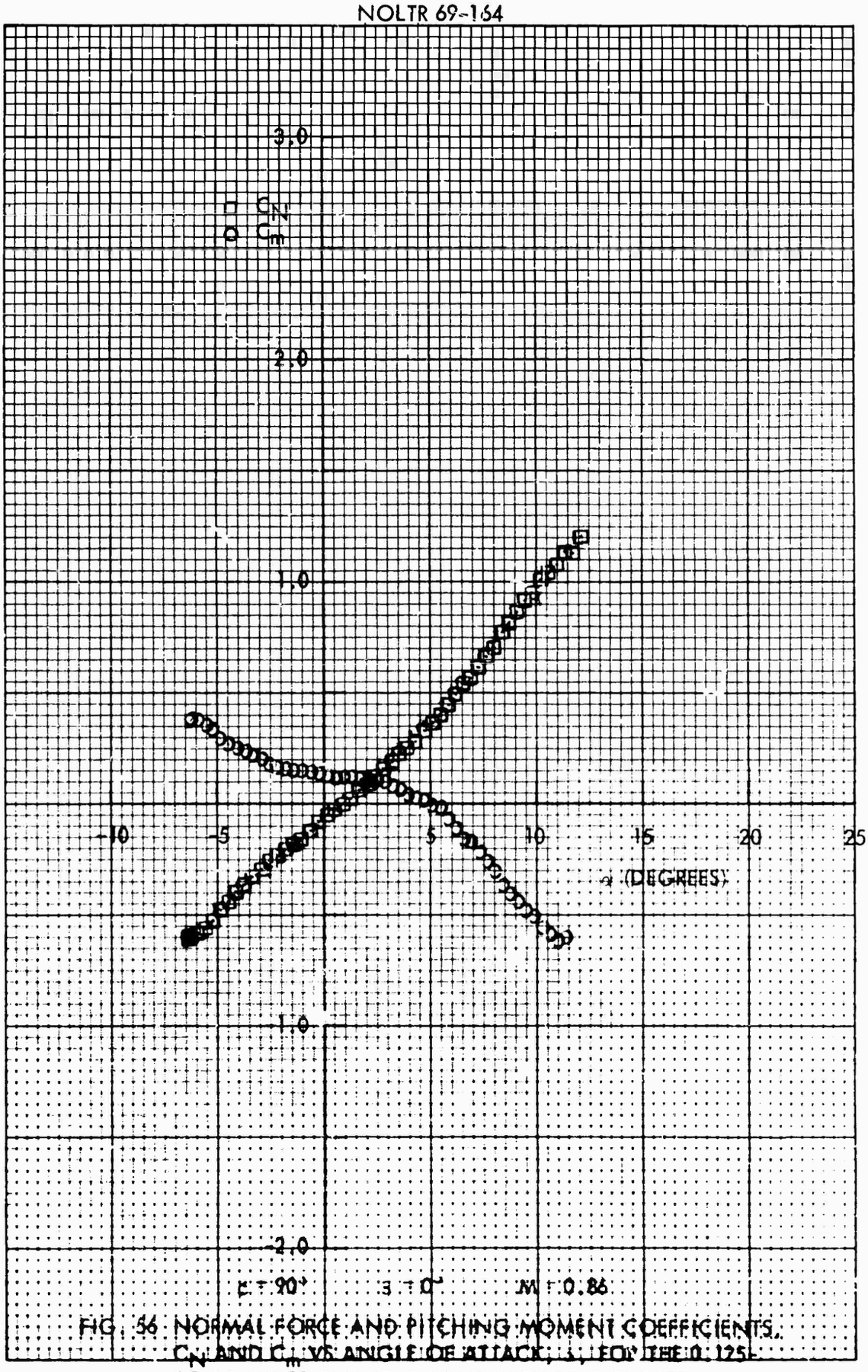

FIG. 56 NORMAL FORCE AND PITCHING MOMENT COEFFICIENTS, C_N AND C_m VS ANGLE OF ATTACK, α, FOR THE 0.125-SCALE MK 82-SNAKEYE BOMB WITH FINS CLOSED

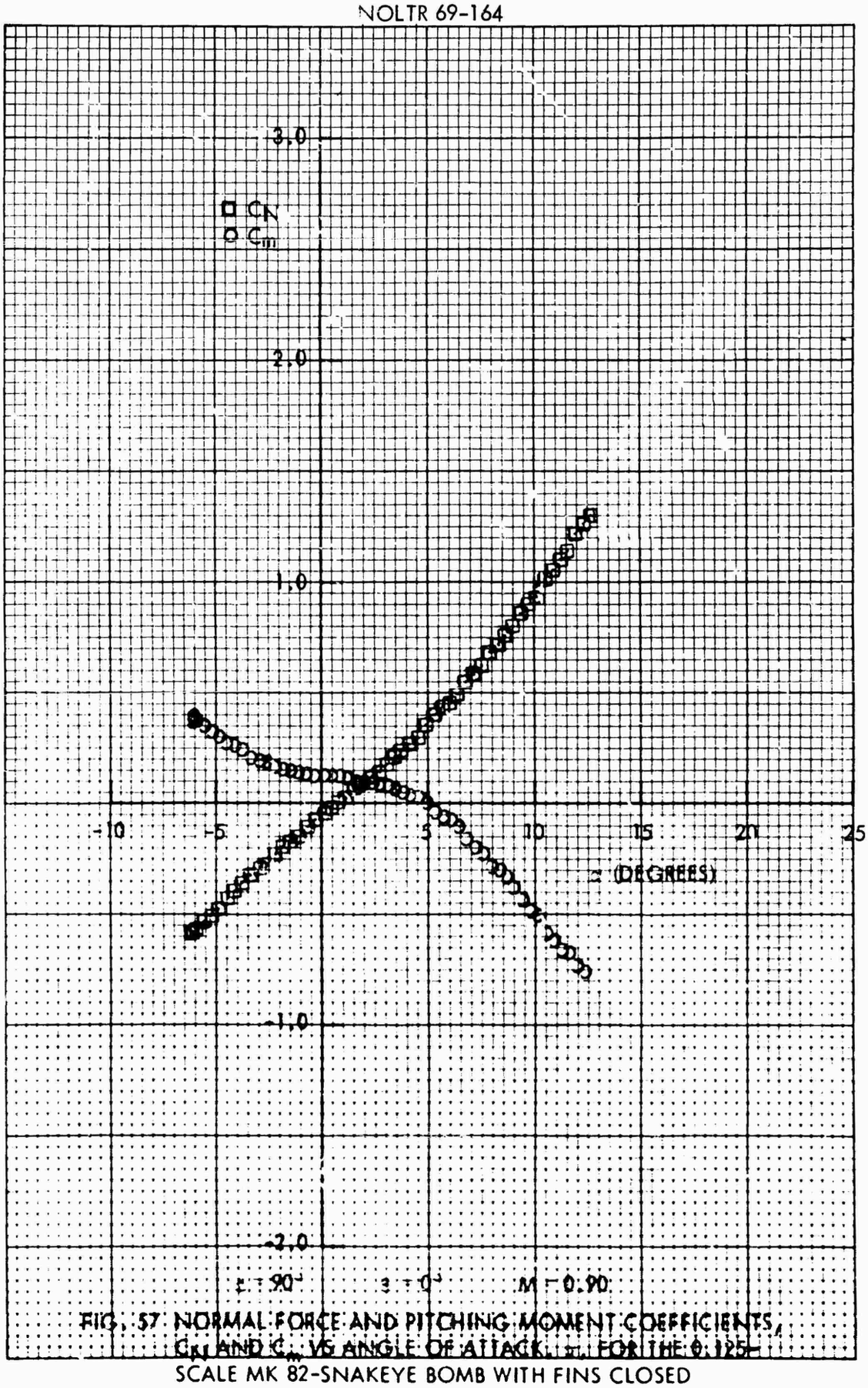

FIG. 57 NORMAL FORCE AND PITCHING MOMENT COEFFICIENTS, C_N AND C_m VS ANGLE OF ATTACK, α, FOR THE 0.125-SCALE MK 82-SNAKEYE BOMB WITH FINS CLOSED

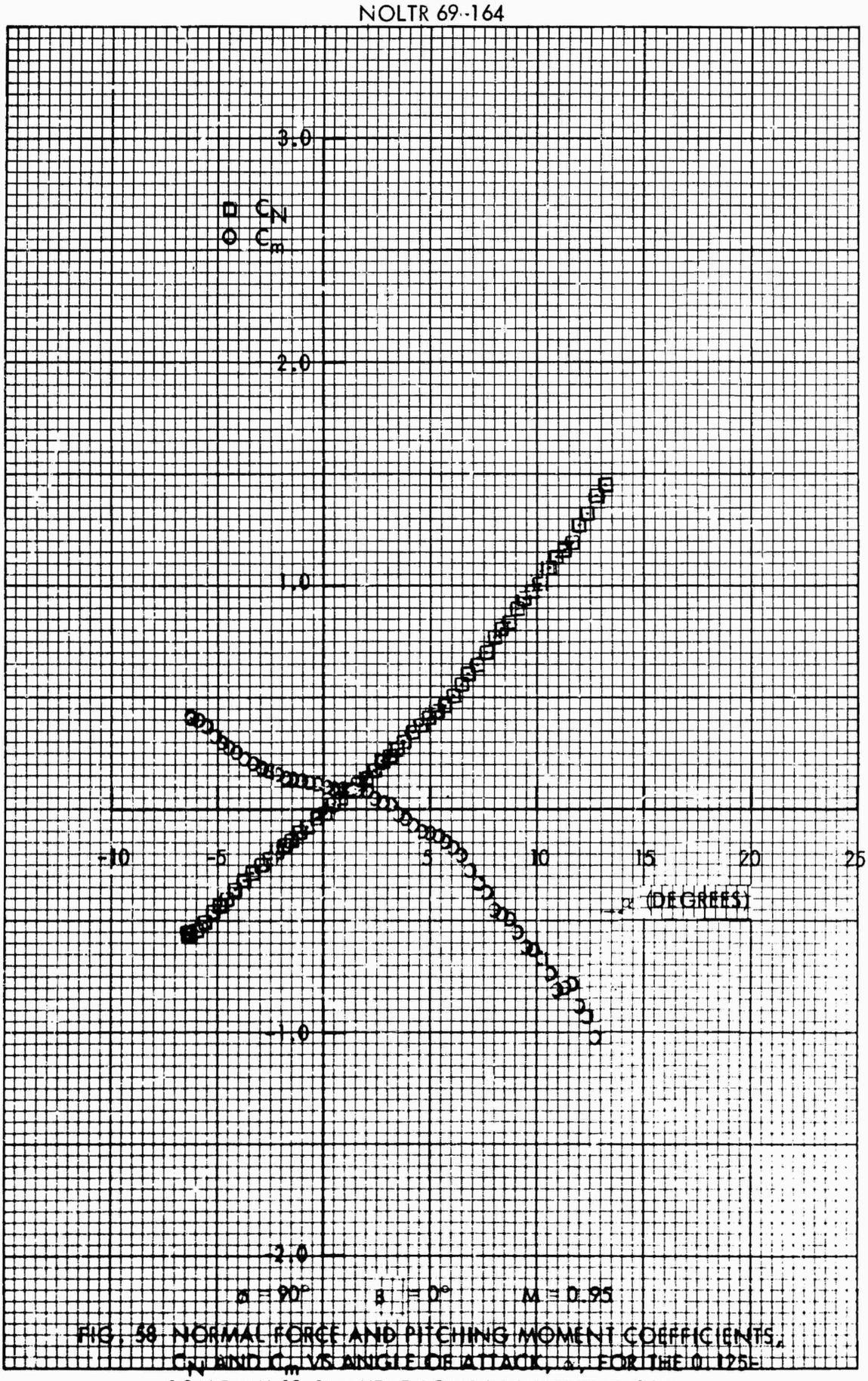

FIG. 58 NORMAL FORCE AND PITCHING MOMENT COEFFICIENTS, C_N AND C_m VS ANGLE OF ATTACK, α, FOR THE 0.125-SCALE MK 82-SNAKEYE BOMB WITH FINS CLOSED

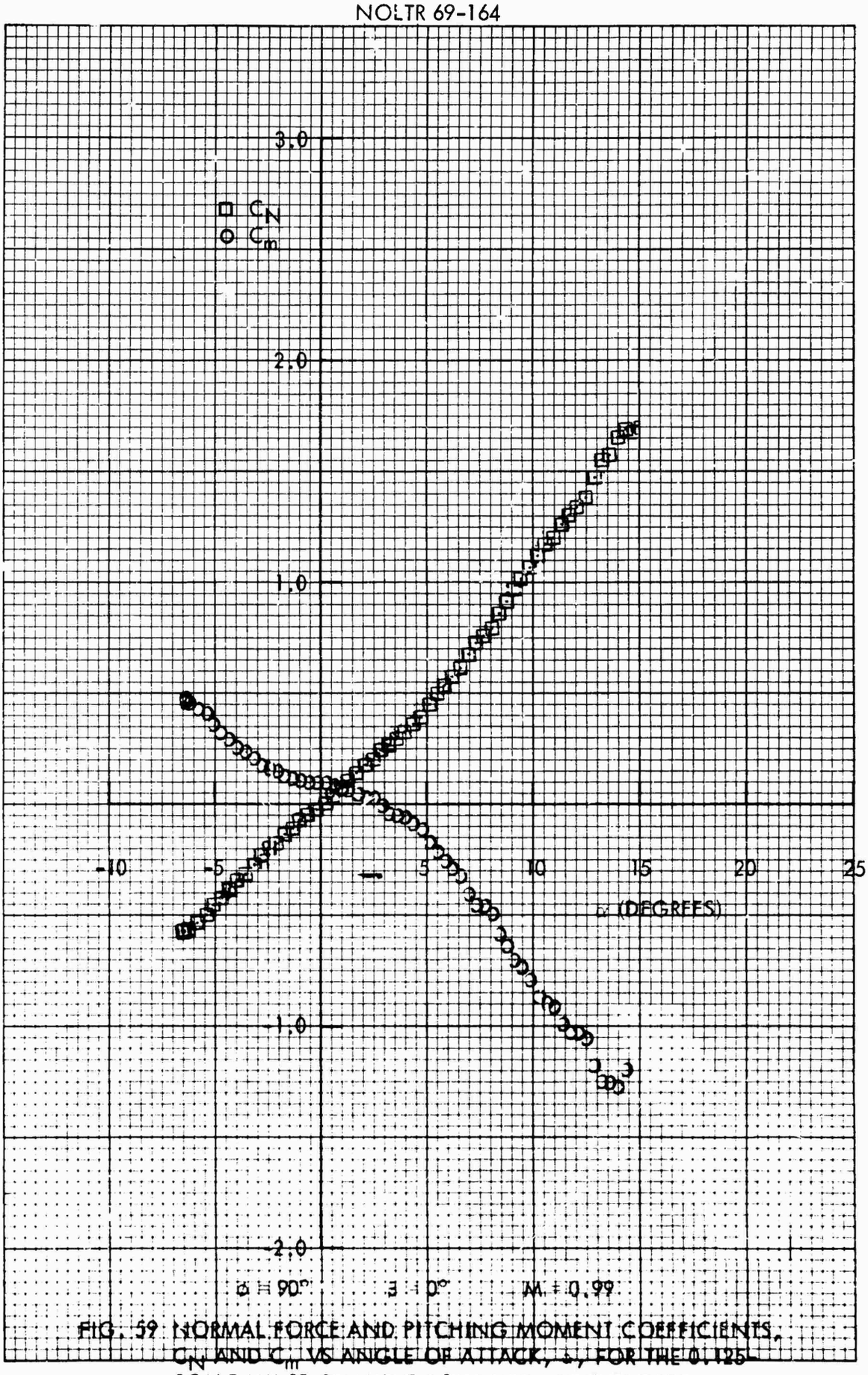

FIG. 59 NORMAL FORCE AND PITCHING MOMENT COEFFICIENTS, C_N AND C_m VS ANGLE OF ATTACK, α, FOR THE 0.125-SCALE MK 82-SNAKEYE BOMB WITH FINS CLOSED

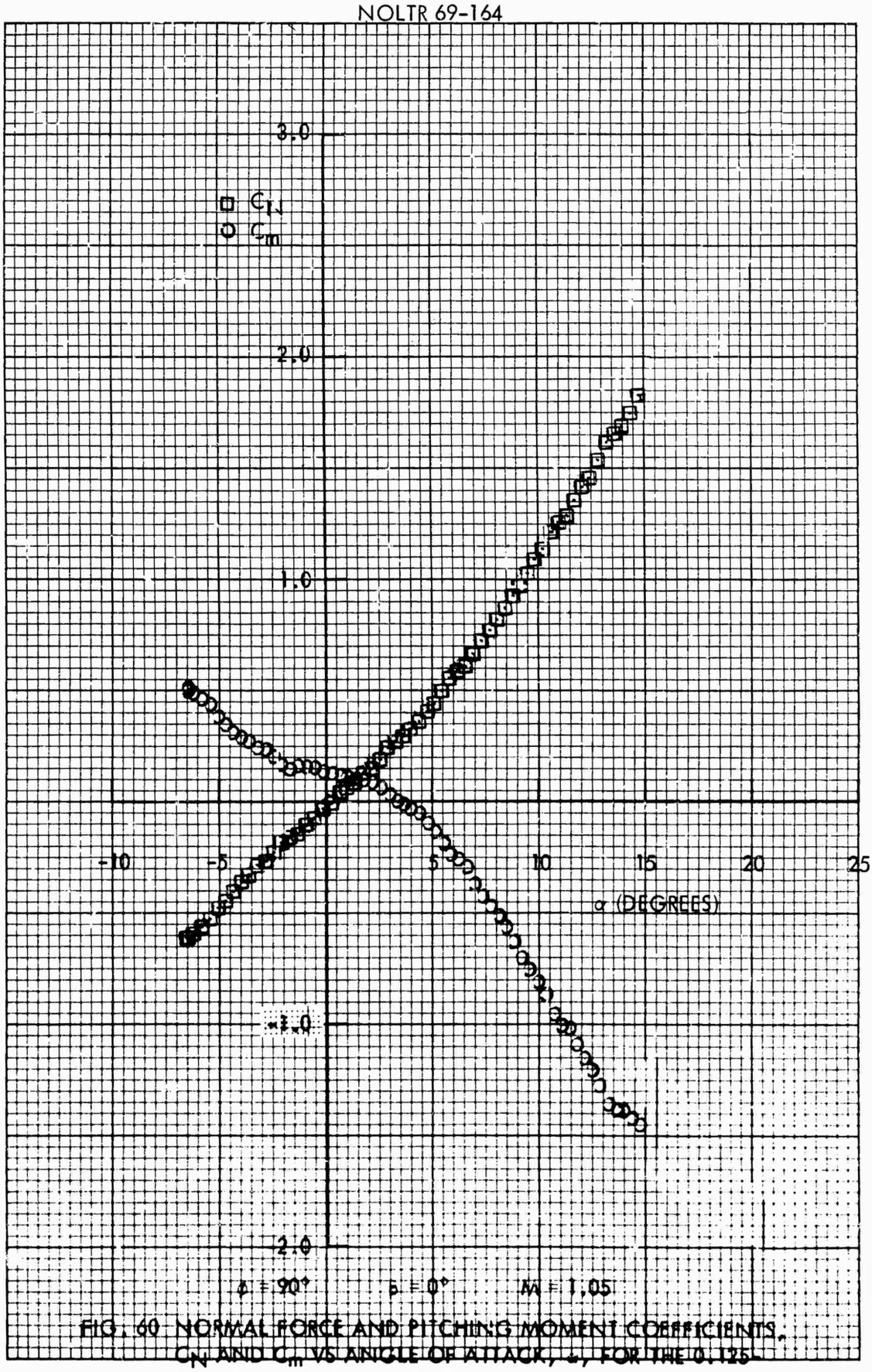

FIG. 60 NORMAL FORCE AND PITCHING MOMENT COEFFICIENTS, C_N AND C_m VS ANGLE OF ATTACK, α, FOR THE 0.125-SCALE MK 82-SNAKEYE BOMB WITH FINS CLOSED

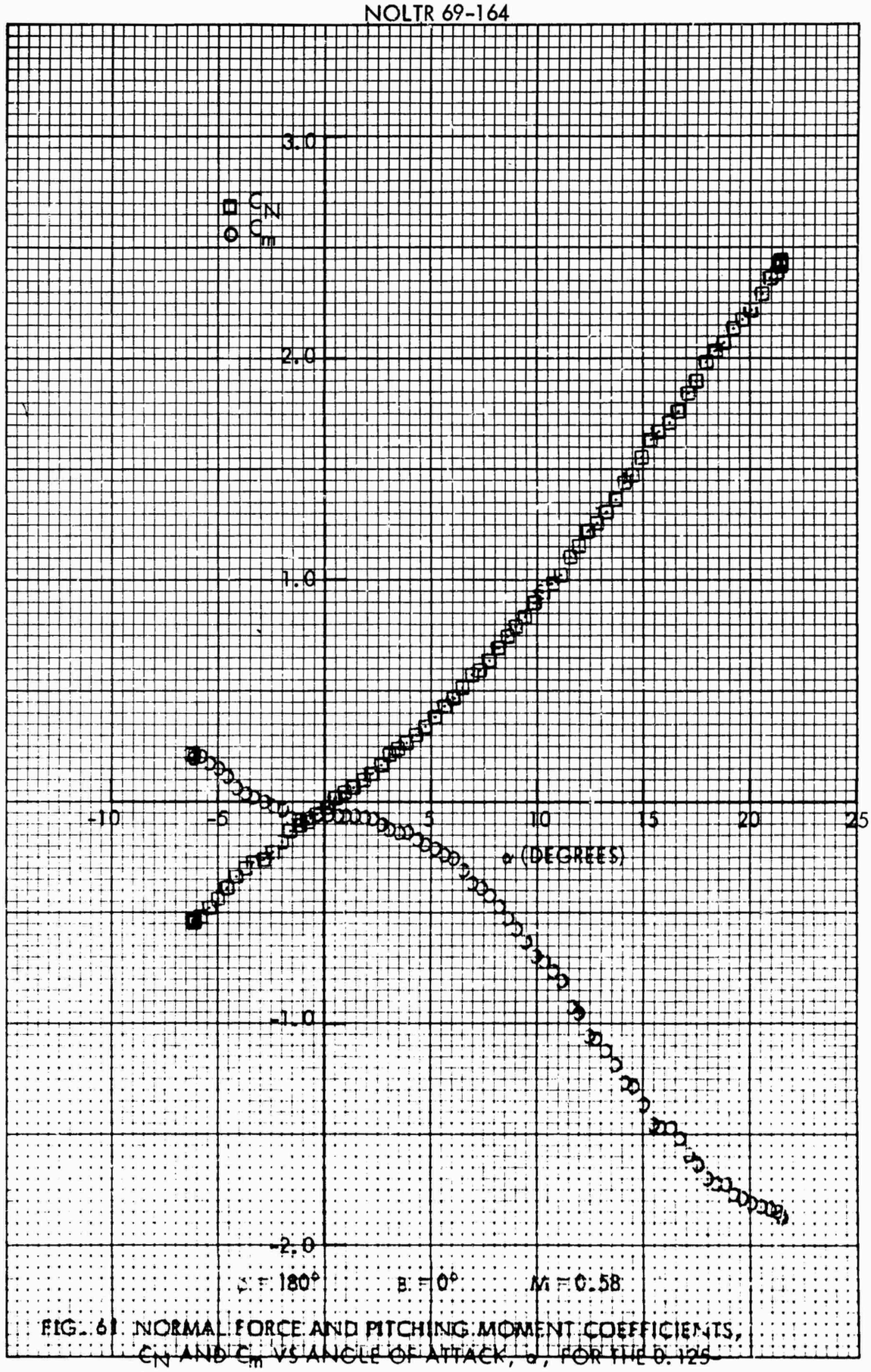

FIG. 61 NORMAL FORCE AND PITCHING MOMENT COEFFICIENTS, C_N AND C_m VS ANGLE OF ATTACK, α, FOR THE 0.125-SCALE MK 82-SNAKEYE BOMB WITH FINS CLOSED

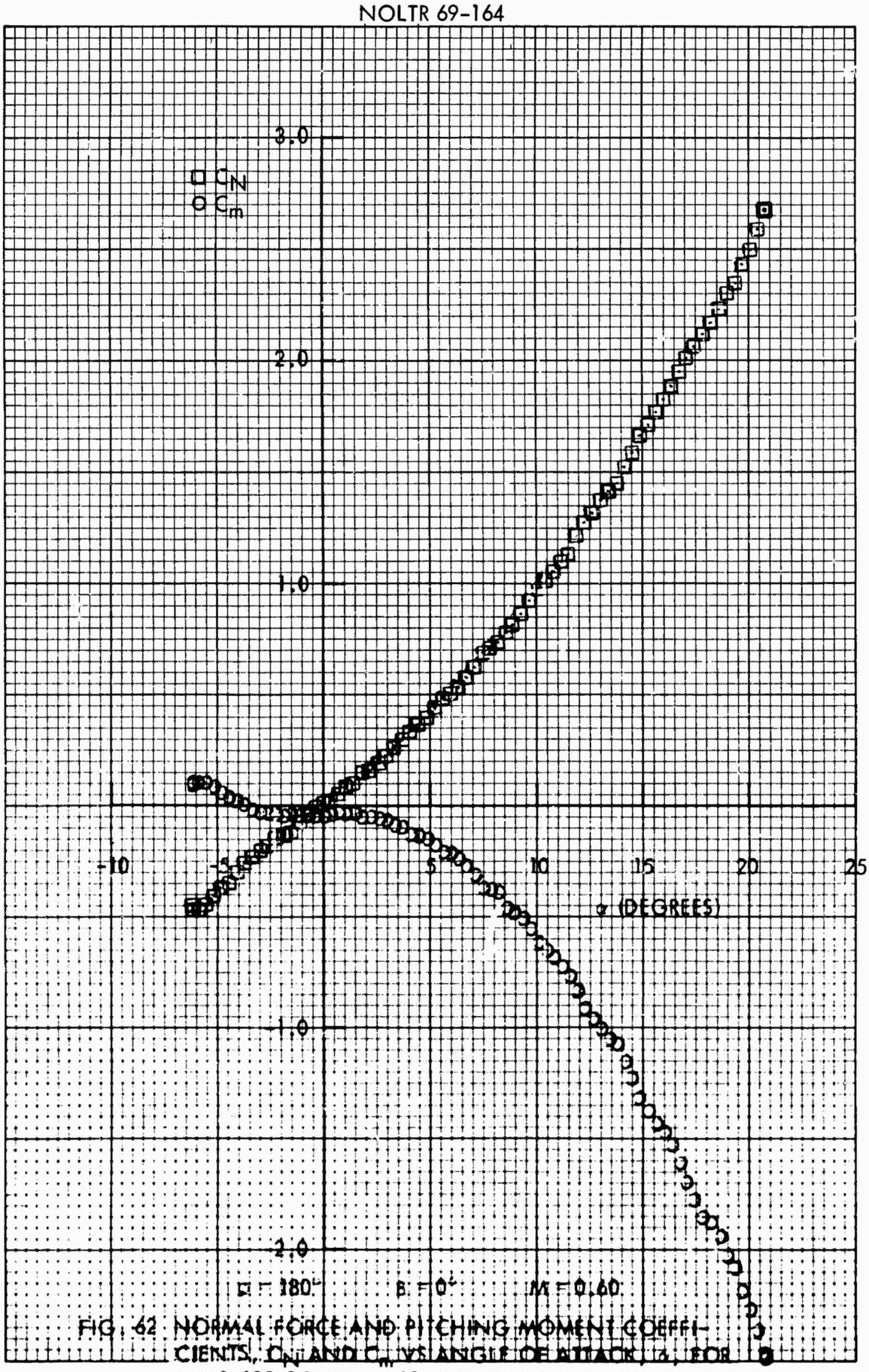

FIG. 62 NORMAL FORCE AND PITCHING MOMENT COEFFICIENTS, C_N AND C_m VS ANGLE OF ATTACK, α, FOR THE 0.125-SCALE MK 82-SNAKEYE BOMB WITH FINS CLOSED

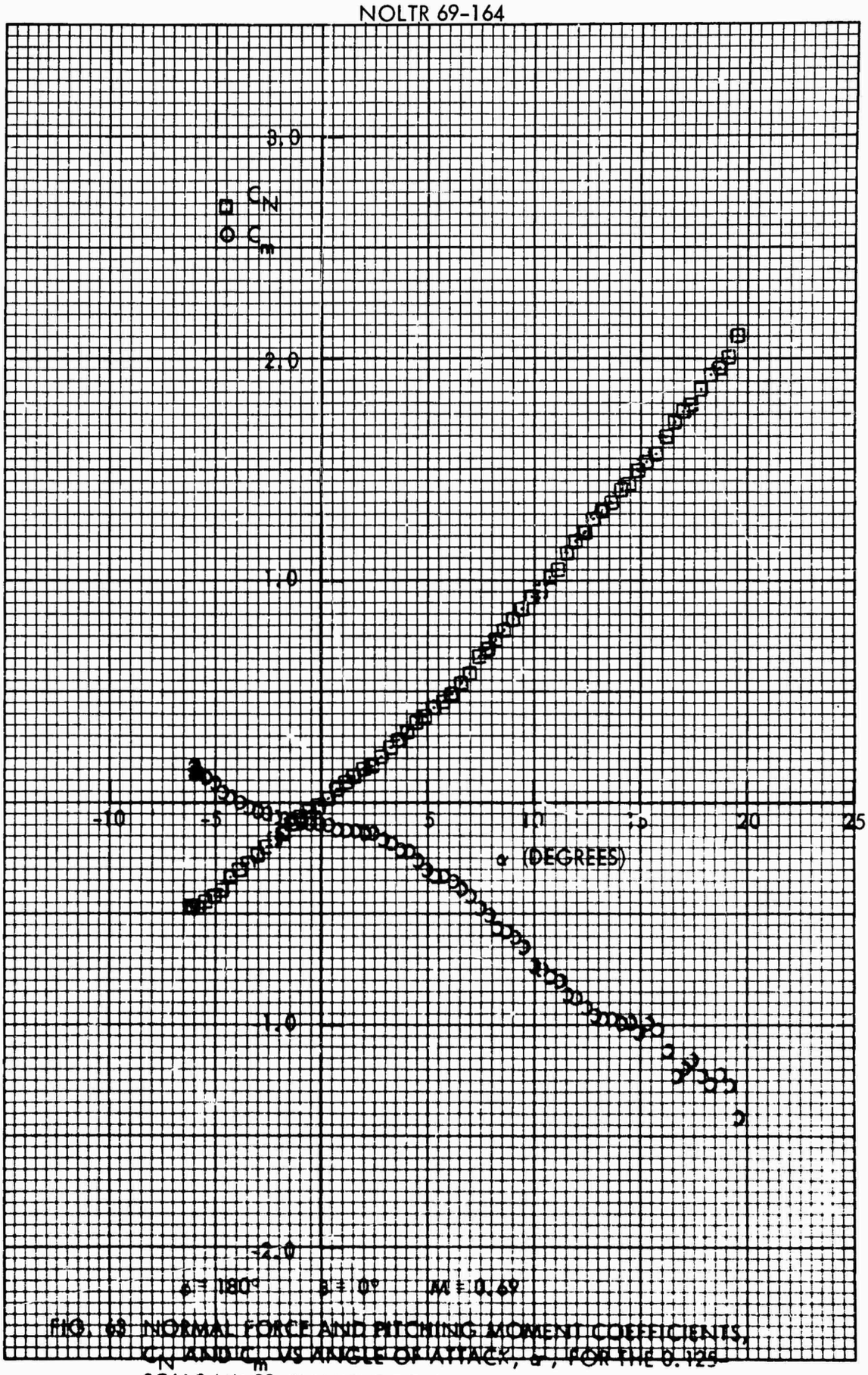

FIG. 63 NORMAL FORCE AND PITCHING MOMENT COEFFICIENTS, C_N AND C_m VS ANGLE OF ATTACK, α, FOR THE 0.125 SCALE MK 82-SNAKEYE BOMB WITH FINS CLOSED

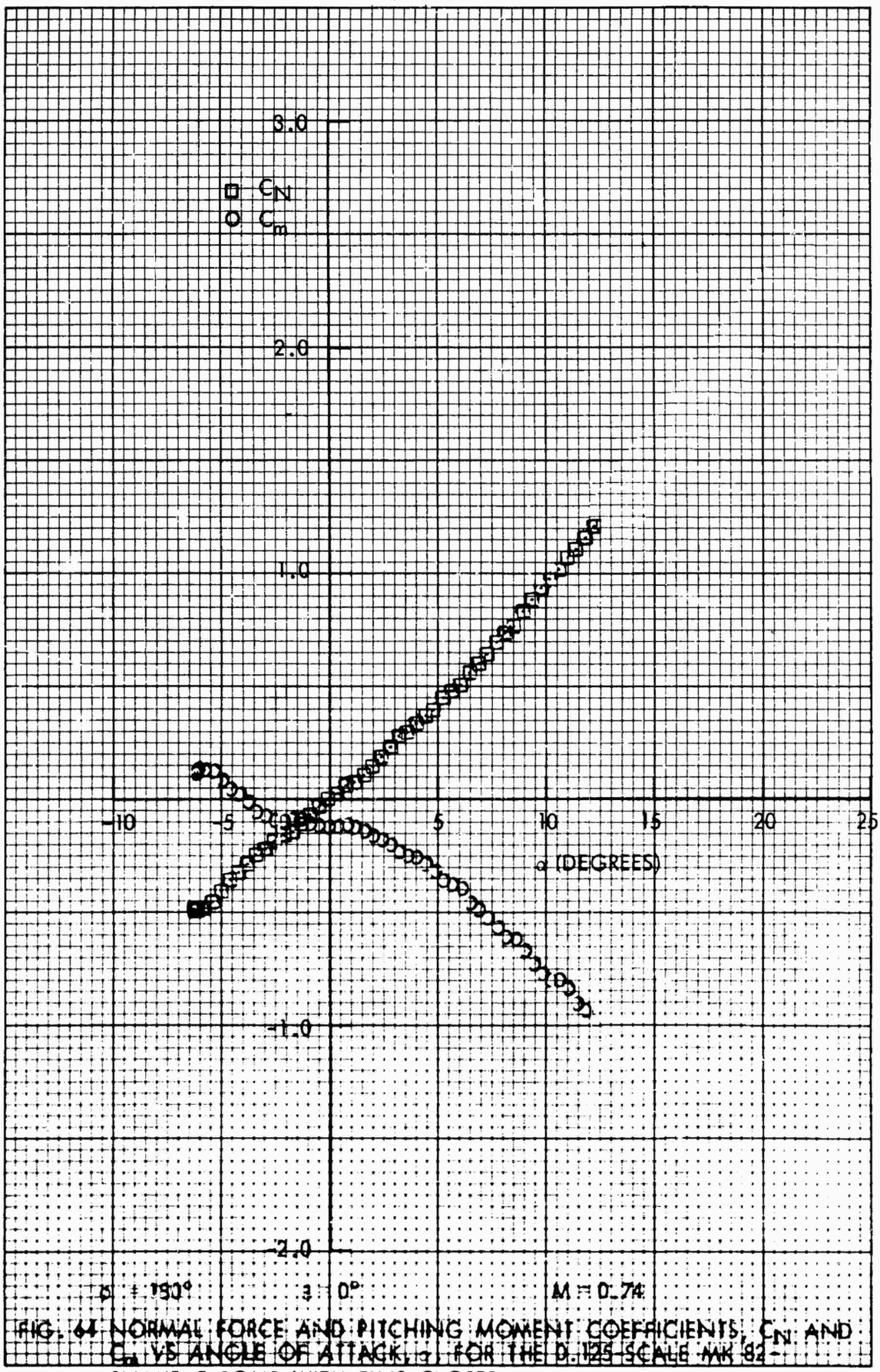

FIG. 64 NORMAL FORCE AND PITCHING MOMENT COEFFICIENTS, C_N AND C_m VS ANGLE OF ATTACK, α, FOR THE 0.125-SCALE MK 82 SNAKEYE BOMB WITH FINS CLOSED

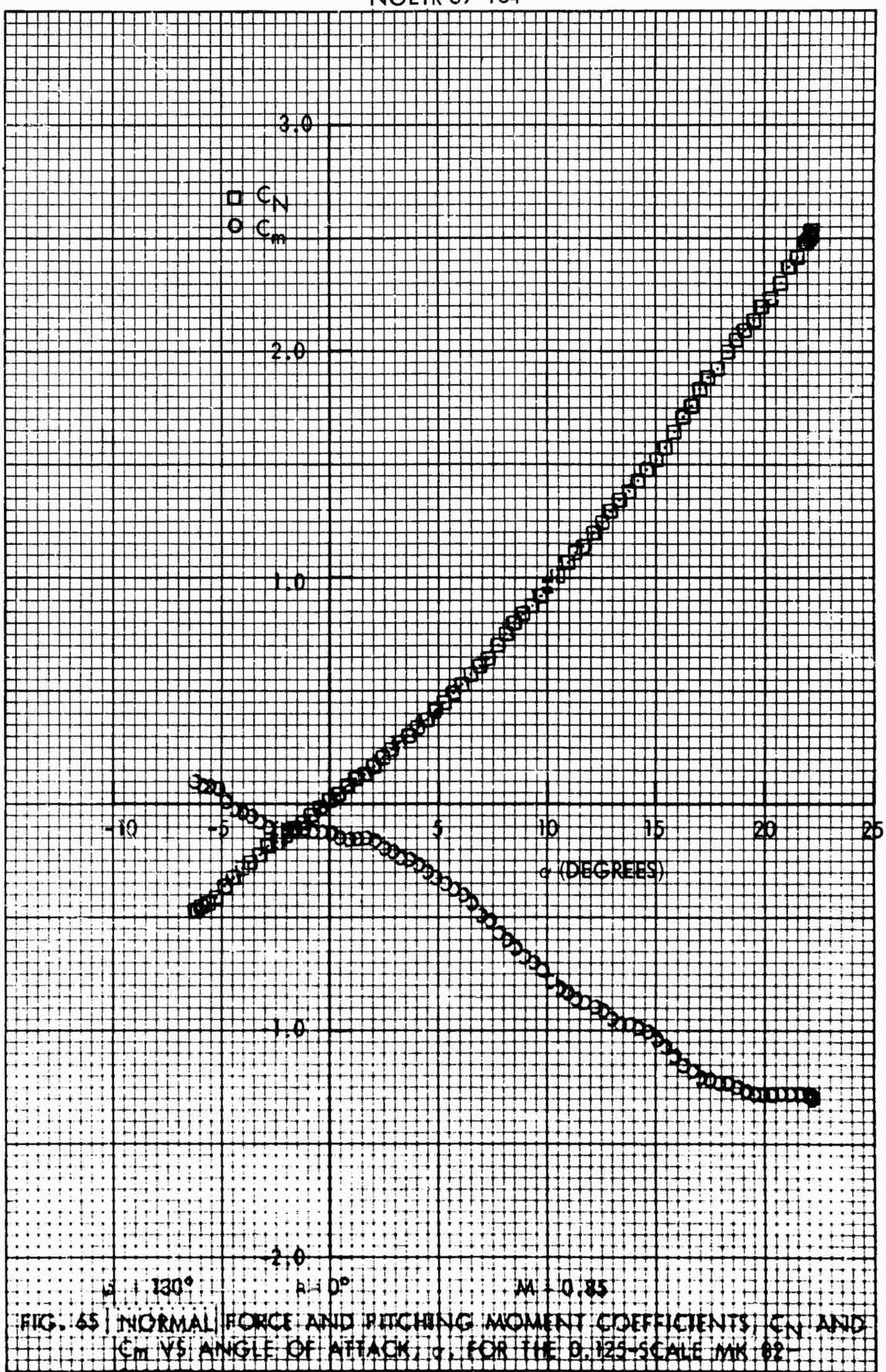

μ = 130° β = 0° M = 0.85

FIG. 65 | NORMAL FORCE AND PITCHING MOMENT COEFFICIENTS, C_N AND C_m VS ANGLE OF ATTACK, α, FOR THE 0.125-SCALE MK 82-SNAKEYE BOMB WITH FINS CLOSED

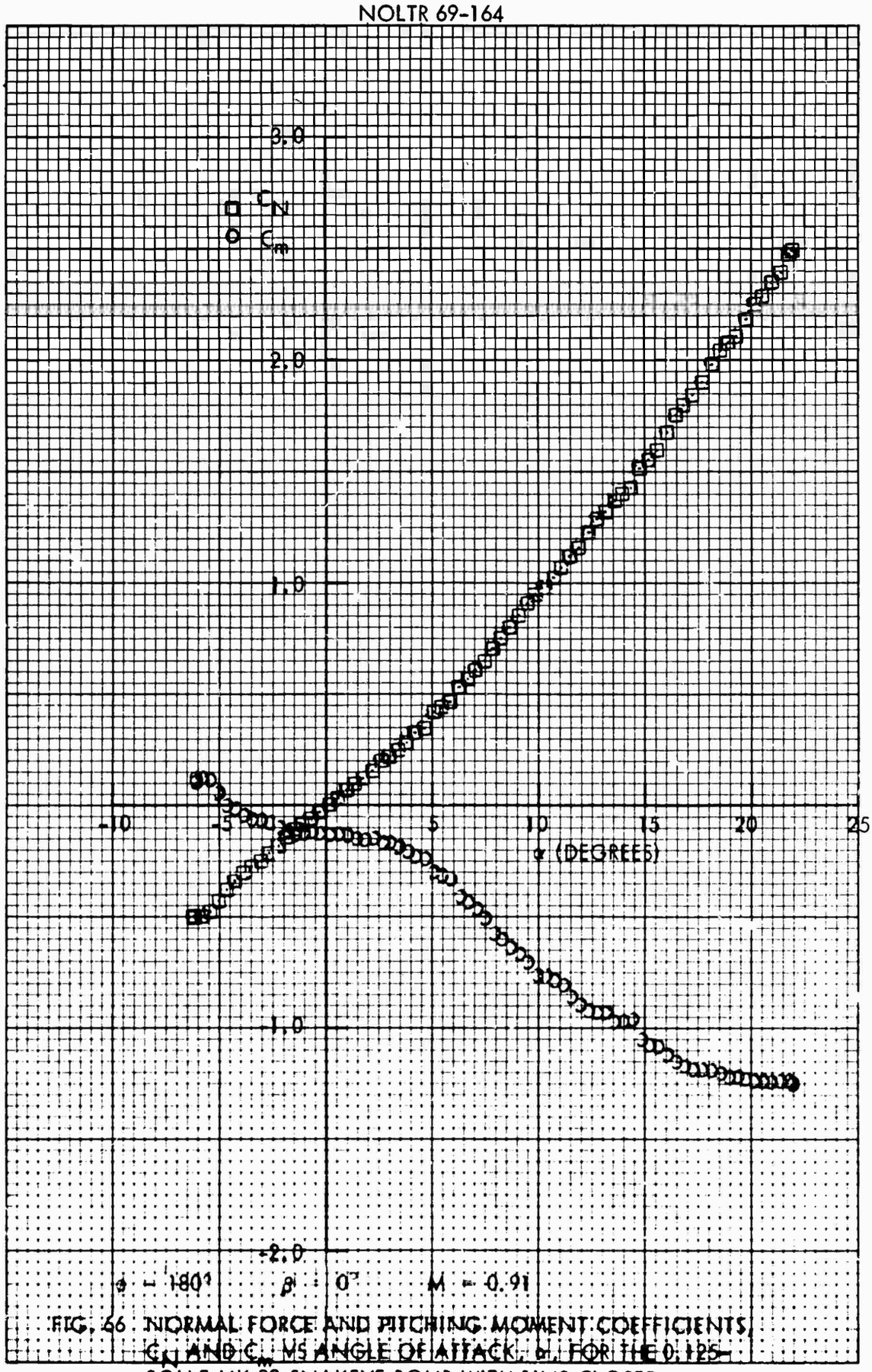

FIG. 66 NORMAL FORCE AND PITCHING MOMENT COEFFICIENTS, C_N AND C_m VS ANGLE OF ATTACK, α, FOR THE 0.125-SCALE MK 82-SNAKEYE BOMB WITH FINS CLOSED

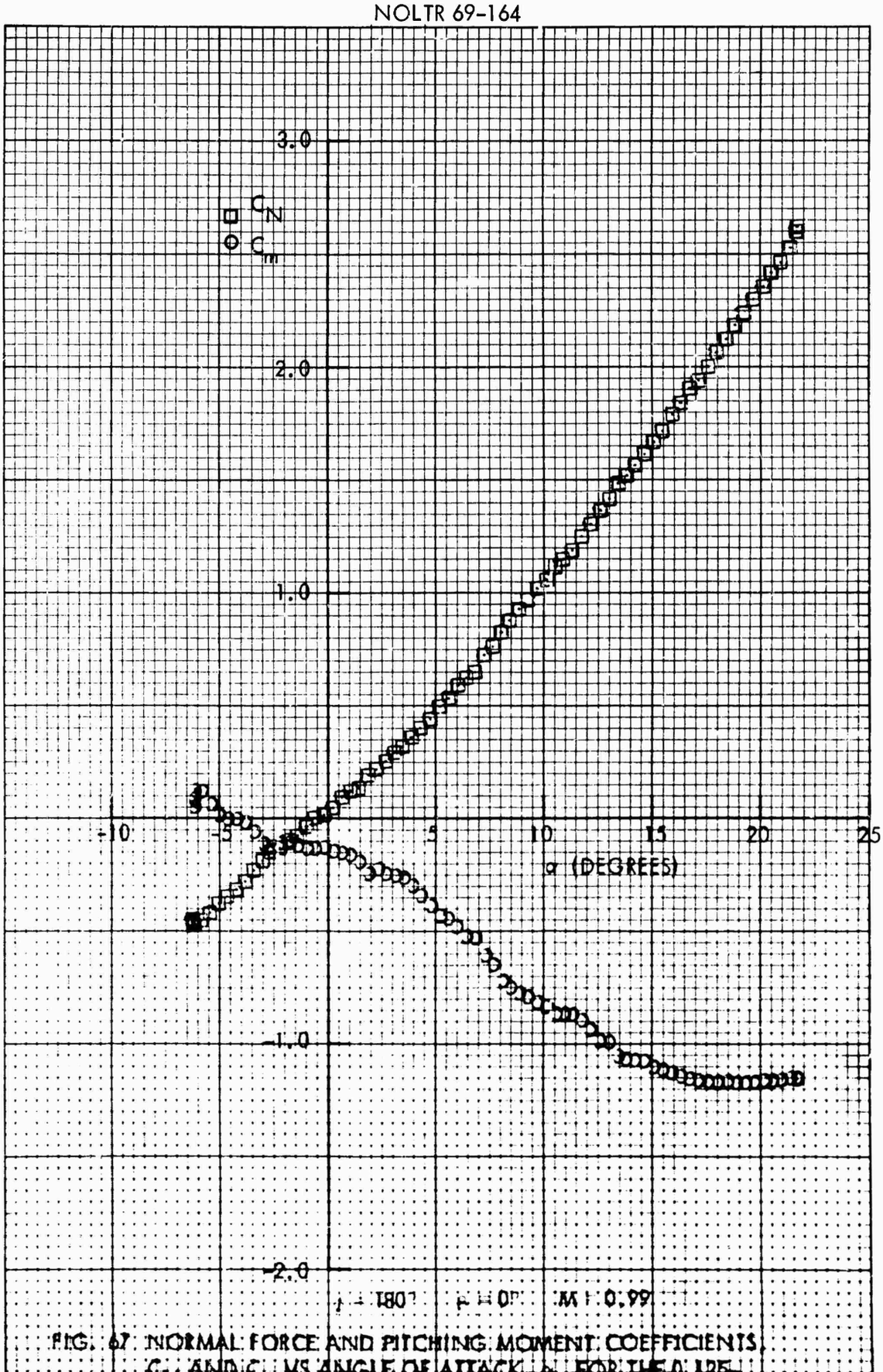

FIG. 67 NORMAL FORCE AND PITCHING MOMENT COEFFICIENTS, C_N AND C_m VS ANGLE OF ATTACK, α, FOR THE 0.125-SCALE MK 82-SNAKEYE BOMB WITH FINS CLOSED

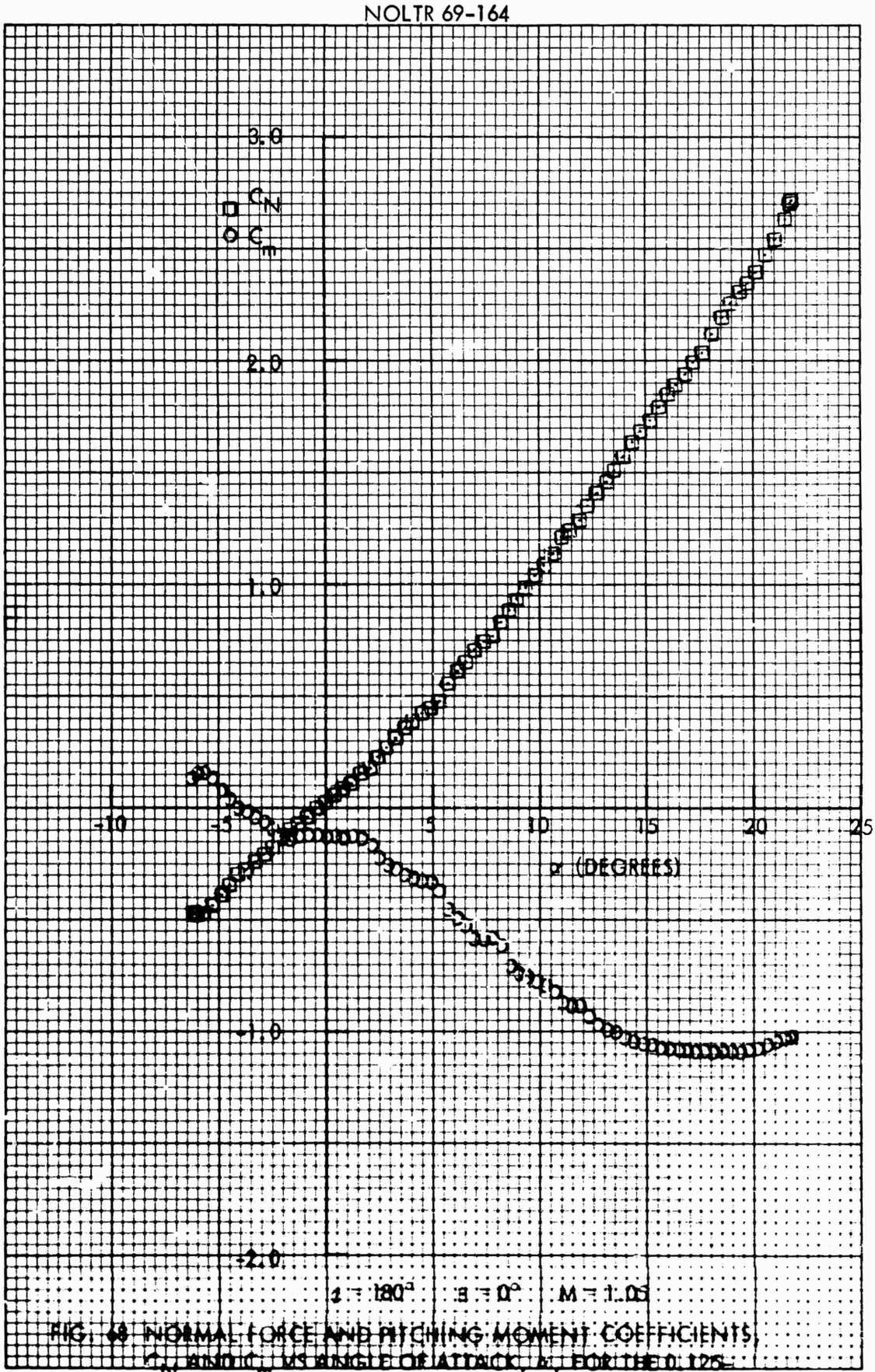

FIG. 69 NORMAL FORCE AND PITCHING MOMENT COEFFICIENTS, C_N AND C_m VS ANGLE OF ATTACK, α, FOR THE 0.125-SCALE MK 82-SNAKEYE BOMB WITH FINS CLOSED

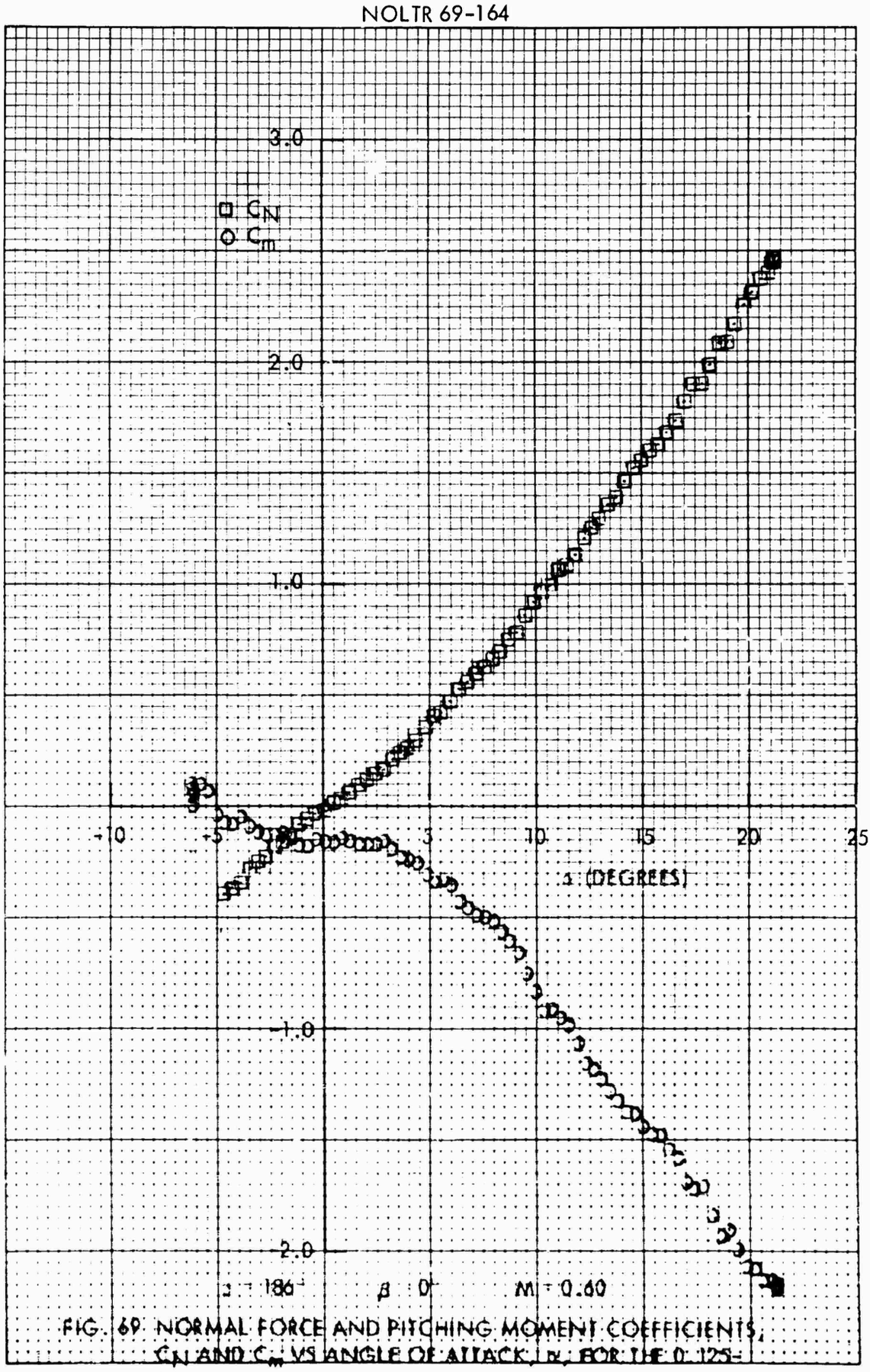

FIG. 69 NORMAL FORCE AND PITCHING MOMENT COEFFICIENTS, C_N AND C_m VS ANGLE OF ATTACK, α, FOR THE 0.125-SCALE MK 82-SNAKEYE BOMB WITH FINS CLOSED

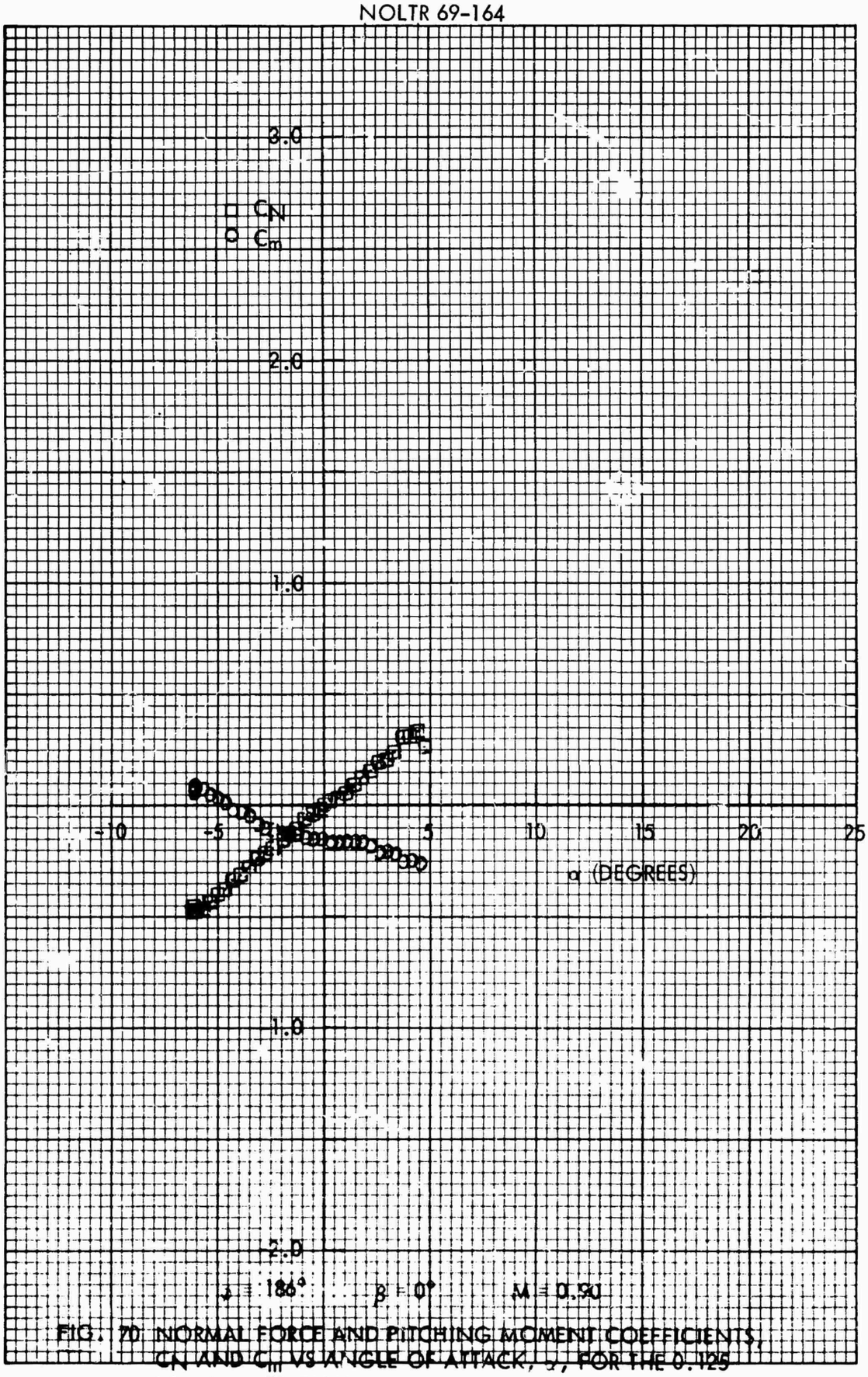

FIG. 70 NORMAL FORCE AND PITCHING MOMENT COEFFICIENTS, C_N AND C_m VS ANGLE OF ATTACK, α, FOR THE 0.125 SCALE MK 82-SNAKEYE BOMB WITH FINS CLOSED

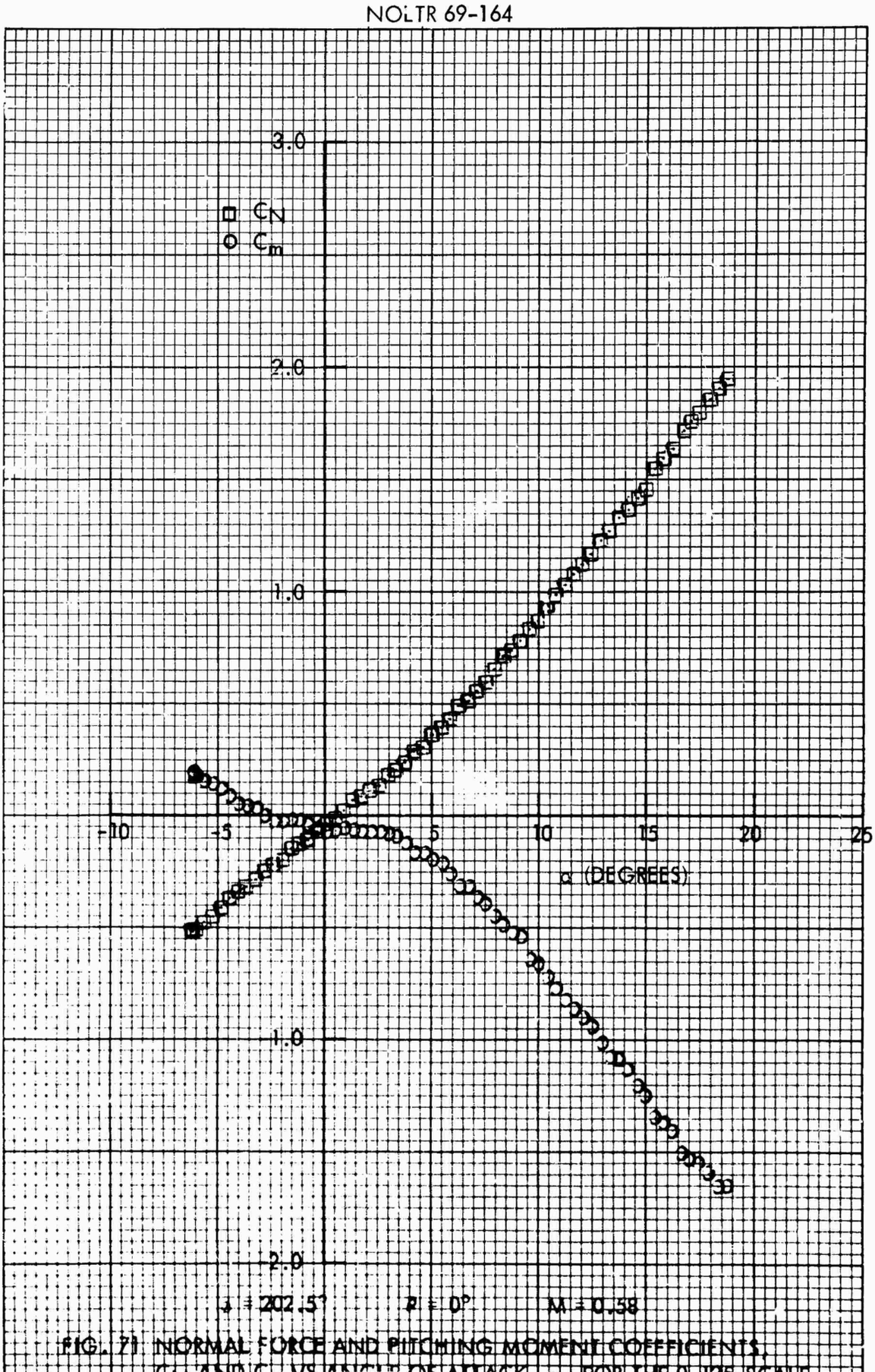

FIG. 71 NORMAL FORCE AND PITCHING MOMENT COEFFICIENTS, C_N AND C_m VS ANGLE OF ATTACK, α, FOR THE 0.125-SCALE MK 82-SNAKEYE BOMB WITH FINS CLOSED

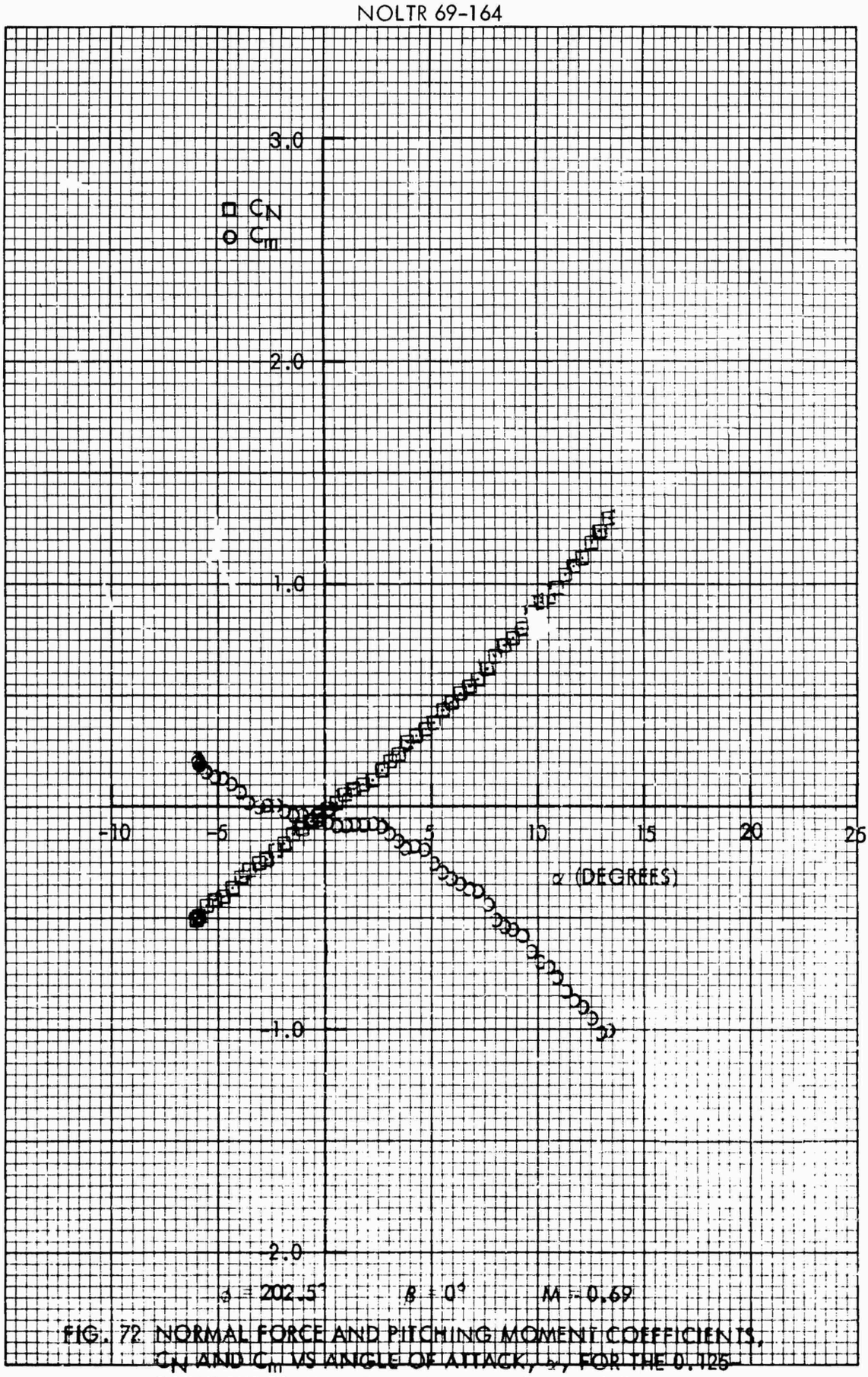

FIG. 72 NORMAL FORCE AND PITCHING MOMENT COEFFICIENTS, C_N AND C_m VS ANGLE OF ATTACK, α, FOR THE 0.125-SCALE MK 82-SNAKEYE BOMB WITH FINS CLOSED

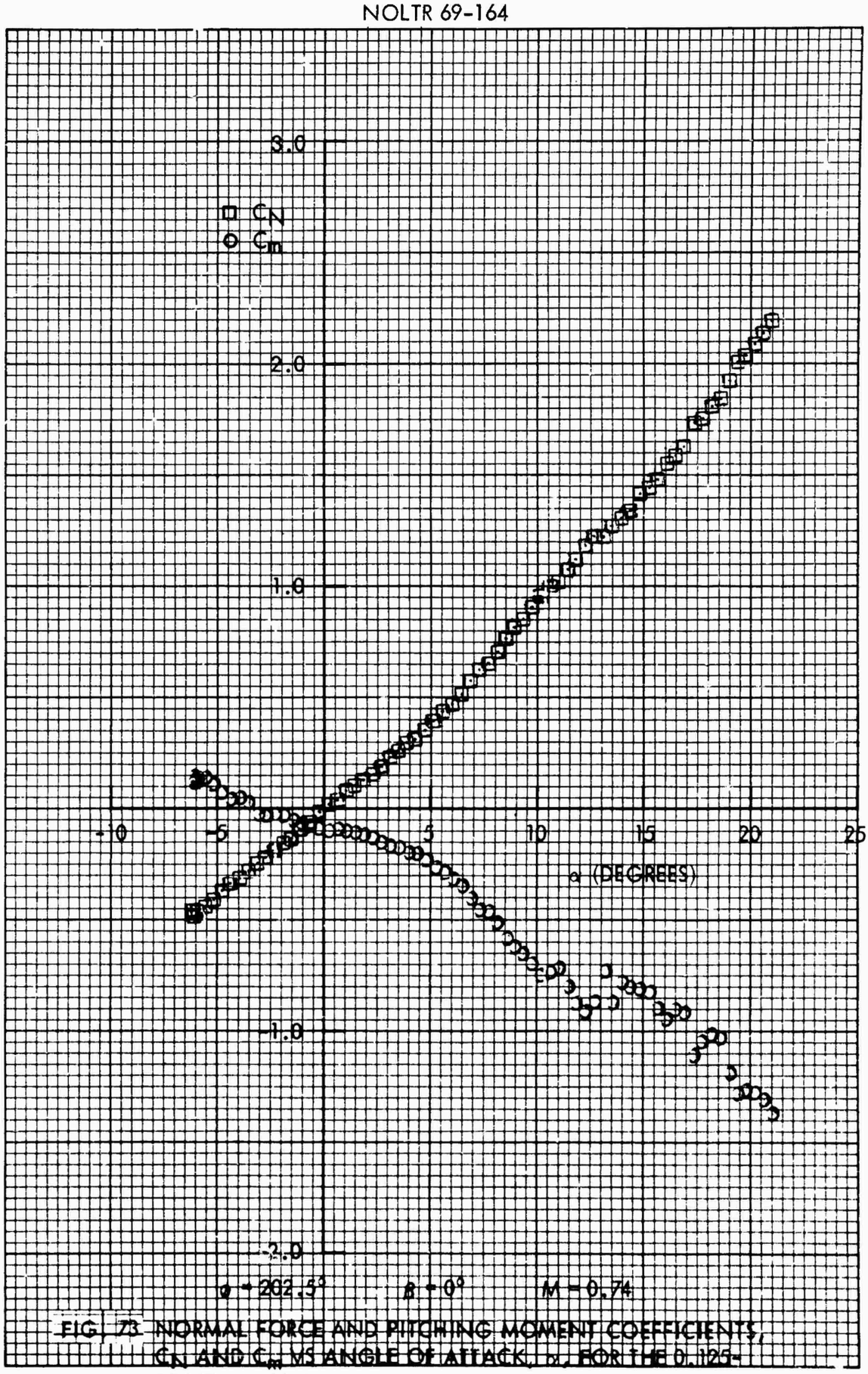

FIG. 73 NORMAL FORCE AND PITCHING MOMENT COEFFICIENTS, C_N AND C_m VS ANGLE OF ATTACK, α, FOR THE 0.125-SCALE MK 82-SNAKEYE BOMB WITH FINS CLOSED

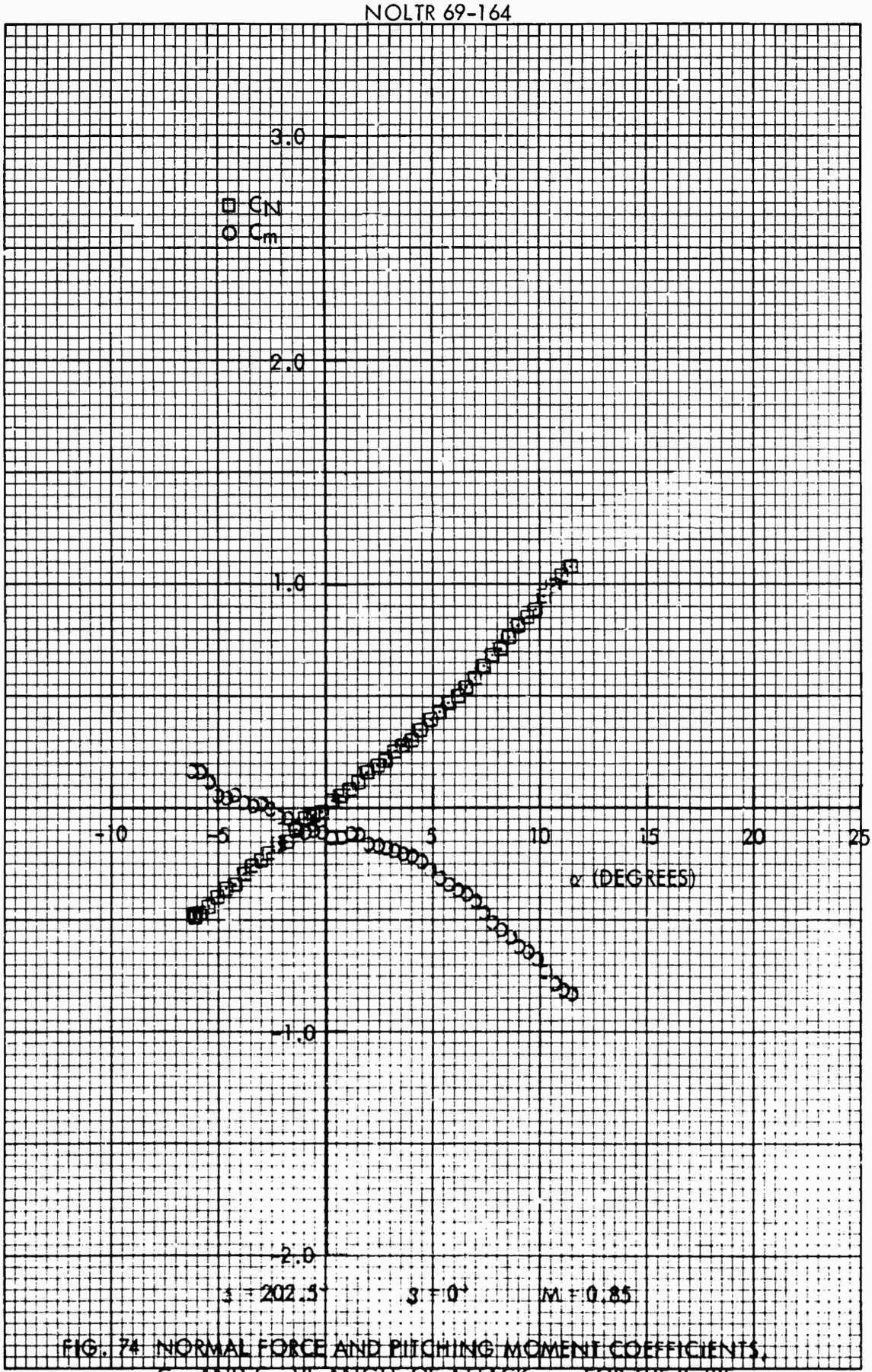

FIG. 74 NORMAL FORCE AND PITCHING MOMENT COEFFICIENTS, C_N AND C_m VS ANGLE OF ATTACK, α, FOR THE 0.125-SCALE MK 82-SNAKEYE BOMB WITH FINS CLOSED

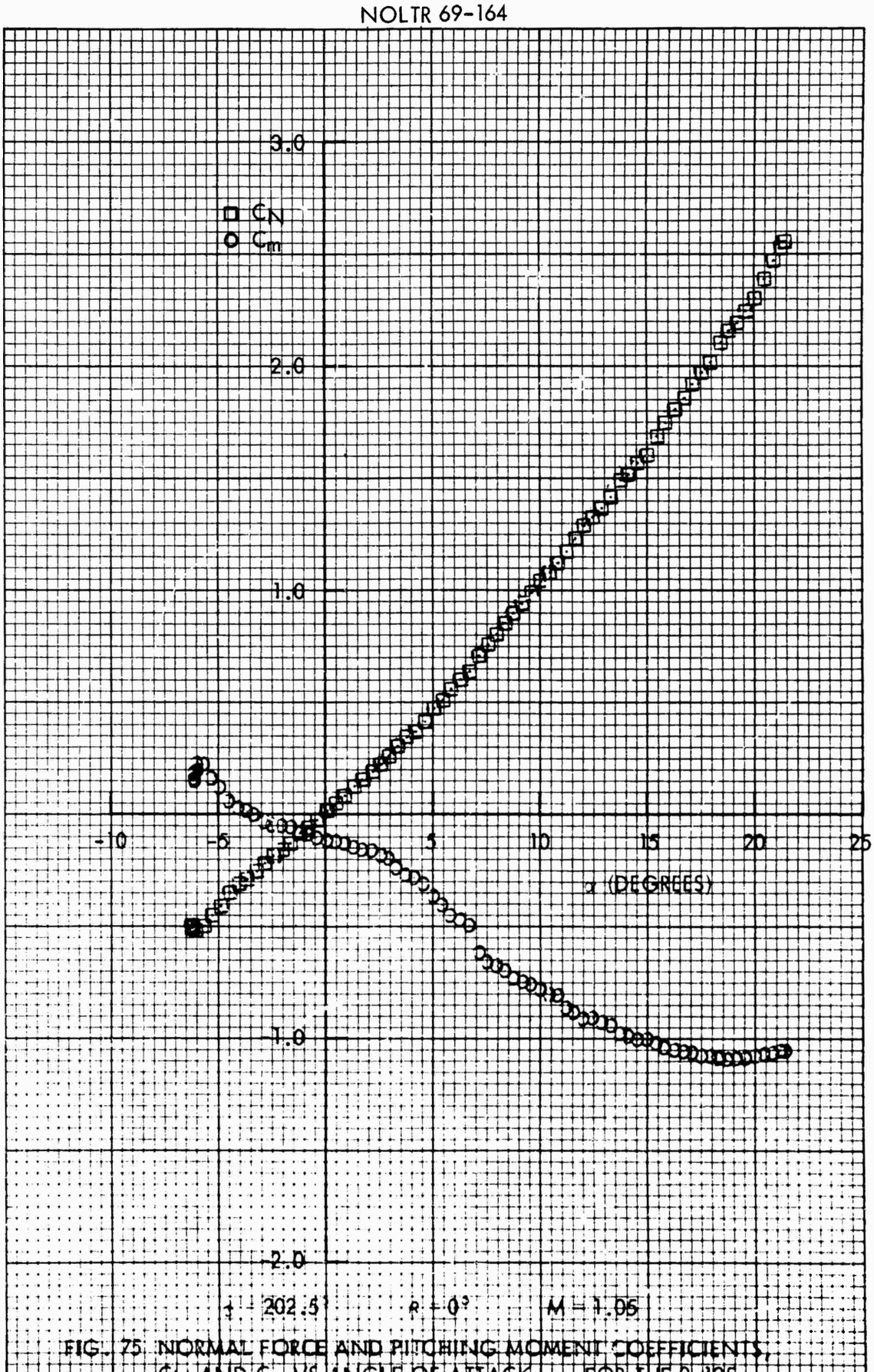

FIG. 75 NORMAL FORCE AND PITCHING MOMENT COEFFICIENTS, C_N AND C_m VS ANGLE OF ATTACK, α, FOR THE 0.125 SCALE MK 82-SNAKEYE BOMB WITH FINS CLOSED

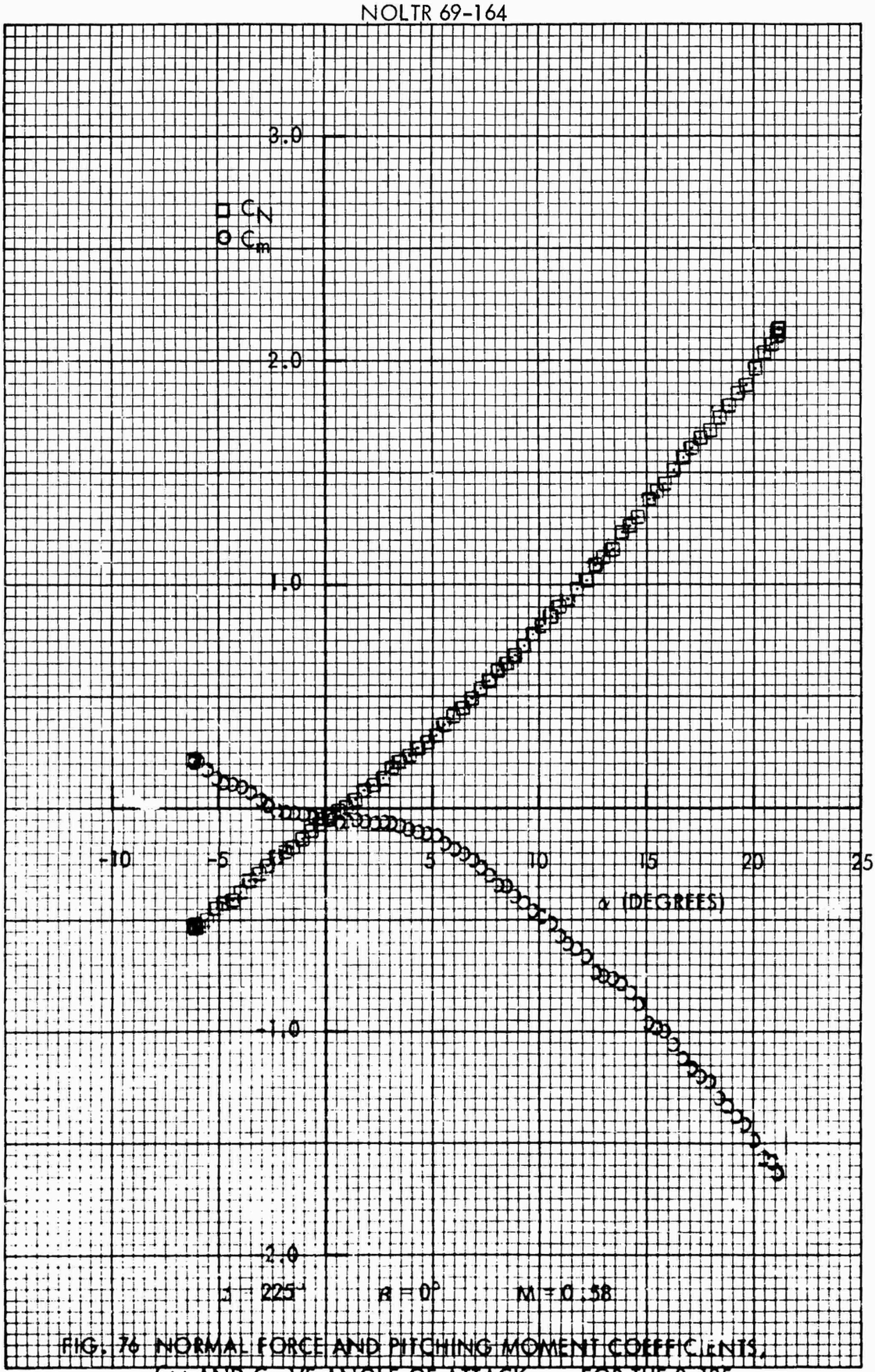

FIG. 76 NORMAL FORCE AND PITCHING MOMENT COEFFICIENTS, C_N AND C_m VS ANGLE OF ATTACK, α, FOR THE 0.125-SCALE MK 82-SNAKEYE BOMB WITH FINS CLOSED

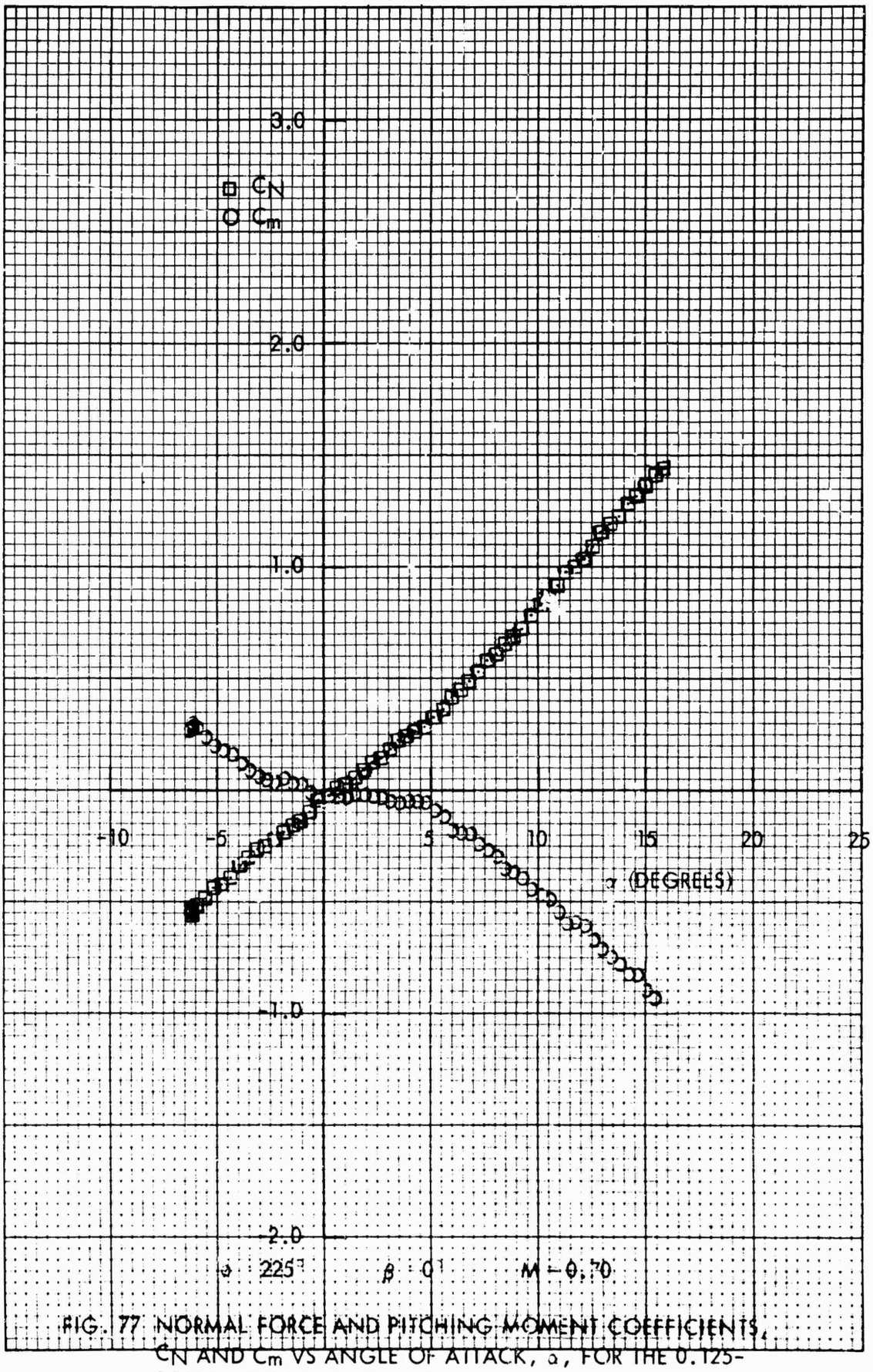

FIG. 77 NORMAL FORCE AND PITCHING MOMENT COEFFICIENTS, C_N AND C_m VS ANGLE OF ATTACK, α, FOR THE 0.125-SCALE MK 82-SNAKEYE BOMB WITH FINS CLOSED

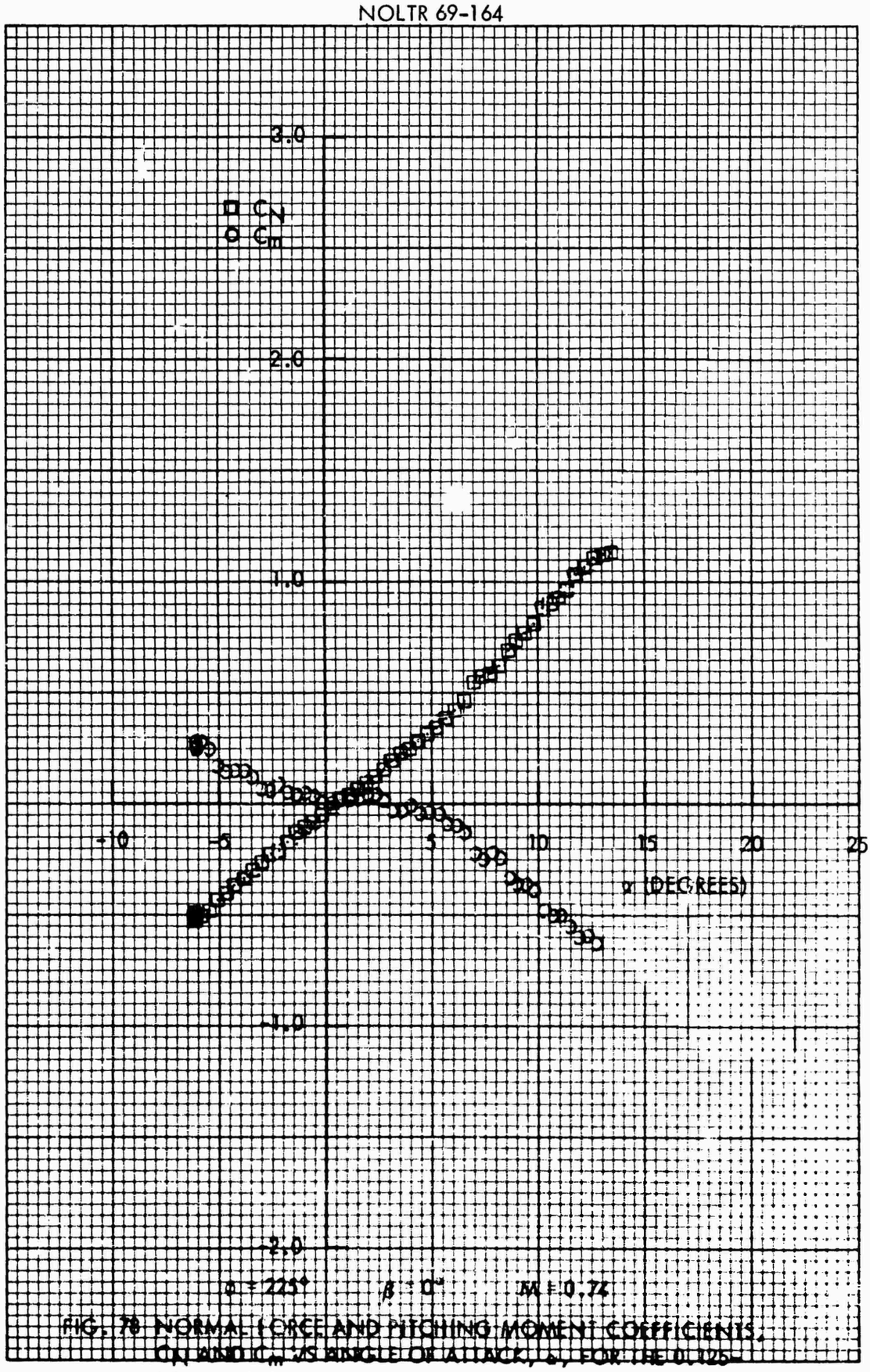

FIG. 78 NORMAL FORCE AND PITCHING MOMENT COEFFICIENTS, C_N AND C_m, AS ANGLE OF ATTACK, α, FOR THE 0.125-SCALE MK 82-SNAKEYE BOMB WITH FINS CLOSED

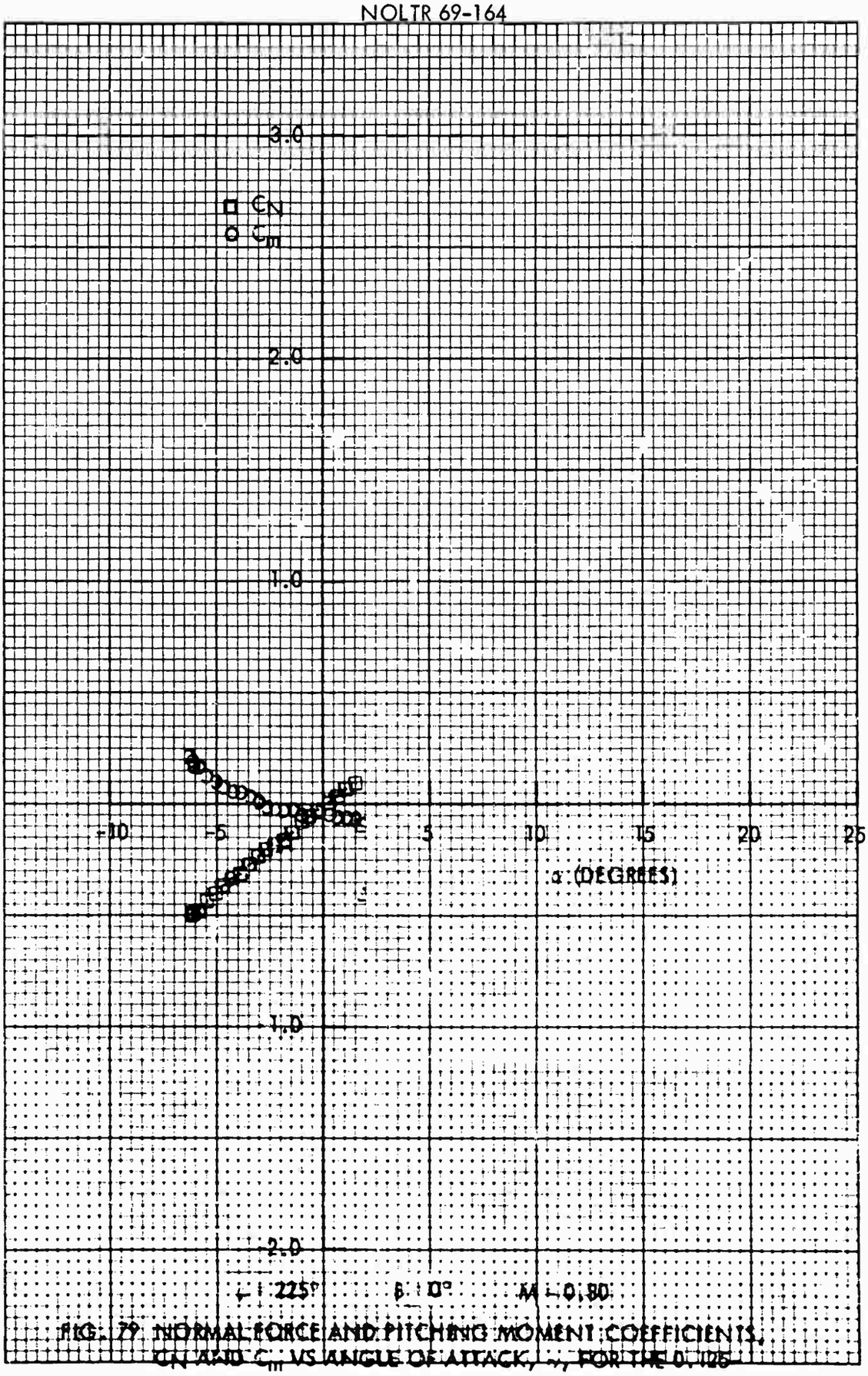

FIG. 79 NORMAL FORCE AND PITCHING MOMENT COEFFICIENTS, C_N AND C_m VS ANGLE OF ATTACK, α, FOR THE 0.125 SCALE MK 82-SNAKEYE BOMB WITH FINS CLOSED

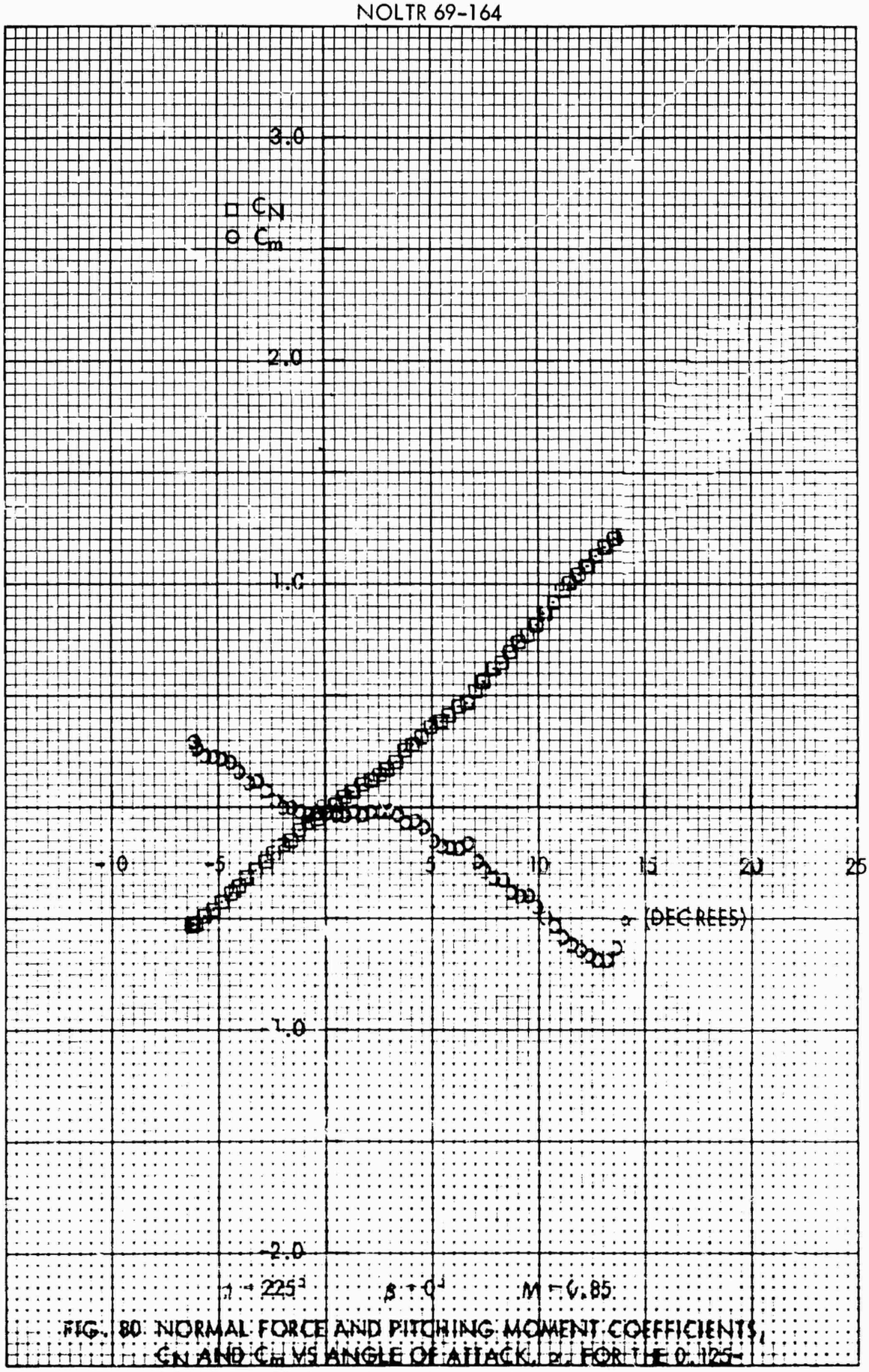

FIG. 80 NORMAL FORCE AND PITCHING MOMENT COEFFICIENTS, C_N AND C_m VS ANGLE OF ATTACK, α, FOR THE 0.125-SCALE MK 82-SNAKEYE BOMB WITH FINS CLOSED

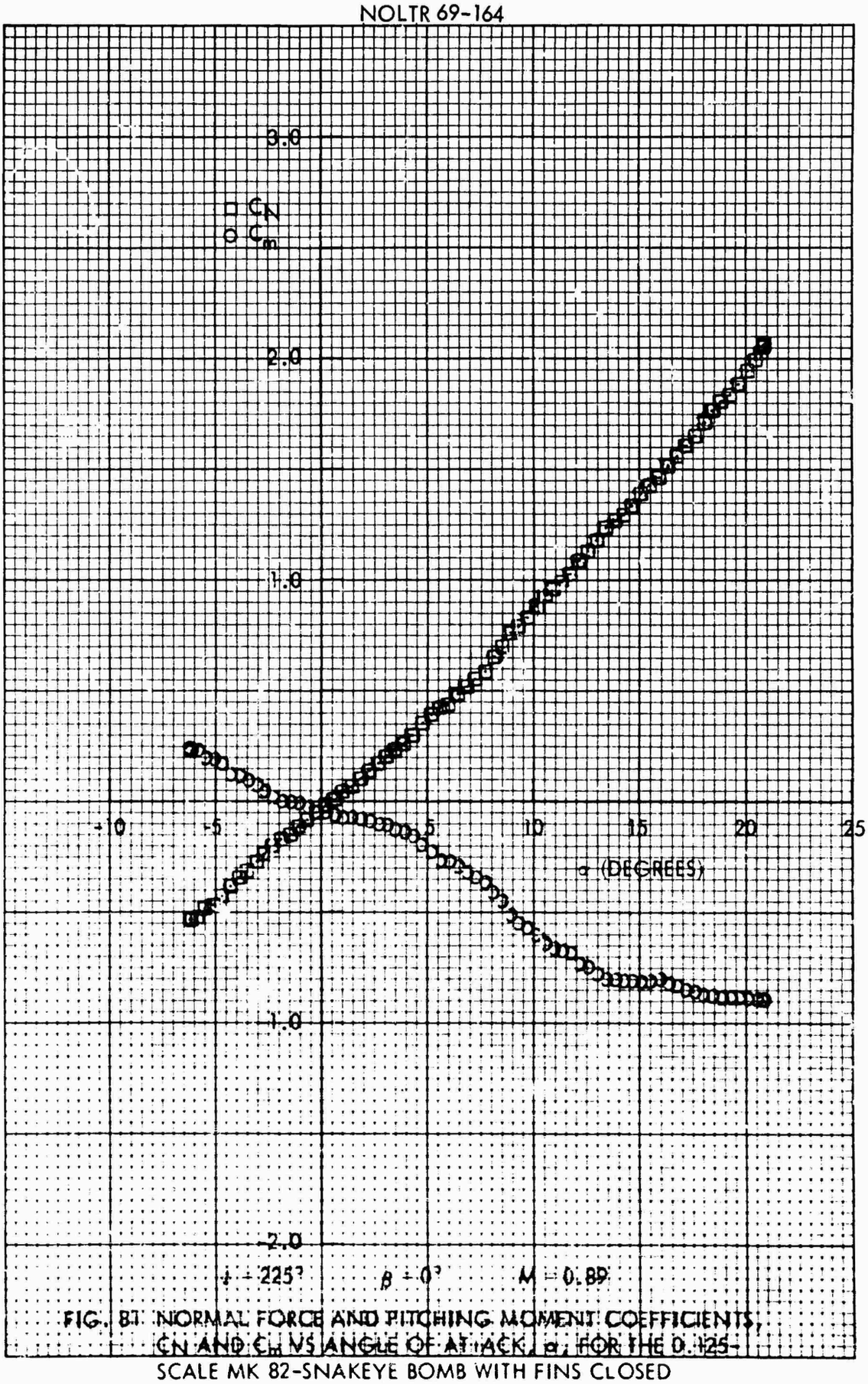

FIG. 87 NORMAL FORCE AND PITCHING MOMENT COEFFICIENTS, C_N AND C_m VS ANGLE OF ATTACK, α, FOR THE 0.125-SCALE MK 82-SNAKEYE BOMB WITH FINS CLOSED

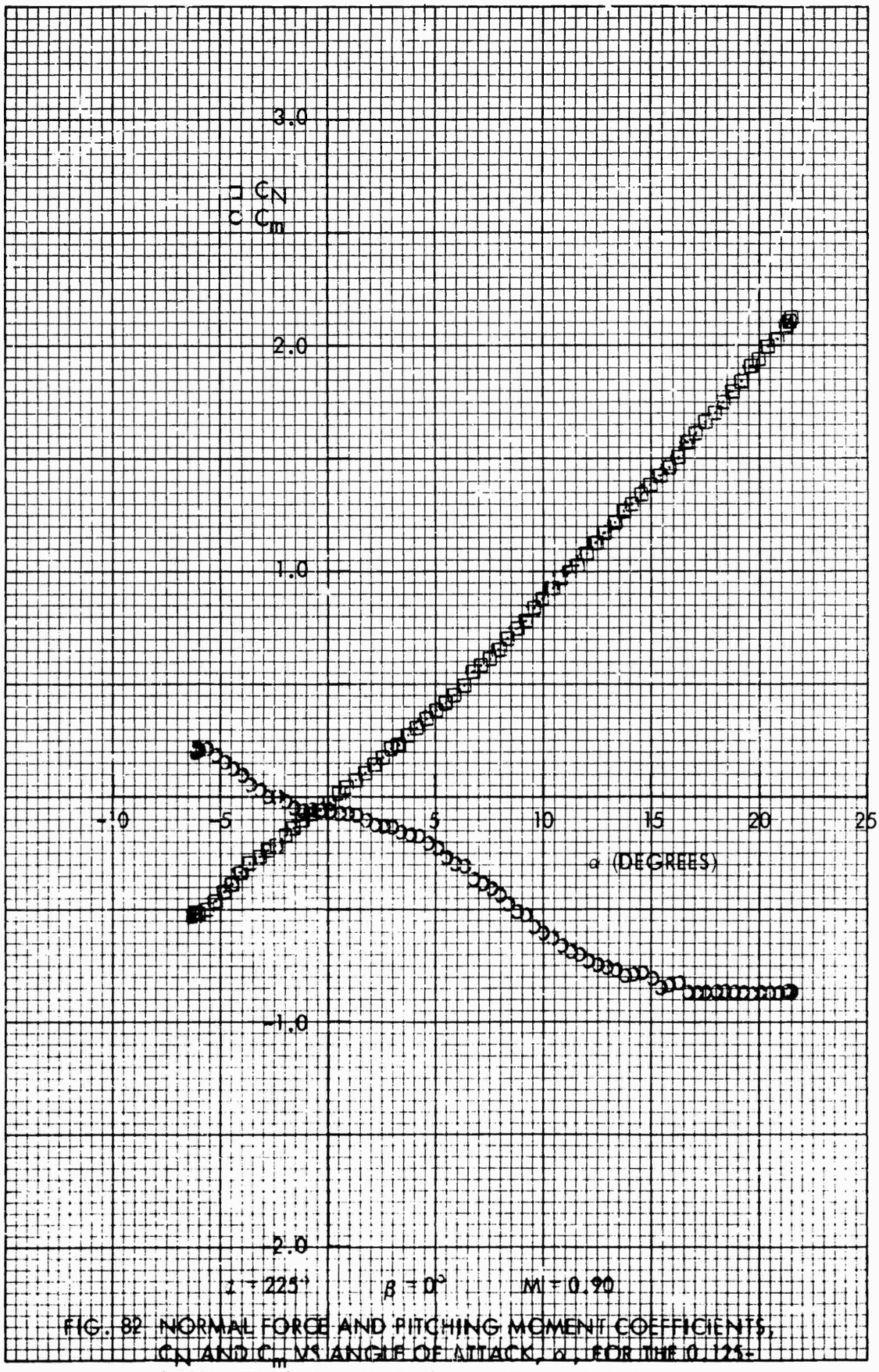

FIG. 82 NORMAL FORCE AND PITCHING MOMENT COEFFICIENTS, C_N AND C_m VS ANGLE OF ATTACK, α, FOR THE 0.125-SCALE MK 82-SNAKEYE BOMB WITH FINS CLOSED

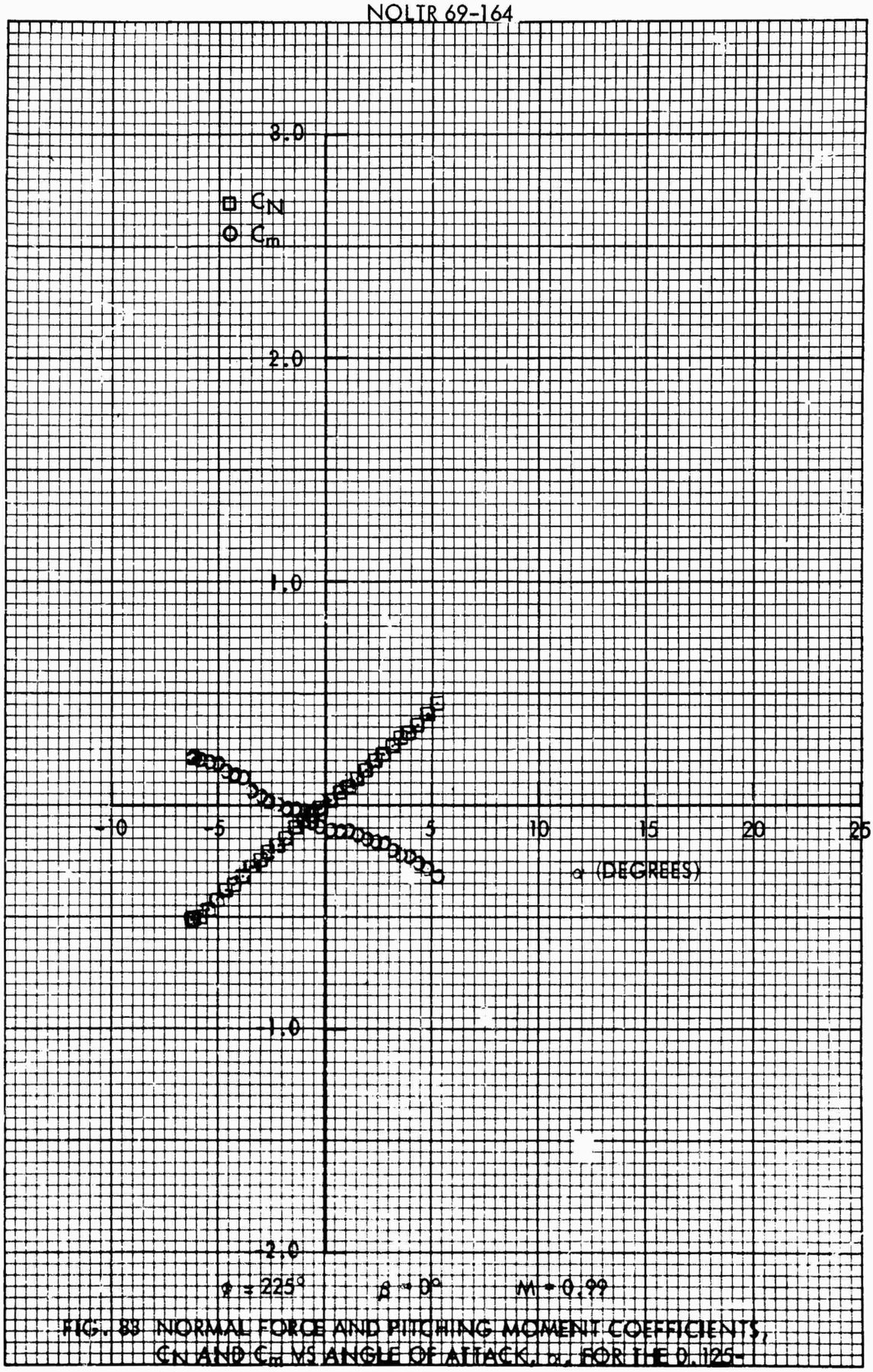

FIG. 83 NORMAL FORCE AND PITCHING MOMENT COEFFICIENTS, C_N AND C_m VS ANGLE OF ATTACK, α, FOR THE 0.126-SCALE MK 82-SNAKEYE BOMB WITH FINS CLOSED

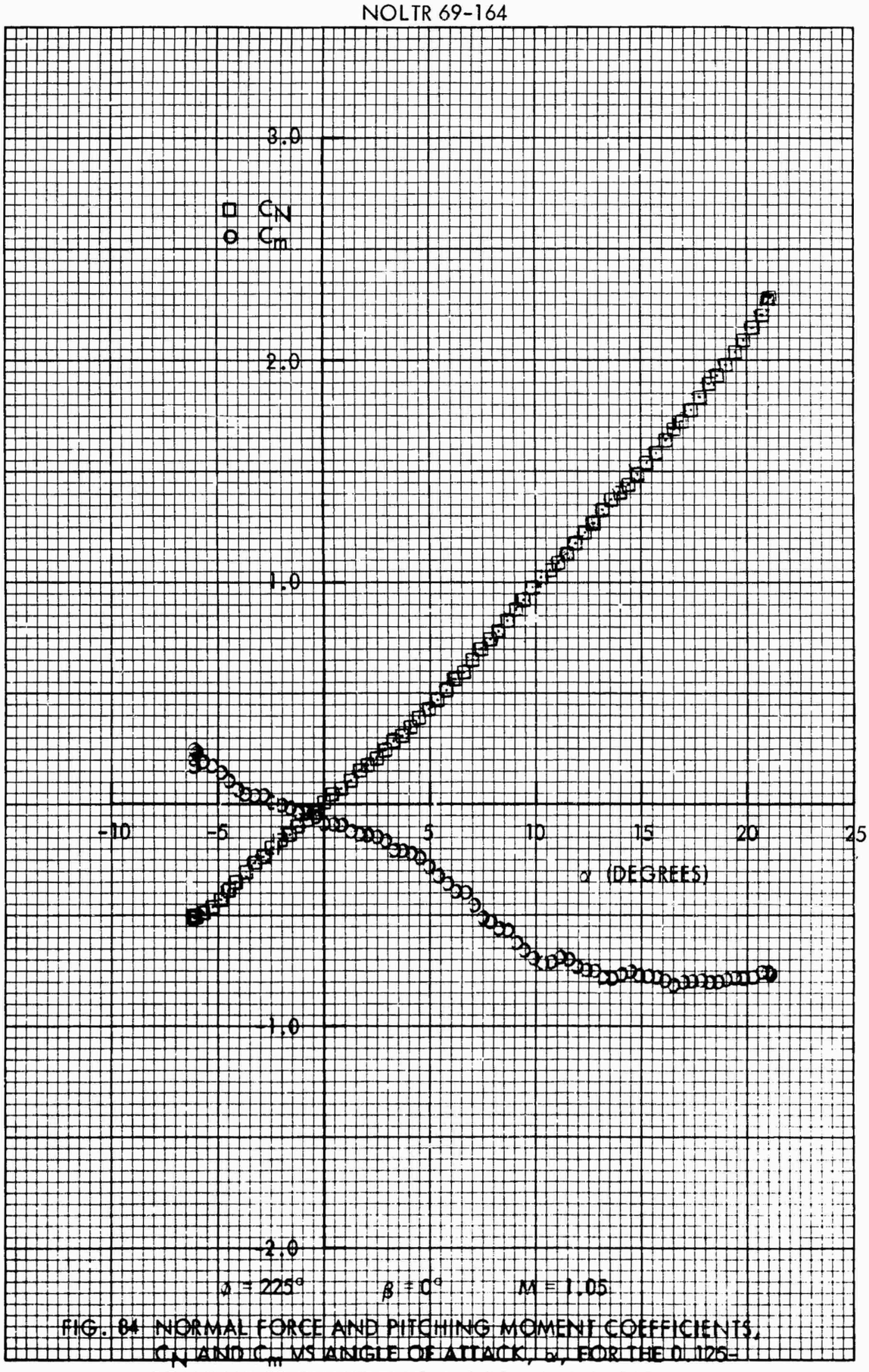

FIG. 84 NORMAL FORCE AND PITCHING MOMENT COEFFICIENTS, C_N AND C_m VS ANGLE OF ATTACK, α, FOR THE 0.125-SCALE MK 82-SNAKEYE BOMB WITH FINS CLOSED

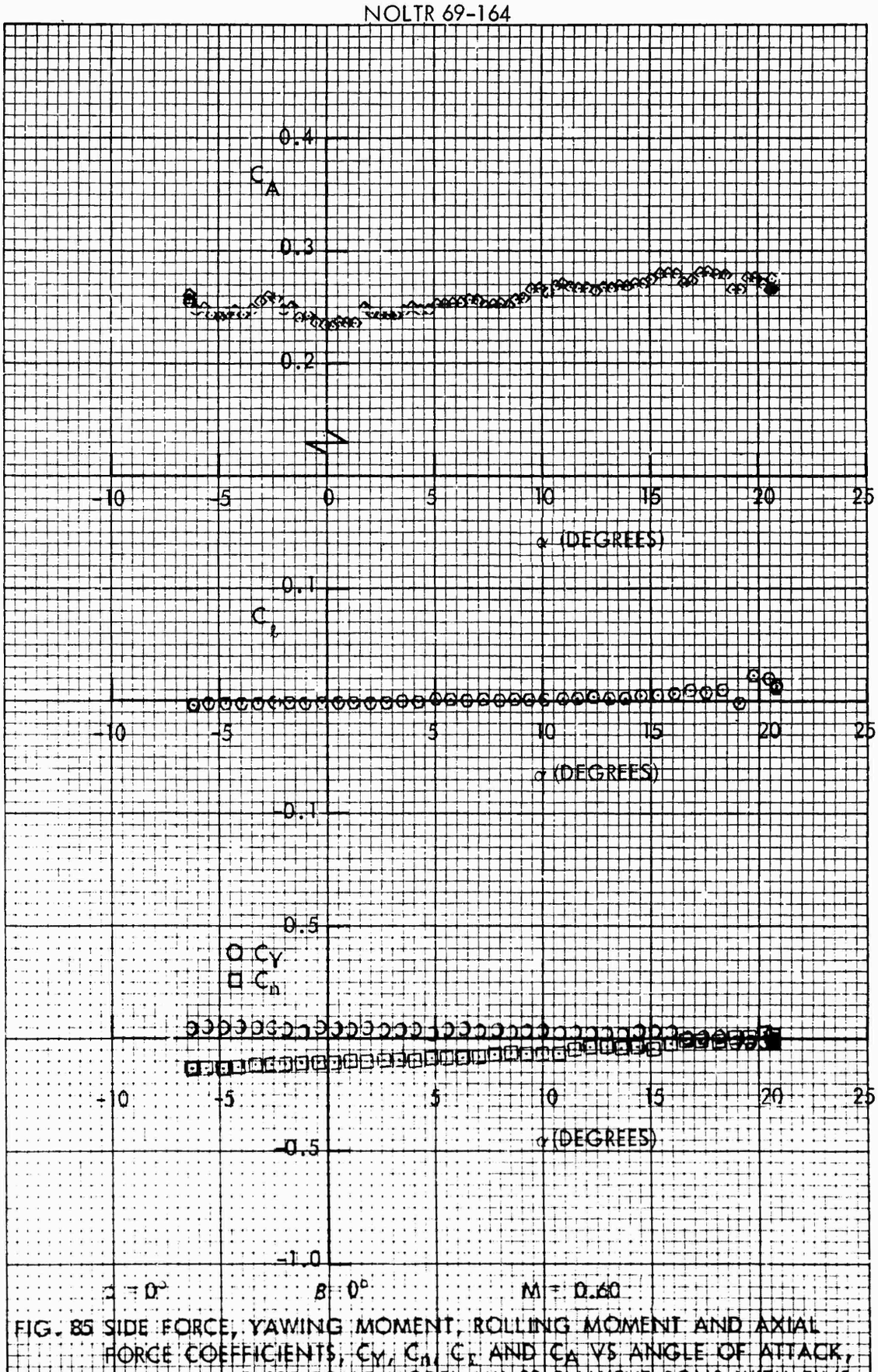

FIG. 85 SIDE FORCE, YAWING MOMENT, ROLLING MOMENT AND AXIAL FORCE COEFFICIENTS, C_Y, C_n, C_ℓ AND C_A VS ANGLE OF ATTACK, α, FOR THE 0.125-SCALE MODEL MK 82-SNAKEYE BOMB WITH FINS CLOSED

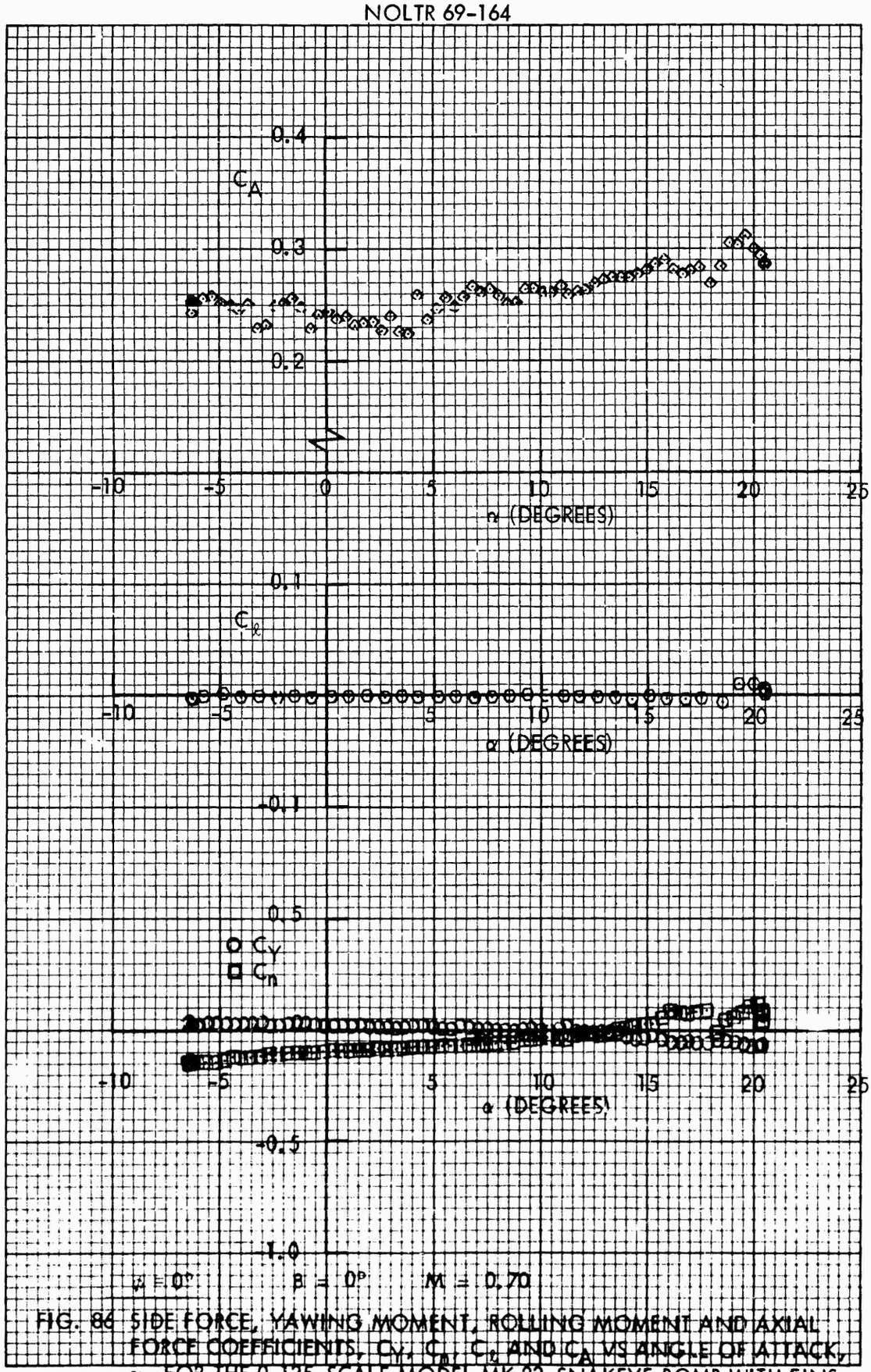

FIG. 86 SIDE FORCE, YAWING MOMENT, ROLLING MOMENT AND AXIAL FORCE COEFFICIENTS, C_Y, C_n, C_ℓ AND C_A VS ANGLE OF ATTACK, α, FOR THE 0.125-SCALE MODEL MK 82-SNAKEYE BOMB WITH FINS CLOSED

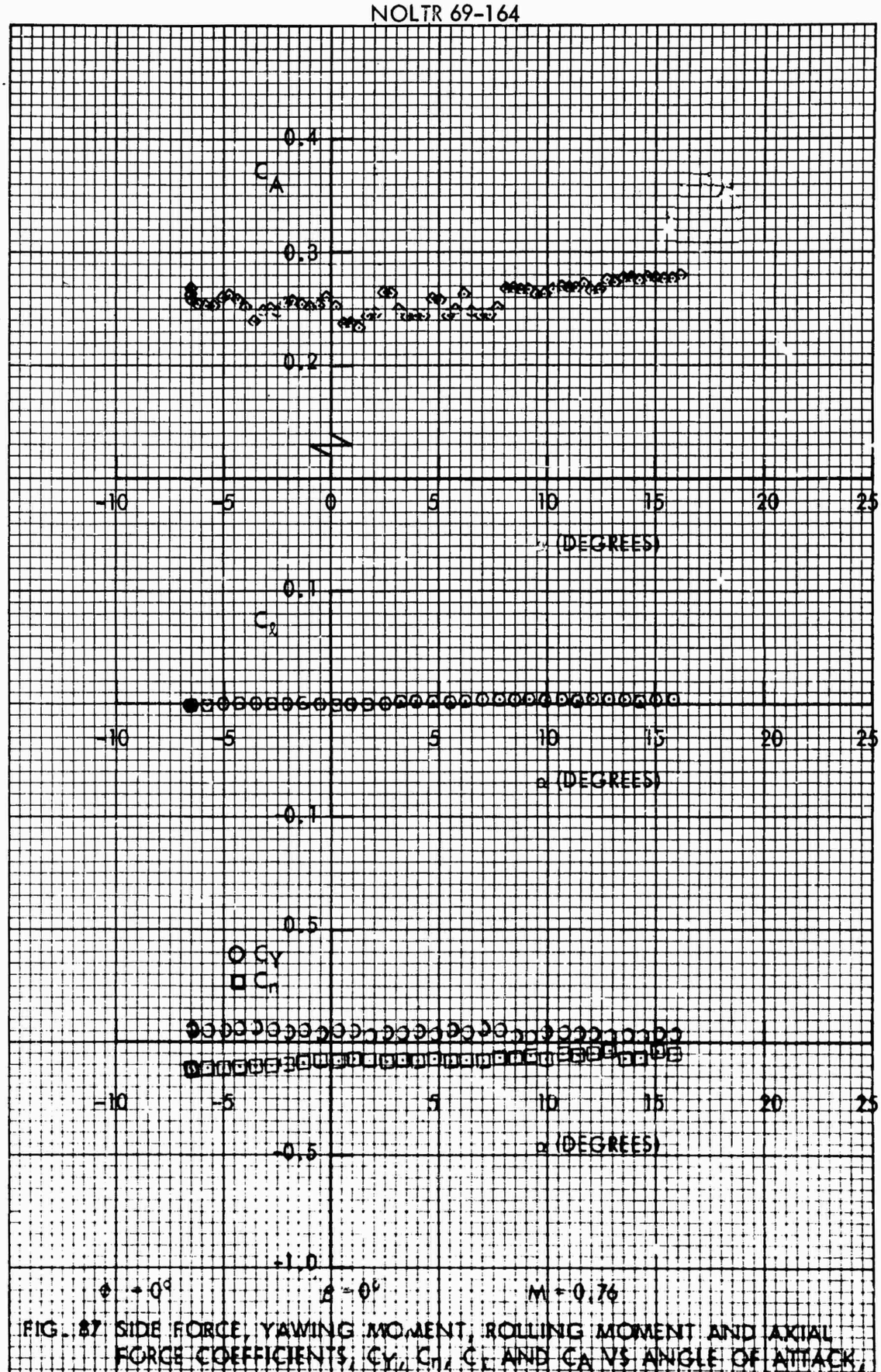

FIG. 87 SIDE FORCE, YAWING MOMENT, ROLLING MOMENT AND AXIAL FORCE COEFFICIENTS, C_Y, C_n, C_ℓ AND C_A VS ANGLE OF ATTACK, α, FOR THE 0.125-SCALE MODEL MK 82-SNAKEYE BOMB WITH FINS CLOSED

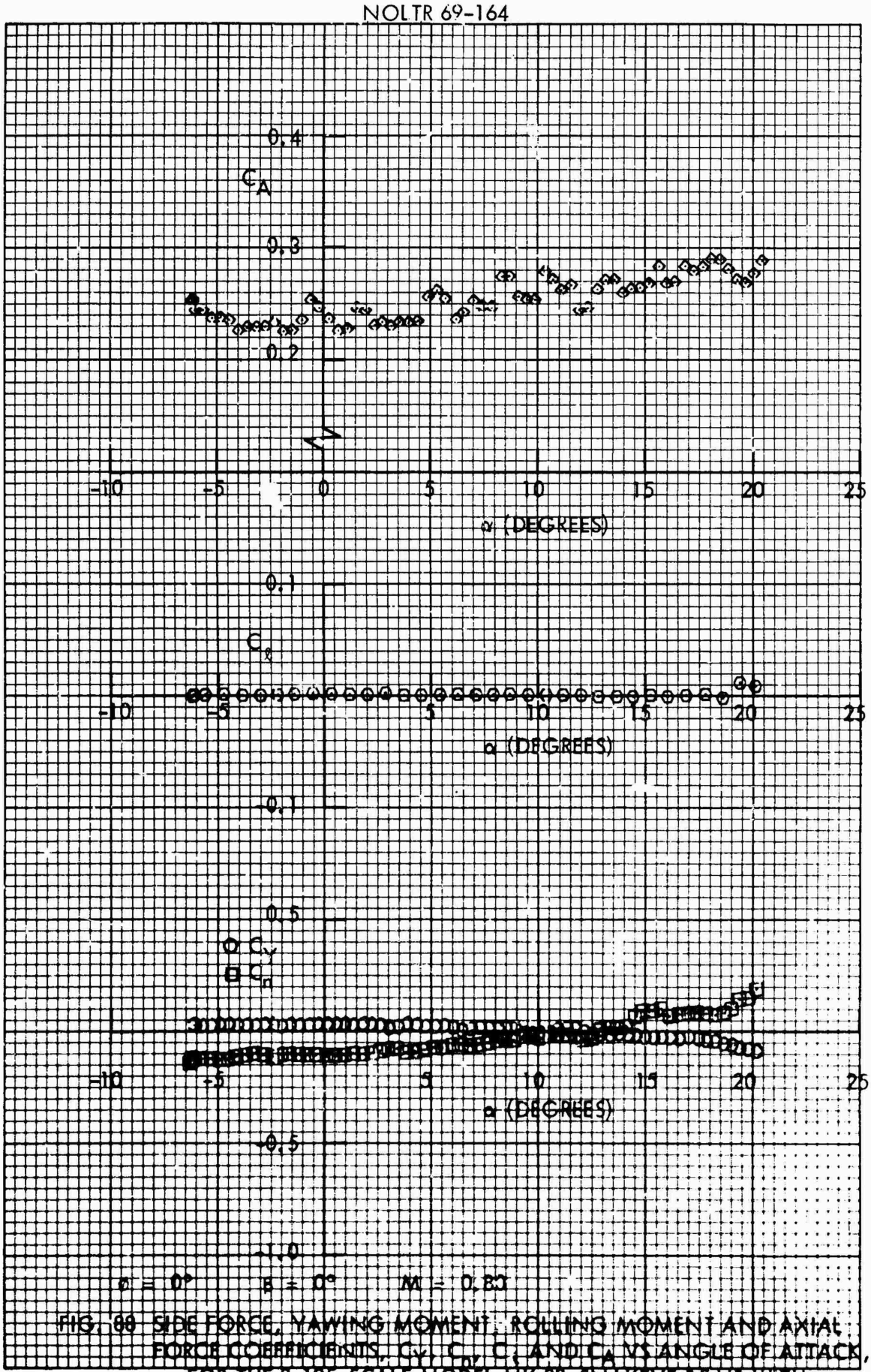

FIG. 88 SIDE FORCE, YAWING MOMENT, ROLLING MOMENT AND AXIAL FORCE COEFFICIENTS, C_Y, C_n, C_ℓ AND C_A VS ANGLE OF ATTACK, α, FOR THE 0.125-SCALE MODEL MK 82-SNAKEYE BOMB WITH FINS CLOSED

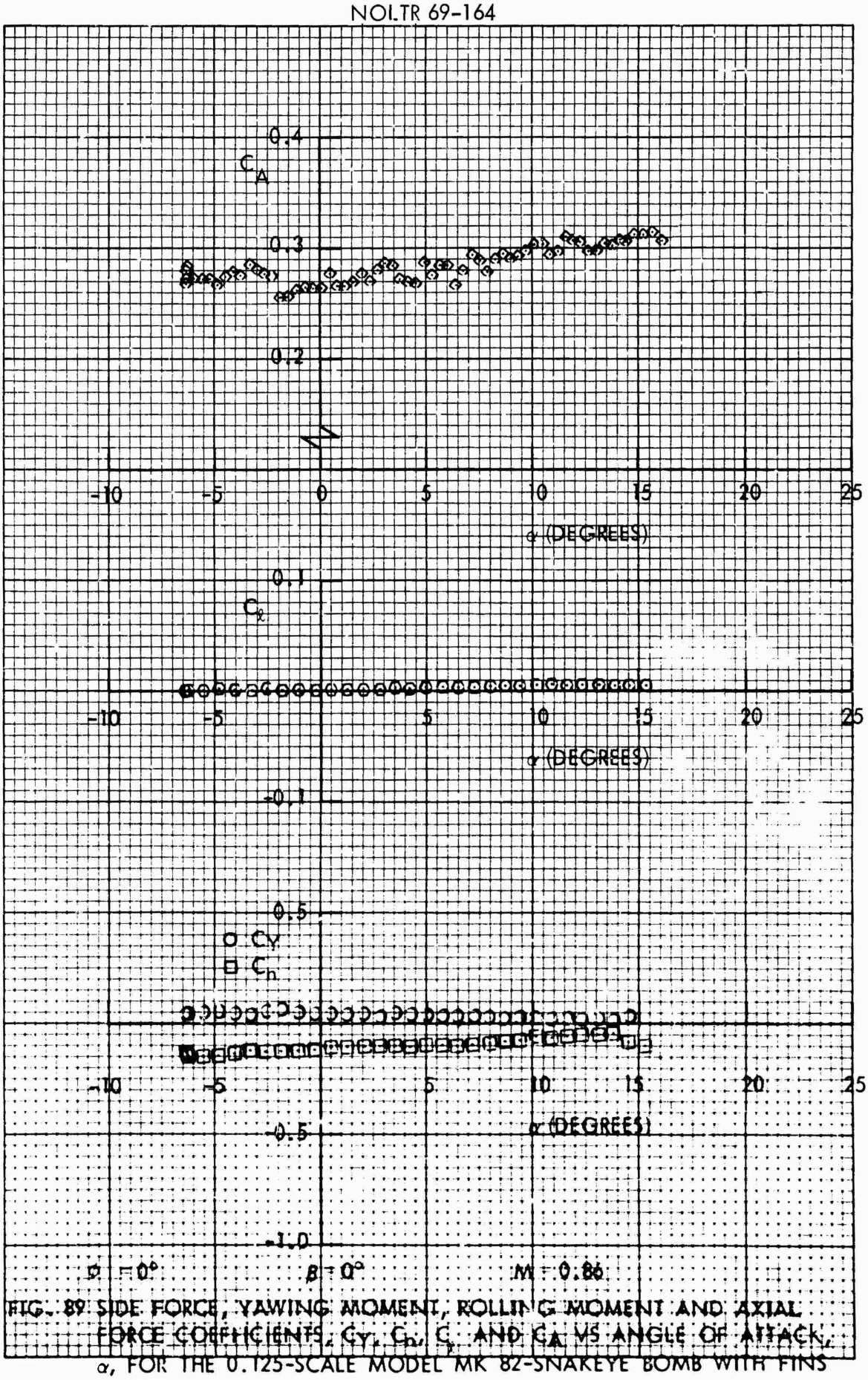

FIG. 89 SIDE FORCE, YAWING MOMENT, ROLLING MOMENT AND AXIAL FORCE COEFFICIENTS, C_Y, C_n, C_ℓ, AND C_A VS ANGLE OF ATTACK, α, FOR THE 0.125-SCALE MODEL MK 82-SNAKEYE BOMB WITH FINS CLOSED

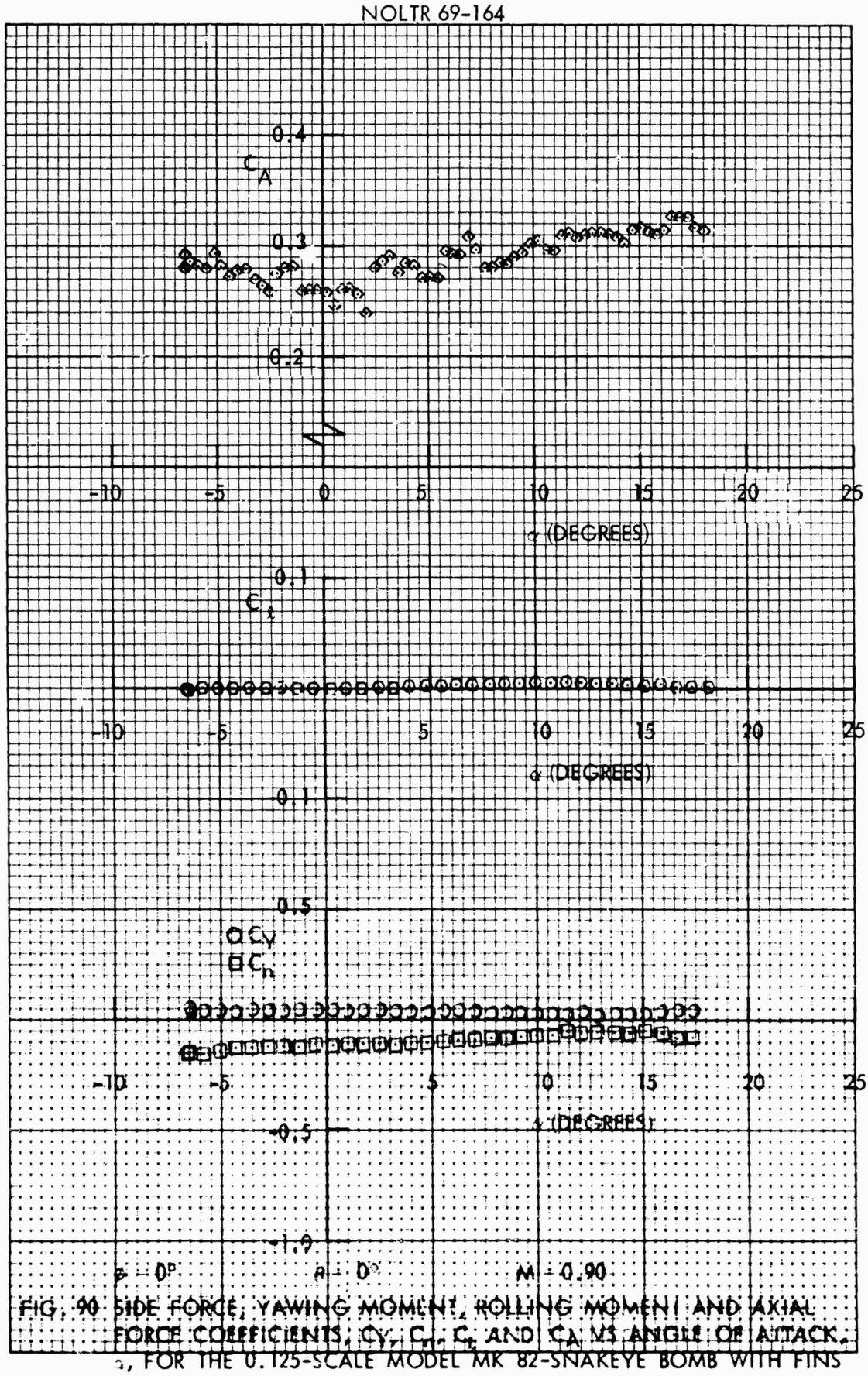

FIG. 90 SIDE FORCE, YAWING MOMENT, ROLLING MOMENT AND AXIAL FORCE COEFFICIENTS, C_Y, C_n, C_ℓ AND C_A VS ANGLE OF ATTACK, α, FOR THE 0.125-SCALE MODEL MK 82-SNAKEYE BOMB WITH FINS CLOSED

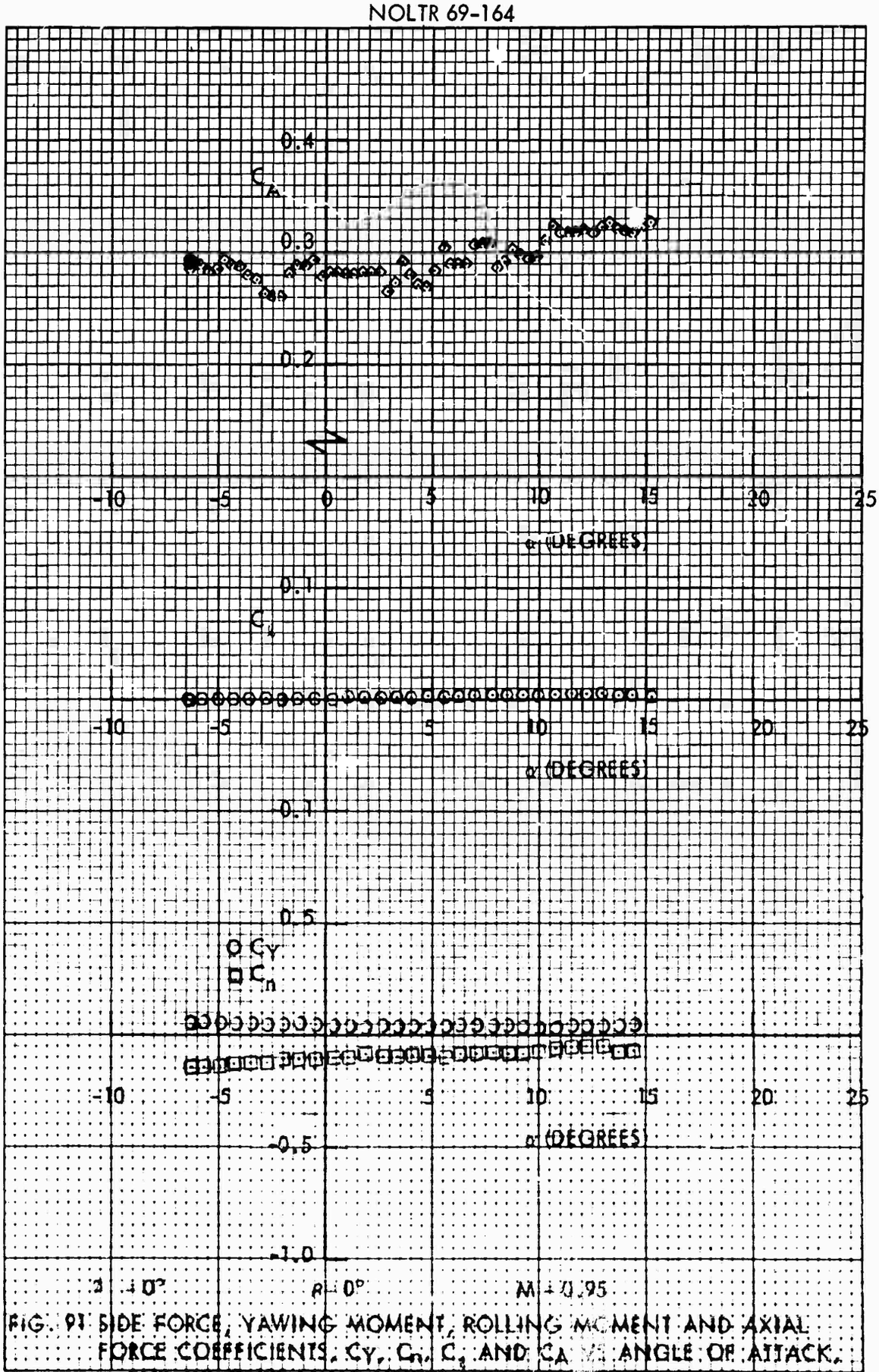

FIG. 91 SIDE FORCE, YAWING MOMENT, ROLLING MOMENT AND AXIAL FORCE COEFFICIENTS, C_Y, C_n, C_l, AND C_A VS. ANGLE OF ATTACK, α, FOR THE 0.125-SCALE MODEL MK 82-SNAKEYE BOMB WITH FINS CLOSED

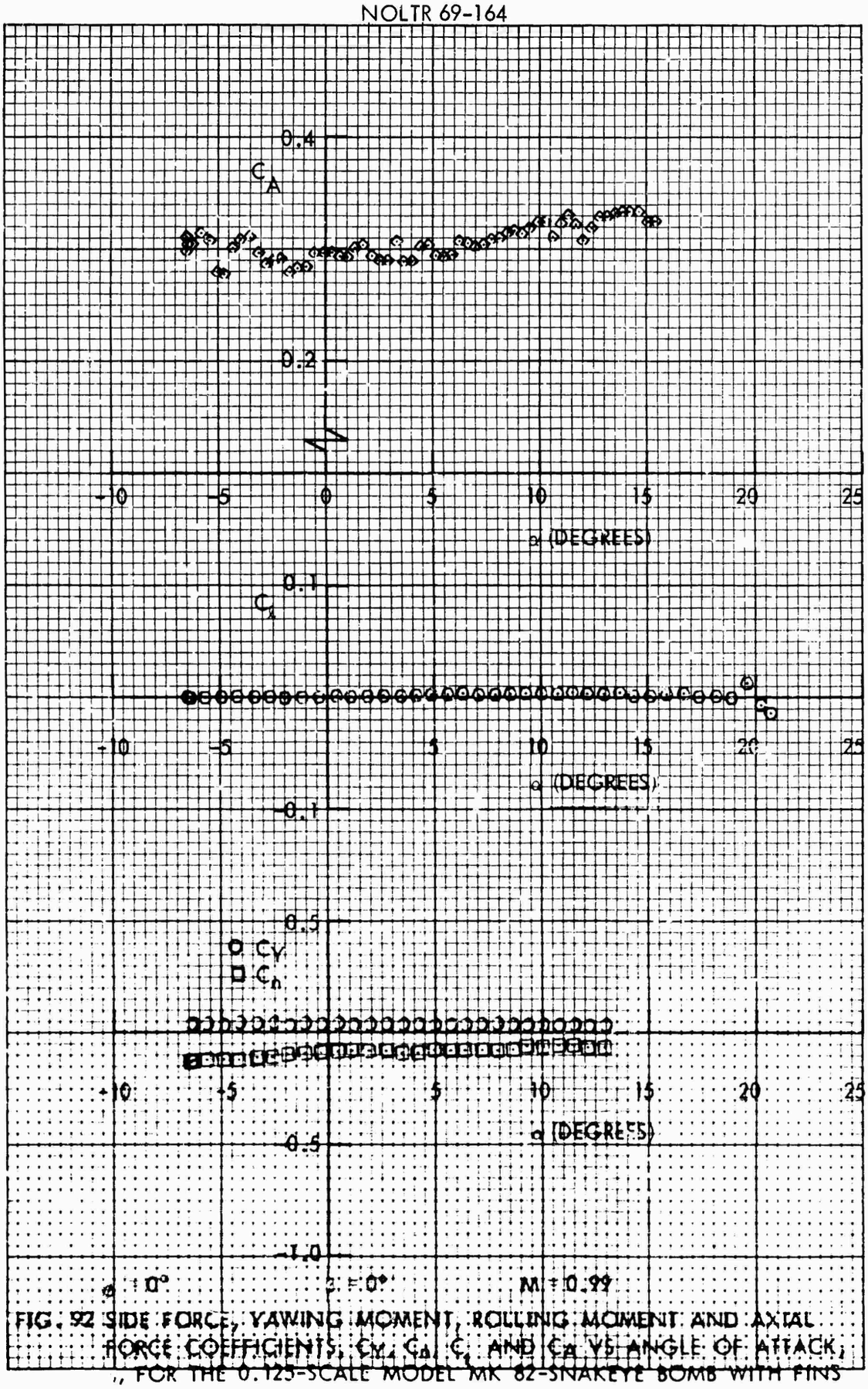

FIG. 92 SIDE FORCE, YAWING MOMENT, ROLLING MOMENT AND AXIAL FORCE COEFFICIENTS, C_M, C_n, C_l, AND C_A VS ANGLE OF ATTACK, FOR THE 0.125-SCALE MODEL MK 82-SNAKEYE BOMB WITH FINS CLOSED

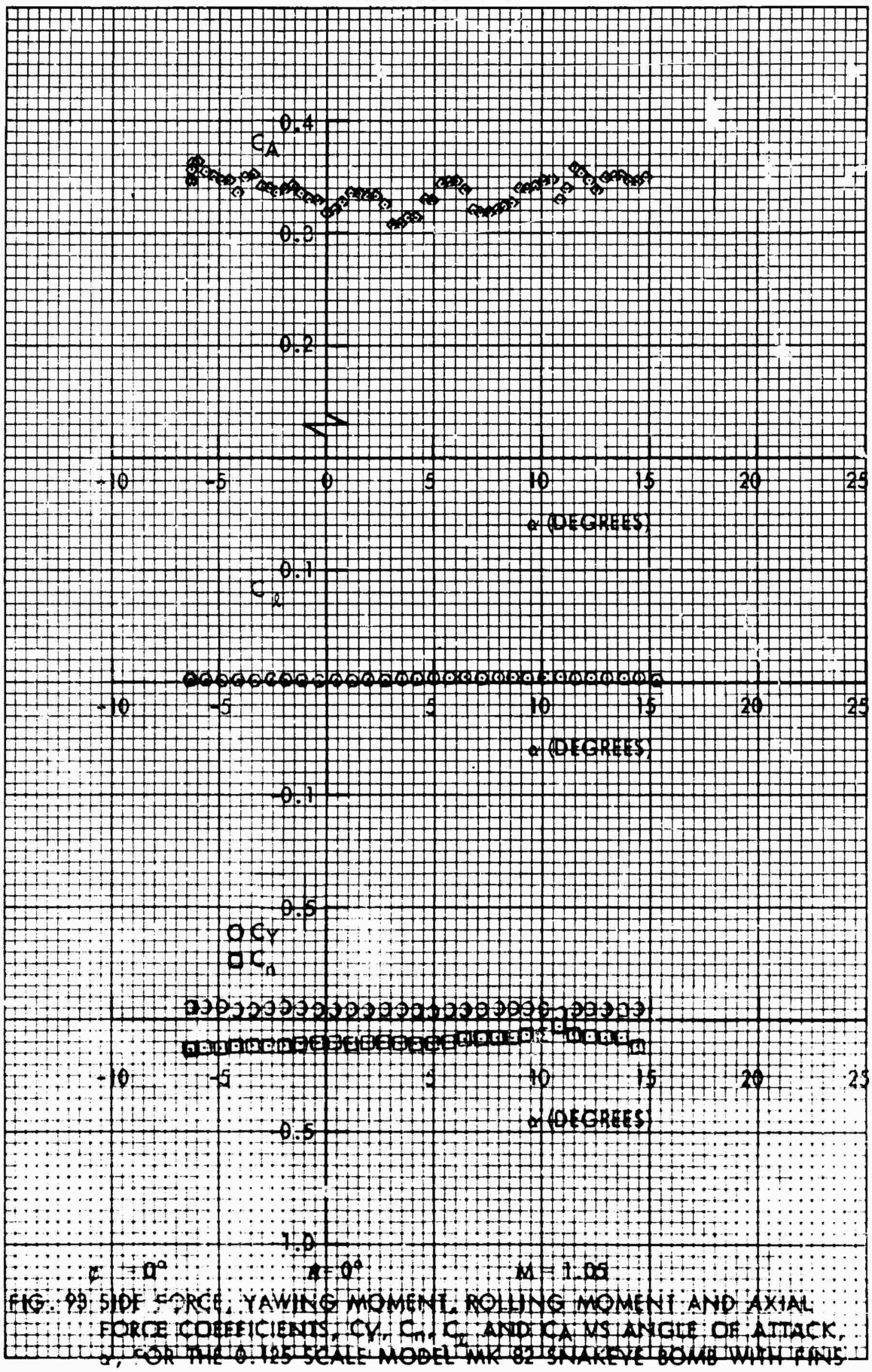

FIG. 93 SIDE FORCE, YAWING MOMENT, ROLLING MOMENT AND AXIAL FORCE COEFFICIENTS, C_Y, C_n, C_ℓ AND C_A VS ANGLE OF ATTACK, α, FOR THE 0.125 SCALE MODEL MK 82 SNAKEYE BOMB WITH FINS CLOSED

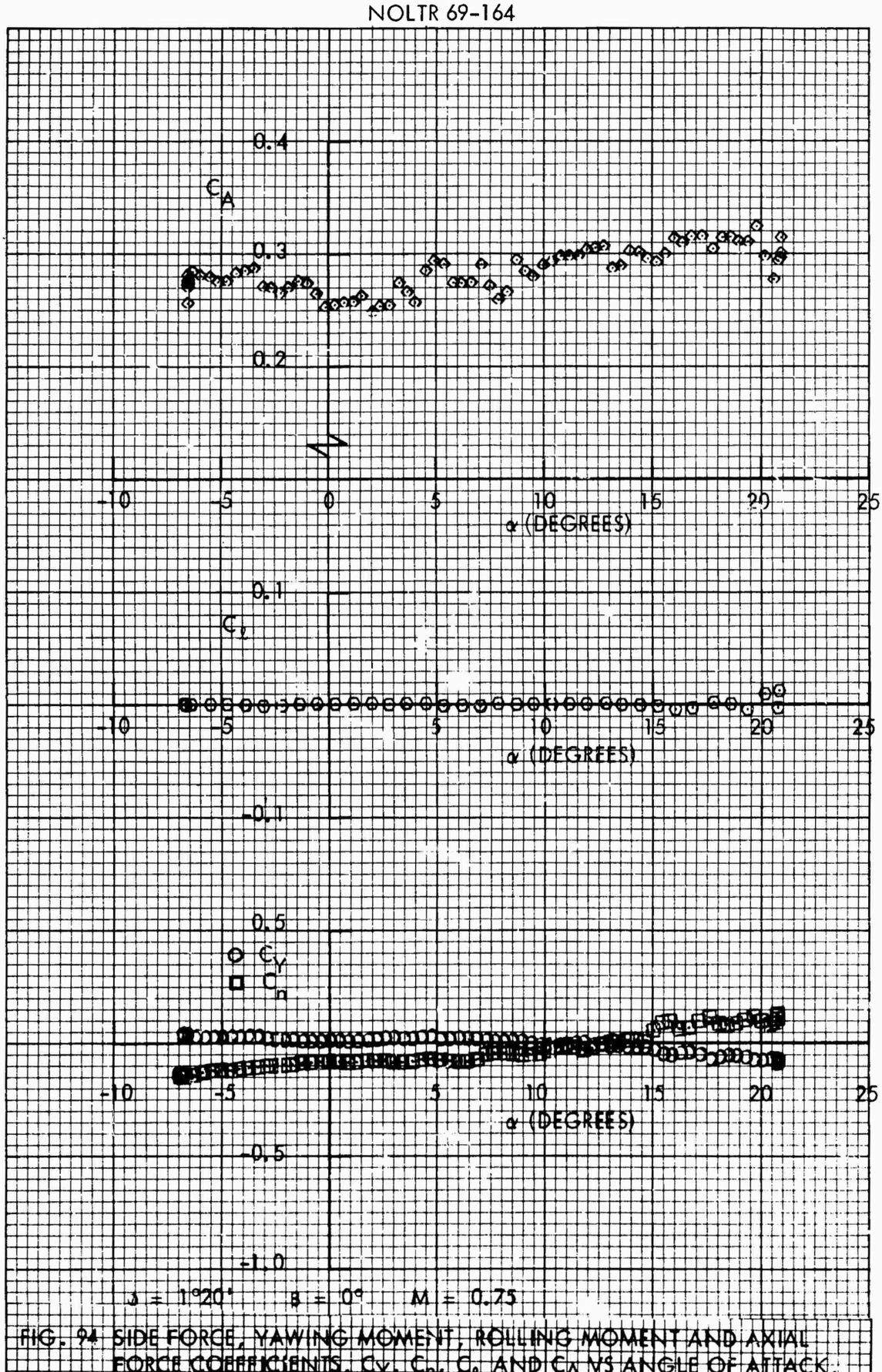

FIG. 94 SIDE FORCE, YAWING MOMENT, ROLLING MOMENT AND AXIAL FORCE COEFFICIENTS, C_Y, C_n, C_ℓ AND C_A VS ANGLE OF ATTACK, α, FOR THE 0.125-SCALE MODEL MK 82-SNAKEYE BOMB WITH FINS CLOSED

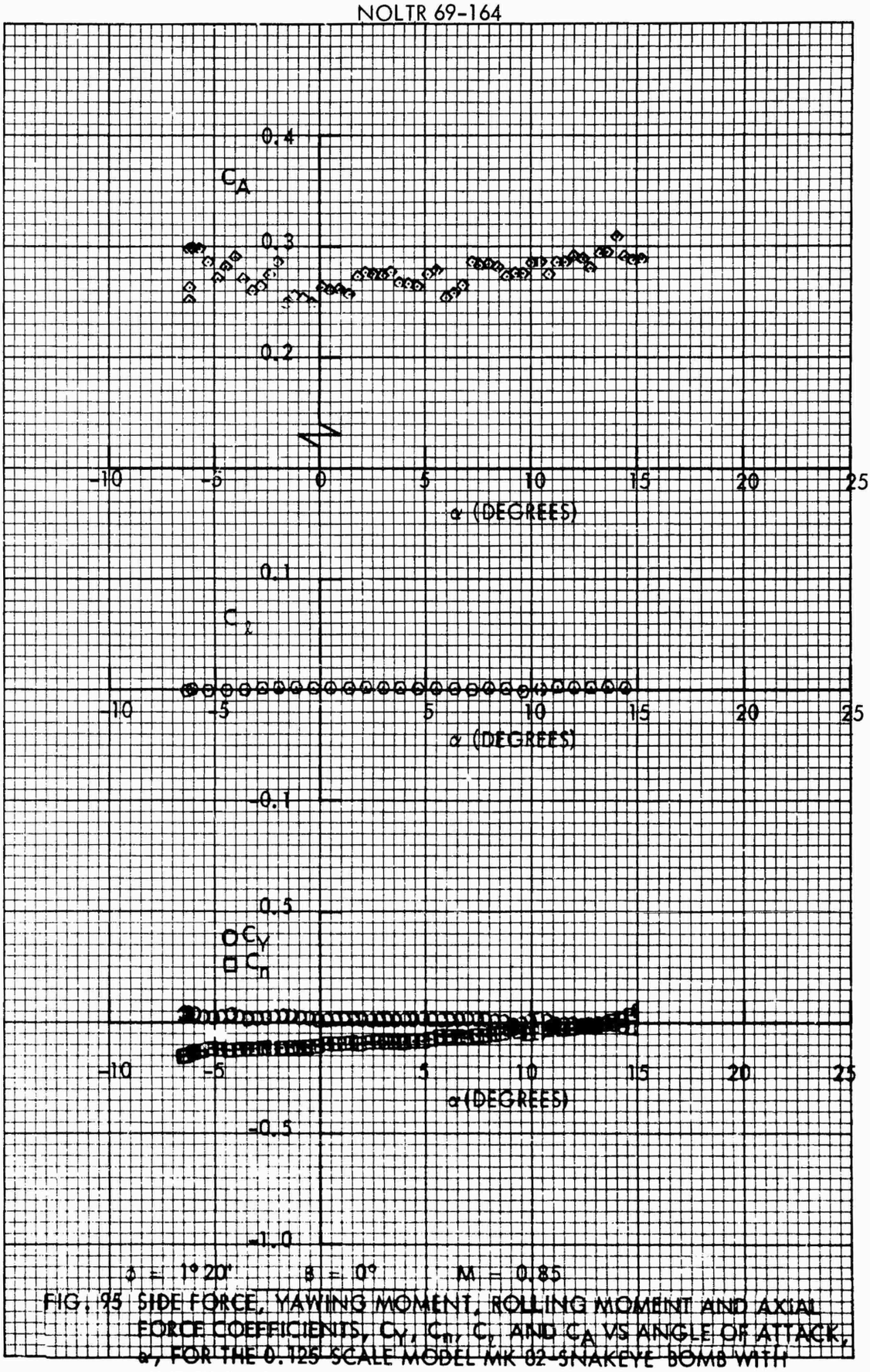

FIG. 95 SIDE FORCE, YAWING MOMENT, ROLLING MOMENT AND AXIAL FORCE COEFFICIENTS, C_Y, C_n, C_ℓ, AND C_A VS ANGLE OF ATTACK, α, FOR THE 0.125 SCALE MODEL MK 82 SNAKEYE BOMB WITH FINS CLOSED

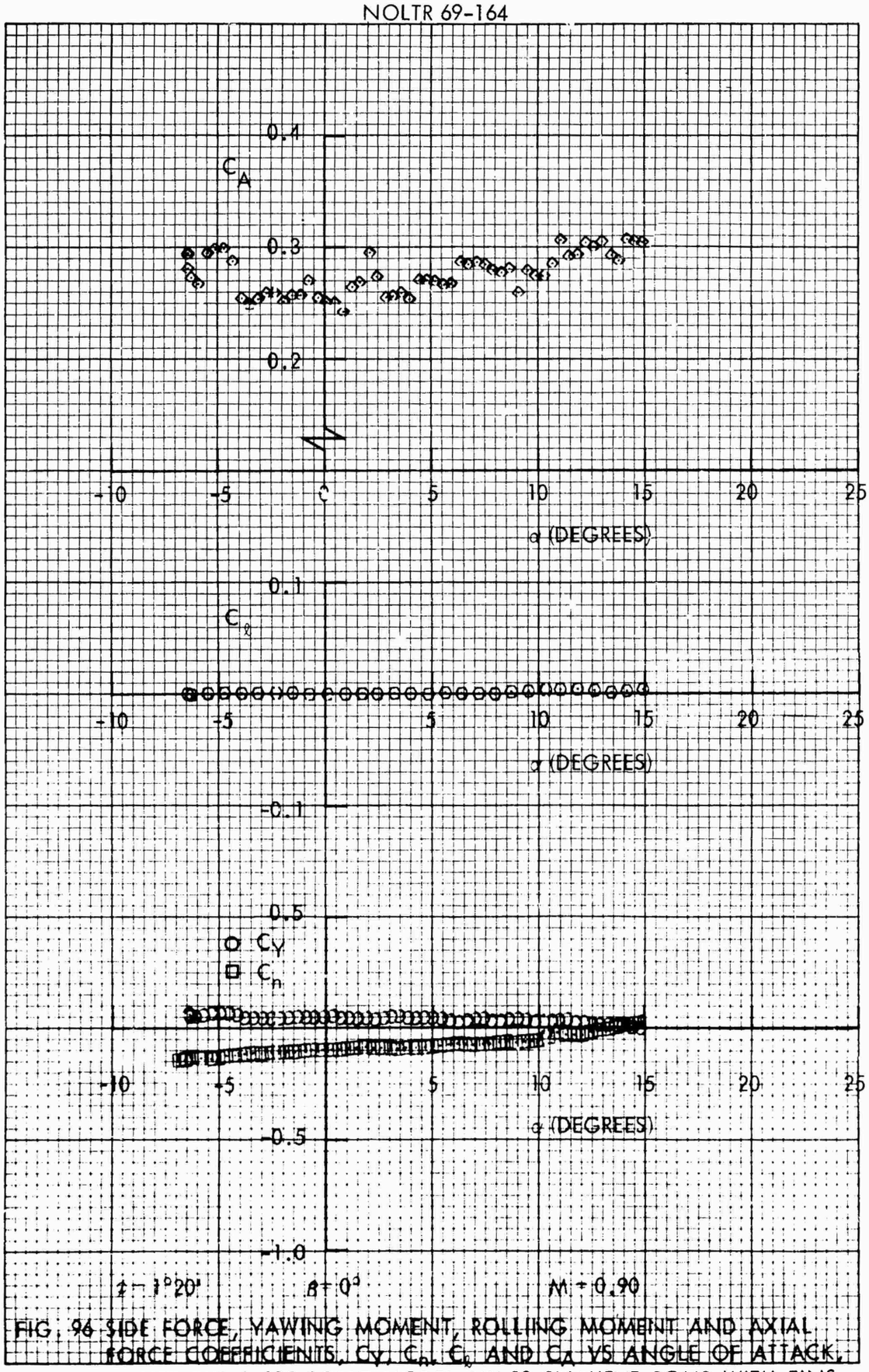

FIG. 96 SIDE FORCE, YAWING MOMENT, ROLLING MOMENT AND AXIAL FORCE COEFFICIENTS, C_Y, C_n, C_ℓ AND C_A VS ANGLE OF ATTACK, α, FOR THE 0.125-SCALE MODEL MK 82-SNAKEYE BOMB WITH FINS CLOSED

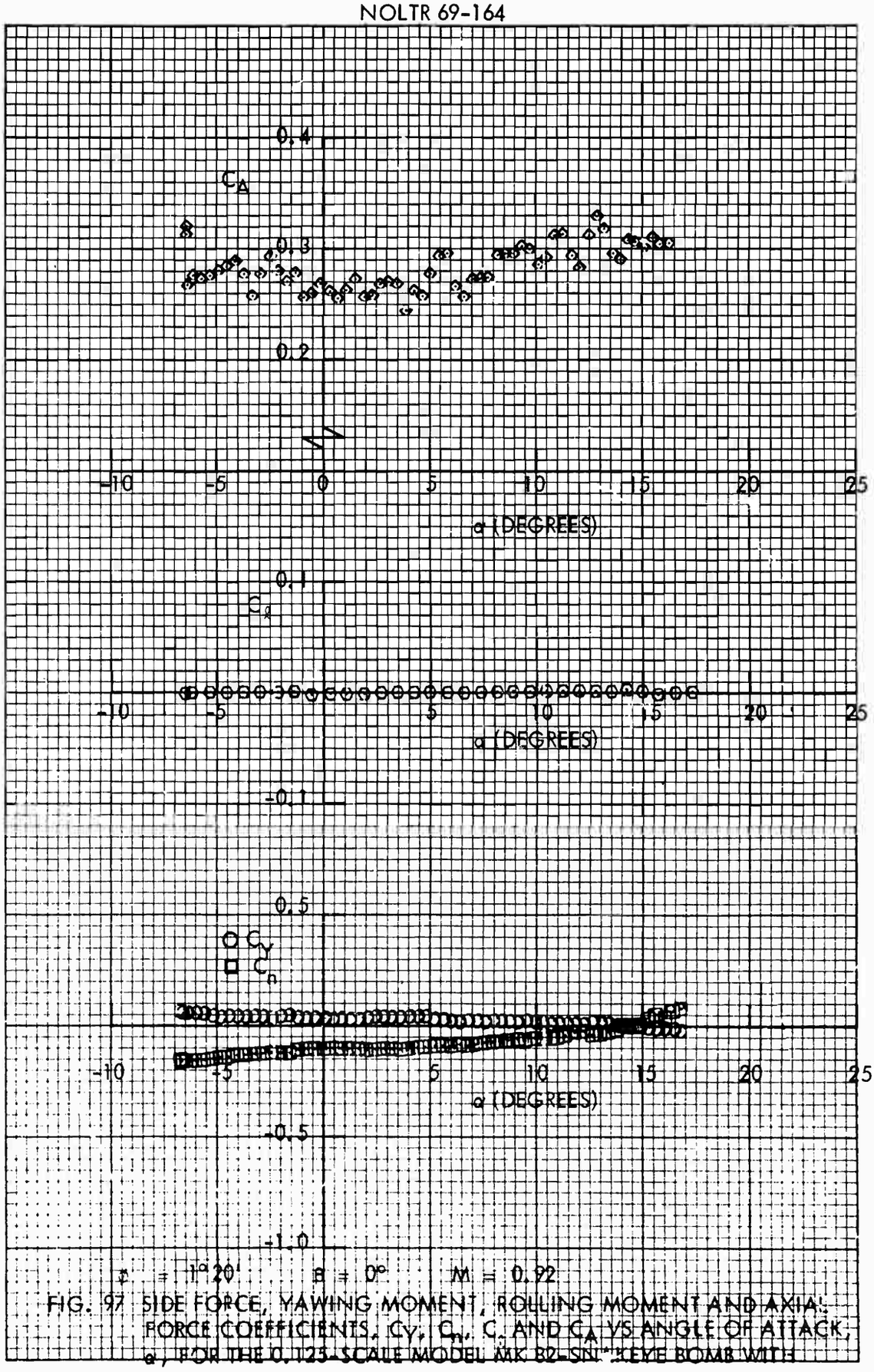

FIG. 97 SIDE FORCE, YAWING MOMENT, ROLLING MOMENT AND AXIAL FORCE COEFFICIENTS, C_Y, C_n, C_ℓ AND C_A VS ANGLE OF ATTACK, α, FOR THE 0.125-SCALE MODEL MK 82-SNT "LEVE BOMB WITH FINS CLOSED

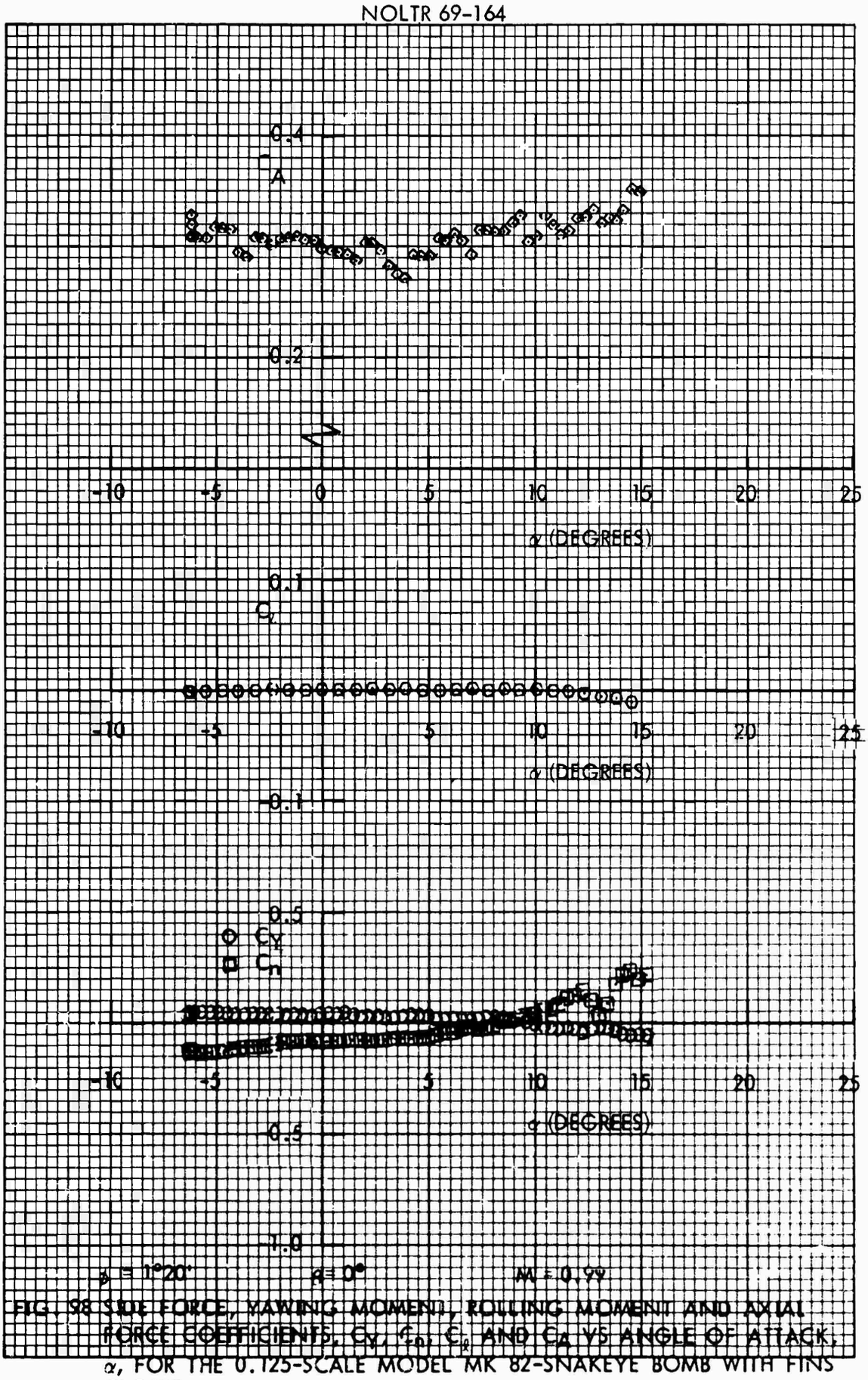

FIG. 98 SIDE FORCE, YAWING MOMENT, ROLLING MOMENT AND AXIAL FORCE COEFFICIENTS, C_Y, C_n, C_ℓ AND C_A VS ANGLE OF ATTACK, α, FOR THE 0.125-SCALE MODEL MK 82-SNAKEYE BOMB WITH FINS CLOSED

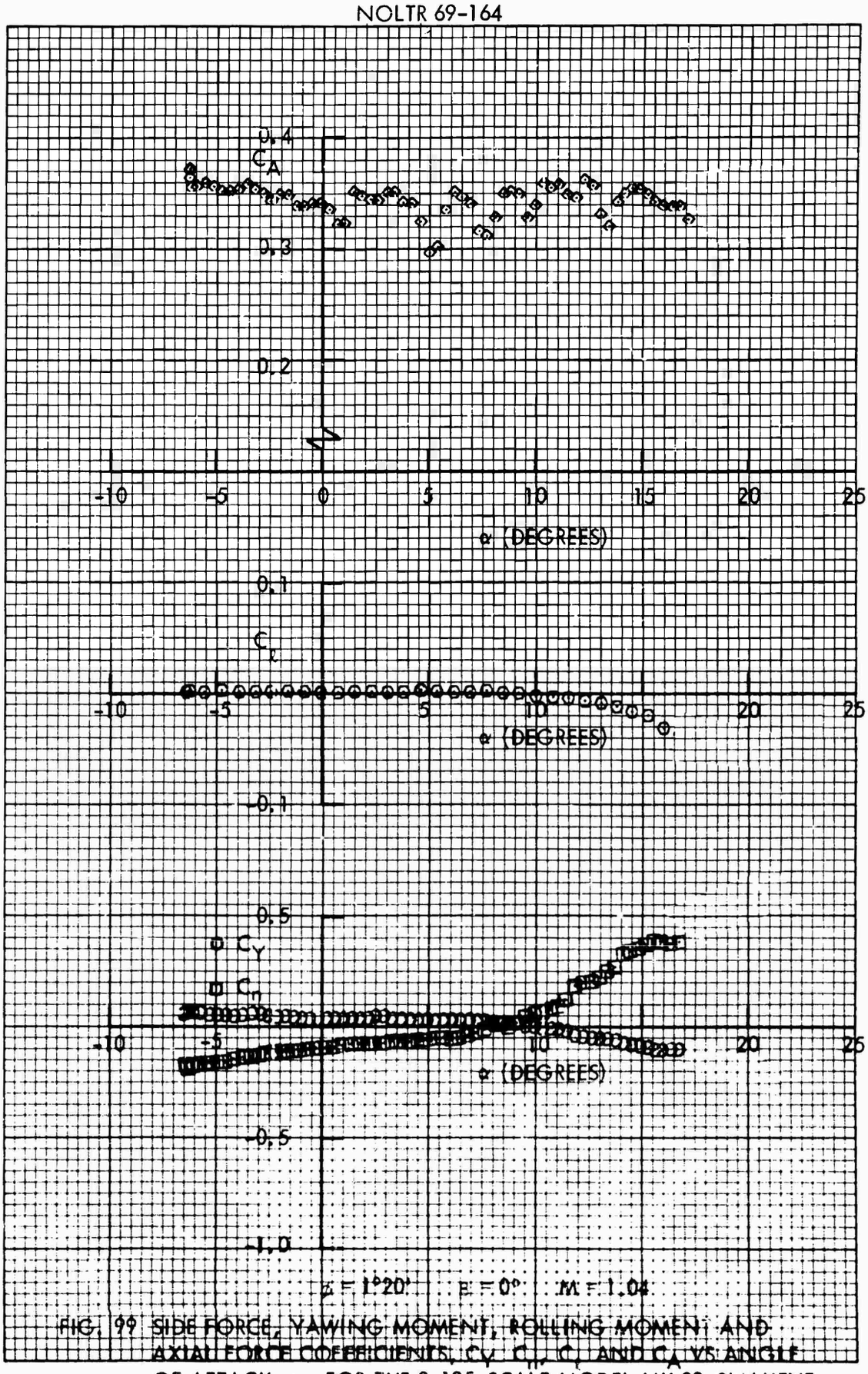

FIG. 99 SIDE FORCE, YAWING MOMENT, ROLLING MOMENT AND AXIAL FORCE COEFFICIENTS, C_Y, C_n, C_ℓ AND C_A VS ANGLE OF ATTACK, α, FOR THE 0.125-SCALE MODEL MK 82-SNAKEYE BOMB WITH FINS CLOSED

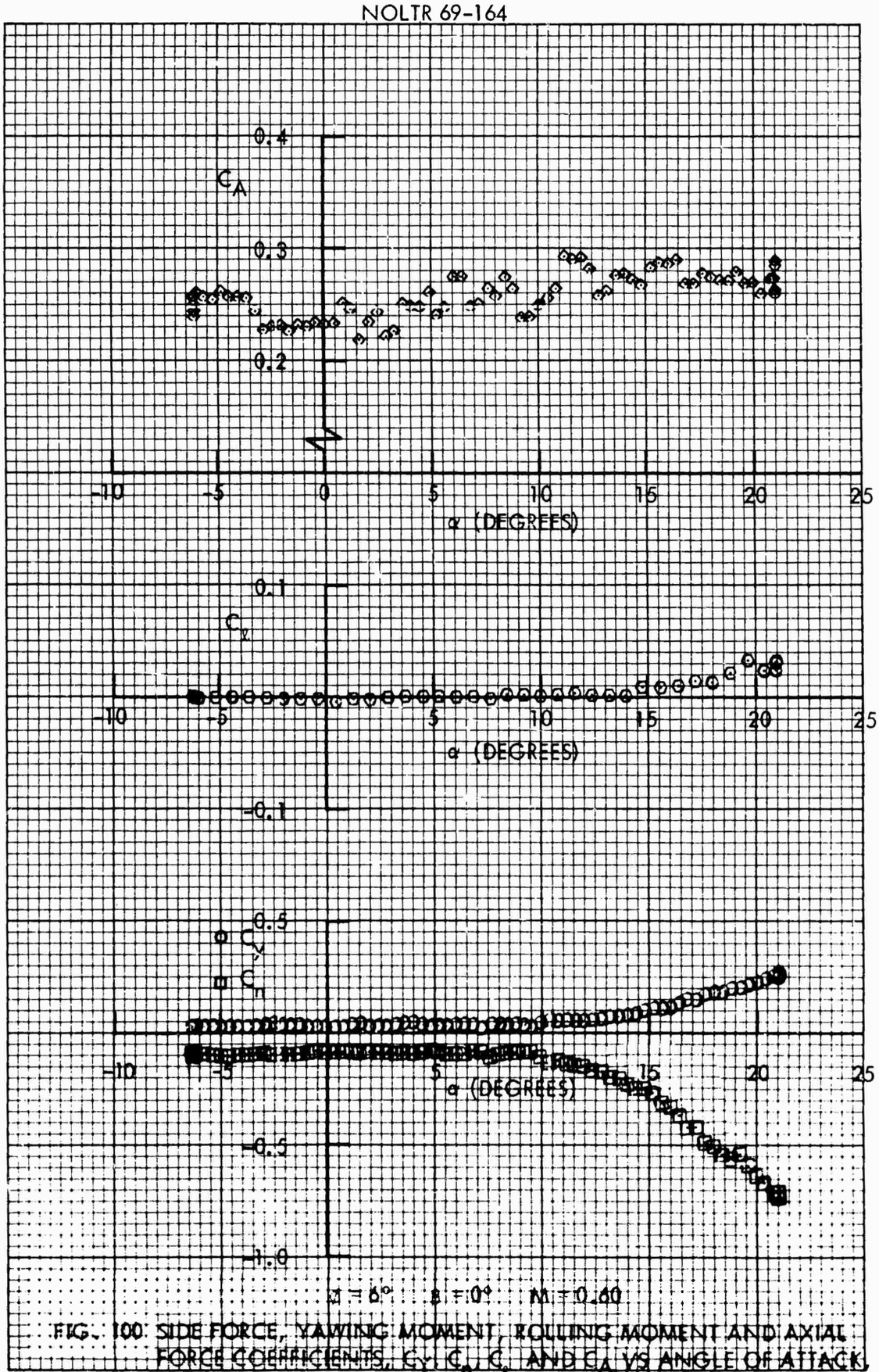

FIG. 100 SIDE FORCE, YAWING MOMENT, ROLLING MOMENT AND AXIAL FORCE COEFFICIENTS, C_Y, C_n, C_ℓ, AND C_A VS ANGLE OF ATTACK, α, FOR THE 0.125-SCALE MODEL MK 82-SNAKEYE BOMB WITH FINS CLOSED

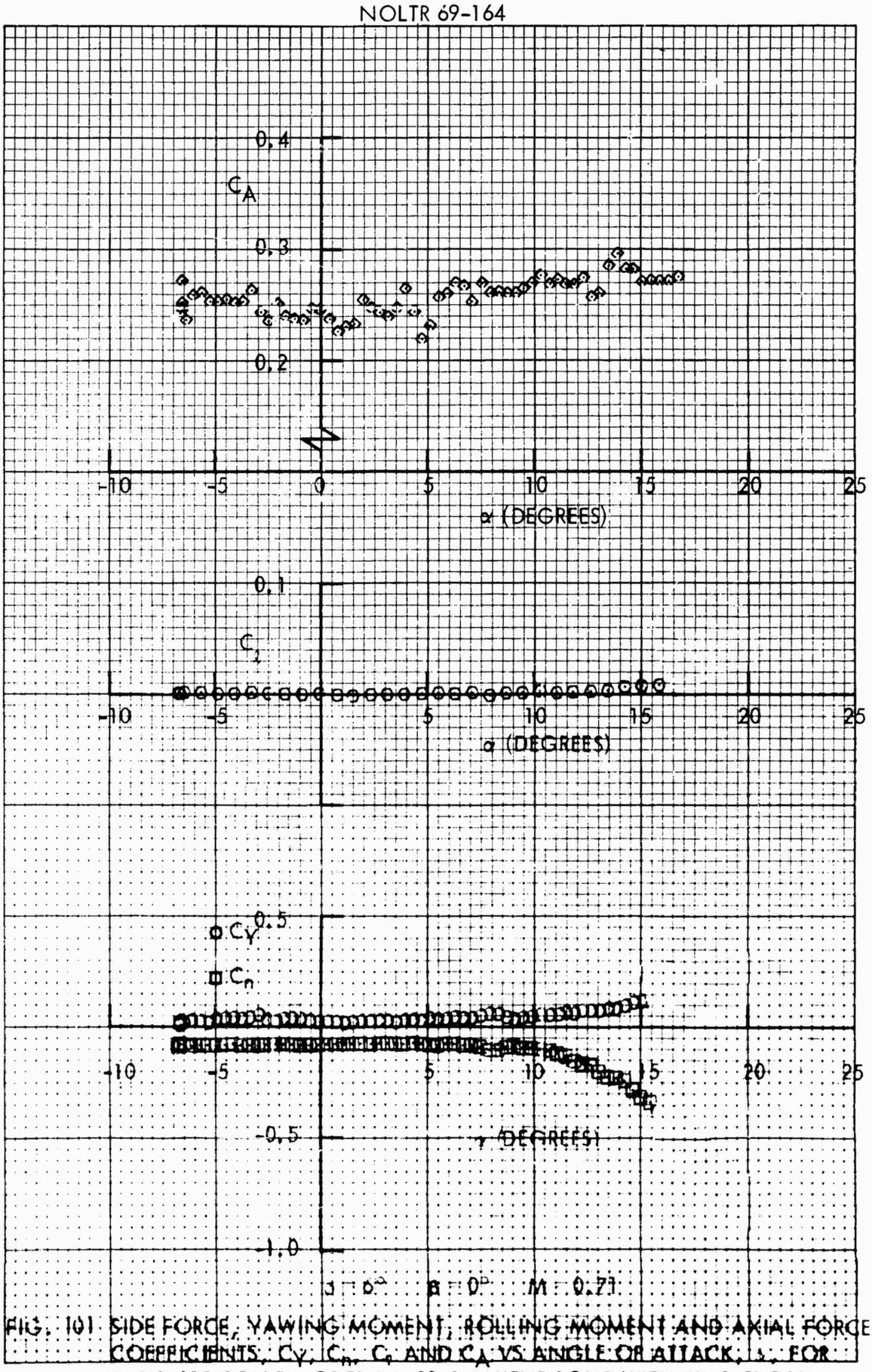

FIG. 101 SIDE FORCE, YAWING MOMENT, ROLLING MOMENT AND AXIAL FORCE COEFFICIENTS, C_Y, C_n, C_l AND C_A VS ANGLE OF ATTACK, α, FOR THE 0.125-SCALE MODEL MK 82-SNAKEYE BOMB WITH FINS CLOSED

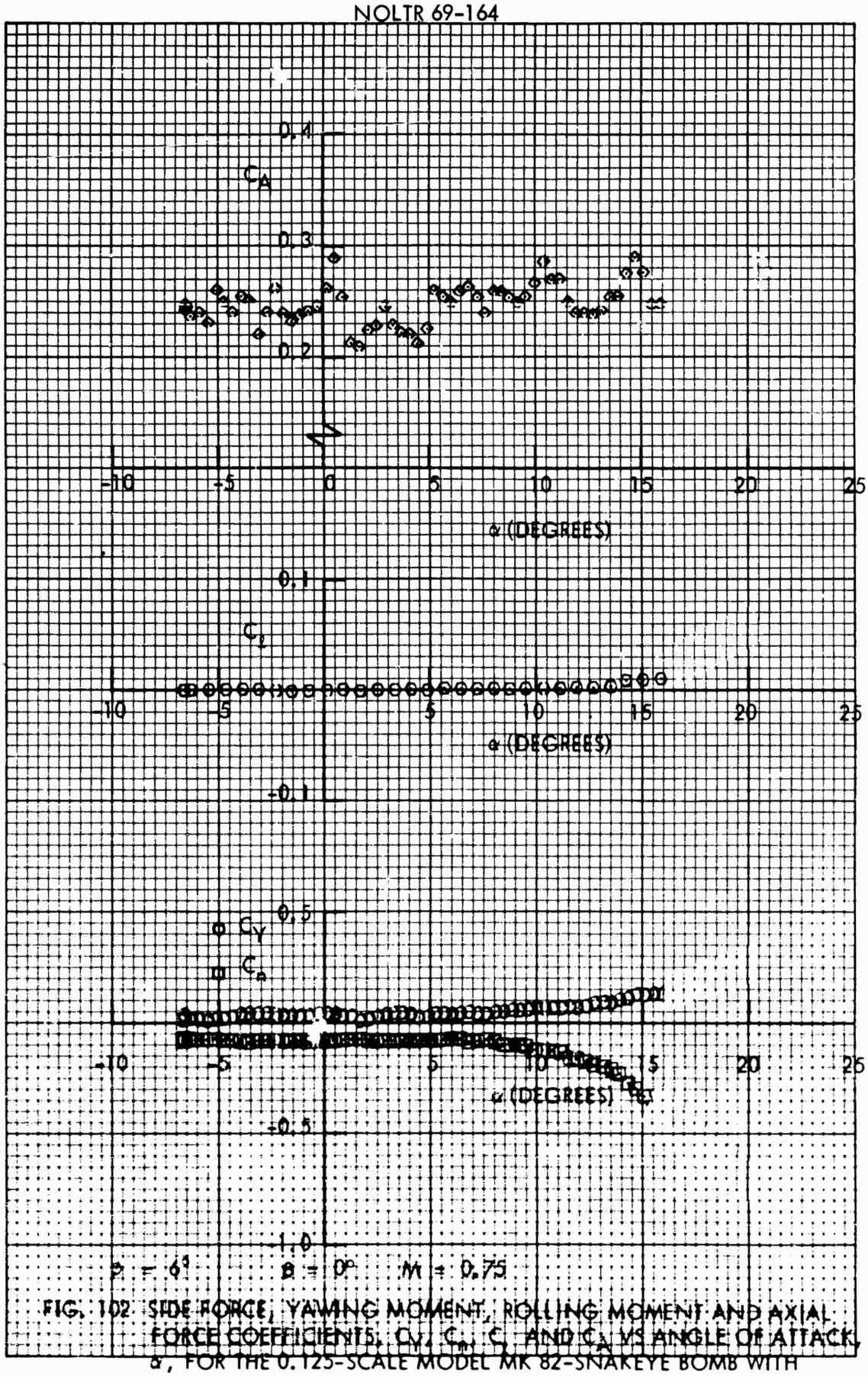

FIG. 102 SIDE FORCE, YAWING MOMENT, ROLLING MOMENT AND AXIAL FORCE COEFFICIENTS, C_Y, C_n, C_l AND C_A VS ANGLE OF ATTACK, α, FOR THE 0.125-SCALE MODEL MK 82-SNAKEYE BOMB WITH FINS CLOSED

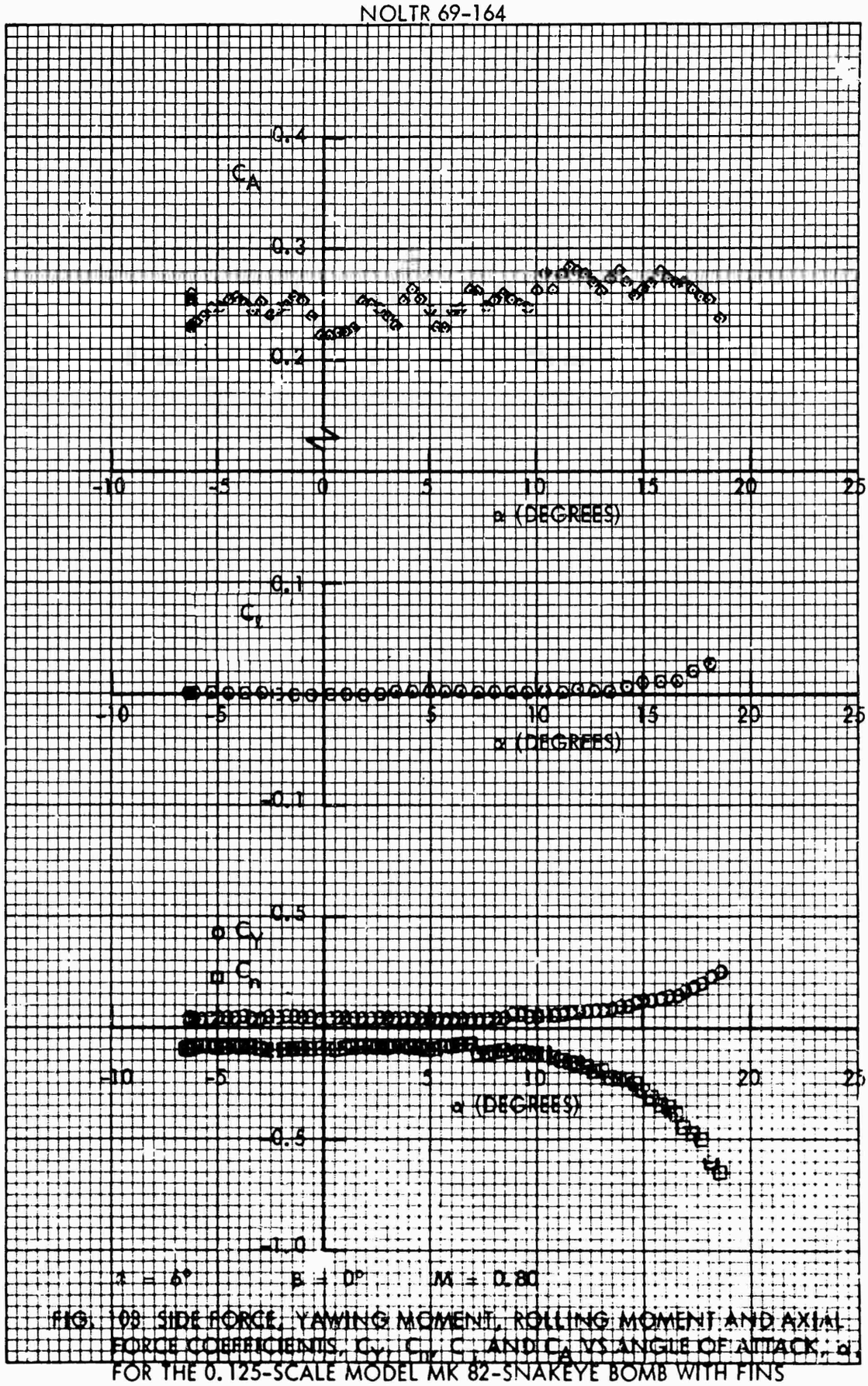

FIG. 109 SIDE FORCE, YAWING MOMENT, ROLLING MOMENT AND AXIAL FORCE COEFFICIENTS, C_Y, C_n, C_ℓ AND C_A VS ANGLE OF ATTACK, α, FOR THE 0.125-SCALE MODEL MK 82-SNAKEYE BOMB WITH FINS CLOSED

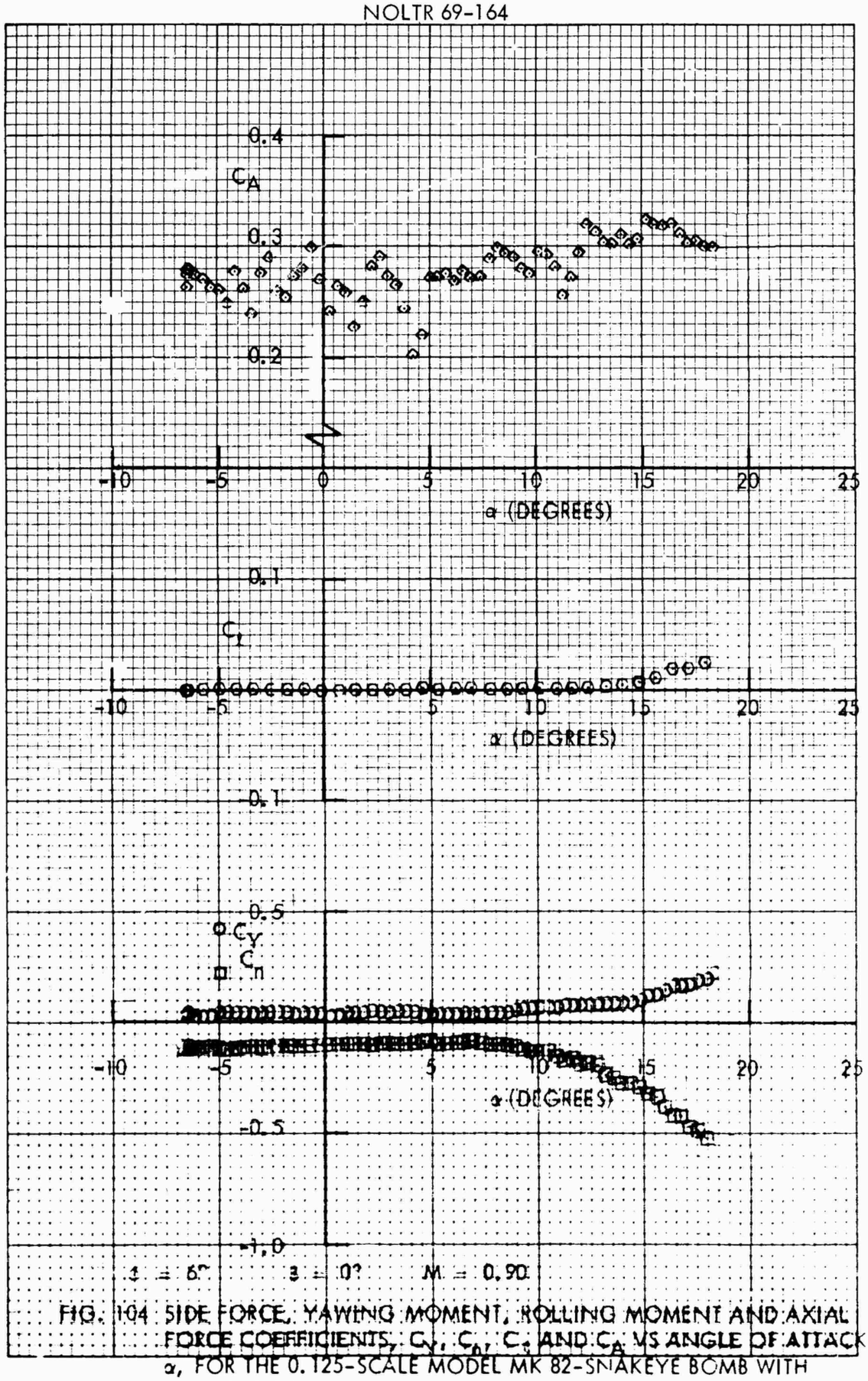

FIG. 104 SIDE FORCE, YAWING MOMENT, ROLLING MOMENT AND AXIAL FORCE COEFFICIENTS, C_Y, C_n, C_l AND C_A VS ANGLE OF ATTACK, α, FOR THE 0.125-SCALE MODEL MK 82-SNAKEYE BOMB WITH FINS CLOSED

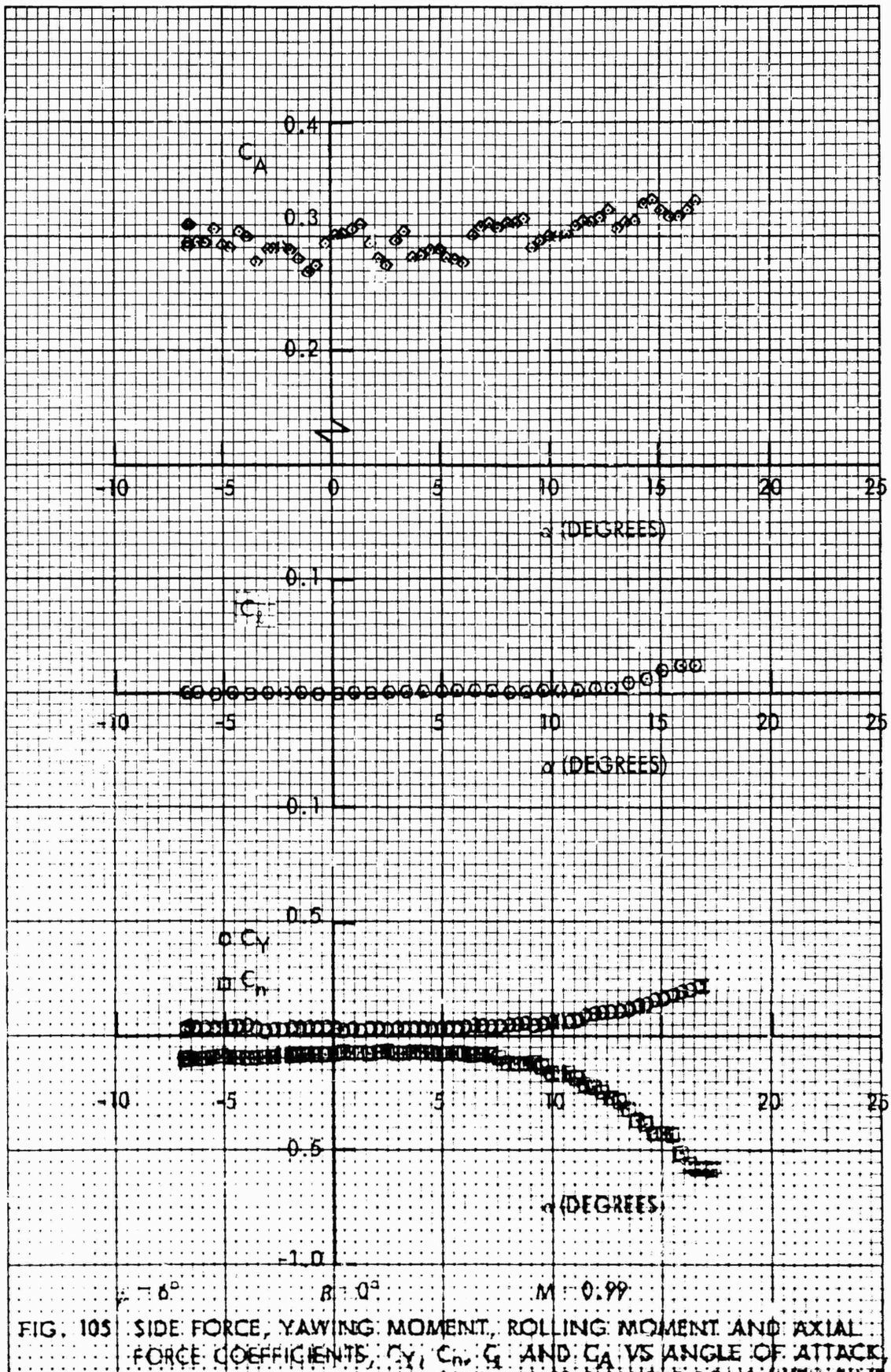

FIG. 105 SIDE FORCE, YAWING MOMENT, ROLLING MOMENT AND AXIAL FORCE COEFFICIENTS, C_Y, C_n, C_l AND C_A VS ANGLE OF ATTACK, α, FOR THE 0.125-SCALE MODEL MK 82 SNAKEYE BOMB WITH FINS CLOSED

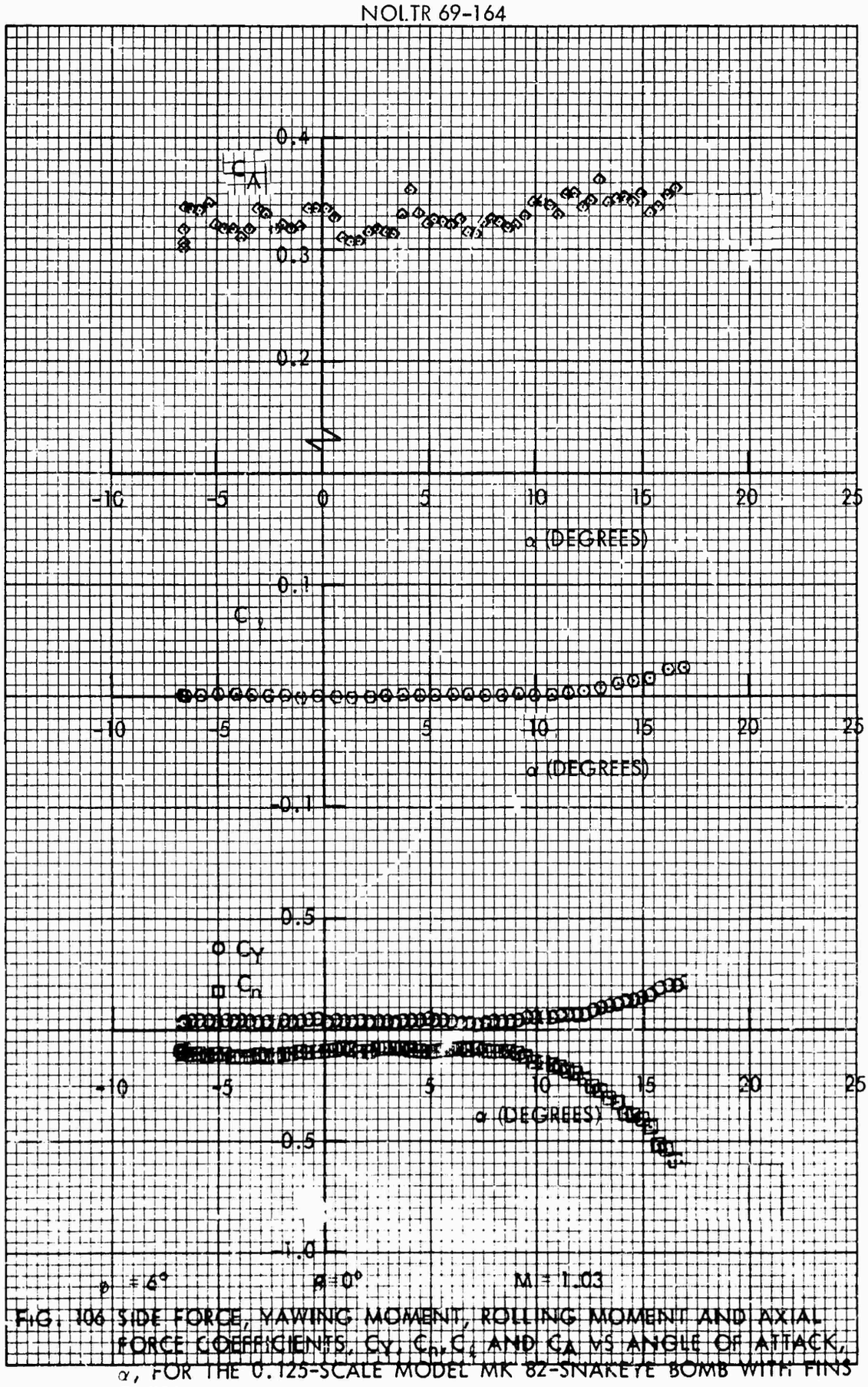

FIG. 106 SIDE FORCE, YAWING MOMENT, ROLLING MOMENT AND AXIAL FORCE COEFFICIENTS, C_Y, C_n, C_l AND C_A VS ANGLE OF ATTACK, α, FOR THE 0.125-SCALE MODEL MK 82-SNAKEYE BOMB WITH FINS CLOSED

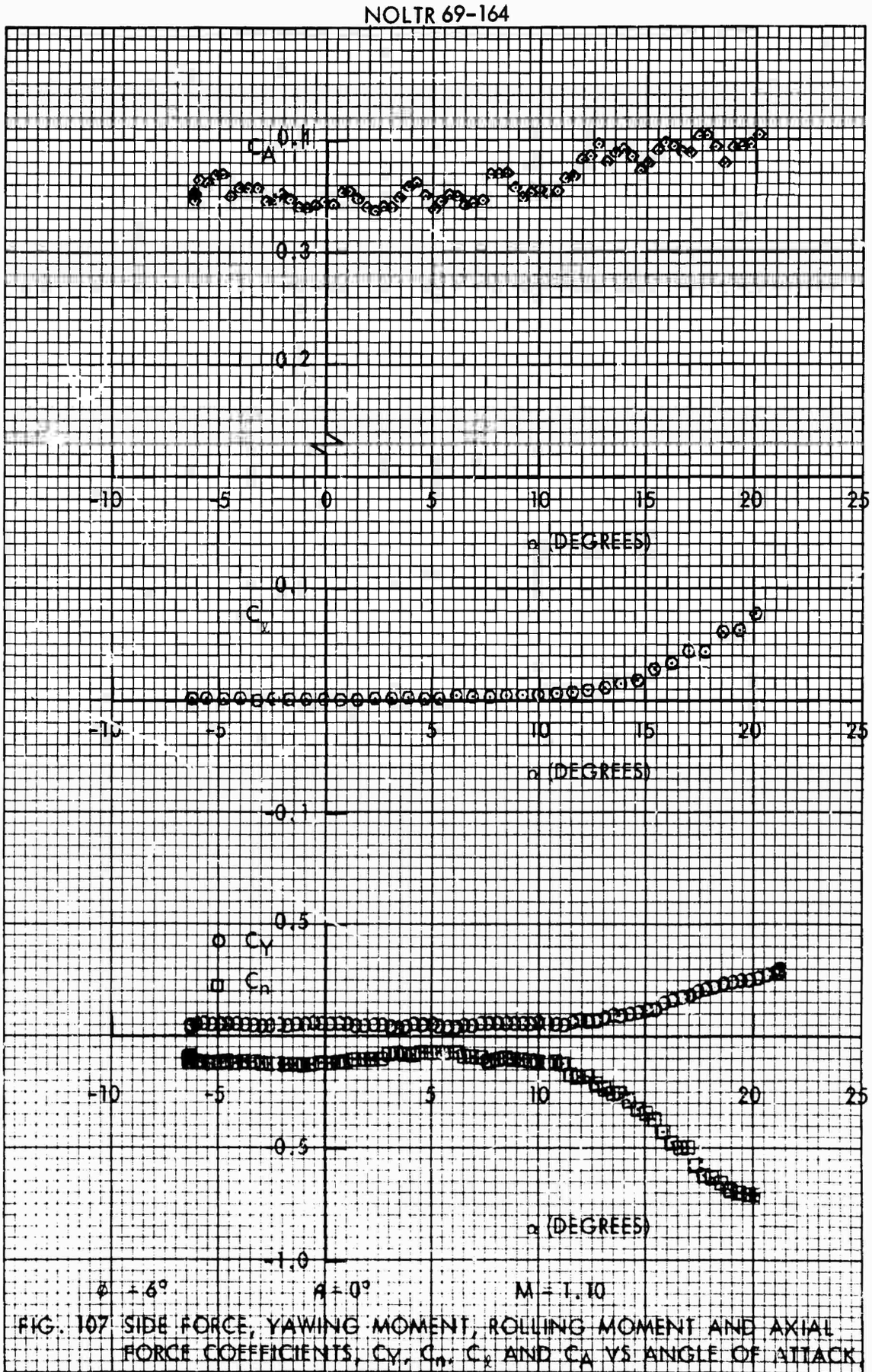

FIG. 107 SIDE FORCE, YAWING MOMENT, ROLLING MOMENT AND AXIAL FORCE COEFFICIENTS, C_Y, C_n, C_ℓ AND C_A VS ANGLE OF ATTACK, α, FOR THE 0.125-SCALE MODEL MK 82-SNAKEYE BOMB WITH FINS CLOSED

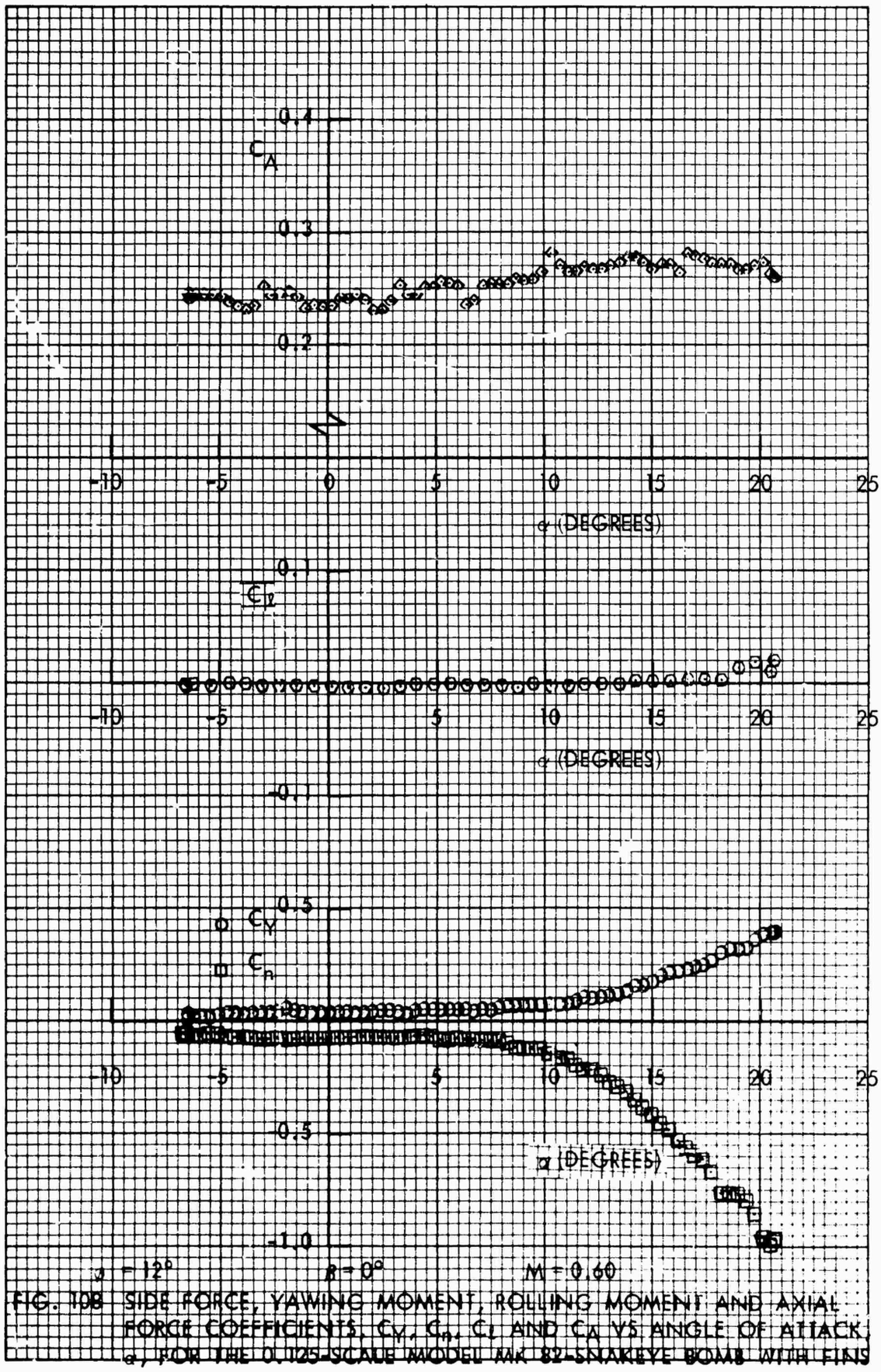

FIG. 108 SIDE FORCE, YAWING MOMENT, ROLLING MOMENT AND AXIAL FORCE COEFFICIENTS, C_Y, C_n, C_l AND C_A VS ANGLE OF ATTACK, α, FOR THE 0.125-SCALE MODEL MK 82-SNAKEYE BOMB WITH FINS CLOSED

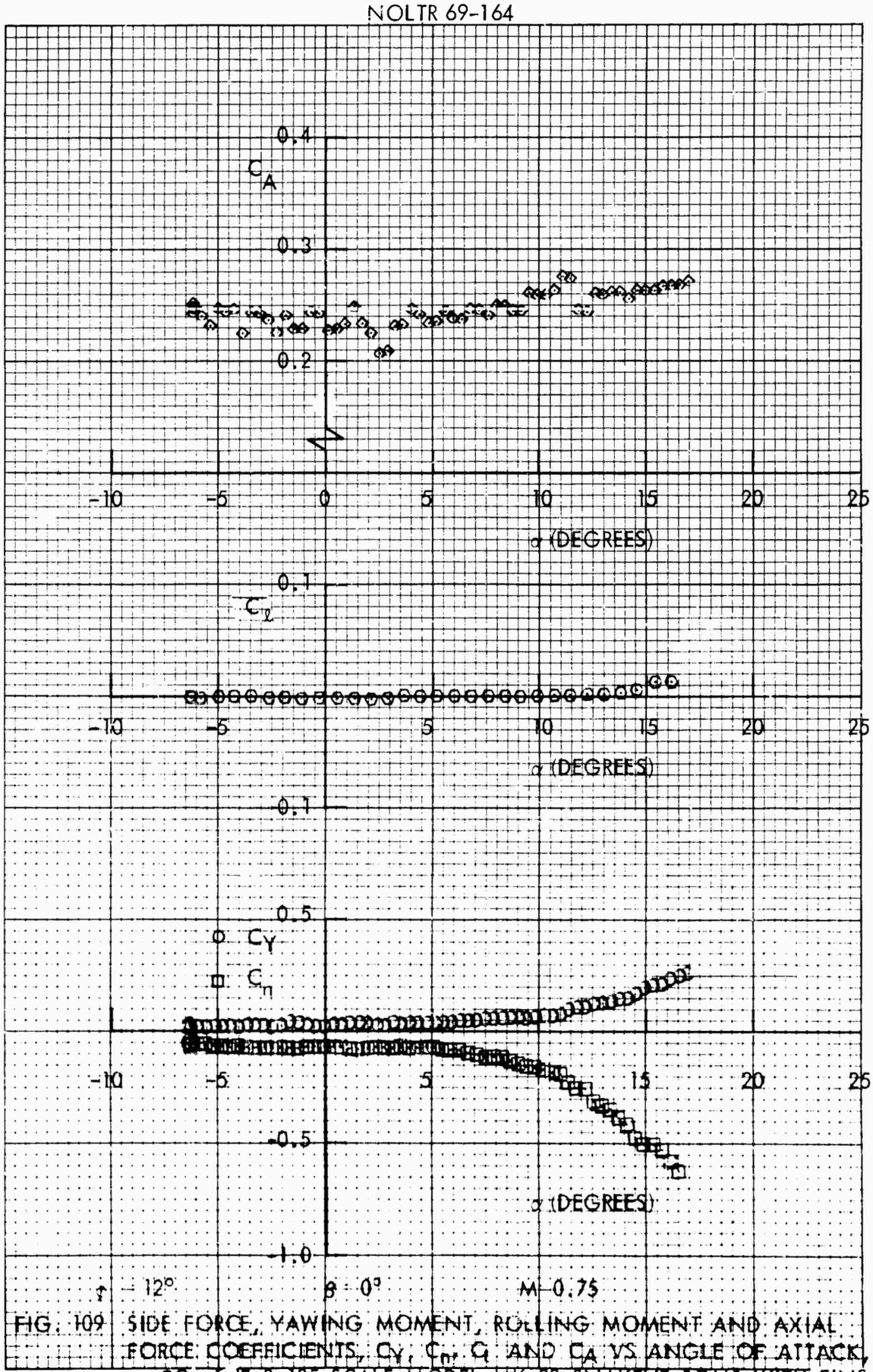

FIG. 109 SIDE FORCE, YAWING MOMENT, ROLLING MOMENT AND AXIAL FORCE COEFFICIENTS, C_Y, C_n, C_l AND C_A VS ANGLE OF ATTACK, α, FOR THE 0.125-SCALE MODEL MK 82-SNAKEYE BOMB WITH FINS CLOSED

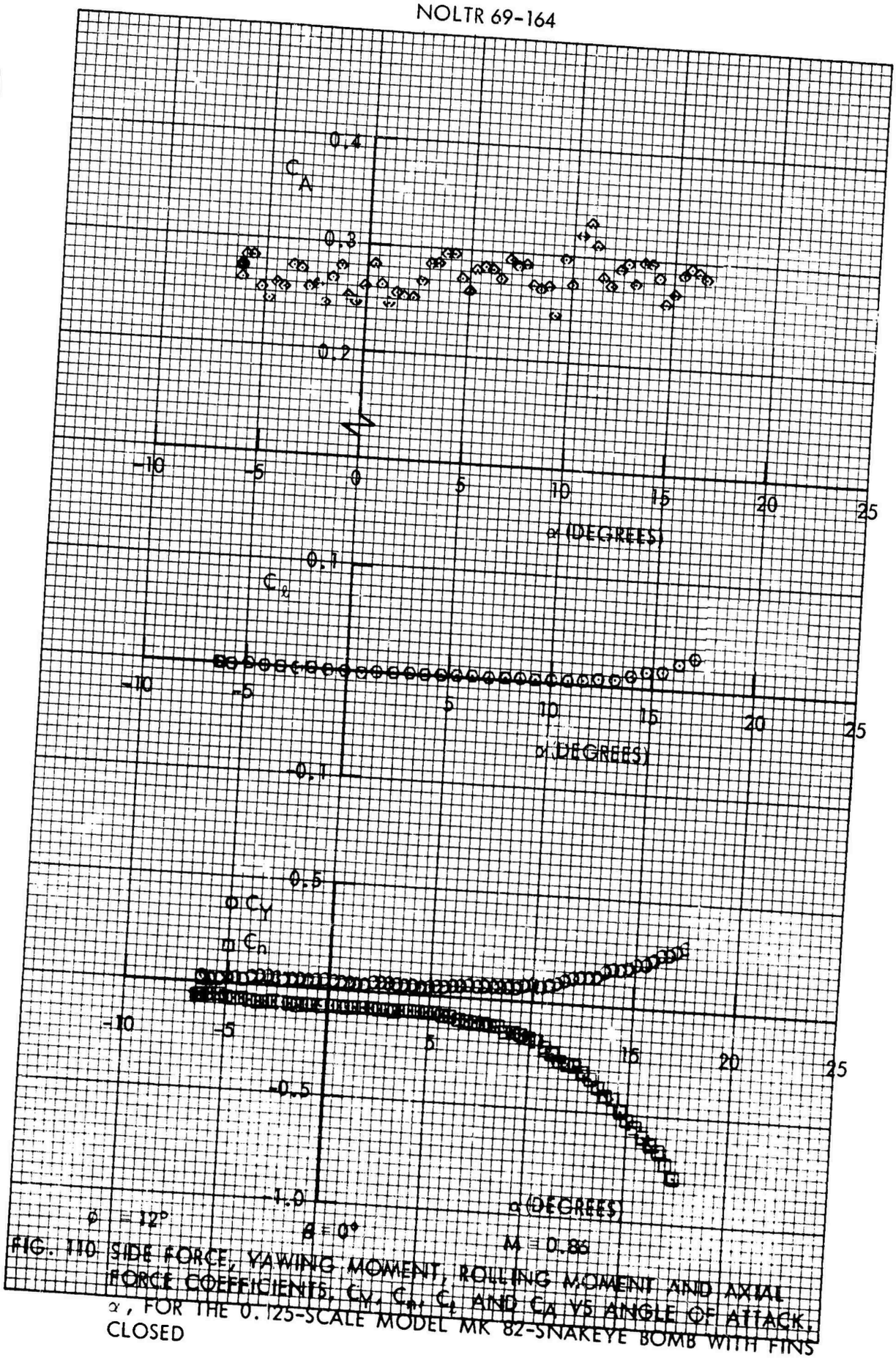

FIG. 110 SIDE FORCE, YAWING MOMENT, ROLLING MOMENT AND AXIAL FORCE COEFFICIENTS, C_Y, C_n, C_ℓ AND C_A VS ANGLE OF ATTACK, α, FOR THE 0.125-SCALE MODEL MK 82-SNAKEYE BOMB WITH FINS CLOSED

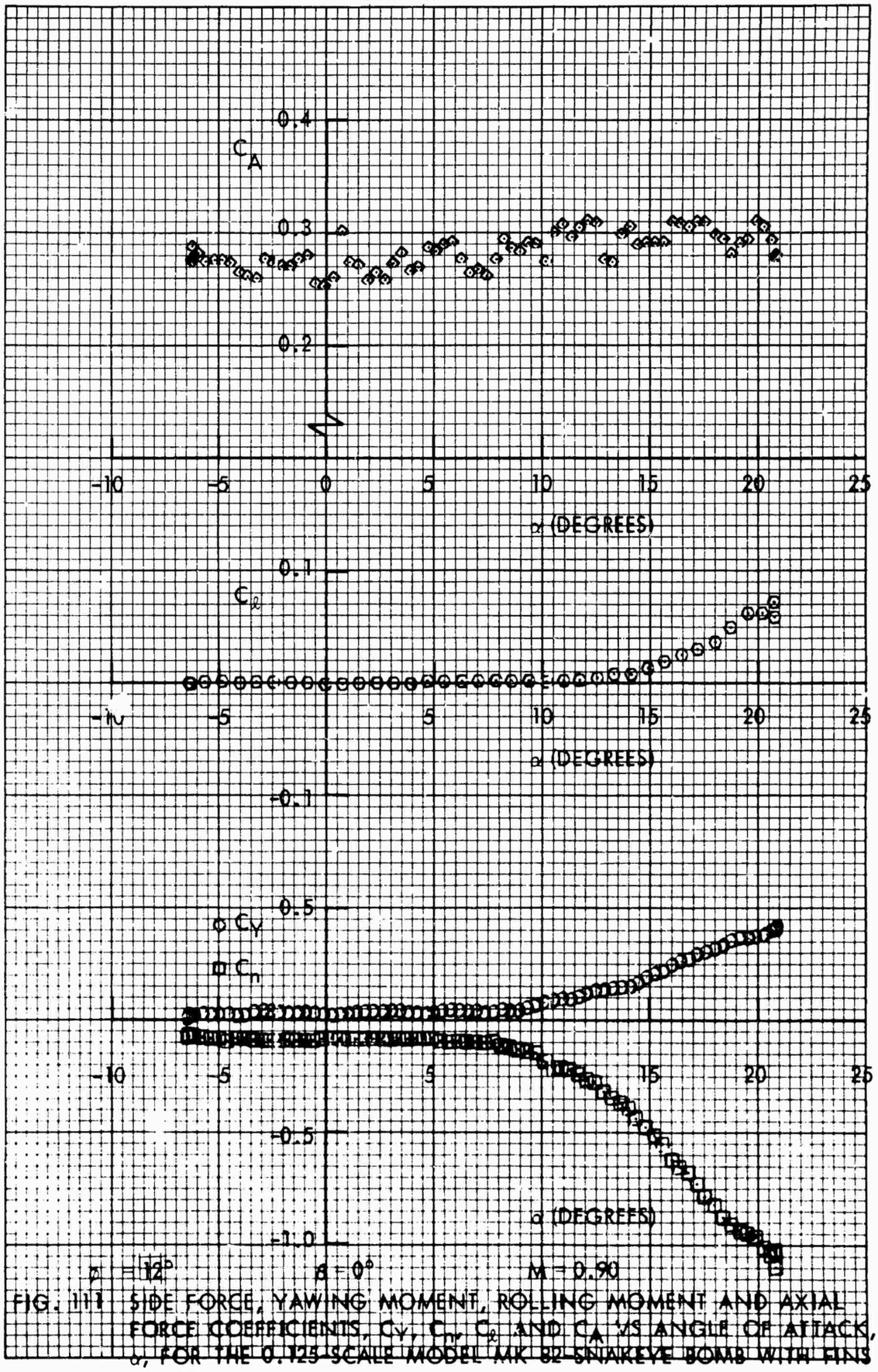

FIG. 111 SIDE FORCE, YAWING MOMENT, ROLLING MOMENT AND AXIAL FORCE COEFFICIENTS, C_Y, C_n, C_ℓ AND C_A VS ANGLE OF ATTACK, α, FOR THE 0.125-SCALE MODEL MK 82-SNAKEYE BOMB WITH FINS CLOSED

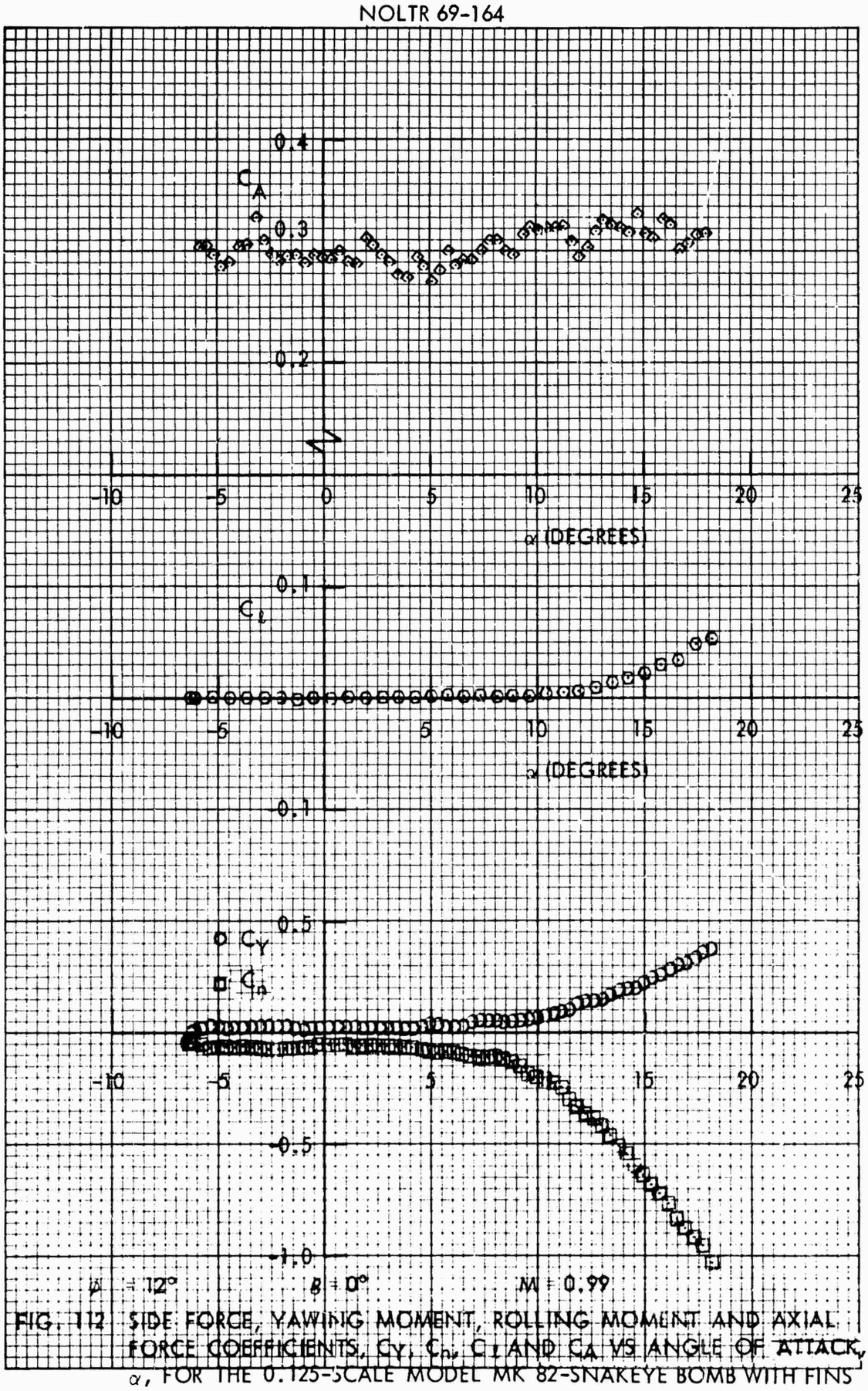

FIG. 112 SIDE FORCE, YAWING MOMENT, ROLLING MOMENT AND AXIAL FORCE COEFFICIENTS, C_Y, C_n, C_ℓ AND C_A VS ANGLE OF ATTACK, α, FOR THE 0.125-SCALE MODEL MK 82-SNAKEYE BOMB WITH FINS CLOSED

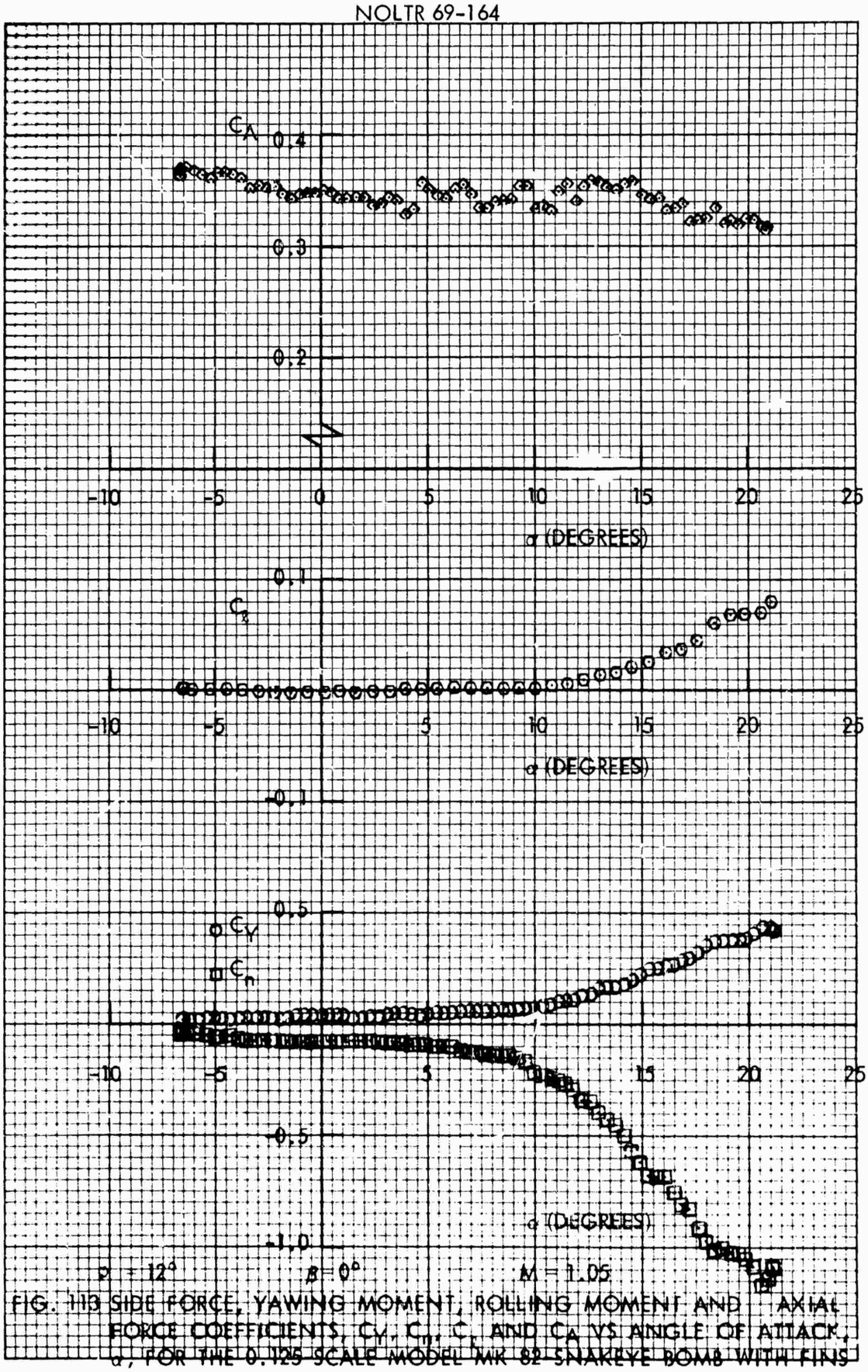

FIG. 113 SIDE FORCE, YAWING MOMENT, ROLLING MOMENT AND AXIAL FORCE COEFFICIENTS, C_Y, C_n, C_ℓ, AND C_A VS ANGLE OF ATTACK, α, FOR THE 0.125 SCALE MODEL MK 82 SNAKEYE BOMB WITH FINS CLOSED

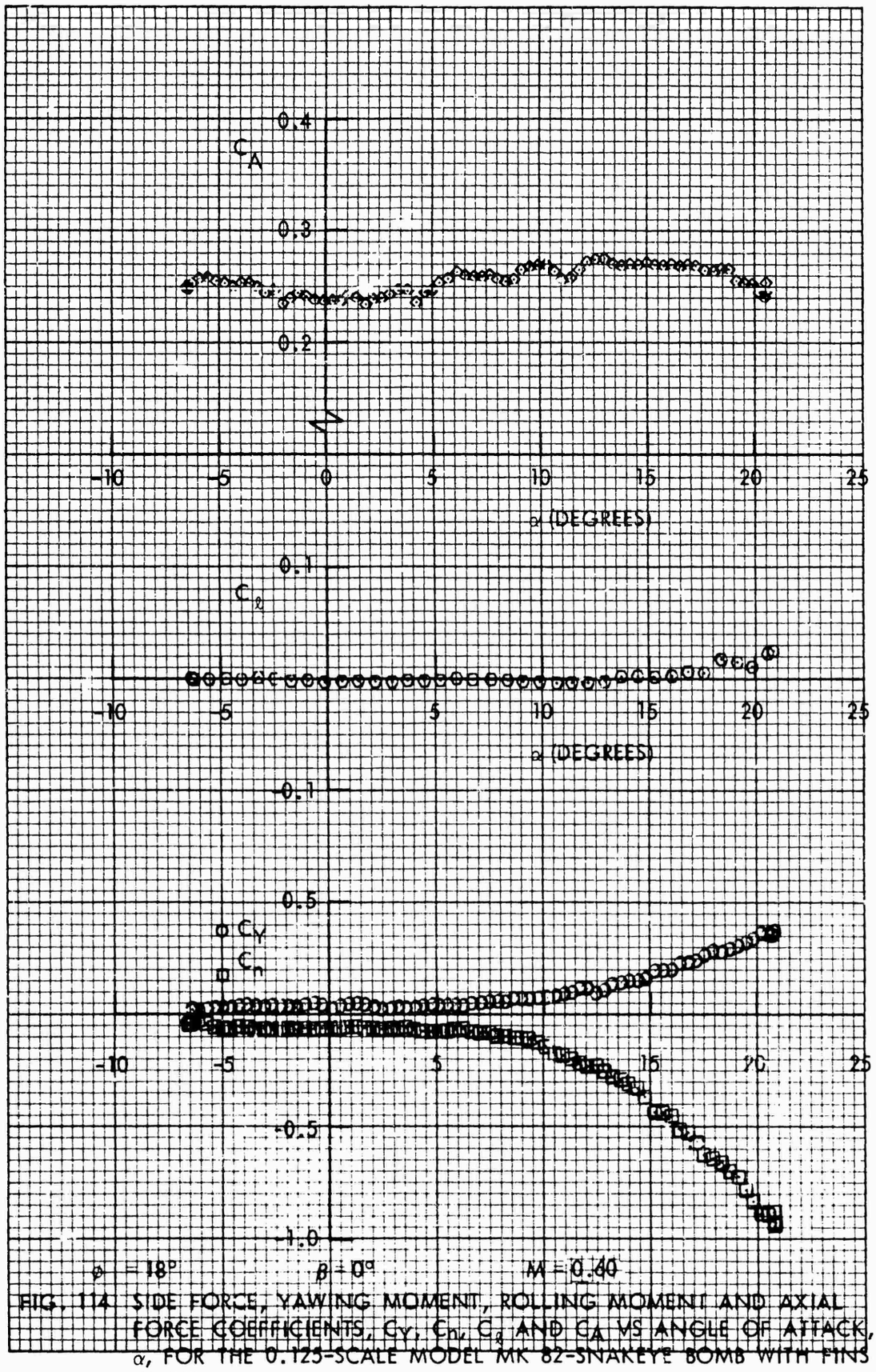

FIG. 114 SIDE FORCE, YAWING MOMENT, ROLLING MOMENT AND AXIAL FORCE COEFFICIENTS, C_Y, C_n, C_ℓ AND C_A VS ANGLE OF ATTACK, α, FOR THE 0.125-SCALE MODEL MK 82-SNAKEYE BOMB WITH FINS CLOSED

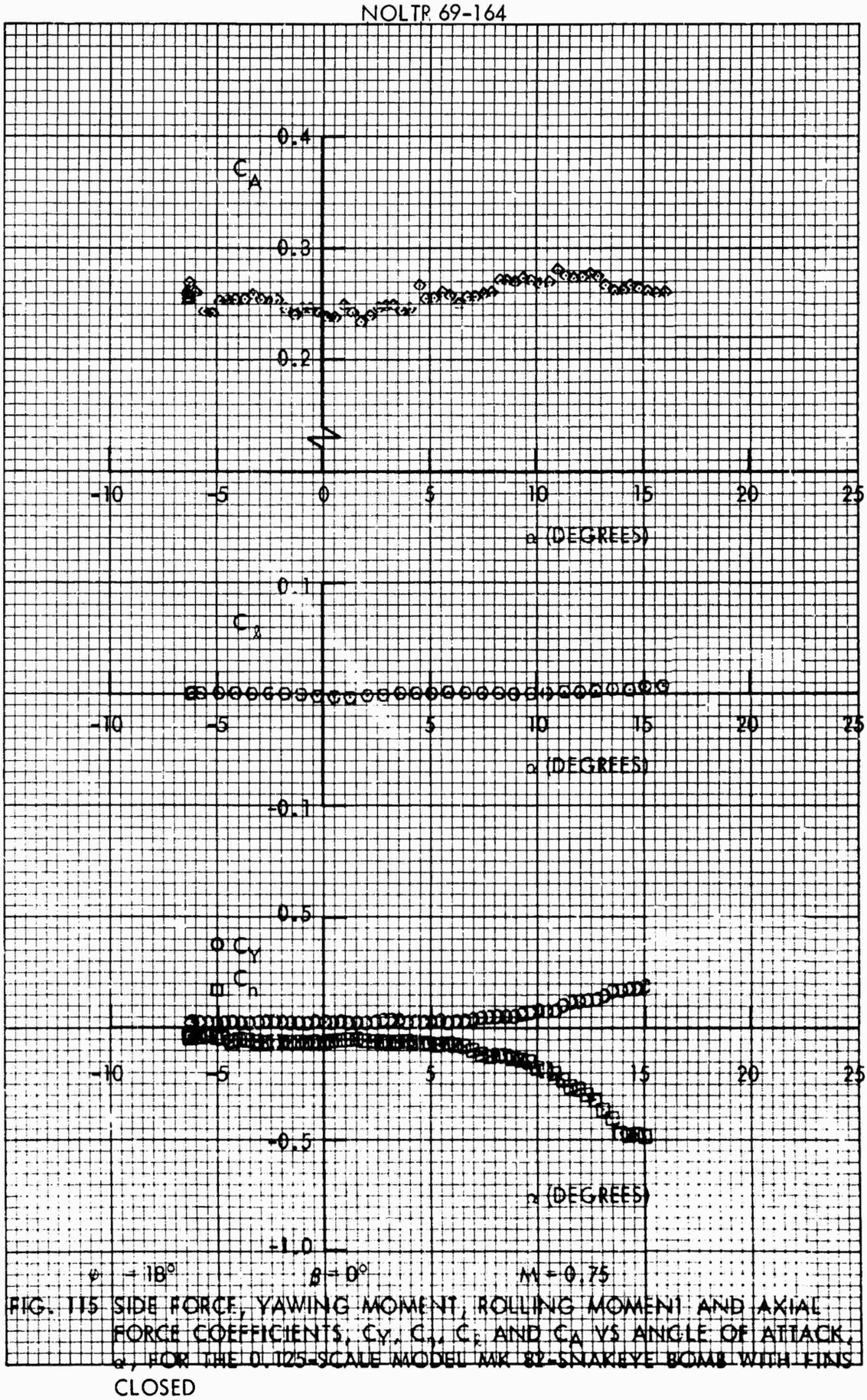

FIG. 115 SIDE FORCE, YAWING MOMENT, ROLLING MOMENT AND AXIAL FORCE COEFFICIENTS, C_Y, C_n, C_ℓ, AND C_A VS ANGLE OF ATTACK, α, FOR THE 0.125-SCALE MODEL MK 82-SNAKEYE BOMB WITH FINS CLOSED

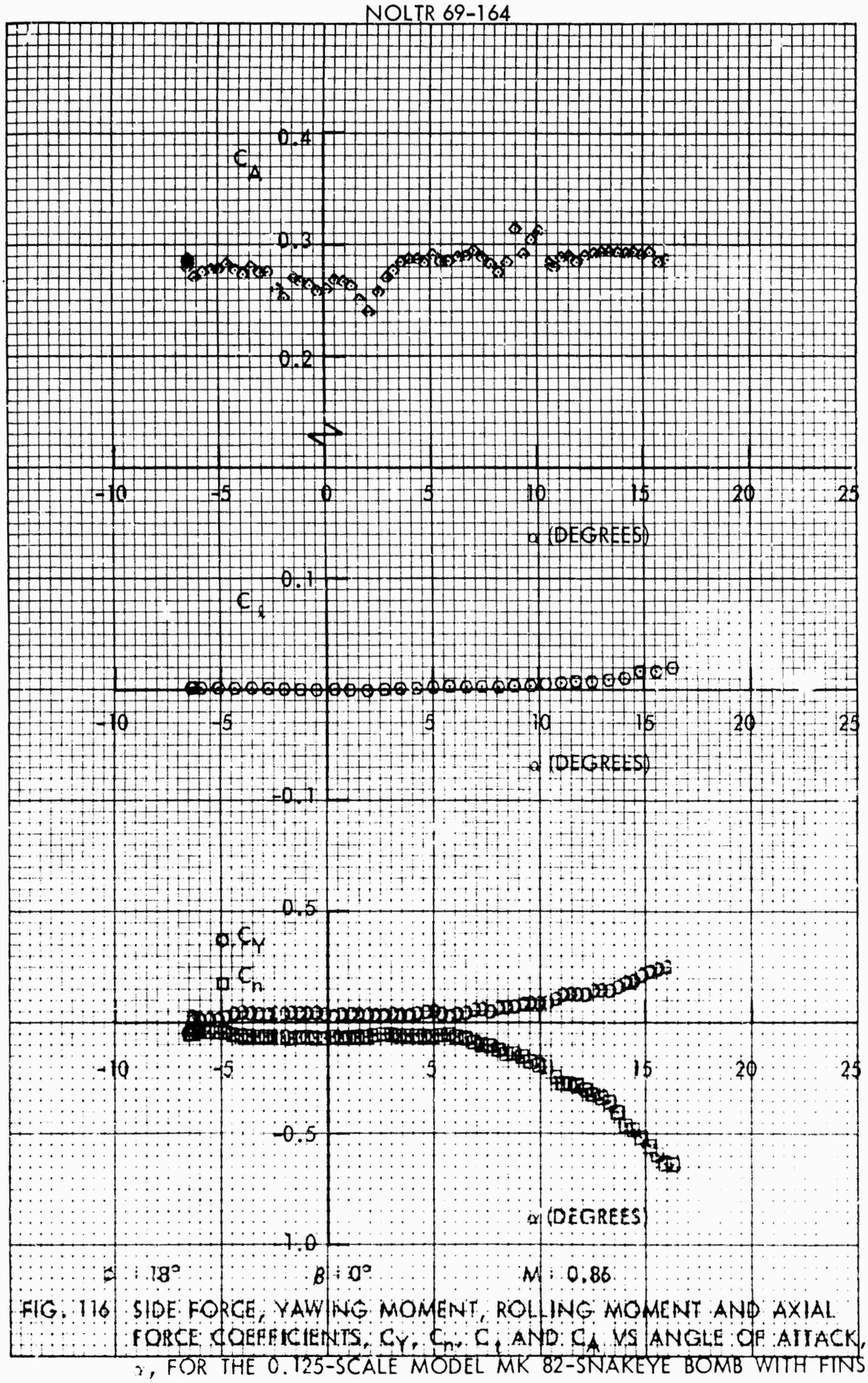

FIG. 116 SIDE FORCE, YAWING MOMENT, ROLLING MOMENT AND AXIAL FORCE COEFFICIENTS, C_Y, C_n, C_ℓ AND C_A VS ANGLE OF ATTACK, α, FOR THE 0.125-SCALE MODEL MK 82-SNAKEYE BOMB WITH FINS CLOSED

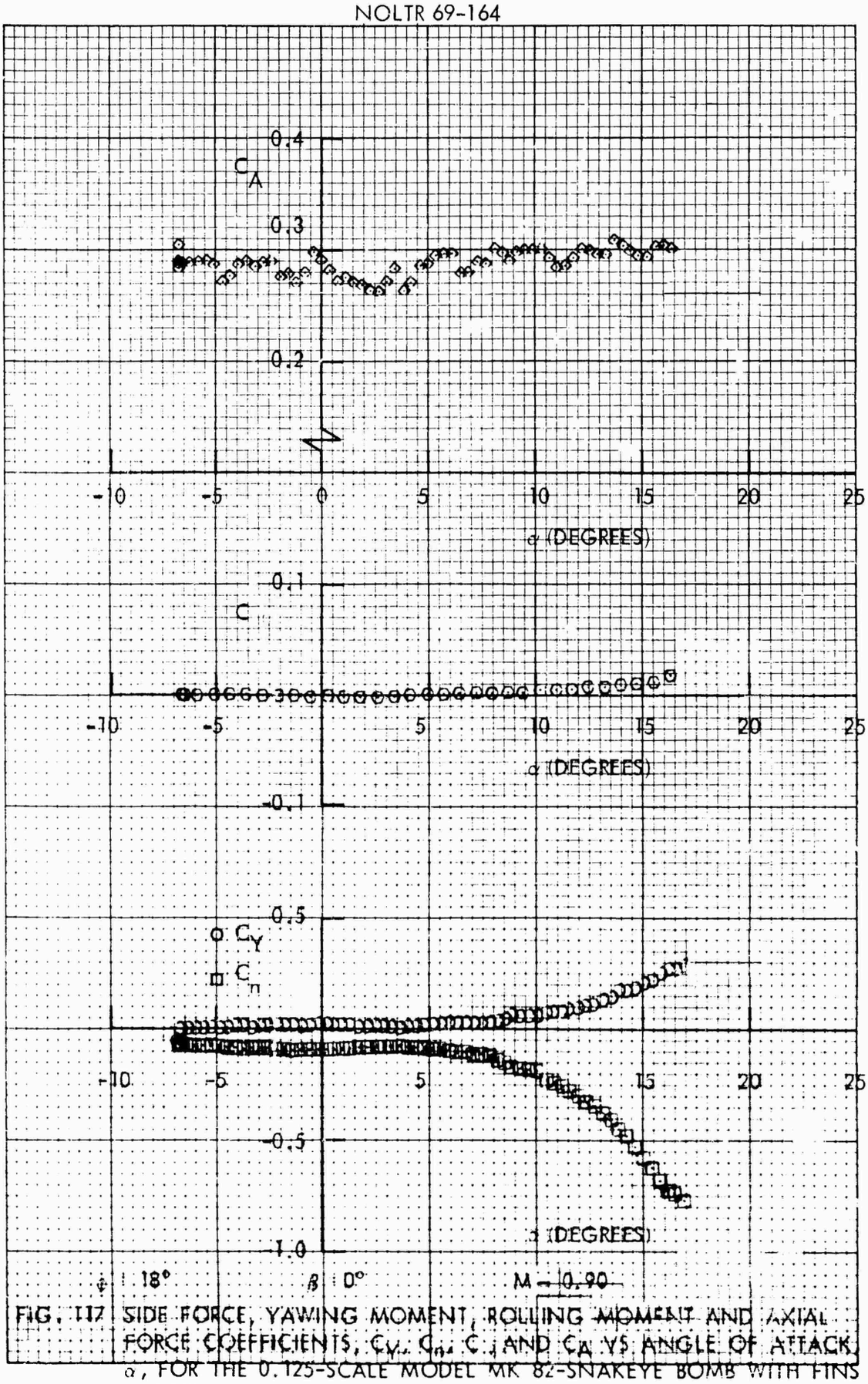

FIG. 117 SIDE FORCE, YAWING MOMENT, ROLLING MOMENT AND AXIAL FORCE COEFFICIENTS, C_Y, C_n, C, AND C_A VS ANGLE OF ATTACK, α, FOR THE 0.125-SCALE MODEL MK 82-SNAKEYE BOMB WITH FINS CLOSED

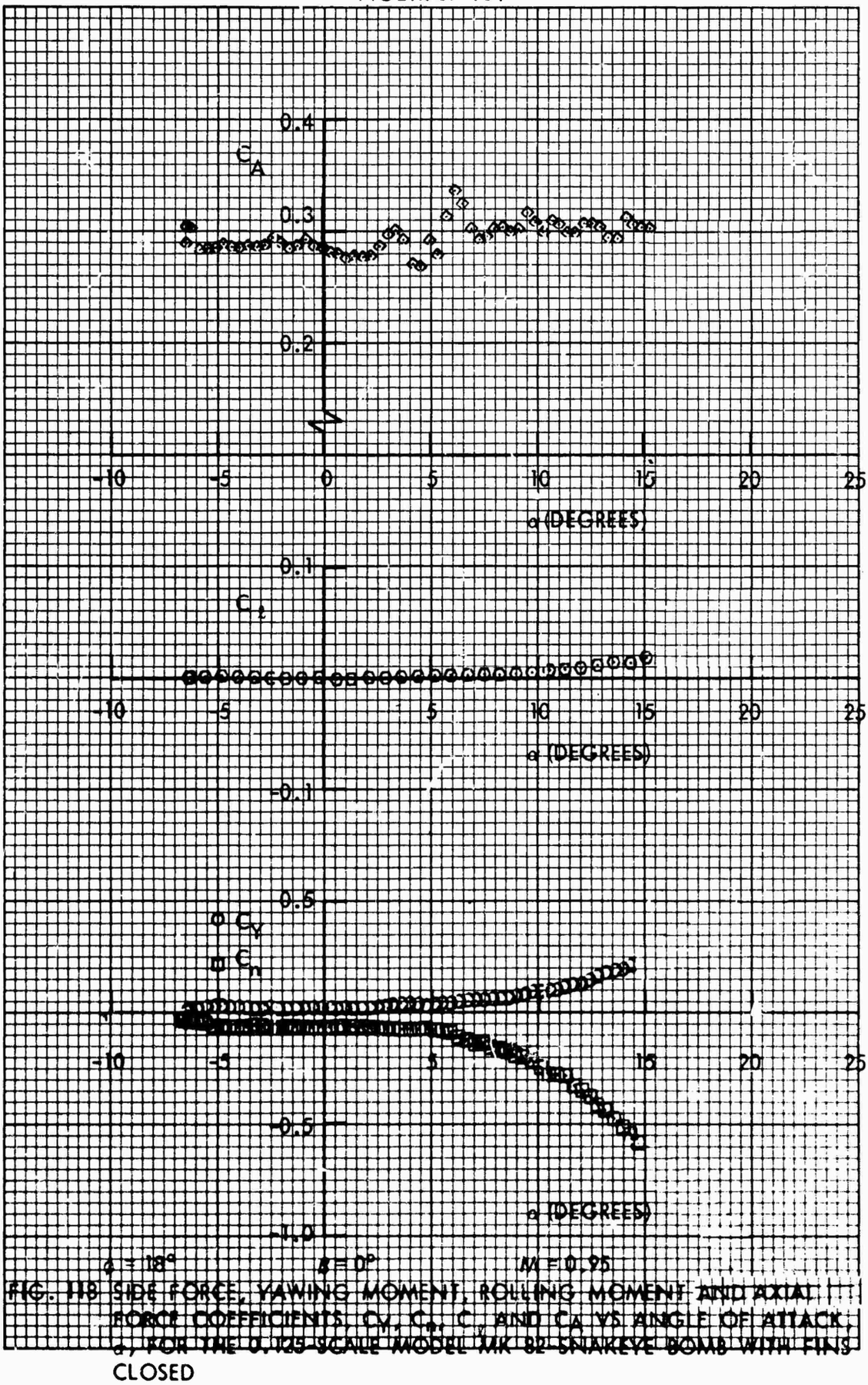

FIG. 118 SIDE FORCE, YAWING MOMENT, ROLLING MOMENT AND AXIAL FORCE COEFFICIENTS, C_Y, C_n, C_ℓ, AND C_A VS ANGLE OF ATTACK, α, FOR THE 0.125-SCALE MODEL MK 82-SNAKEYE BOMB WITH FINS CLOSED

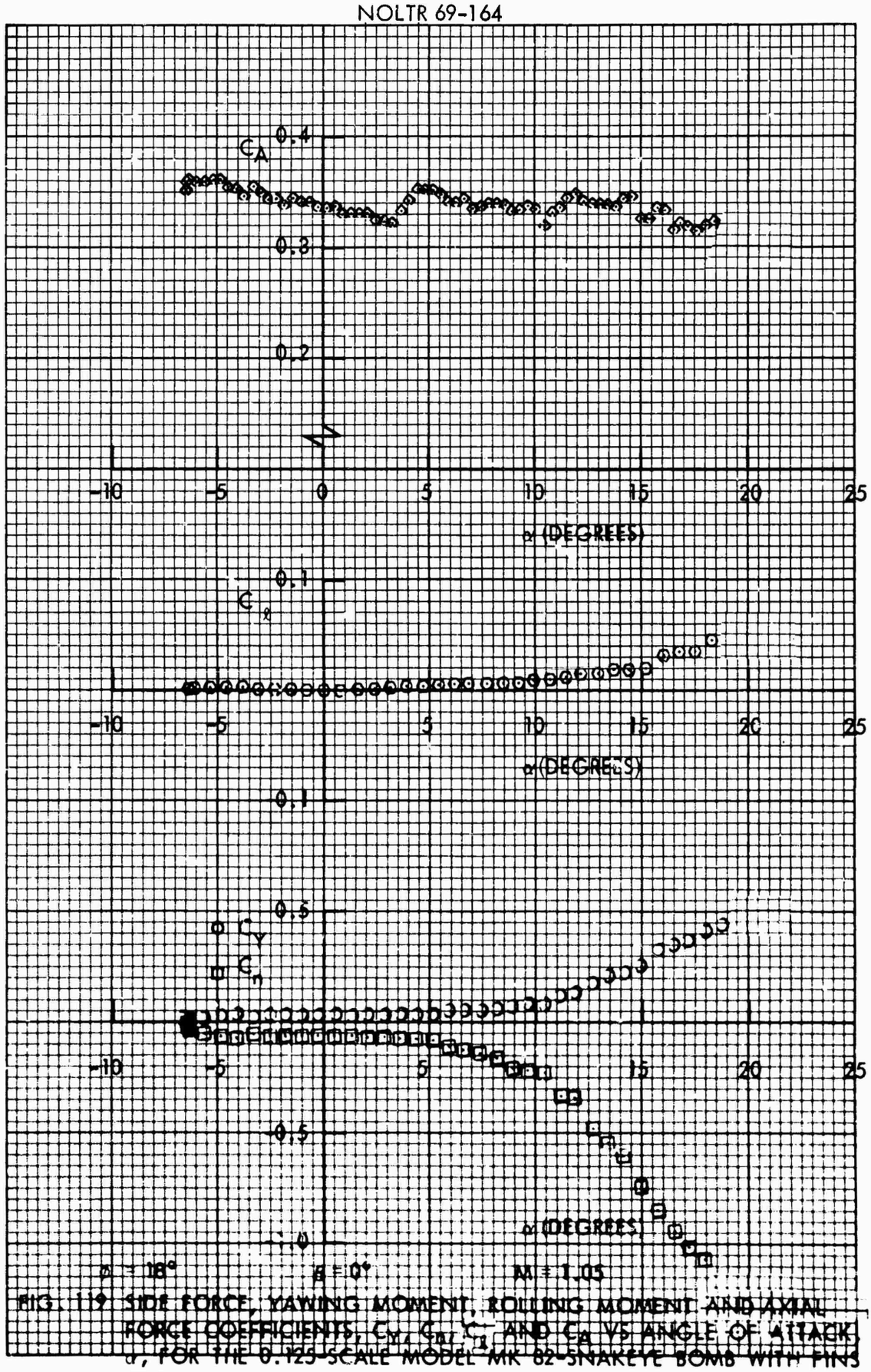

FIG. 119 SIDE FORCE, YAWING MOMENT, ROLLING MOMENT AND AXIAL FORCE COEFFICIENTS, C_Y, C_n, C_ℓ, AND C_A VS ANGLE OF ATTACK, α, FOR THE 0.125-SCALE MODEL MK 82-SNAKEYE BOMB WITH FINS CLOSED

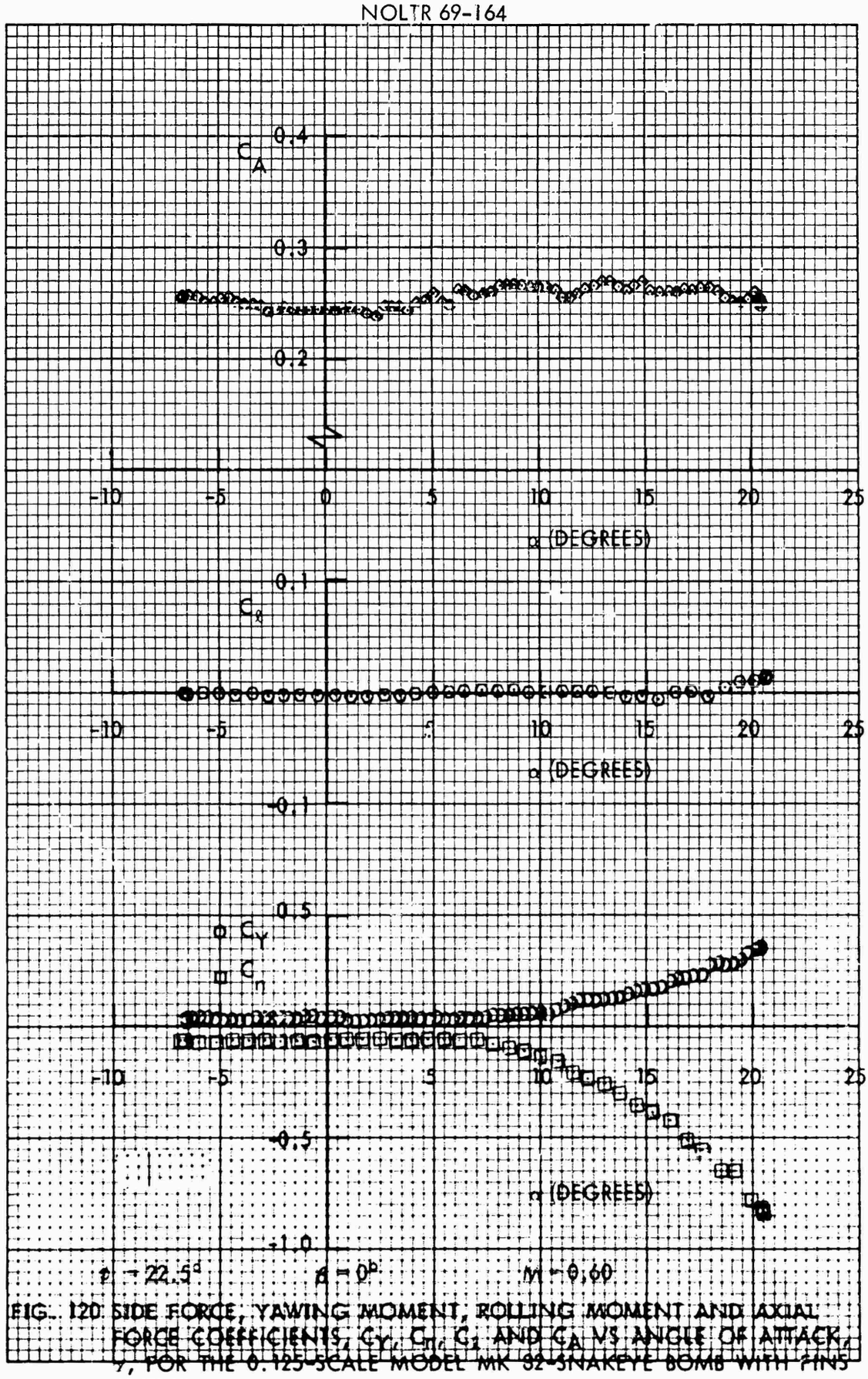

FIG. 120 SIDE FORCE, YAWING MOMENT, ROLLING MOMENT AND AXIAL FORCE COEFFICIENTS, C_Y, C_n, C_ℓ AND C_A VS ANGLE OF ATTACK, γ, FOR THE 0.125-SCALE MODEL MK 82-SNAKEYE BOMB WITH FINS CLOSED

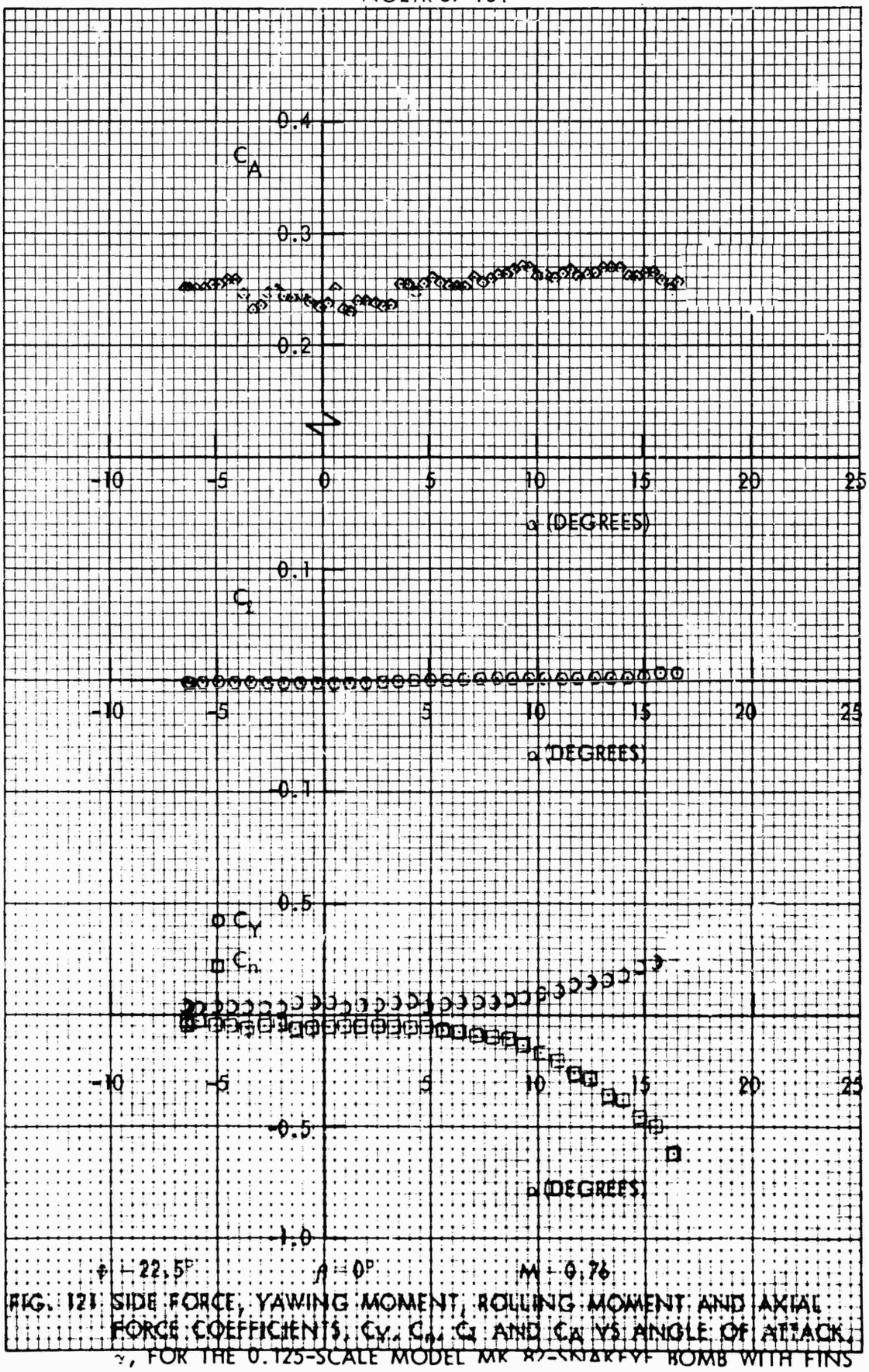

FIG. 121 SIDE FORCE, YAWING MOMENT, ROLLING MOMENT AND AXIAL FORCE COEFFICIENTS, C_Y, C_n, C_l AND C_A VS ANGLE OF ATTACK, α, FOR THE 0.125-SCALE MODEL MK 82-SNAKEYE BOMB WITH FINS CLOSED

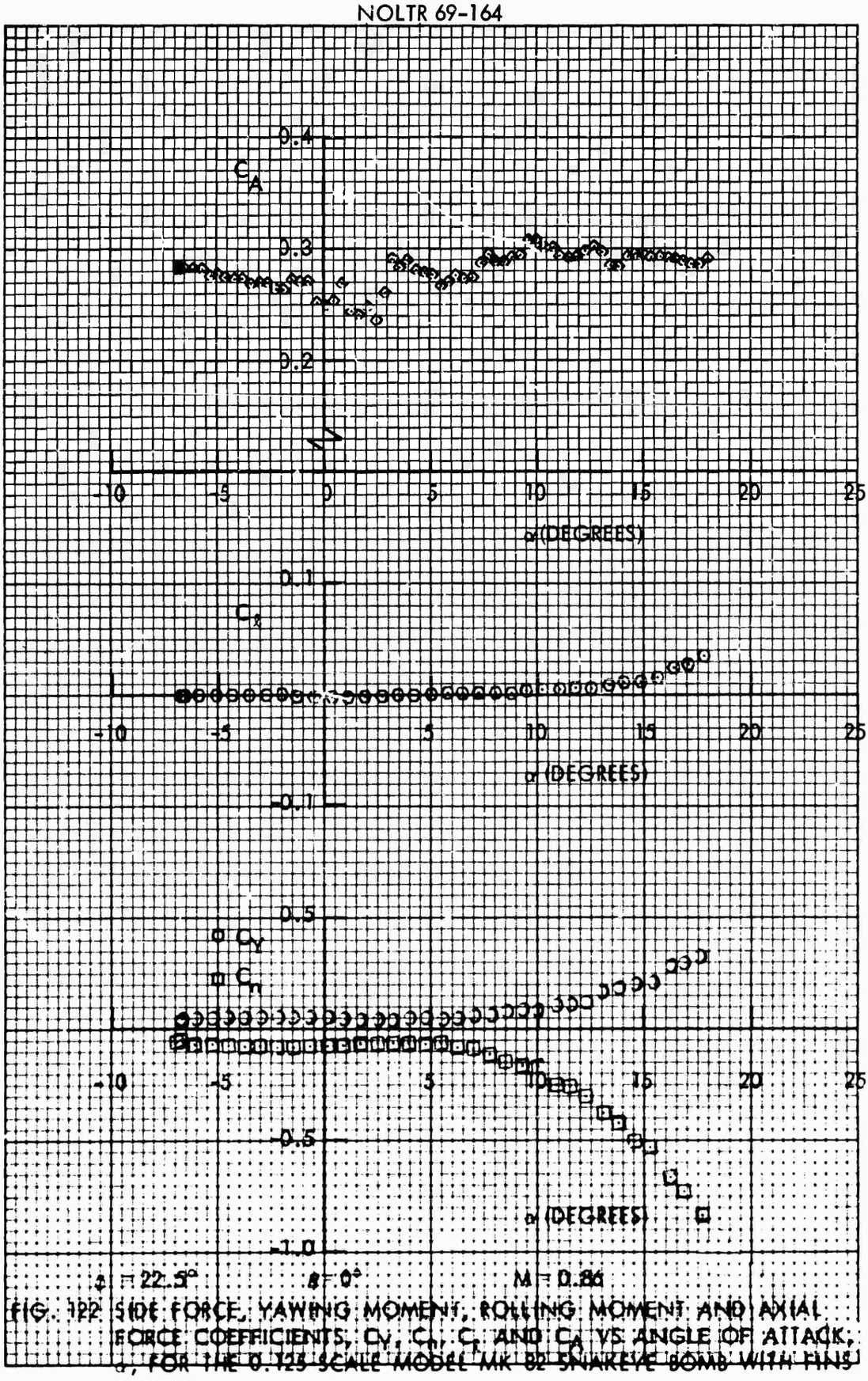

FIG. 122 SIDE FORCE, YAWING MOMENT, ROLLING MOMENT AND AXIAL FORCE COEFFICIENTS, C_Y, C_n, C_l AND C_A VS ANGLE OF ATTACK, α, FOR THE 0.125 SCALE MODEL MK 82 SNAKEYE BOMB WITH FINS CLOSED

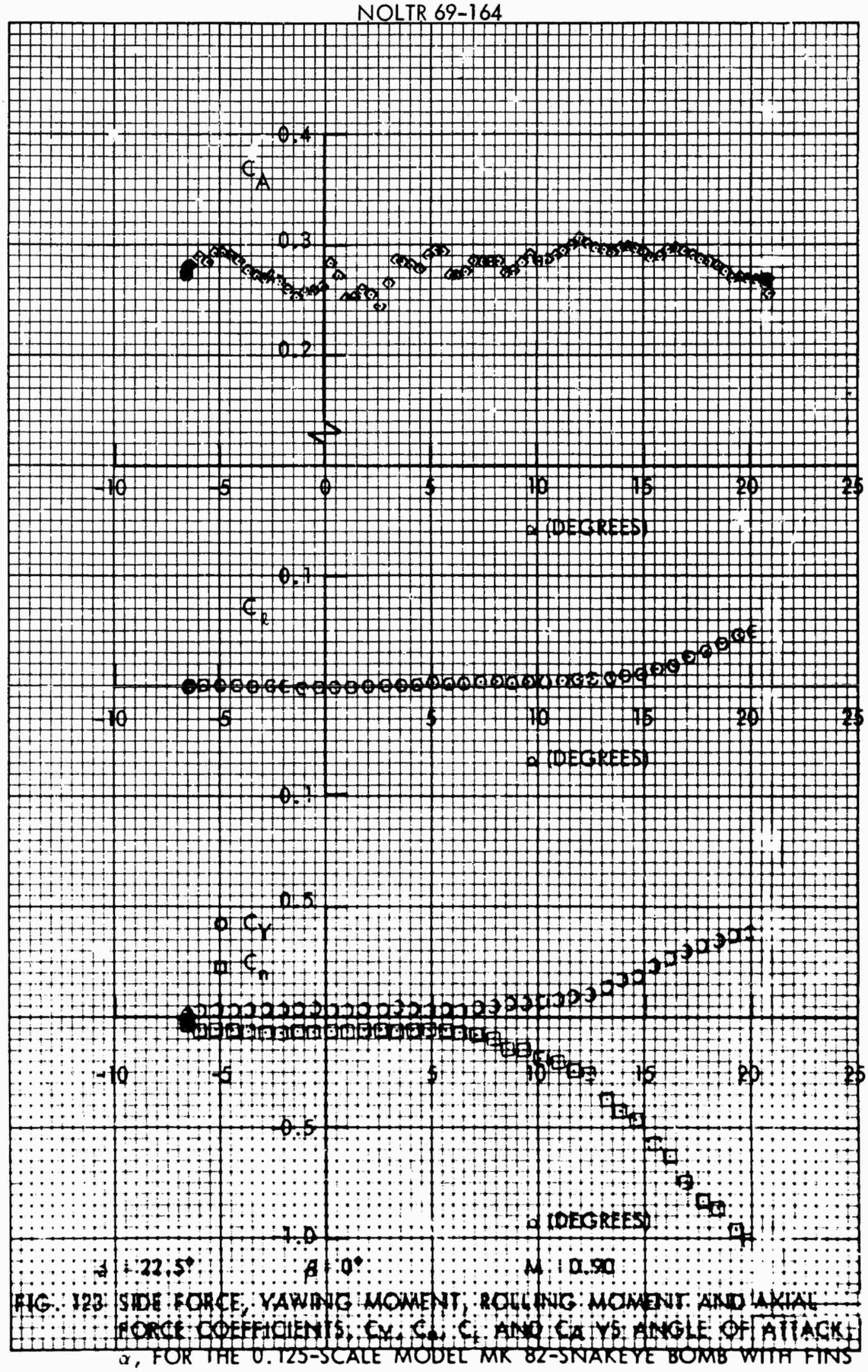

FIG. 123 SIDE FORCE, YAWING MOMENT, ROLLING MOMENT AND AXIAL FORCE COEFFICIENTS, C_Y, C_n, C_ℓ AND C_A VS ANGLE OF ATTACK, α, FOR THE 0.125-SCALE MODEL MK 82-SNAKEYE BOMB WITH FINS CLOSED

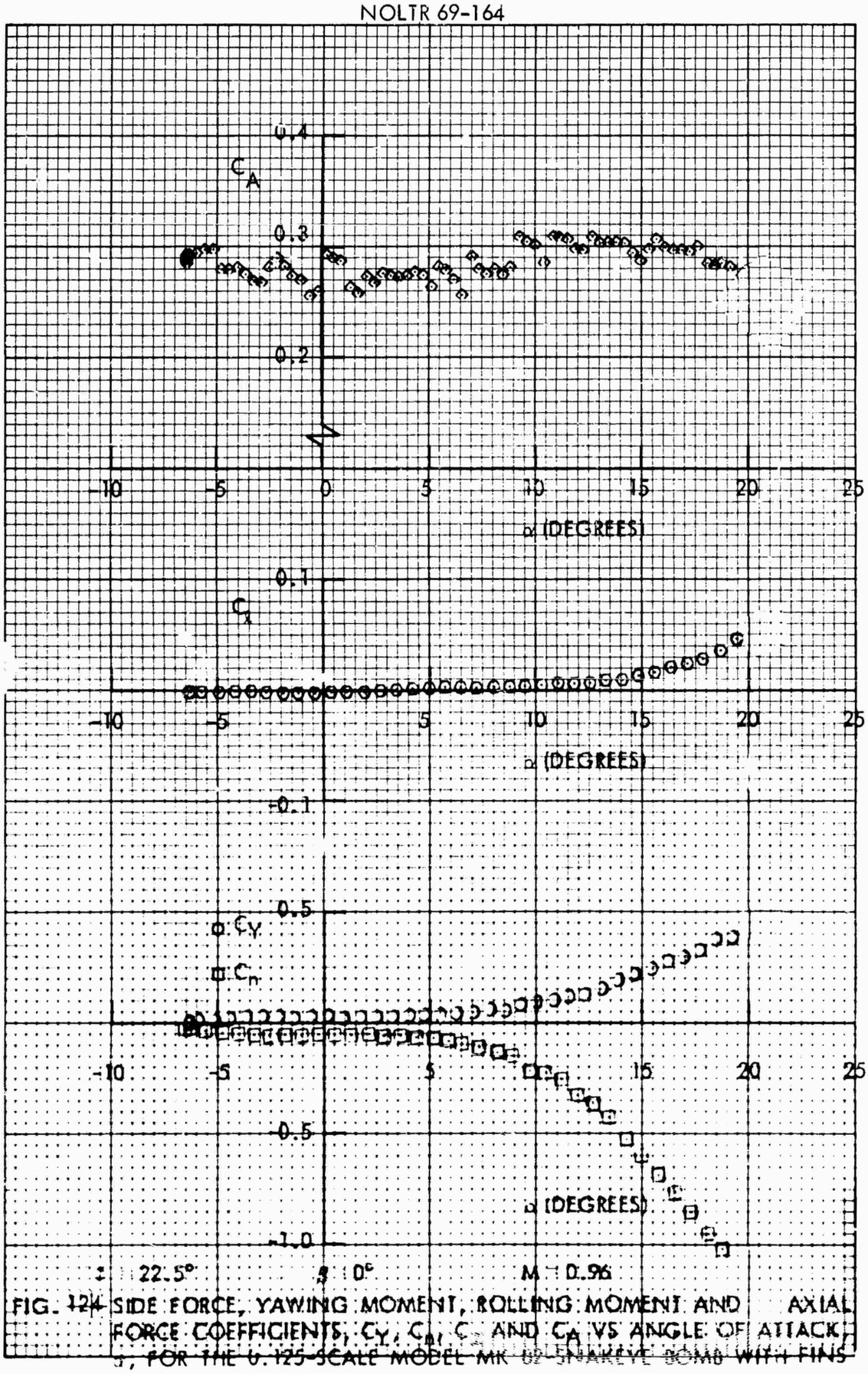

FIG. 124 SIDE FORCE, YAWING MOMENT, ROLLING MOMENT AND AXIAL FORCE COEFFICIENTS, C_Y, C_n, C_ℓ AND C_A VS ANGLE OF ATTACK, α, FOR THE 0.125-SCALE MODEL MK 82 SNAKEYE BOMB WITH FINS CLOSED

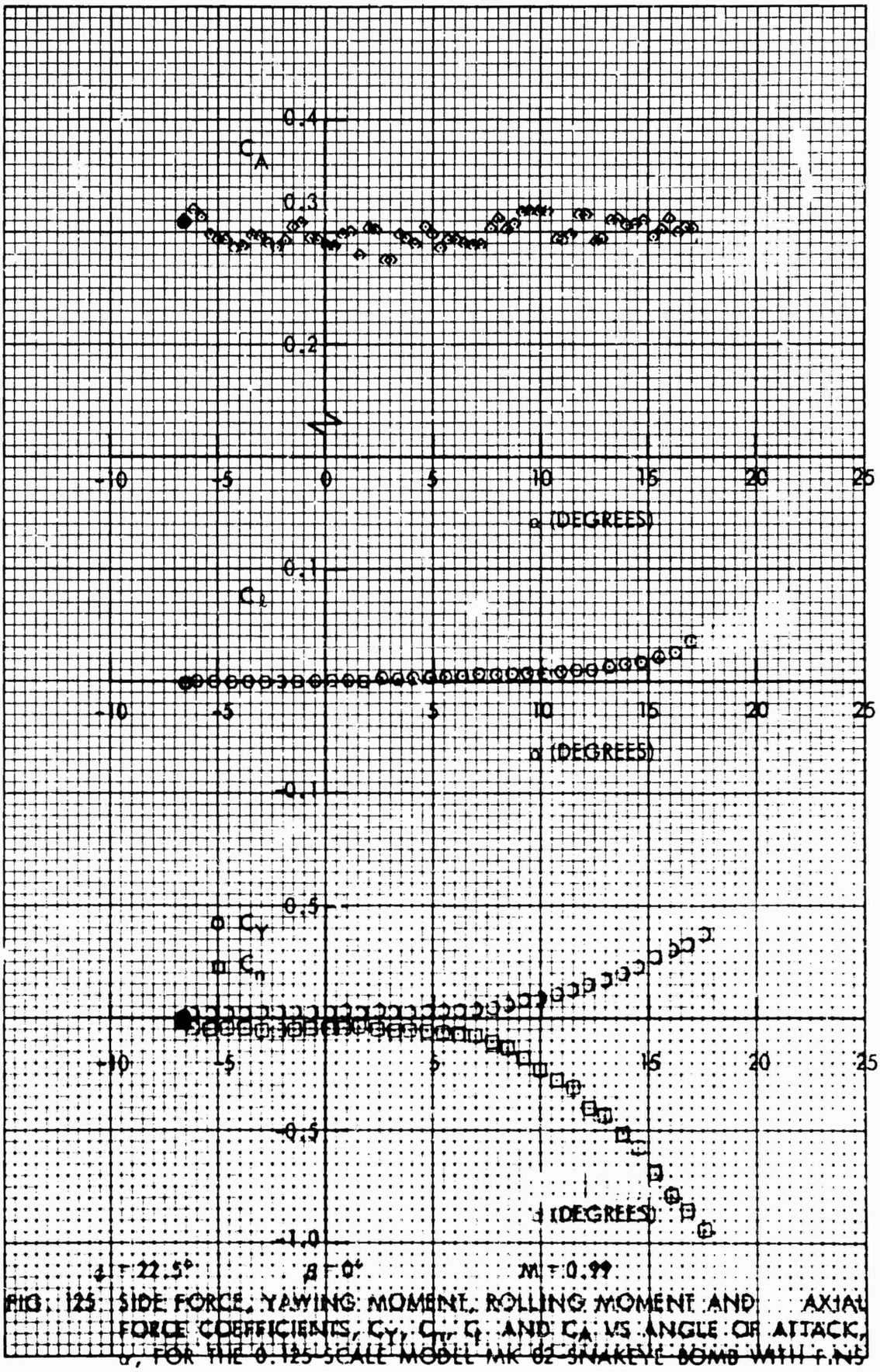

FIG. 125 SIDE FORCE, YAWING MOMENT, ROLLING MOMENT AND AXIAL FORCE COEFFICIENTS, C_Y, C_n, C_l AND C_A VS ANGLE OF ATTACK, α, FOR THE 0.125 SCALE MODEL MK 82 SNAKEYE BOMB WITH FINS CLOSED

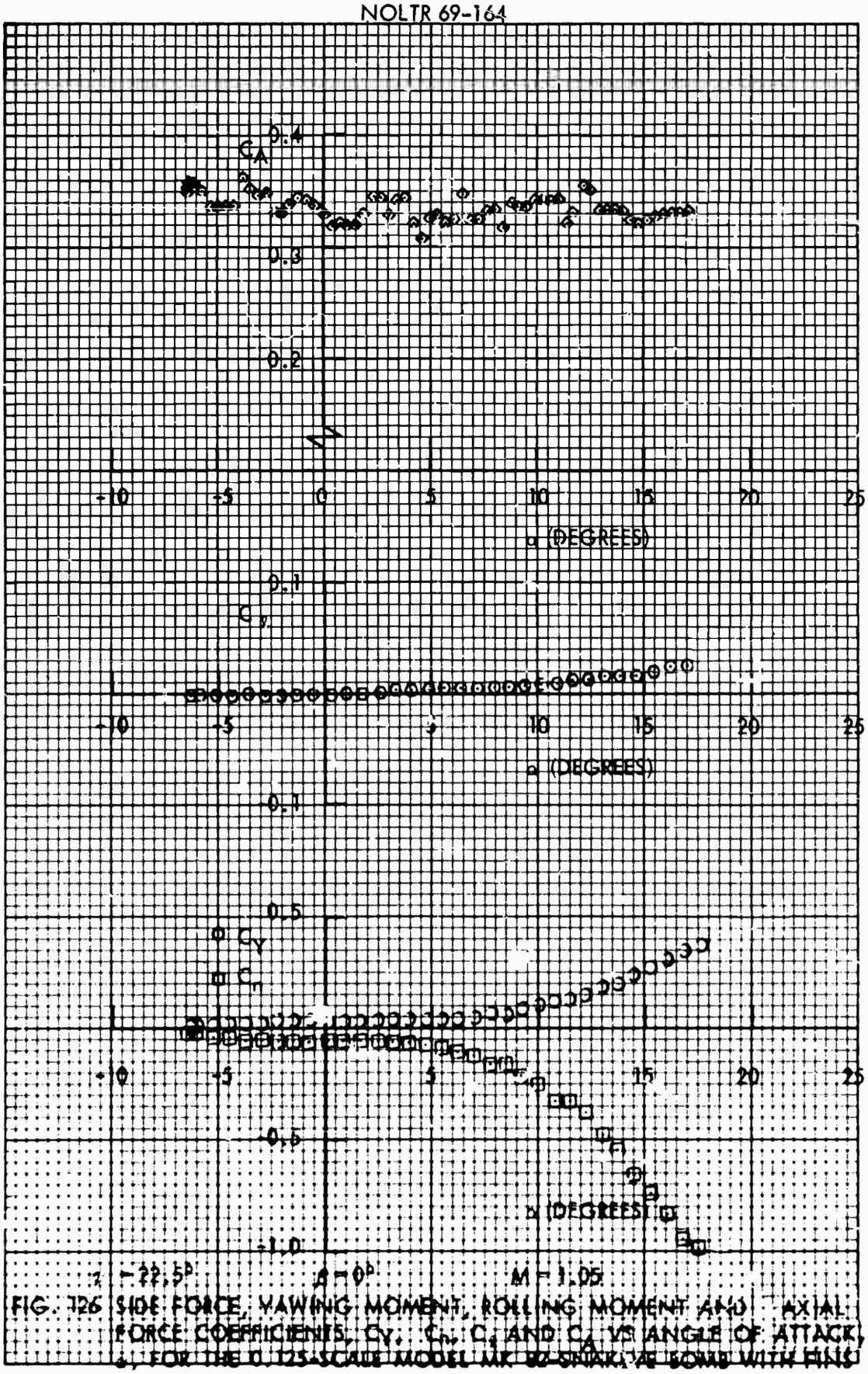

FIG. 126 SIDE FORCE, YAWING MOMENT, ROLLING MOMENT AND AXIAL FORCE COEFFICIENTS, C_Y, C_n, C_l AND C_A VS ANGLE OF ATTACK, α, FOR THE 0.125-SCALE MODEL MK 82 SNAKEYE BOMB WITH FINS CLOSED

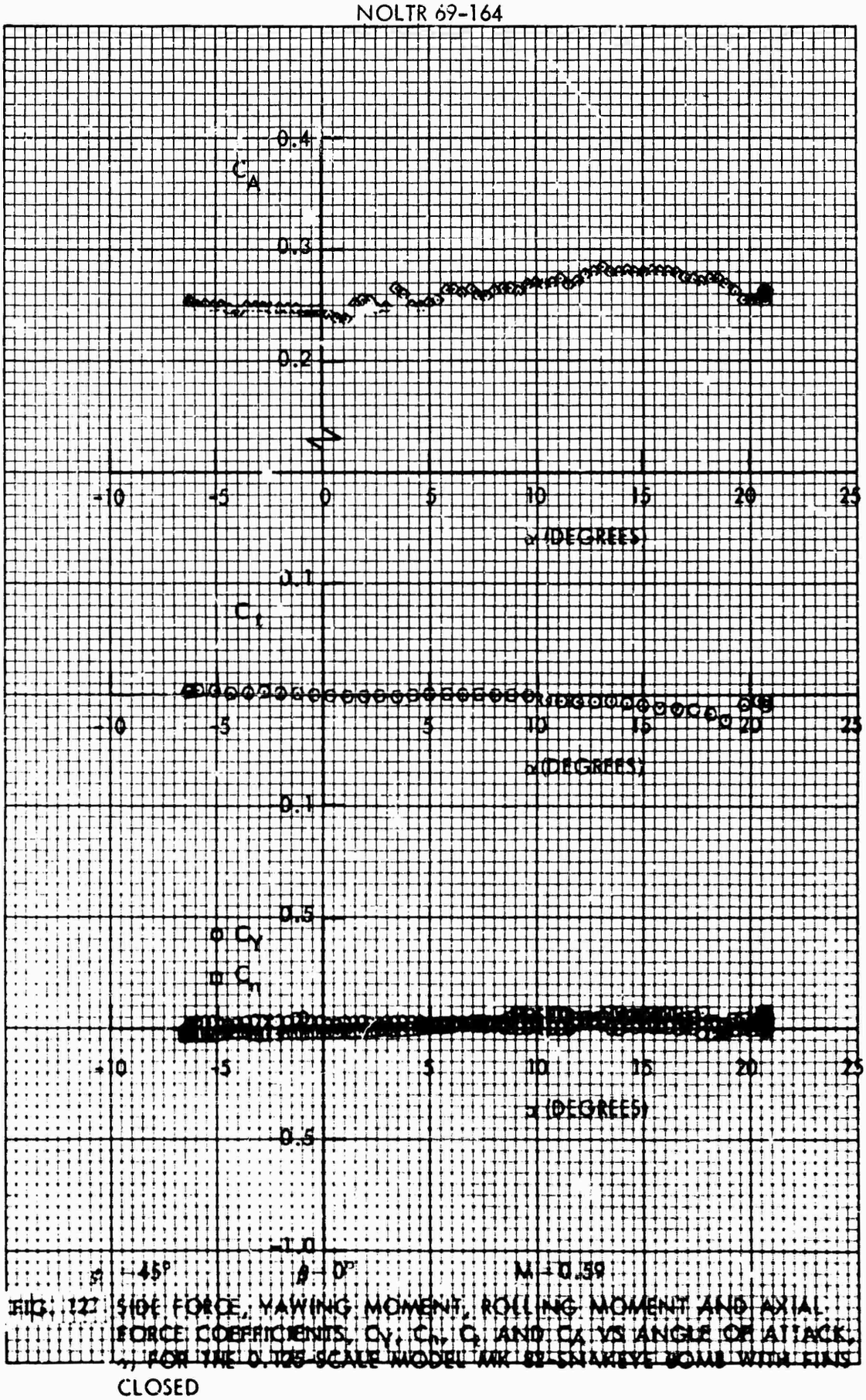

FIG. 122 SIDE FORCE, YAWING MOMENT, ROLLING MOMENT AND AXIAL FORCE COEFFICIENTS, C_Y, C_n, C_t AND C_A VS ANGLE OF ATTACK, α, FOR THE 0.105-SCALE MODEL MK 82 SNAKEYE BOMB WITH FINS CLOSED

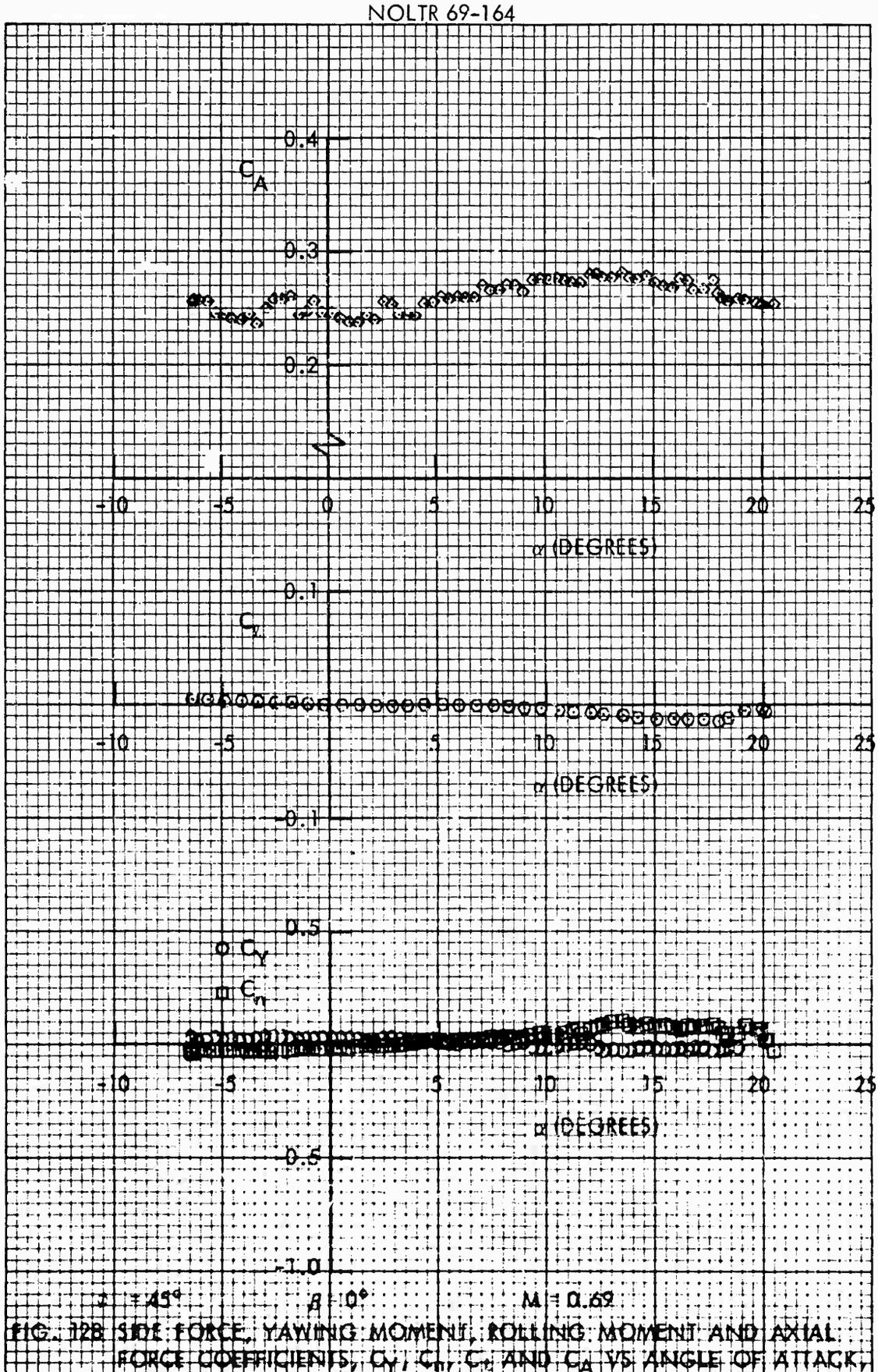

FIG. 12B SIDE FORCE, YAWING MOMENT, ROLLING MOMENT AND AXIAL FORCE COEFFICIENTS, C_Y, C_n, C_ℓ AND C_A VS ANGLE OF ATTACK, α, FOR THE 0.125-SCALE MODEL MK 82-SNAKEYE BOMB WITH FINS CLOSED

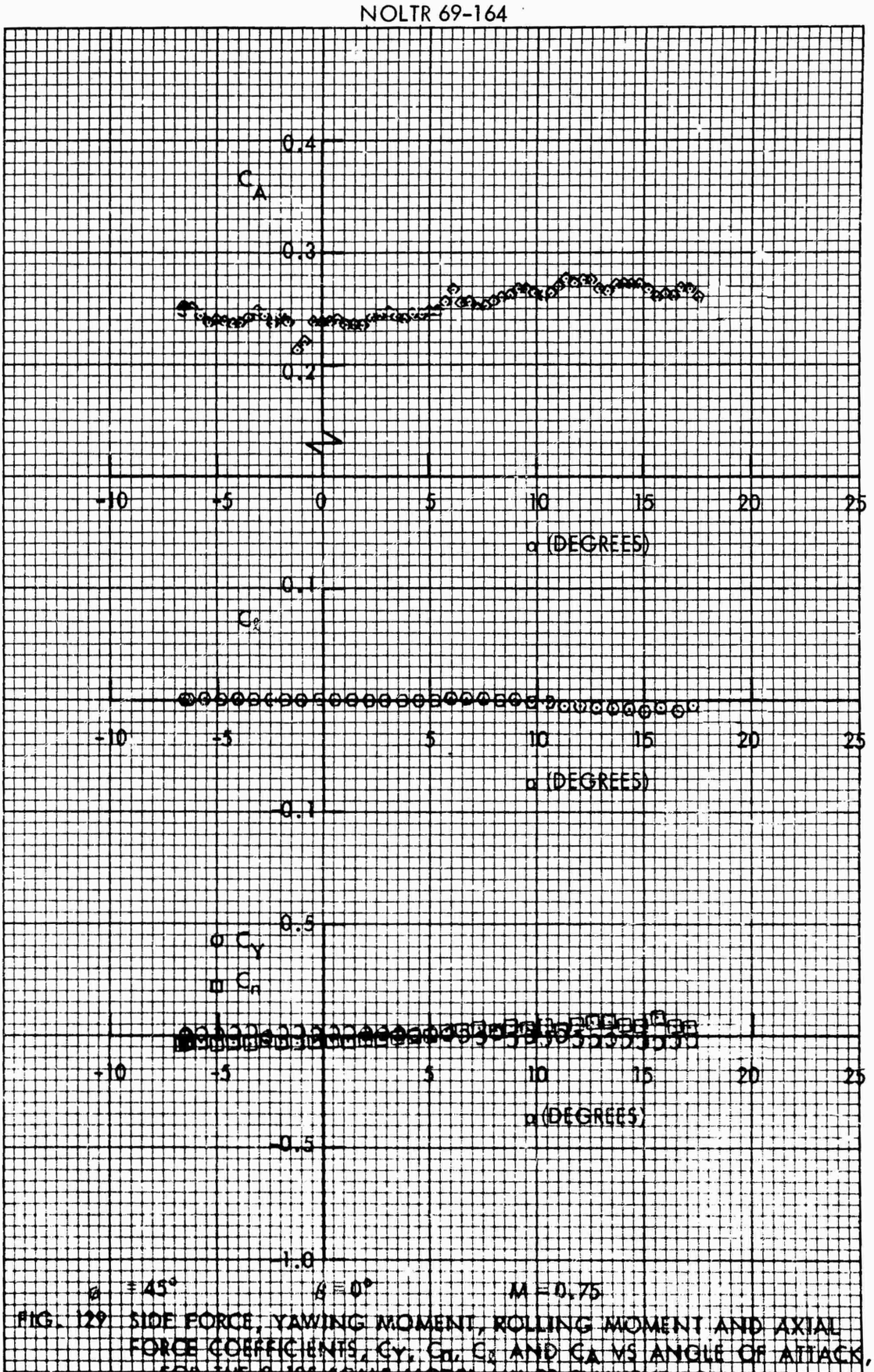

$\phi = 45°$ $\beta = 0°$ $M = 0.75$

FIG. 129 SIDE FORCE, YAWING MOMENT, ROLLING MOMENT AND AXIAL FORCE COEFFICIENTS, C_Y, C_n, C_ℓ AND C_A VS ANGLE OF ATTACK, α, FOR THE 0.125-SCALE MODEL MK 82-SNAKEYE BOMB WITH FINS CLOSED

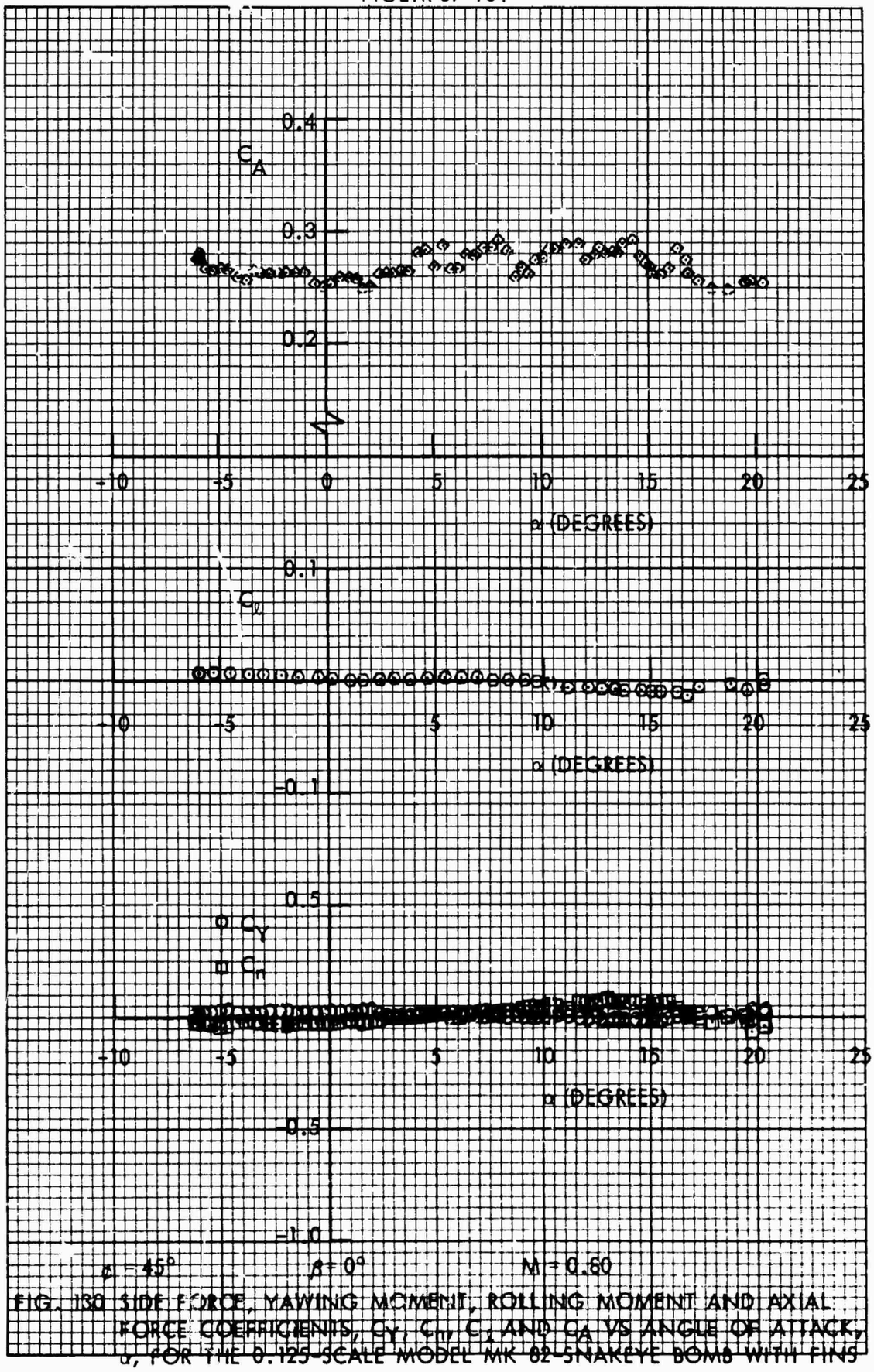

FIG. 130 SIDE FORCE, YAWING MOMENT, ROLLING MOMENT AND AXIAL FORCE COEFFICIENTS, C_Y, C_n, C_ℓ AND C_A VS ANGLE OF ATTACK, α, FOR THE 0.125-SCALE MODEL MK 82 SNAKEYE BOMB WITH FINS CLOSED

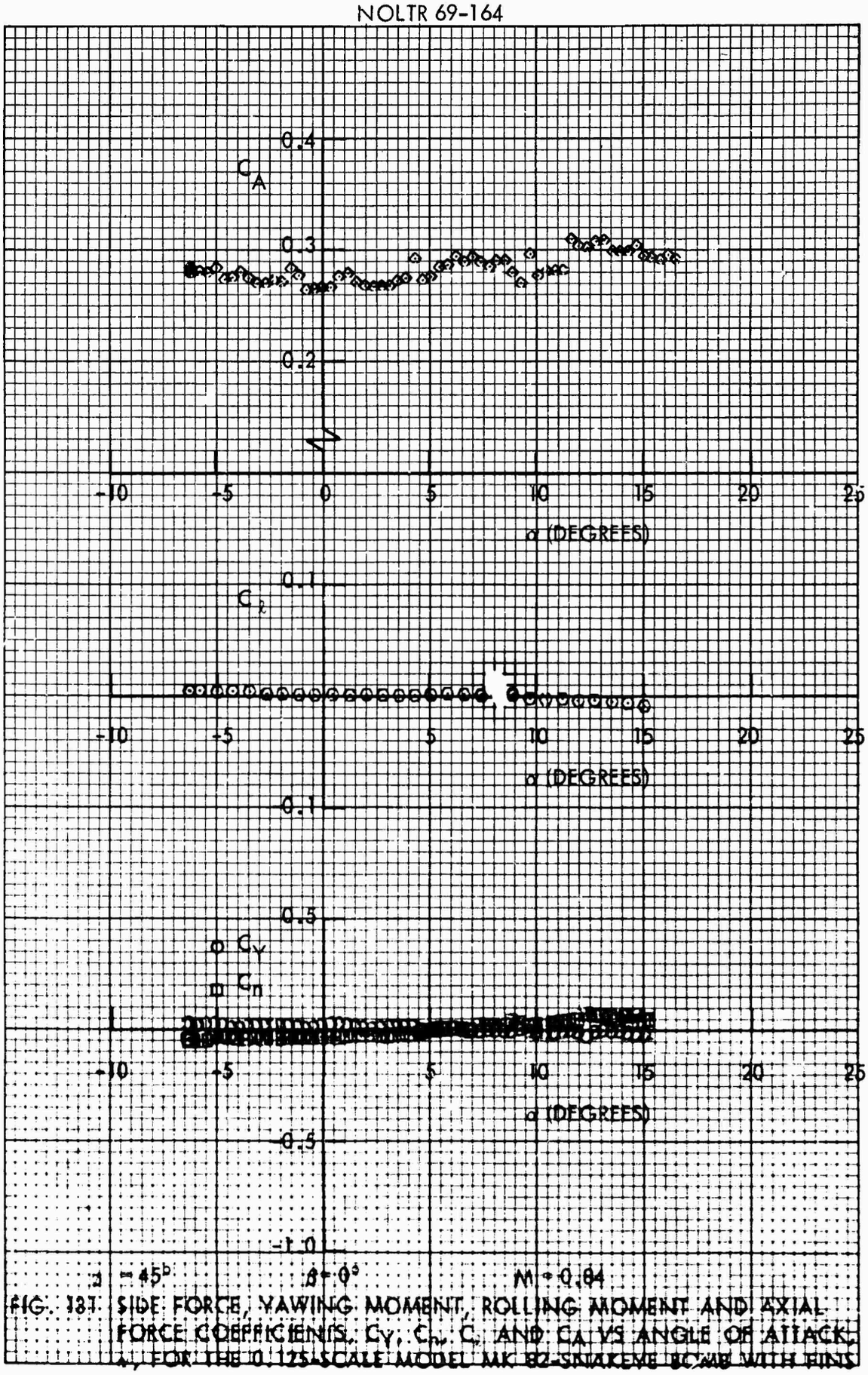

FIG. 137 SIDE FORCE, YAWING MOMENT, ROLLING MOMENT AND AXIAL FORCE COEFFICIENTS, C_Y, C_n, C_l AND C_A VS ANGLE OF ATTACK, α, FOR THE 0.125-SCALE MODEL MK 82-SNAKEYE BCMB WITH FINS CLOSED

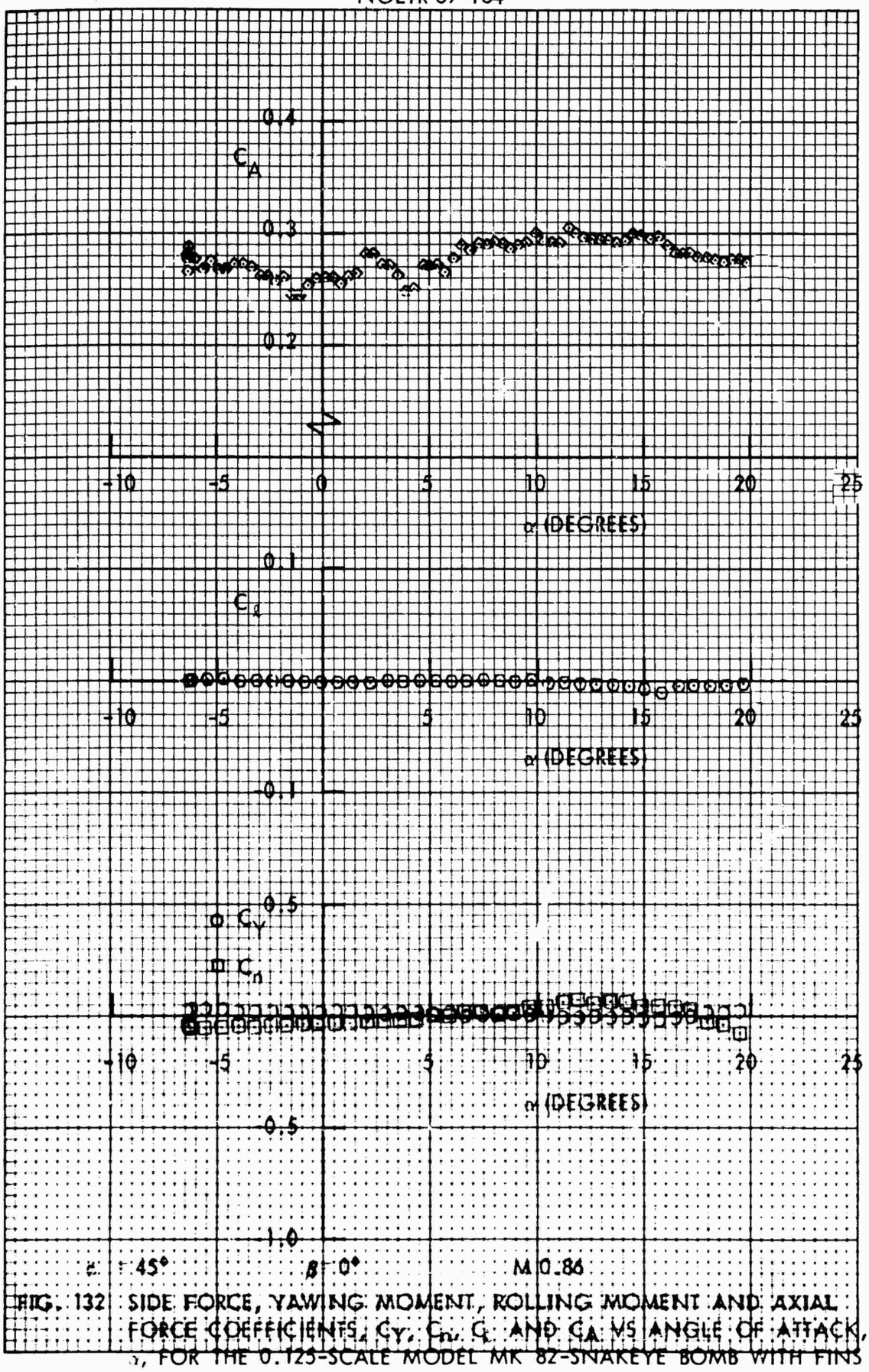

FIG. 132 SIDE FORCE, YAWING MOMENT, ROLLING MOMENT AND AXIAL FORCE COEFFICIENTS, C_Y, C_n, C_{l_α} AND C_A VS ANGLE OF ATTACK, α, FOR THE 0.125-SCALE MODEL MK 82-SNAKEYE BOMB WITH FINS CLOSED

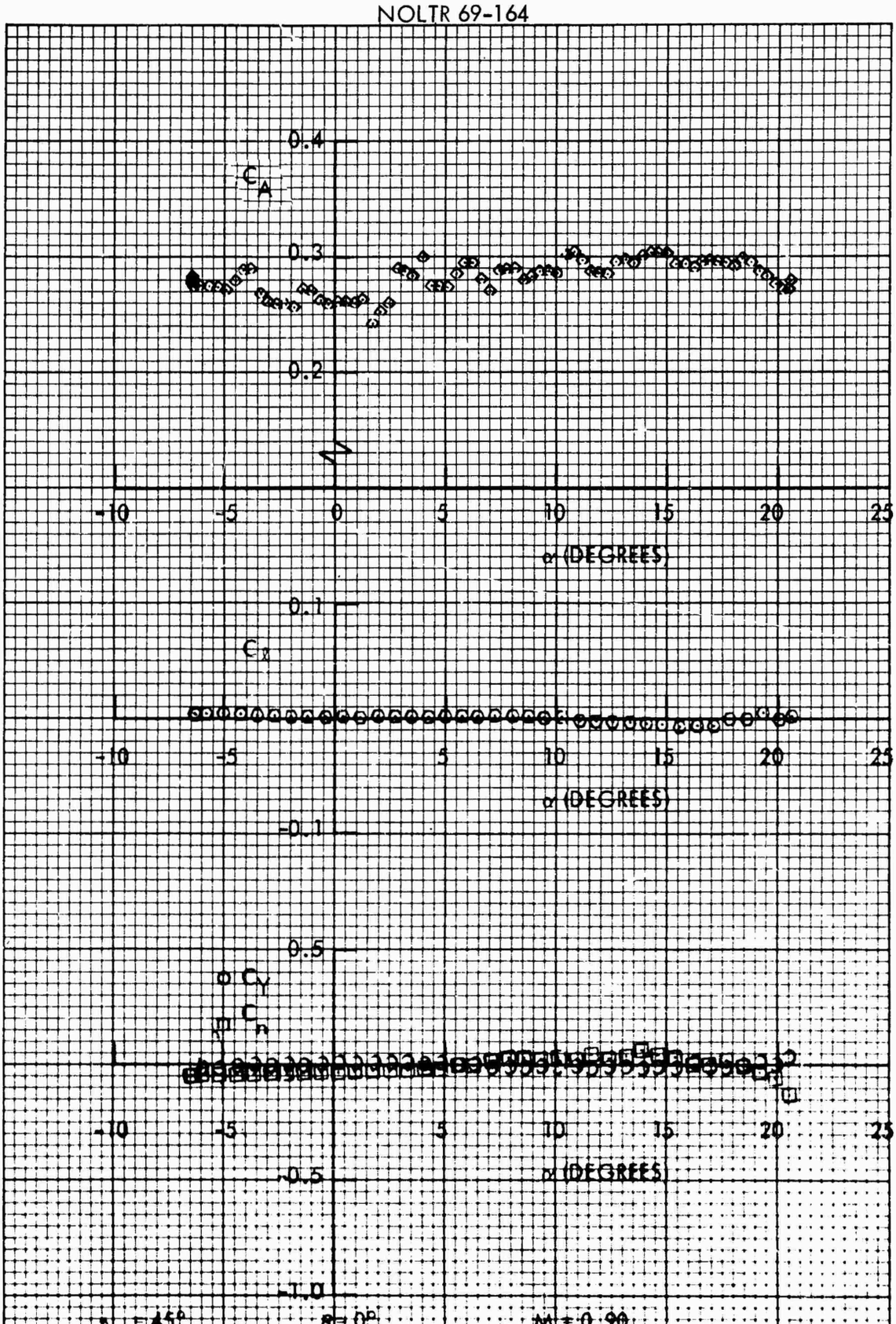

FIG. 33 SIDE FORCE, YAWING MOMENT, ROLLING MOMENT AND AXIAL FORCE COEFFICIENTS, C_Y, C_n, C_ℓ AND C_A VS ANGLE OF ATTACK, α, FOR THE 0.125-SCALE MODEL MK 82 SNAKEYE BOMB WITH FINS CLOSED

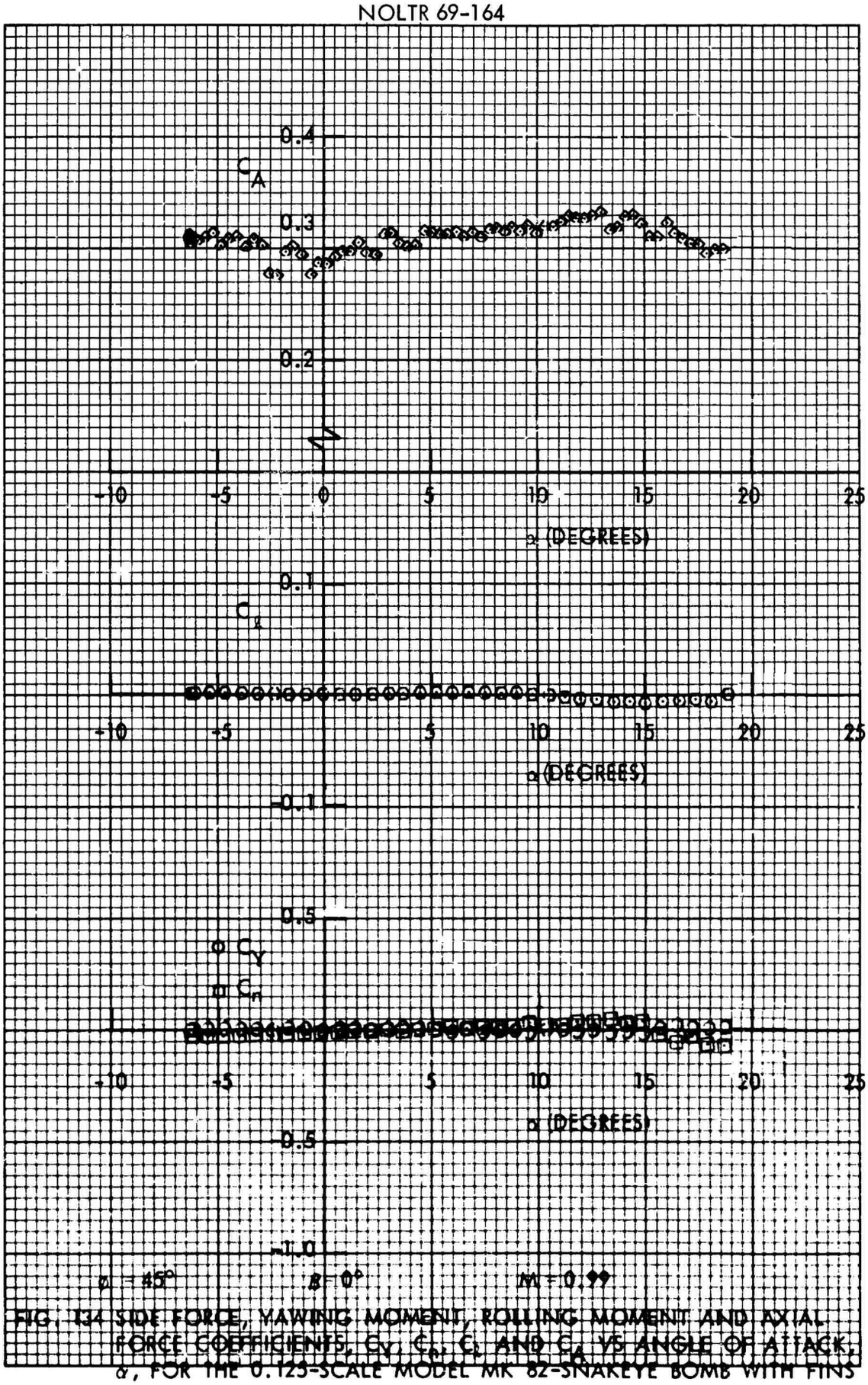

FIG. 134 SIDE FORCE, YAWING MOMENT, ROLLING MOMENT AND AXIAL FORCE COEFFICIENTS, C_Y, C_n, C_ℓ AND C_A VS ANGLE OF ATTACK, α, FOR THE 0.125-SCALE MODEL MK 82-SNAKEYE BOMB WITH FINS CLOSED

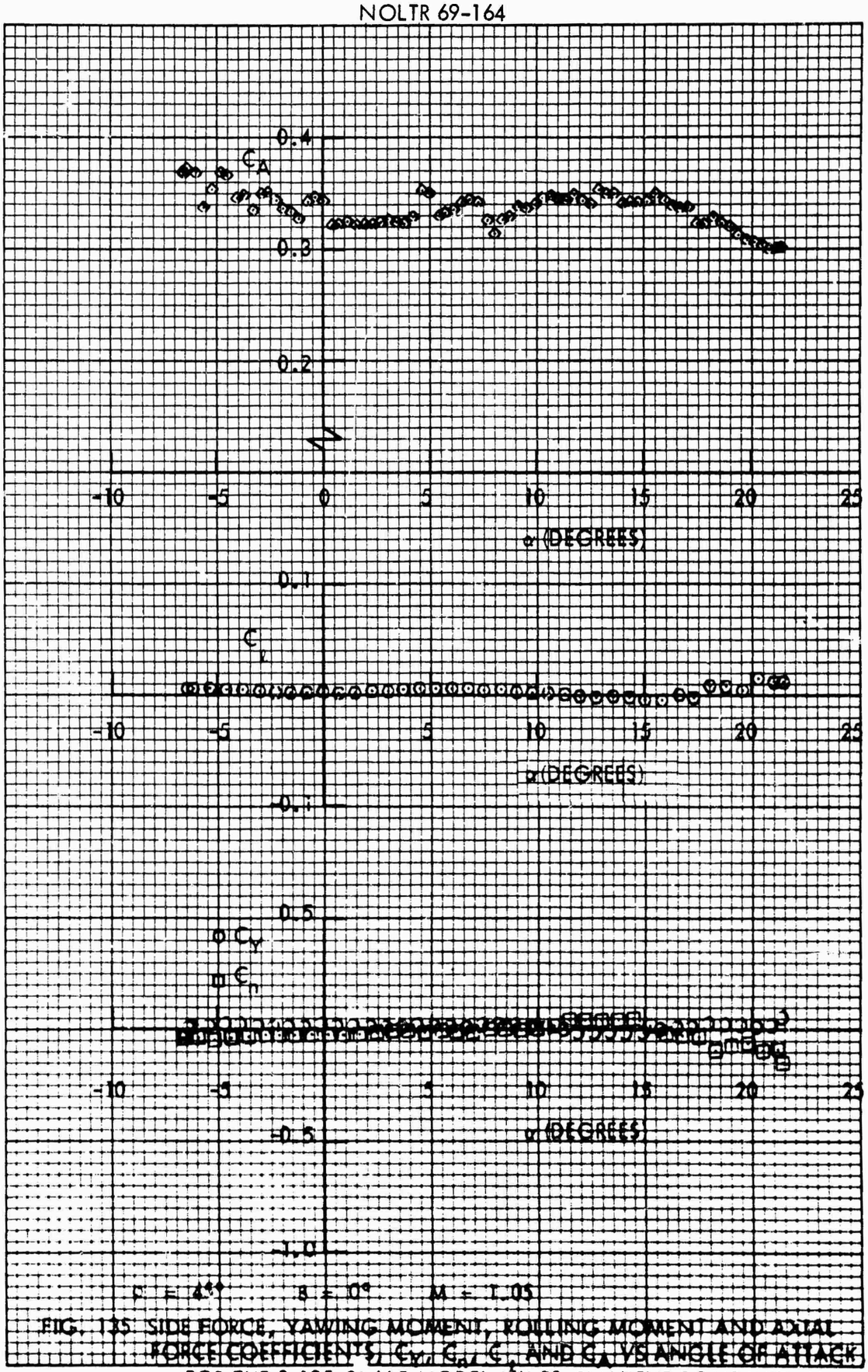

FIG. 135 SIDE FORCE, YAWING MOMENT, ROLLING MOMENT AND AXIAL FORCE COEFFICIENTS, C_Y, $C_{l'}$, C_n, AND C_A VS ANGLE OF ATTACK α, FOR THE 0.125-SCALE MODEL MK 82-SNAKEYE BOMB WITH FINS CLOSED

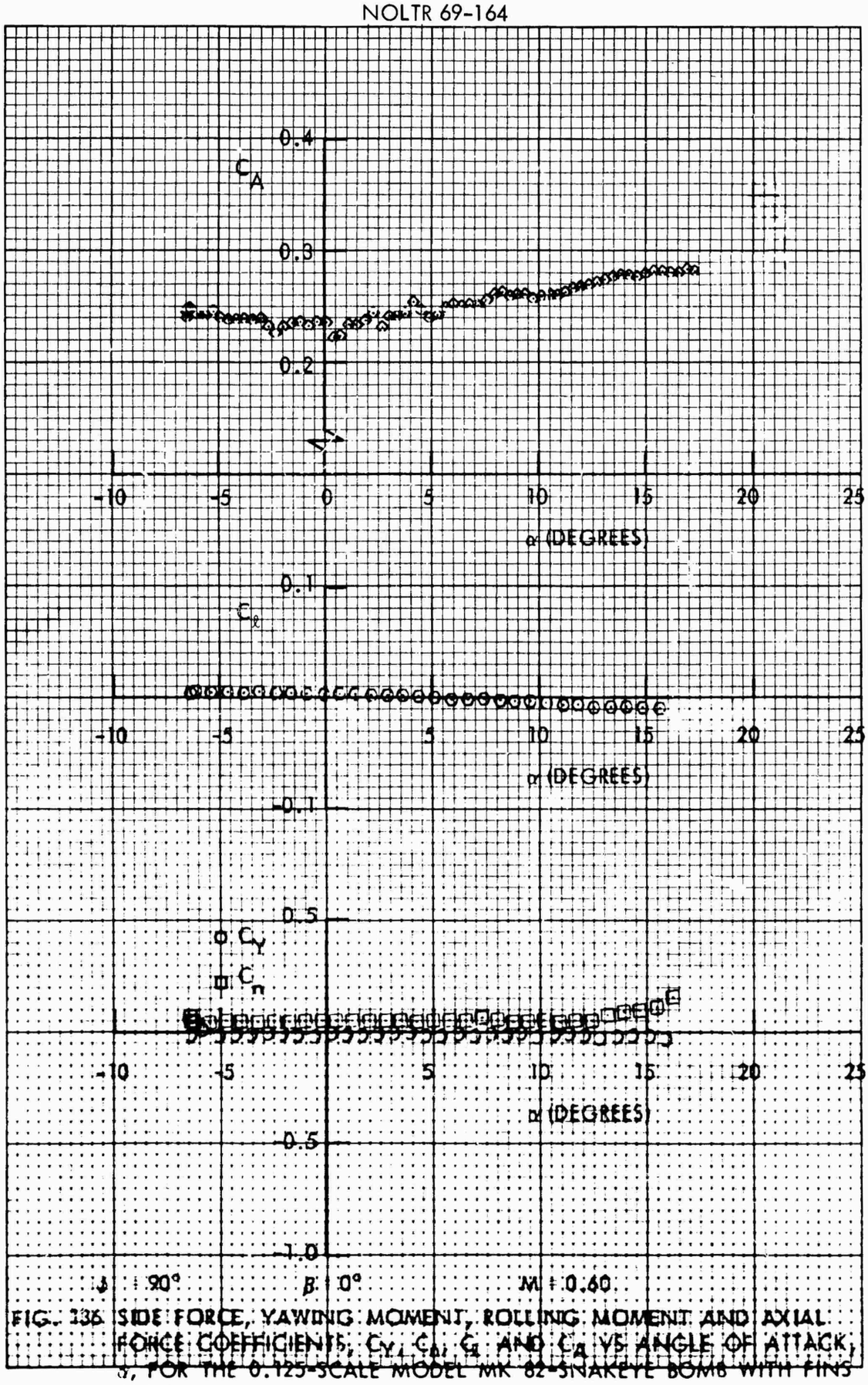

FIG. 136 SIDE FORCE, YAWING MOMENT, ROLLING MOMENT AND AXIAL FORCE COEFFICIENTS, C_Y, C_n, C_ℓ AND C_A VS ANGLE OF ATTACK, α, FOR THE 0.125-SCALE MODEL MK 82-SNAKEYE BOMB WITH FINS CLOSED

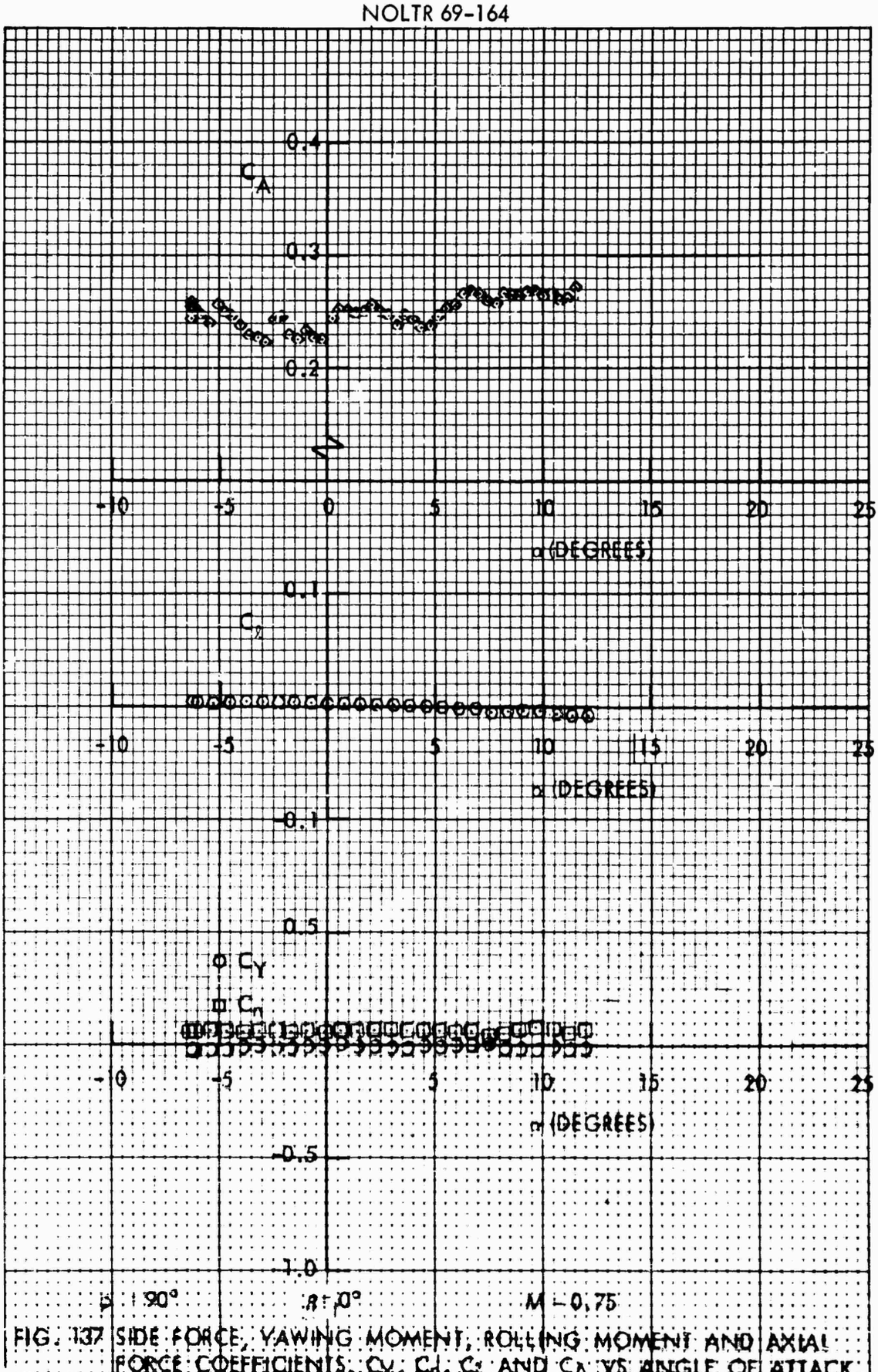

FIG. 137 SIDE FORCE, YAWING MOMENT, ROLLING MOMENT AND AXIAL FORCE COEFFICIENTS, C_Y, C_n, C_ℓ AND C_A VS ANGLE OF ATTACK, α, FOR THE 0.125-SCALE MODEL MK 82-SNAKEYE BOMB WITH FINS CLOSED

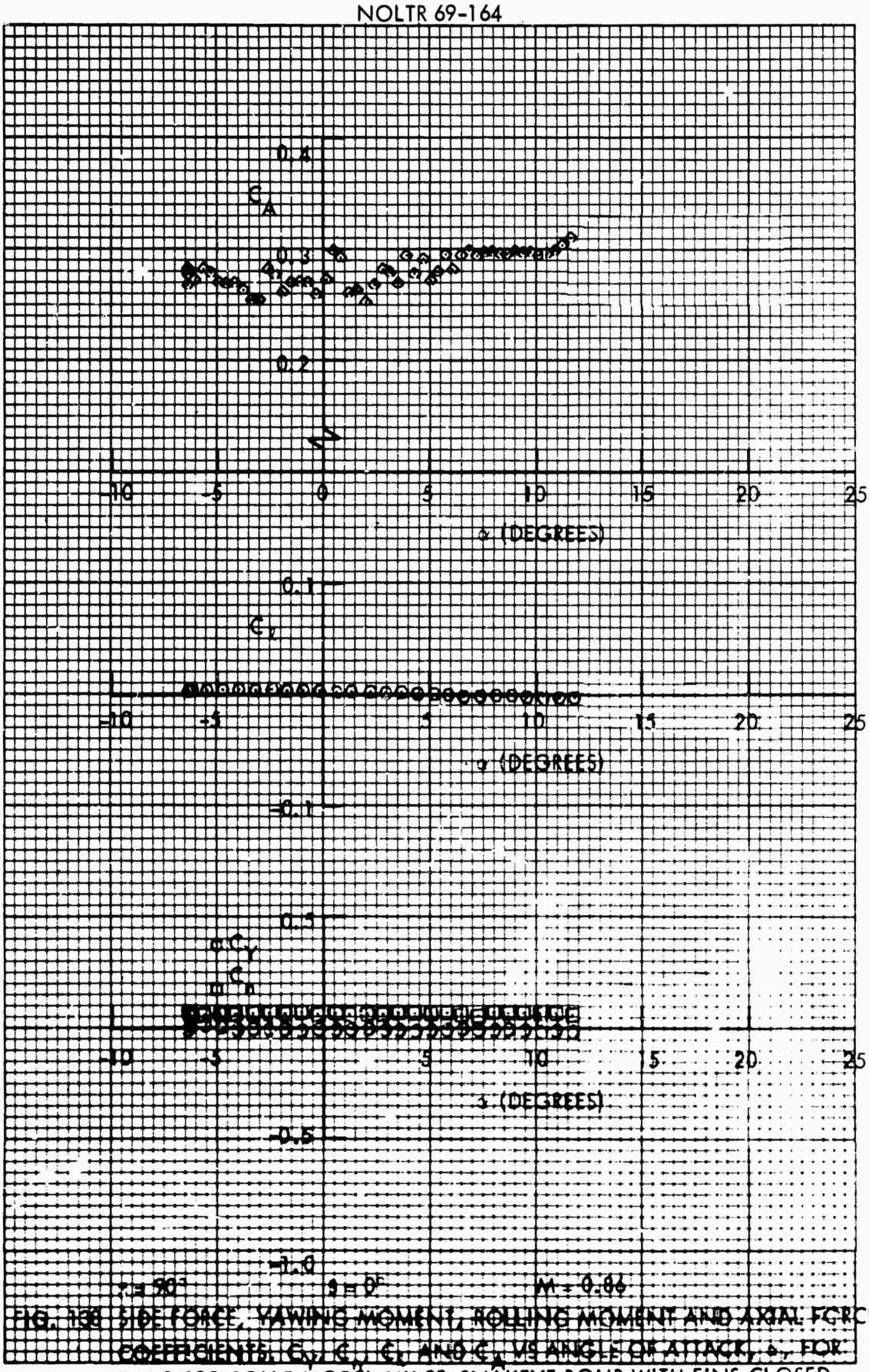

FIG. 138 SIDE FORCE, YAWING MOMENT, ROLLING MOMENT AND AXIAL FORCE COEFFICIENTS, C_Y, C_n, C_l AND C_A VS ANGLE OF ATTACK, α, FOR THE 0.125-SCALE MODEL MK 82-SNAKEYE BOMB WITH FINS CLOSED

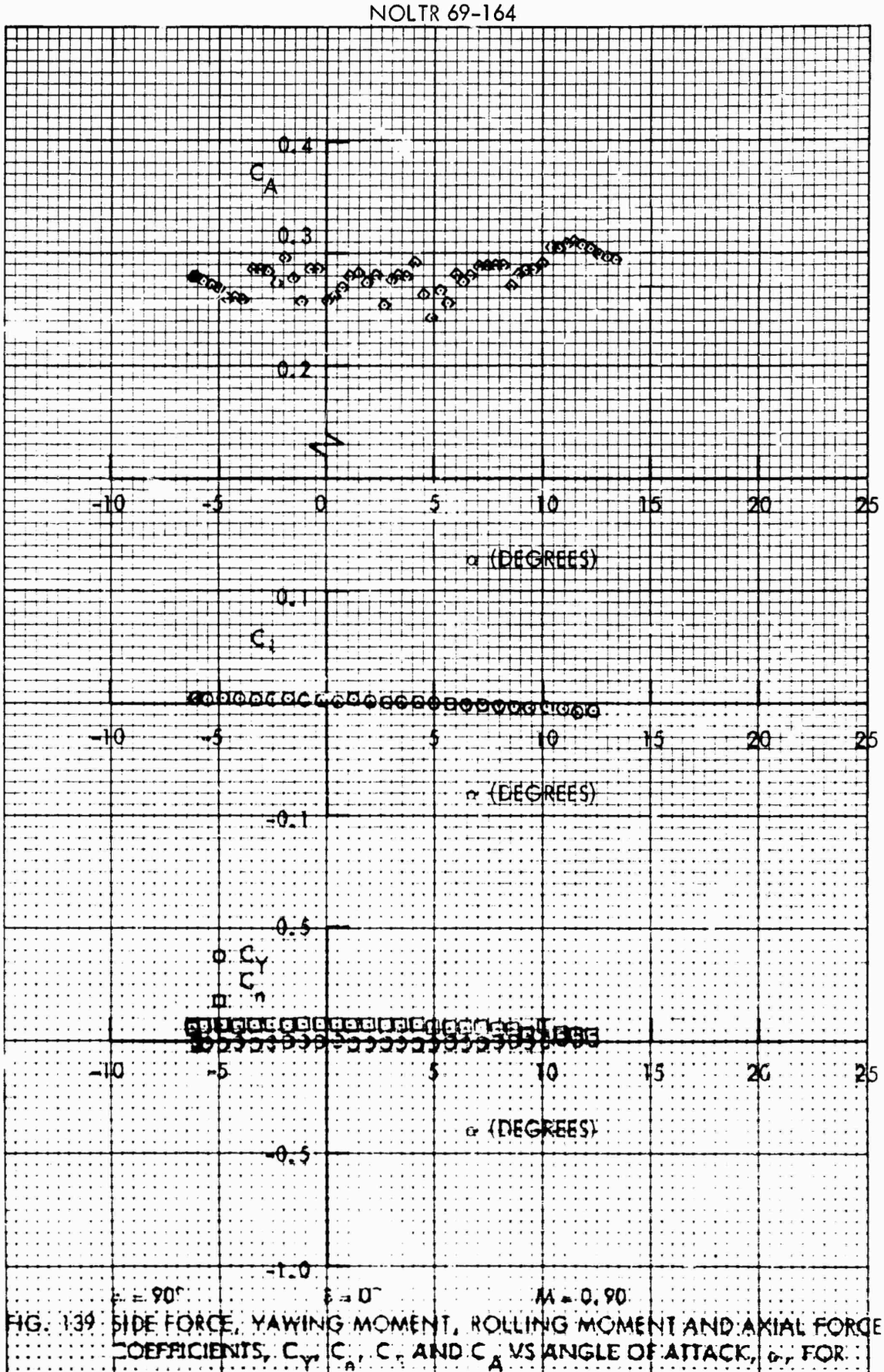

FIG. 139 SIDE FORCE, YAWING MOMENT, ROLLING MOMENT AND AXIAL FORCE COEFFICIENTS, C_Y, C_n, C_l AND C_A VS ANGLE OF ATTACK, α, FOR THE 0.125-SCALE MODEL MK 82-SNAKEYE BOMB WITH FINS CLOSED

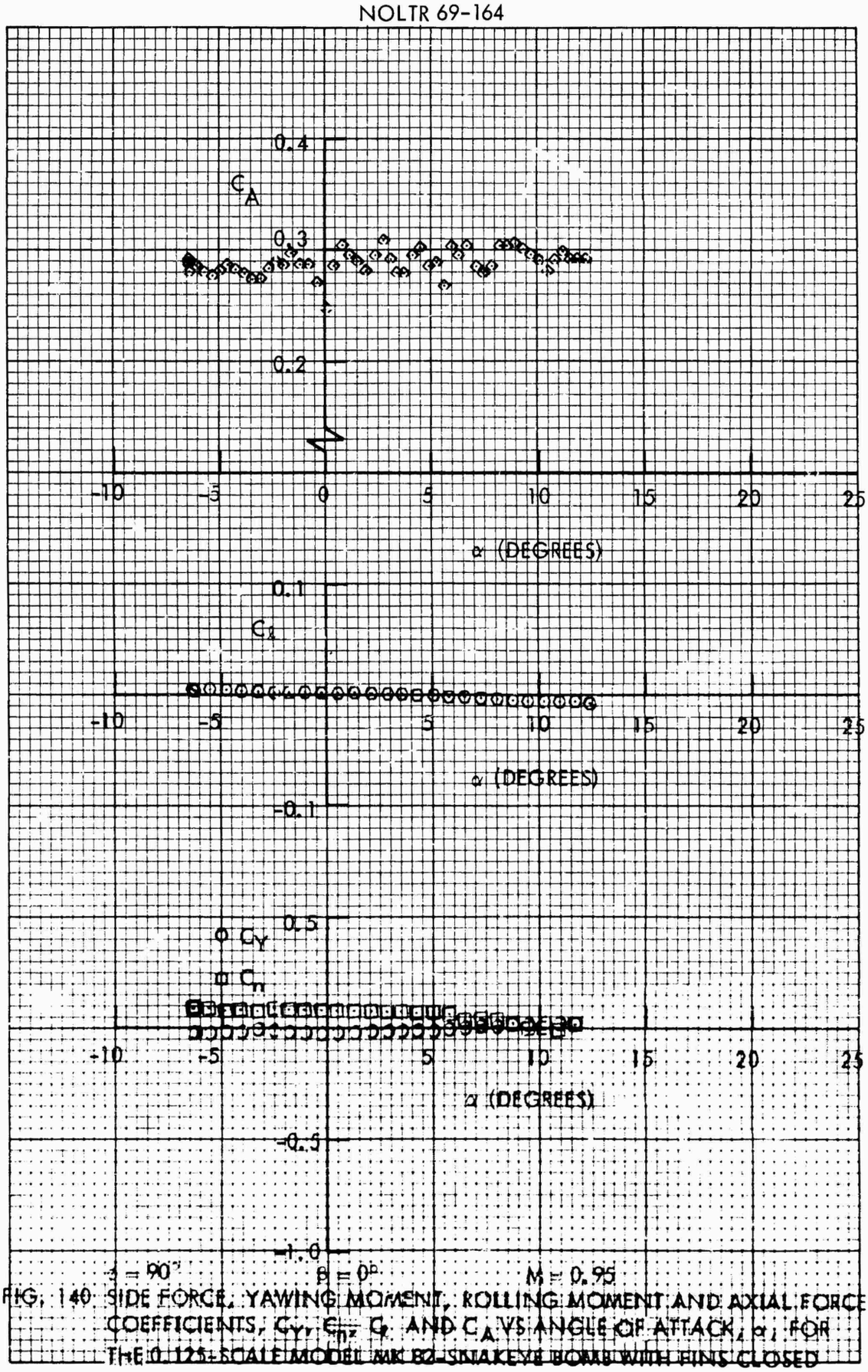

FIG. 140 SIDE FORCE, YAWING MOMENT, ROLLING MOMENT AND AXIAL FORCE COEFFICIENTS, C_Y, C_n, C_l, AND C_A VS ANGLE OF ATTACK, α_i, FOR THE 0.125-SCALE MODEL MK 82-SNAKEYE BOMB WITH FINS CLOSED

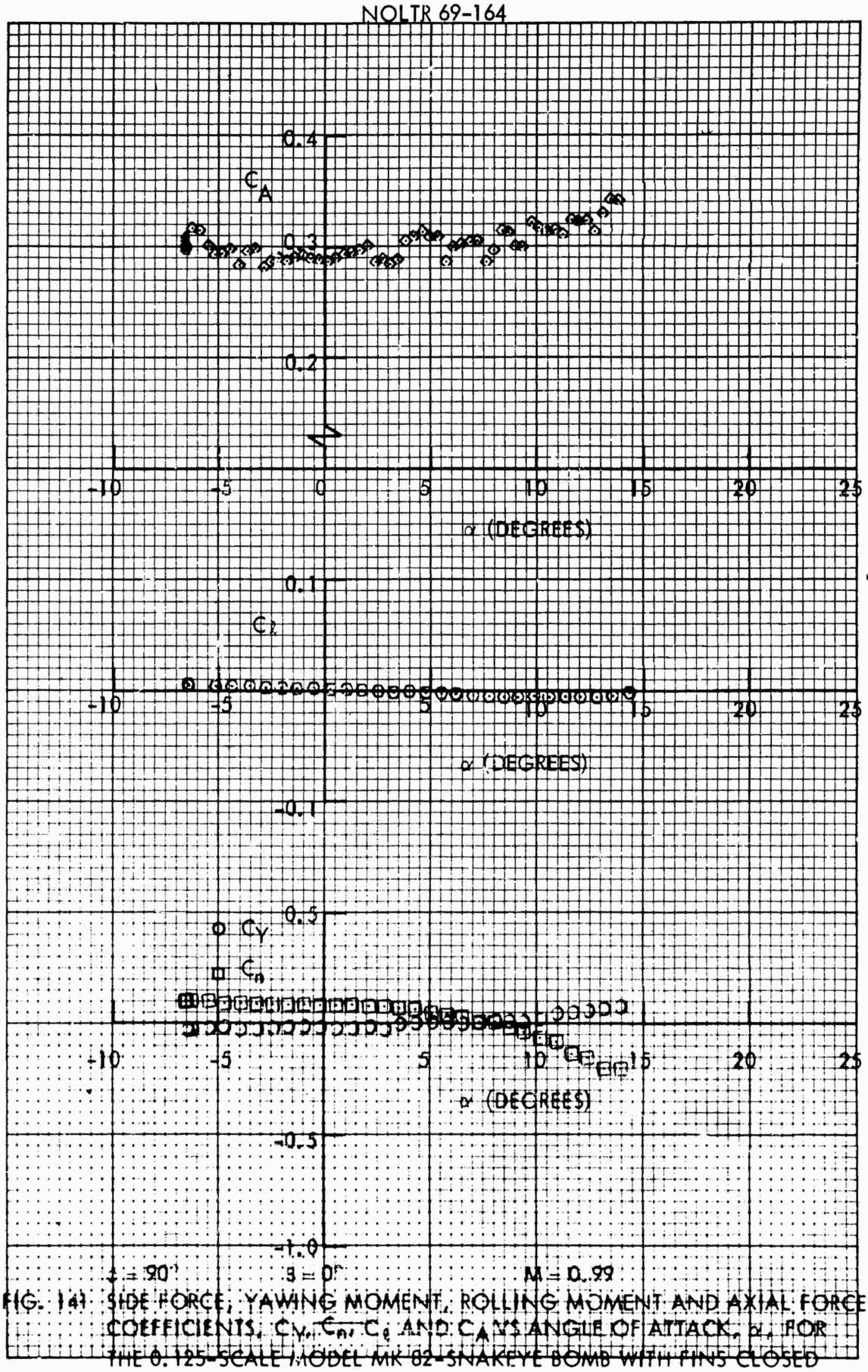

FIG. 141 SIDE FORCE, YAWING MOMENT, ROLLING MOMENT AND AXIAL FORCE COEFFICIENTS, C_Y, C_n, C_ℓ AND C_A VS ANGLE OF ATTACK, α, FOR THE 0.125-SCALE MODEL MK 82-SNAKEYE BOMB WITH FINS CLOSED

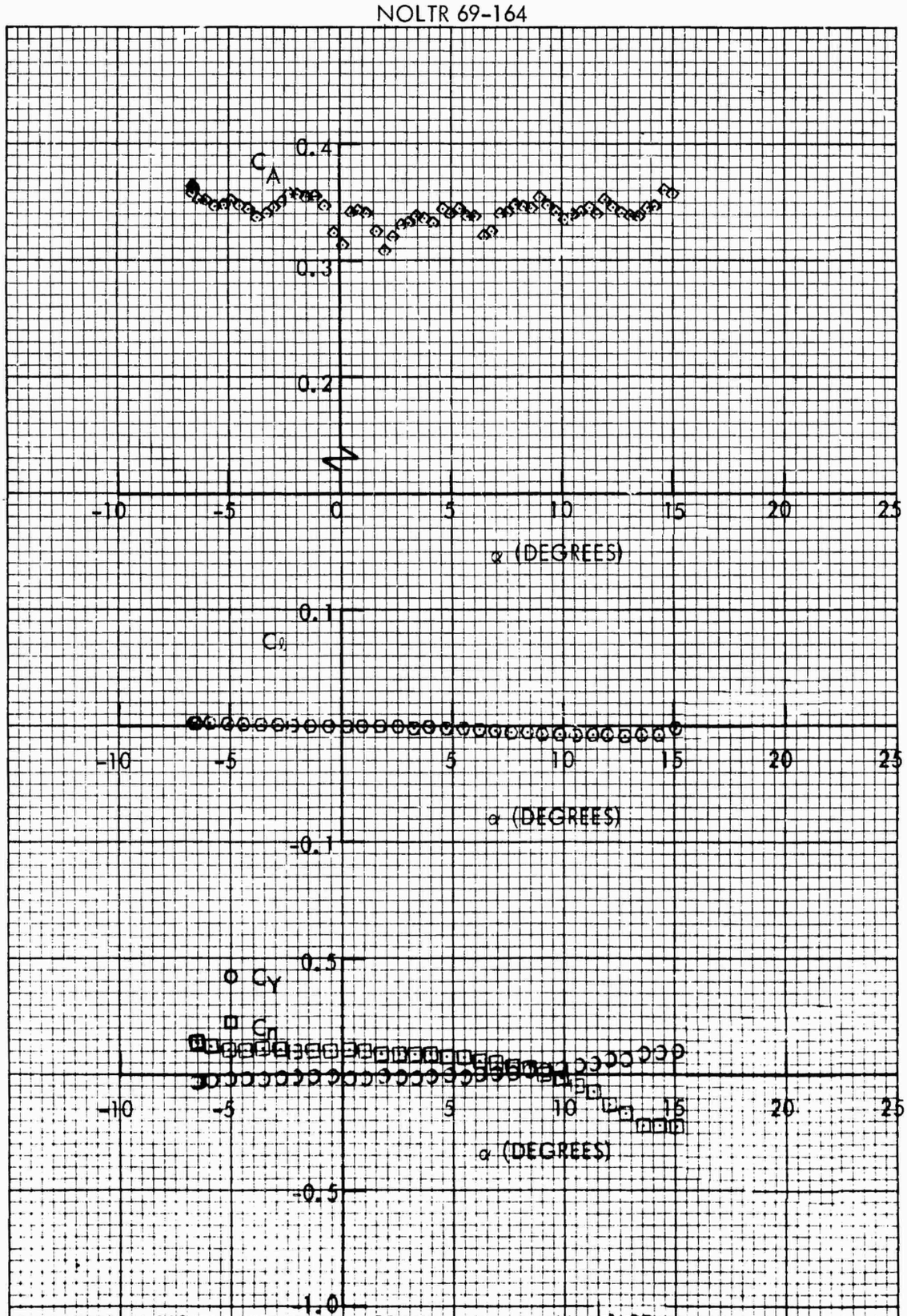

FIG. 142 SIDE FORCE, YAWING MOMENT, ROLLING MOMENT AND AXIAL FORCE COEFFICIENTS, C_Y, C_n, C_ℓ AND C_A VS ANGLE OF ATTACK, α, FOR THE 0.125-SCALE MODEL MK 82 SNAKEYE BOMB WITH FINS CLOSED

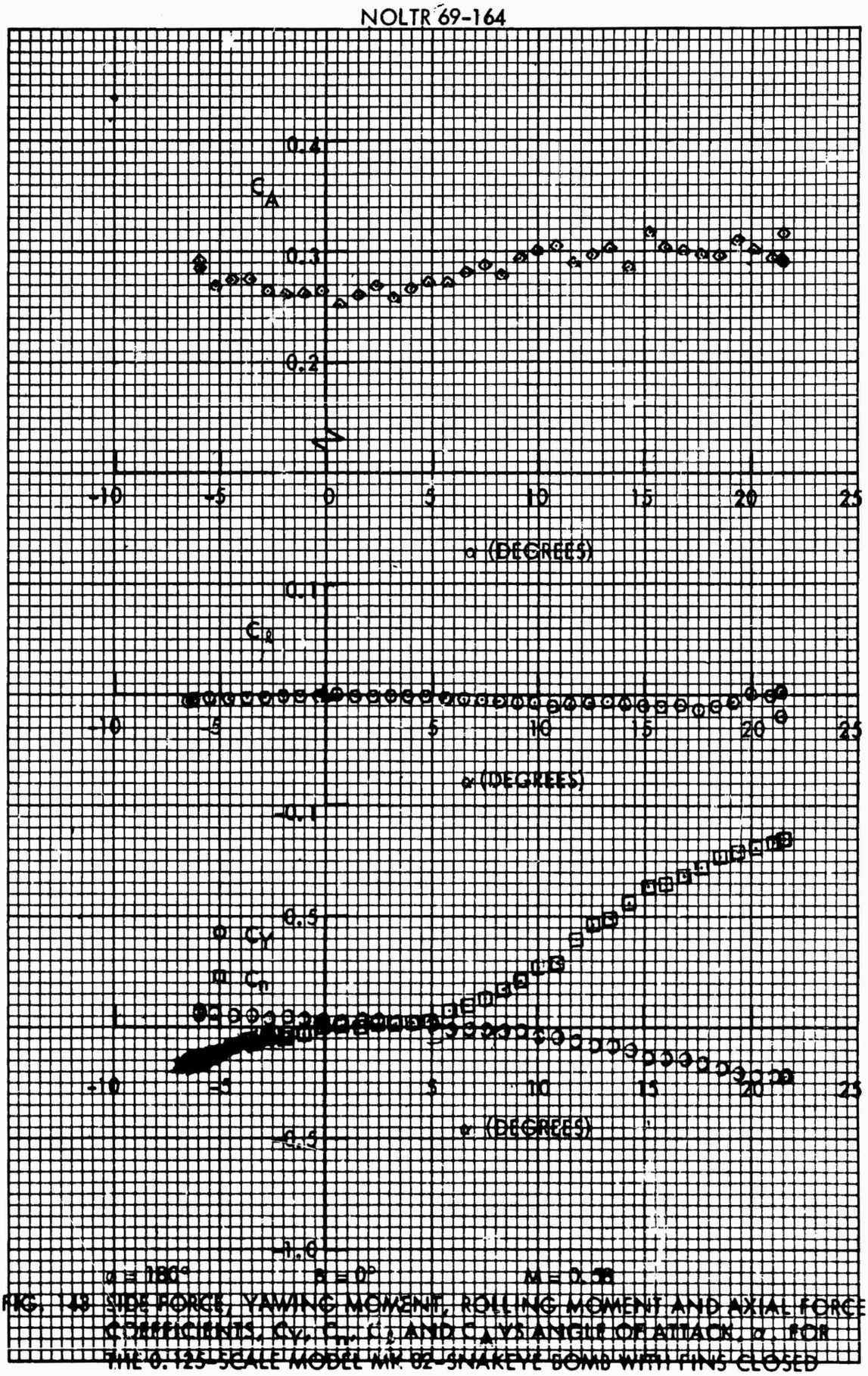

FIG. 148 SIDE FORCE, YAWING MOMENT, ROLLING MOMENT AND AXIAL FORCE COEFFICIENTS, C_Y, C_n, C_ℓ, AND C_A VS ANGLE OF ATTACK, α, FOR THE 0.125-SCALE MODEL MK 82-SNAKEYE BOMB WITH FINS CLOSED

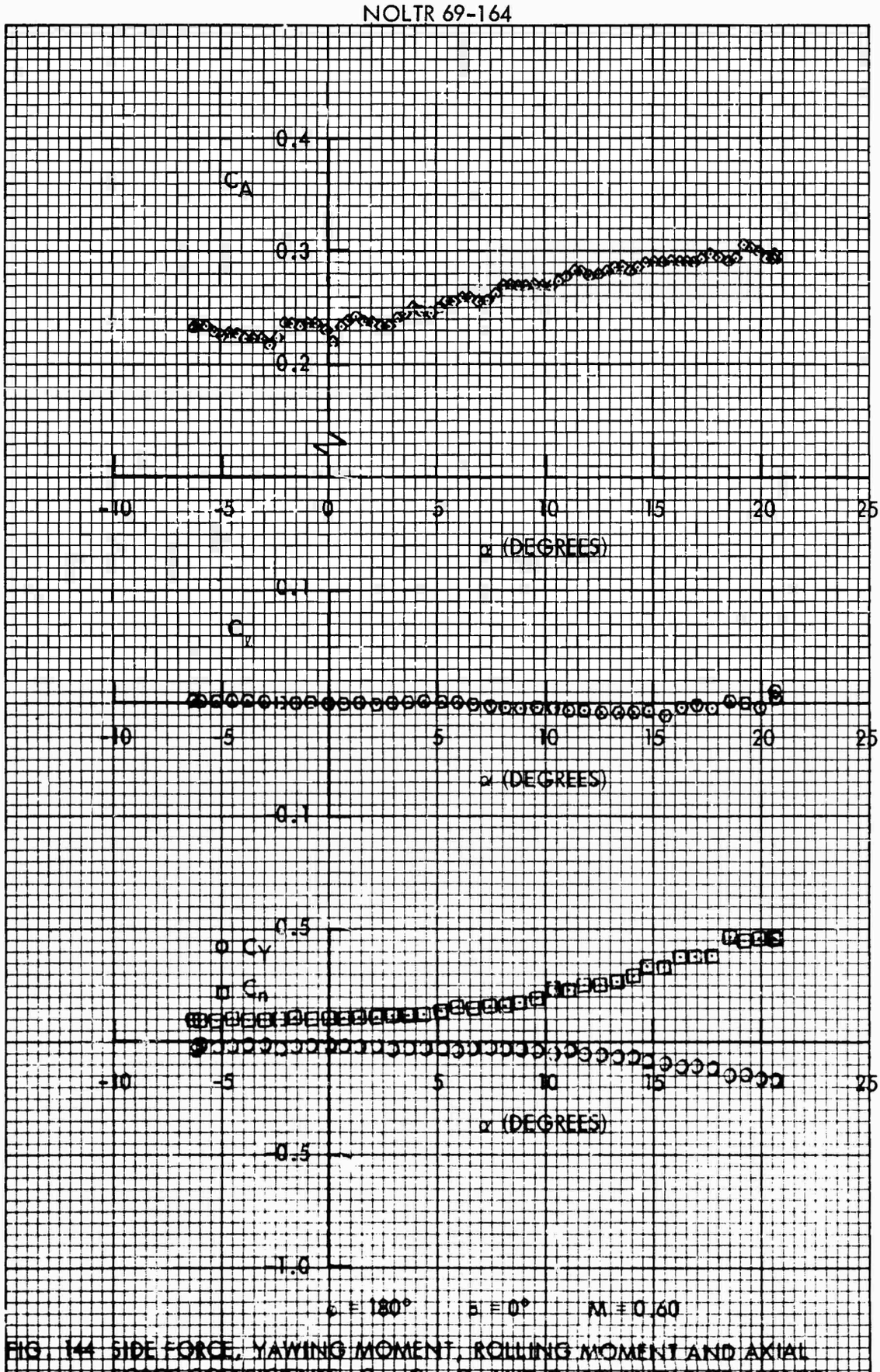

FIG. 144 SIDE FORCE, YAWING MOMENT, ROLLING MOMENT AND AXIAL FORCE COEFFICIENTS, C_Y, C_n, C_ℓ AND C_A VS ANGLE OF ATTACK, α, FOR THE 0.125-SCALE MODEL MK 82-SNAKEYE BOMB WITH FINS CLOSED

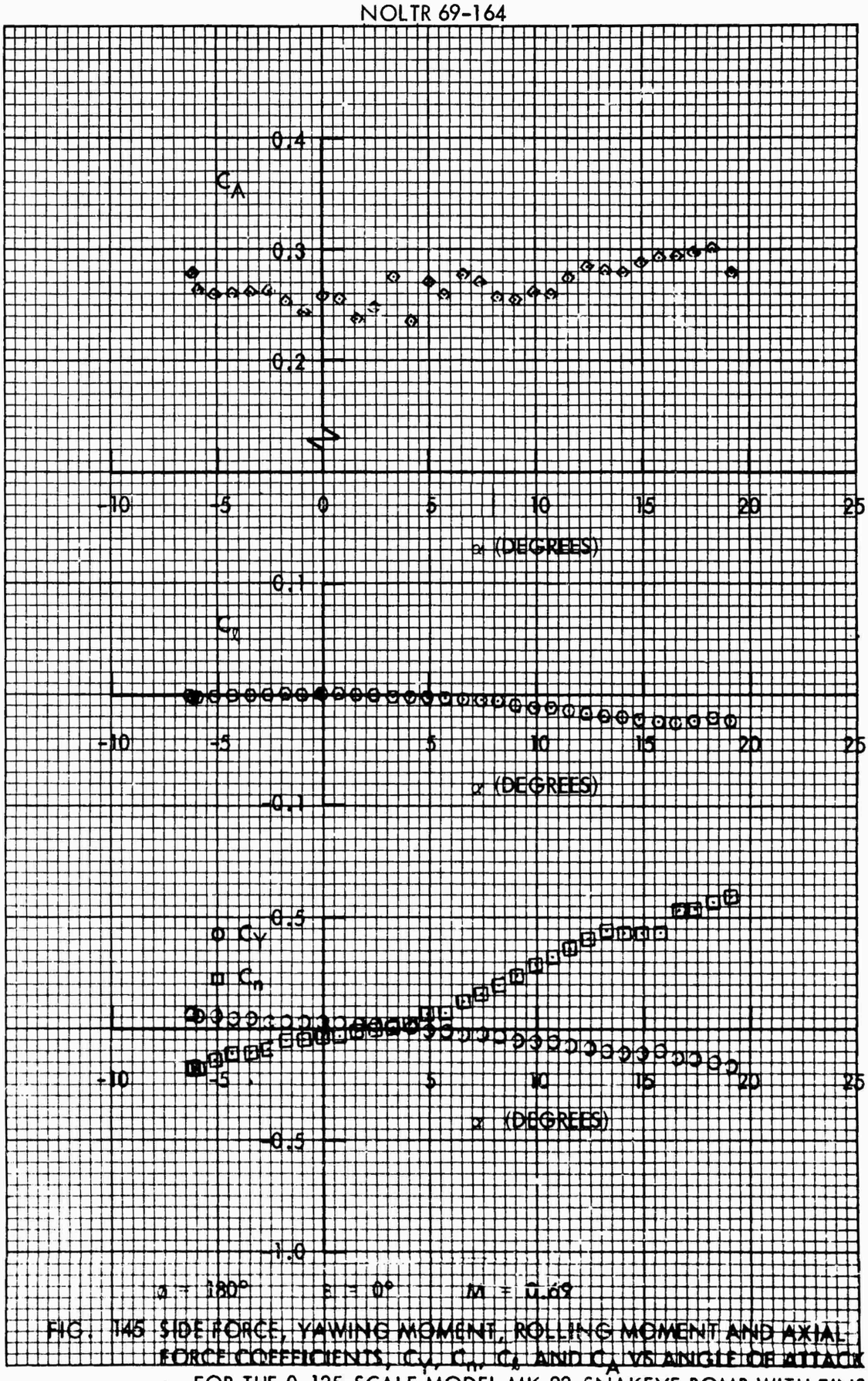

FIG. 145 SIDE FORCE, YAWING MOMENT, ROLLING MOMENT AND AXIAL FORCE COEFFICIENTS, C_Y, C_n, C_ℓ AND C_A VS ANGLE OF ATTACK α, FOR THE 0.125-SCALE MODEL MK 82-SNAKEYE BOMB WITH FINS CLOSED

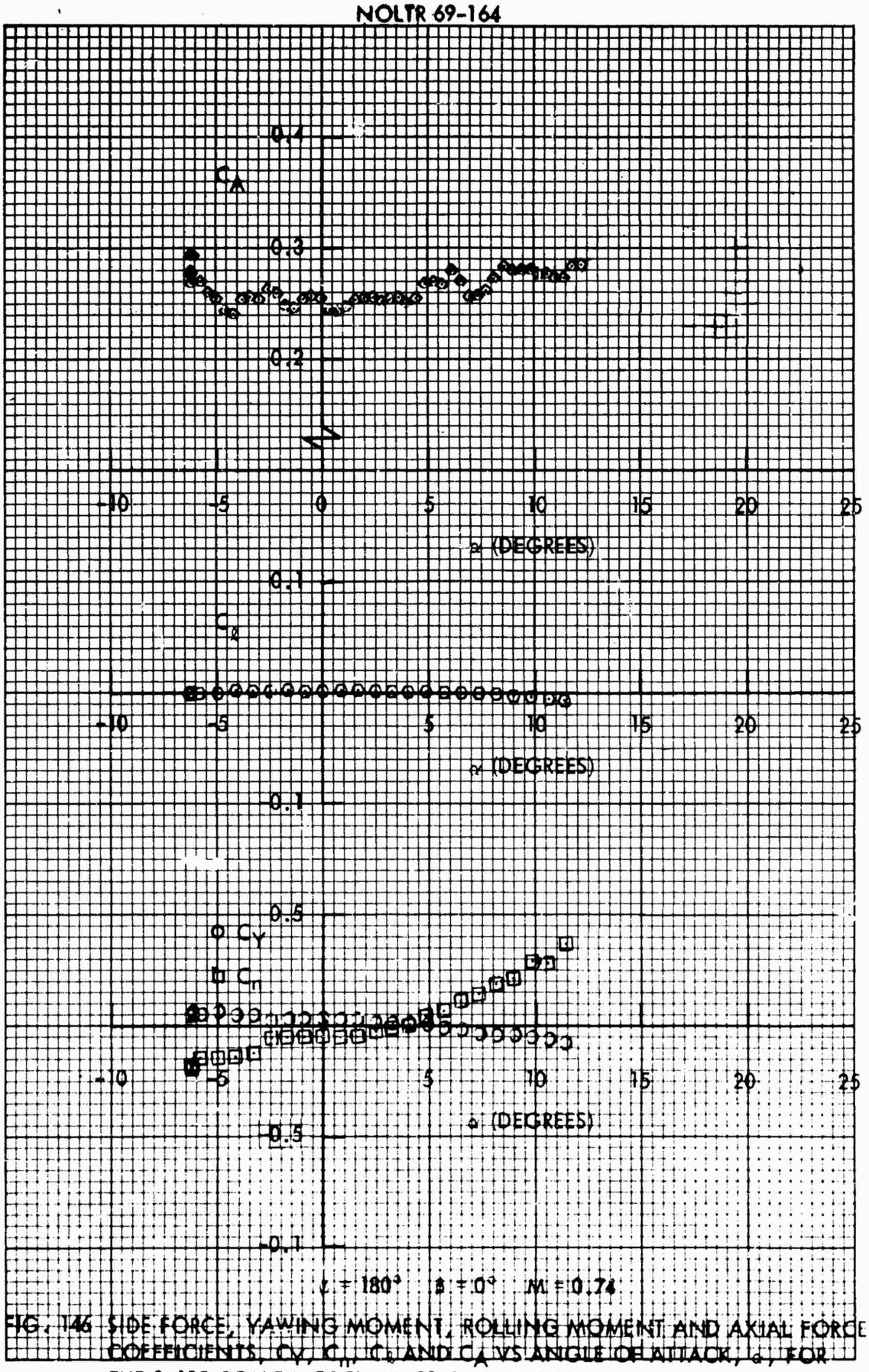

FIG. 146 SIDE FORCE, YAWING MOMENT, ROLLING MOMENT AND AXIAL FORCE COEFFICIENTS, C_Y, C_n, C_ℓ AND C_A VS ANGLE OF ATTACK, α, FOR THE 0.125-SCALE MODEL MK 82-SNAKEYE BOMB WITH FINS CLOSED

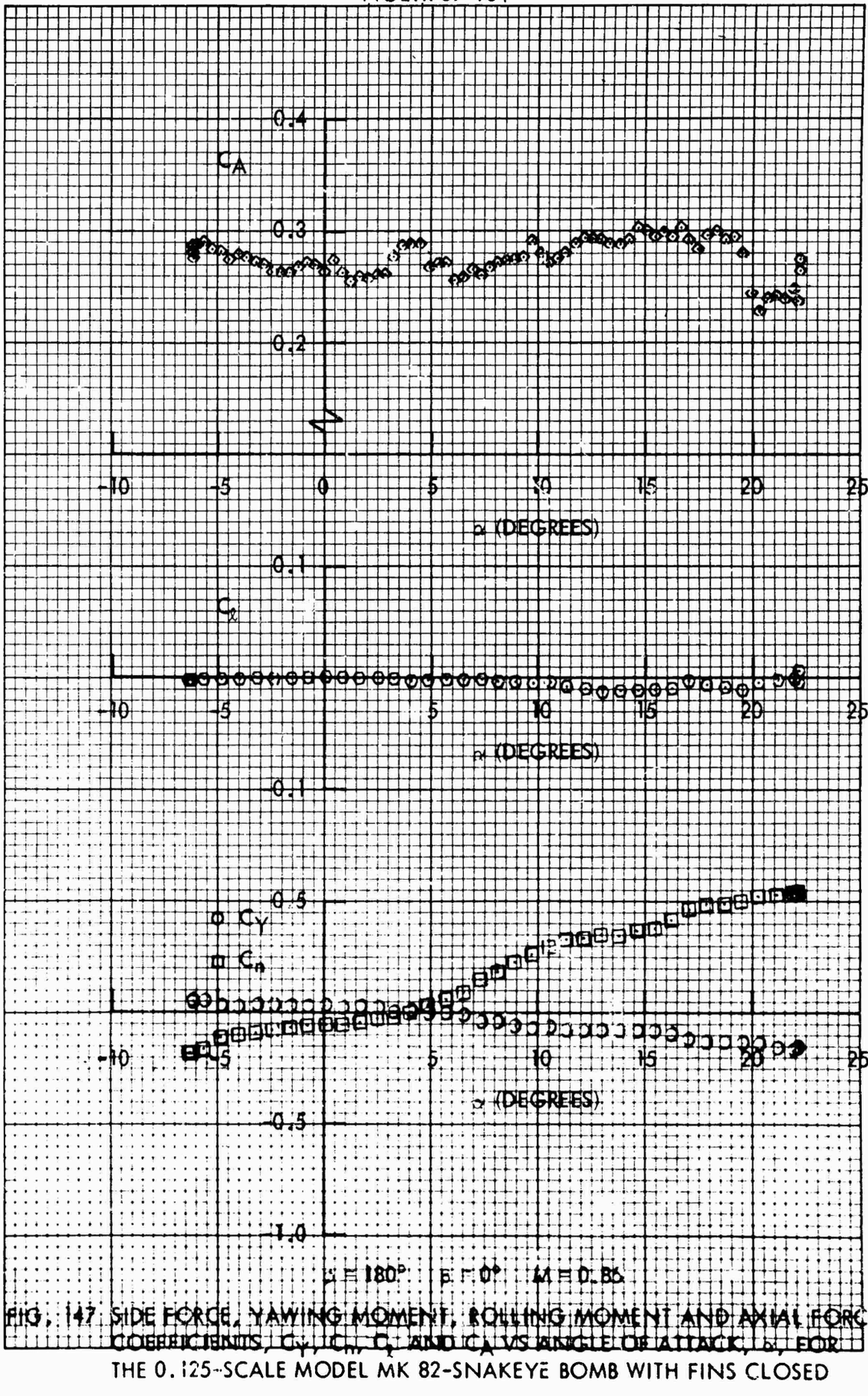

FIG. 147 SIDE FORCE, YAWING MOMENT, ROLLING MOMENT AND AXIAL FORCE COEFFICIENTS, C_Y, C_n, C_ℓ AND C_A VS ANGLE OF ATTACK, α, FOR THE 0.125-SCALE MODEL MK 82-SNAKEYE BOMB WITH FINS CLOSED

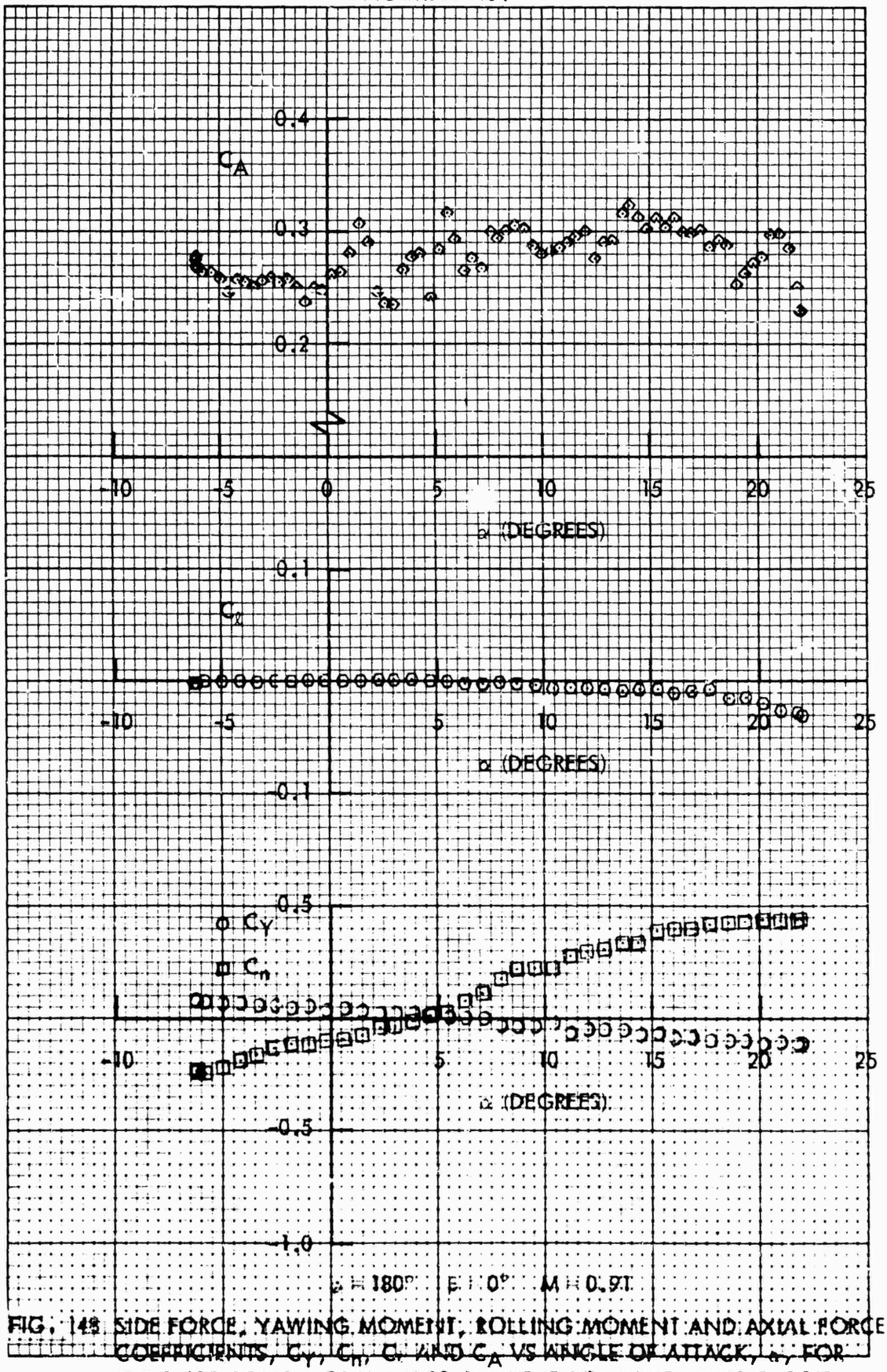

FIG. 148 SIDE FORCE, YAWING MOMENT, ROLLING MOMENT AND AXIAL FORCE COEFFICIENTS, C_Y, C_n, C_ℓ AND C_A VS ANGLE OF ATTACK, α, FOR THE 0.125-SCALE MODEL MK 82-SNAKEYE BOMB WITH FINS CLOSED

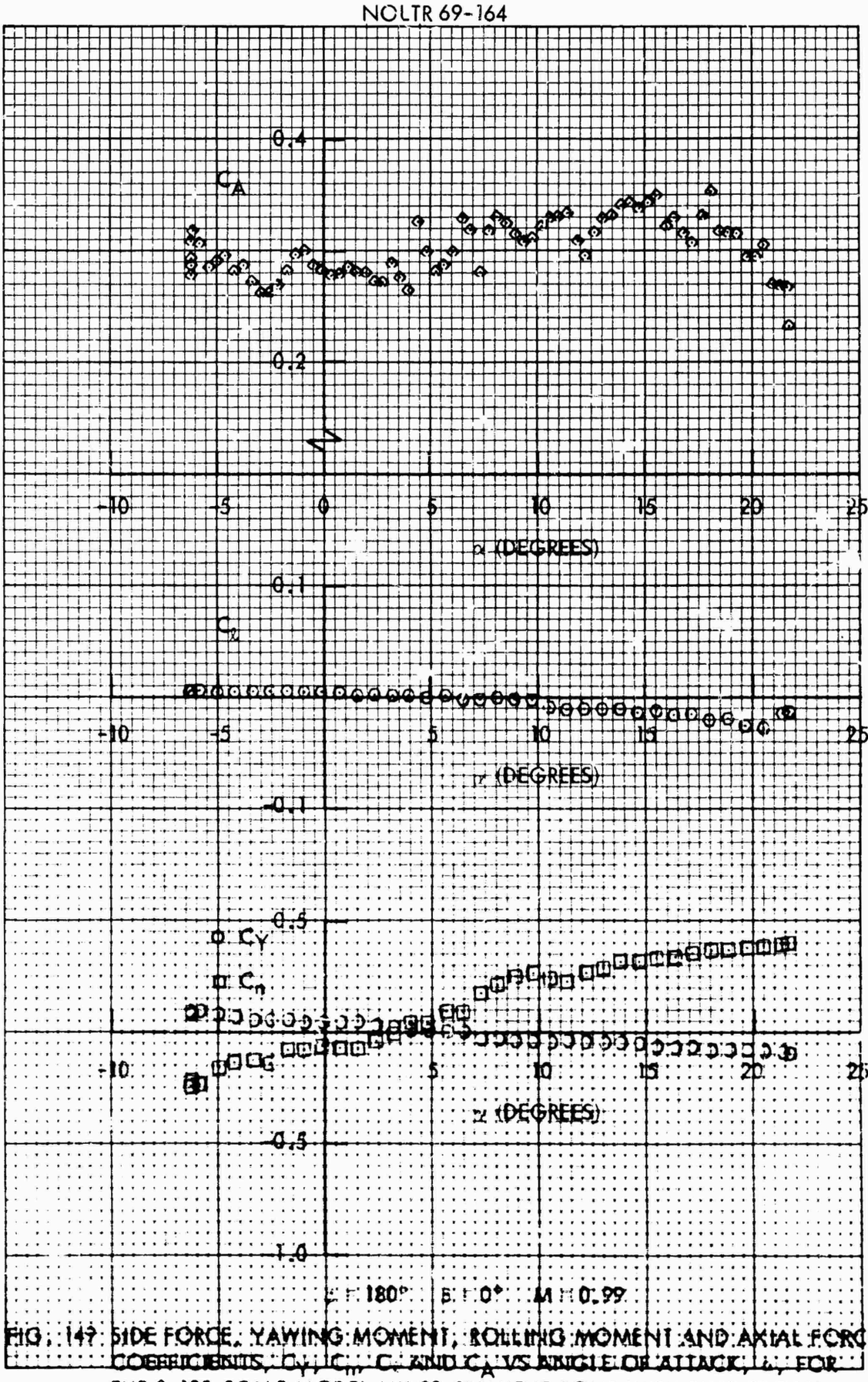

FIG. 14? SIDE FORCE, YAWING MOMENT, ROLLING MOMENT AND AXIAL FORCE COEFFICIENTS, C_Y, C_n, C_l AND C_A VS ANGLE OF ATTACK, α, FOR THE 0.125-SCALE MODEL MK 82-SNAKEYE BOMB WITH FINS CLOSED

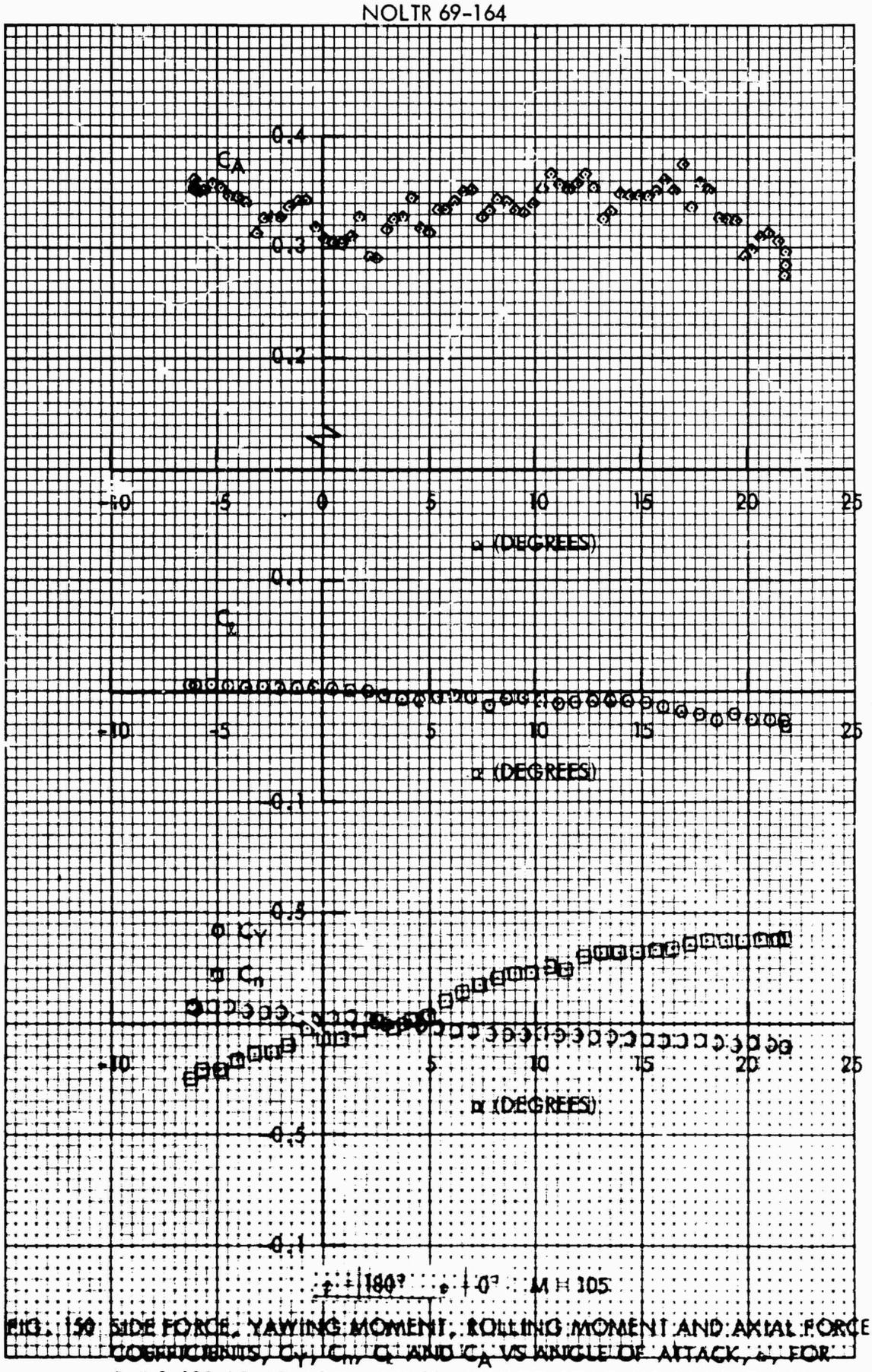

FIG. 150 SIDE FORCE, YAWING MOMENT, ROLLING MOMENT AND AXIAL FORCE COEFFICIENTS, C_Y, C_n, C_l AND C_A VS ANGLE OF ATTACK, α, FOR THE 0.125-SCALE MODEL MK 82-SNAKEYE BOMB WITH FINS CLOSED

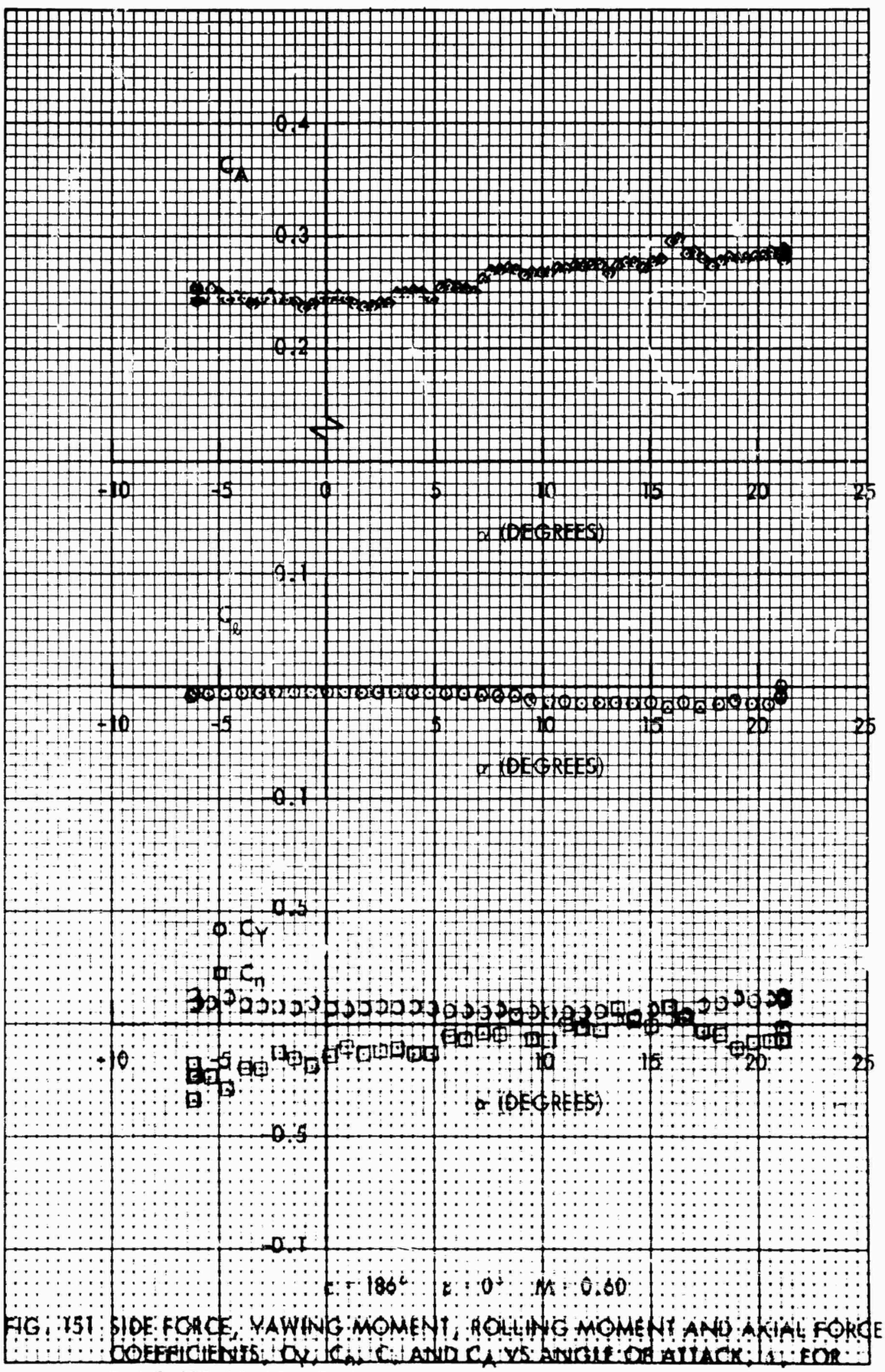

FIG. 151 SIDE FORCE, YAWING MOMENT, ROLLING MOMENT AND AXIAL FORCE COEFFICIENTS, C_Y, C_n, C_ℓ AND C_A VS ANGLE OF ATTACK, α, FOR THE 0.125-SCALE MODEL MK 82-SNAKEYE BOMB WITH FINS CLOSED

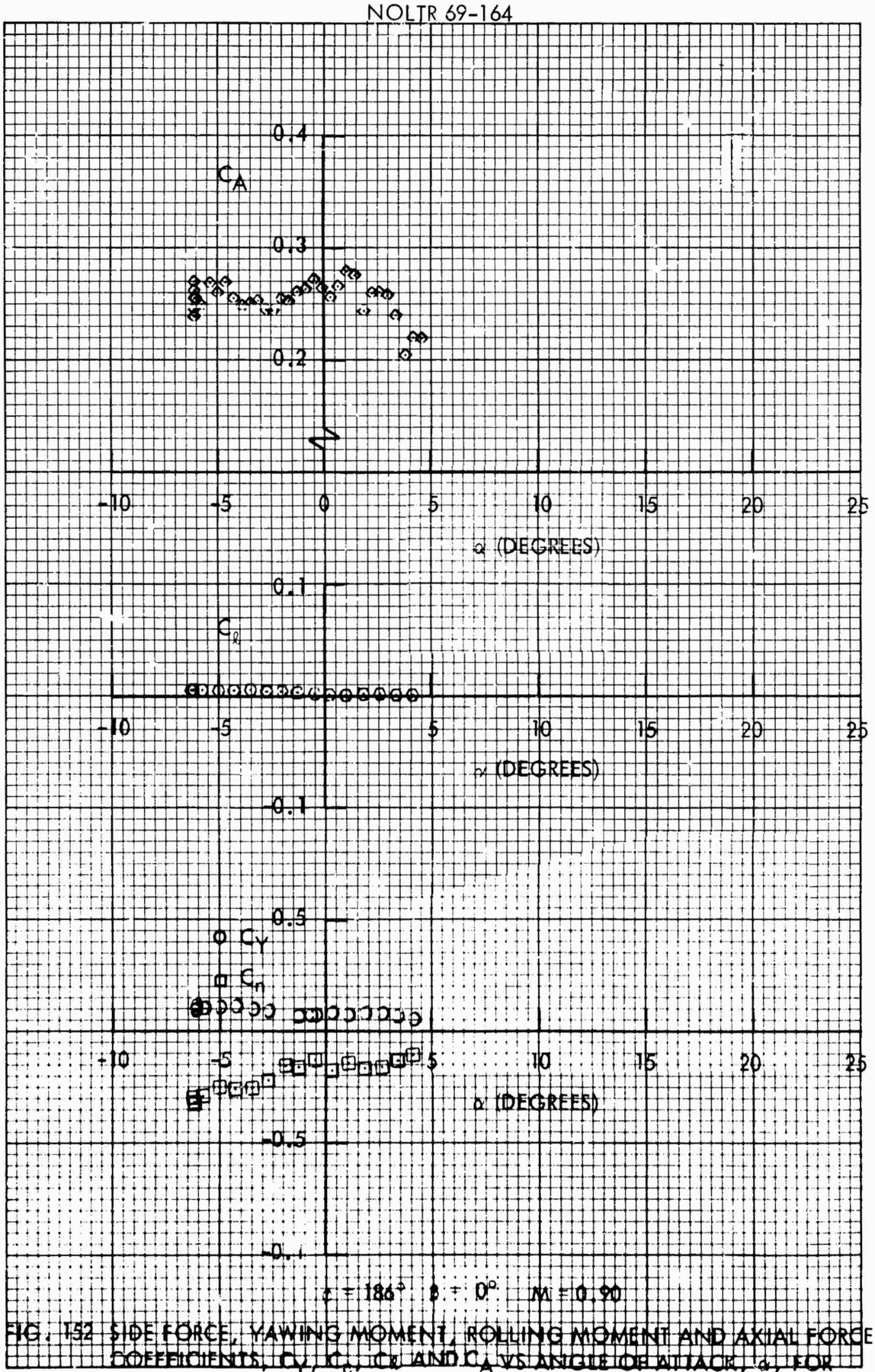

FIG. 152 SIDE FORCE, YAWING MOMENT, ROLLING MOMENT AND AXIAL FORCE COEFFICIENTS, C_Y, C_n, C_ℓ AND C_A VS ANGLE OF ATTACK, α, FOR THE 0.125-SCALE MODEL MK 82-SNAKEYE BOMB WITH FINS CLOSED

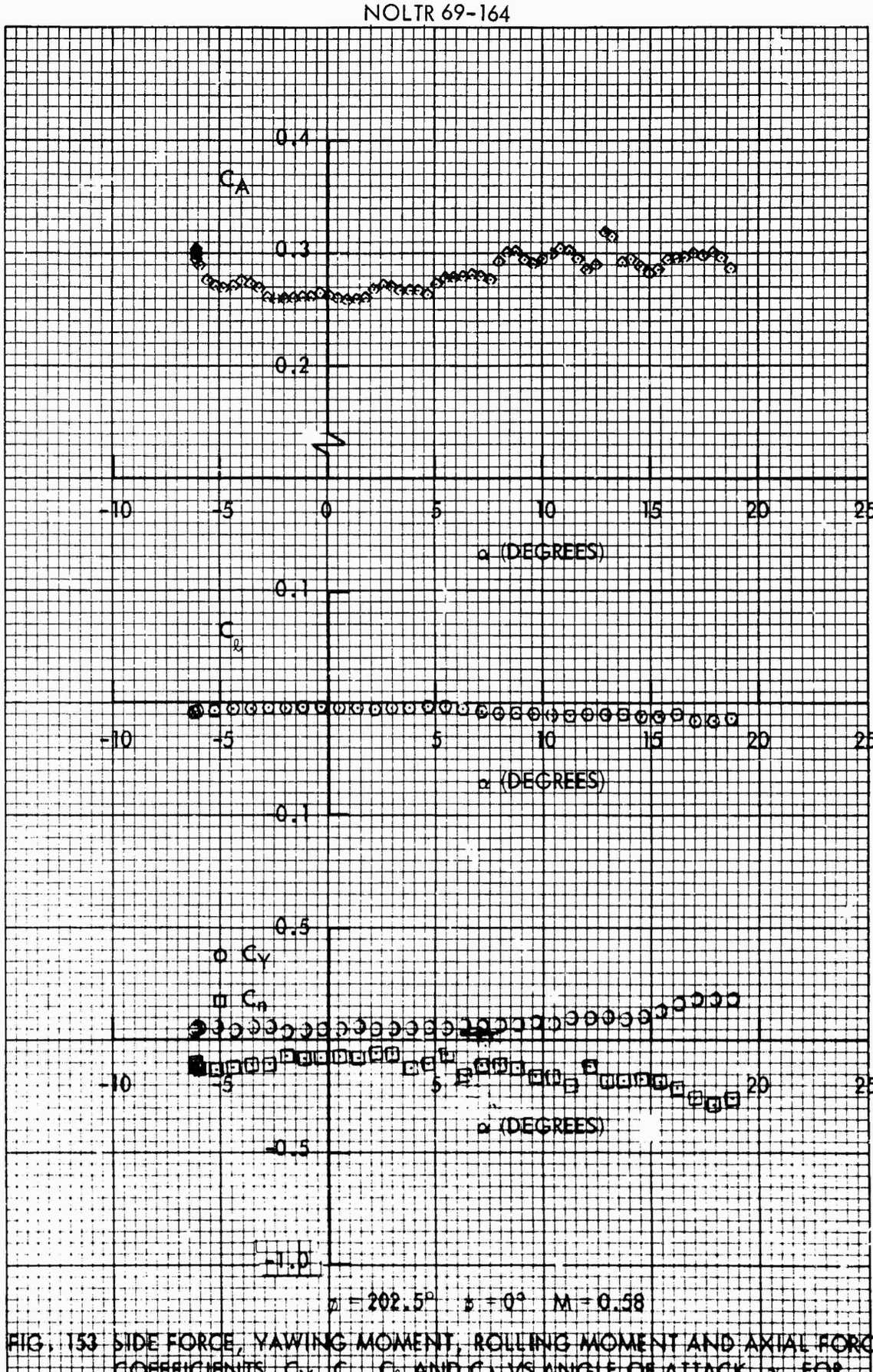

FIG. 153 SIDE FORCE, YAWING MOMENT, ROLLING MOMENT AND AXIAL FORCE COEFFICIENTS, C_Y, C_n, C_ℓ AND C_A VS ANGLE OF ATTACK, α, FOR THE 0.125-SCALE MODEL MK 82-SNAKEYE BOMB WITH FINS CLOSED

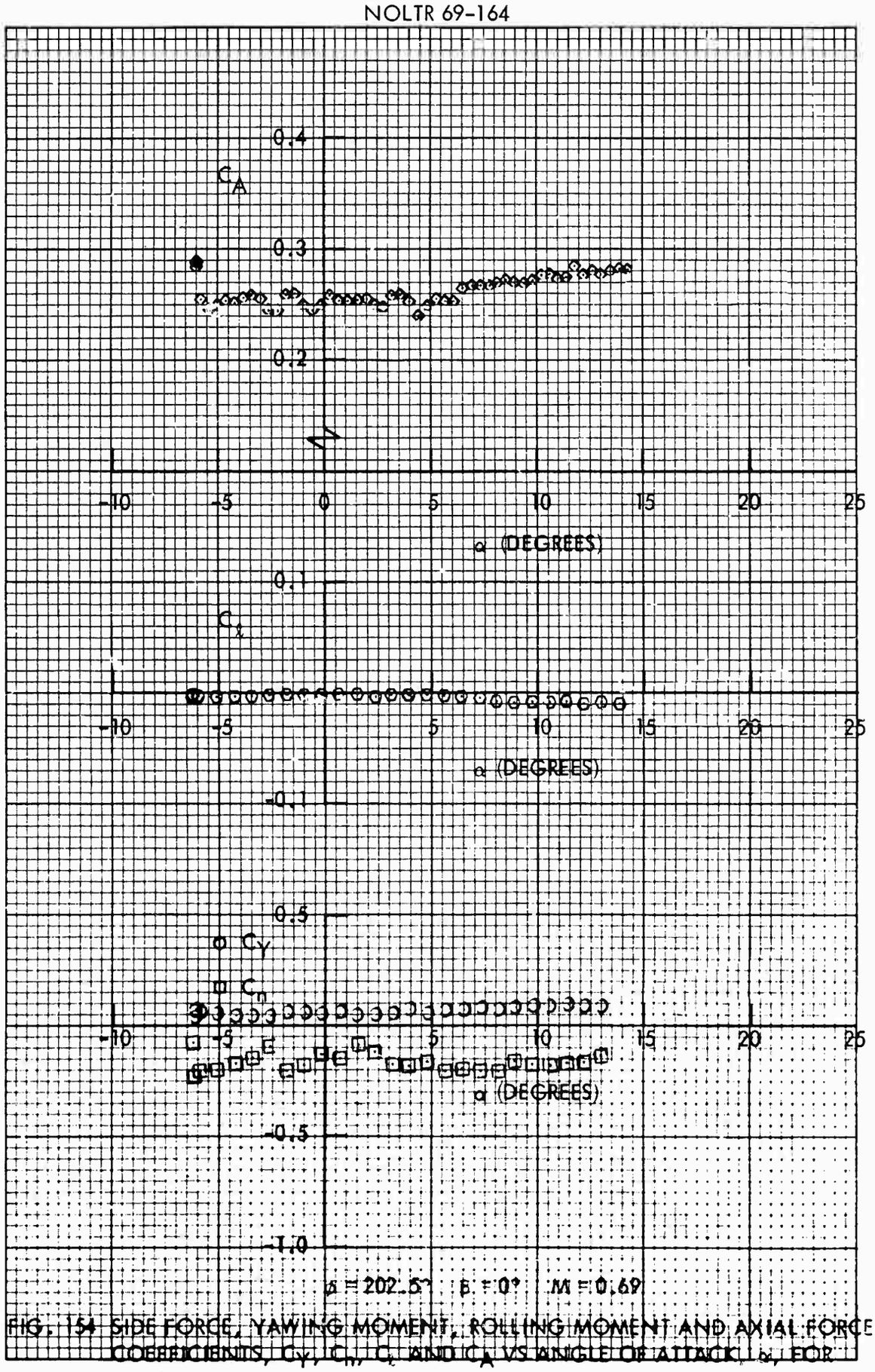

FIG. 154 SIDE FORCE, YAWING MOMENT, ROLLING MOMENT AND AXIAL FORCE COEFFICIENTS, C_Y, C_n, C_ℓ AND C_A VS ANGLE OF ATTACK, α, FOR THE 0.125-SCALE MODEL MK 82-SNAKEYE BOMB WITH FINS CLOSED

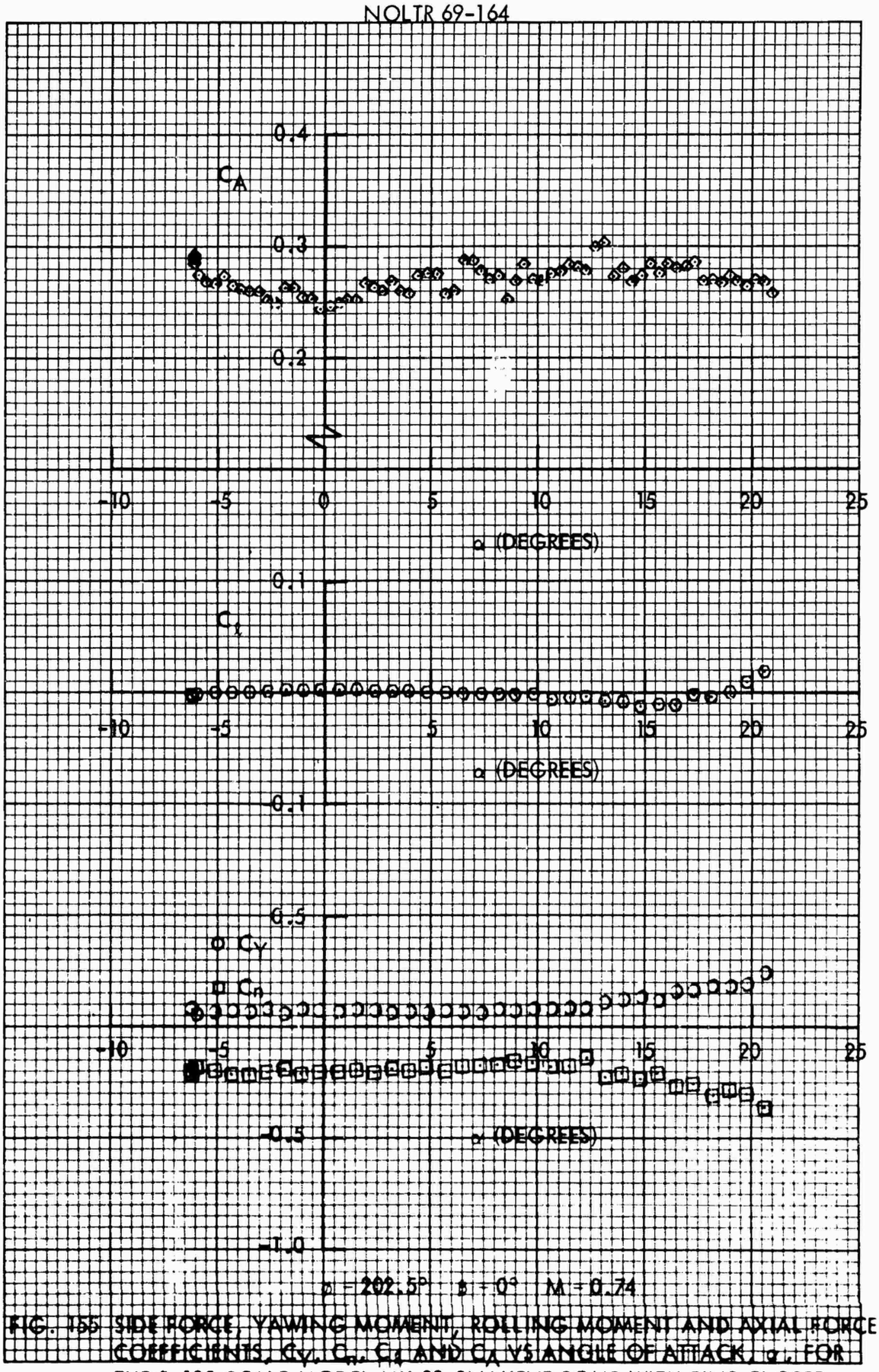

FIG. 155 SIDE FORCE, YAWING MOMENT, ROLLING MOMENT AND AXIAL FORCE COEFFICIENTS, C_Y, C_n, C_ℓ AND C_A VS ANGLE OF ATTACK, α, FOR THE 0.125-SCALE MODEL MK 82-SNAKEYE BOMB WITH FINS CLOSED

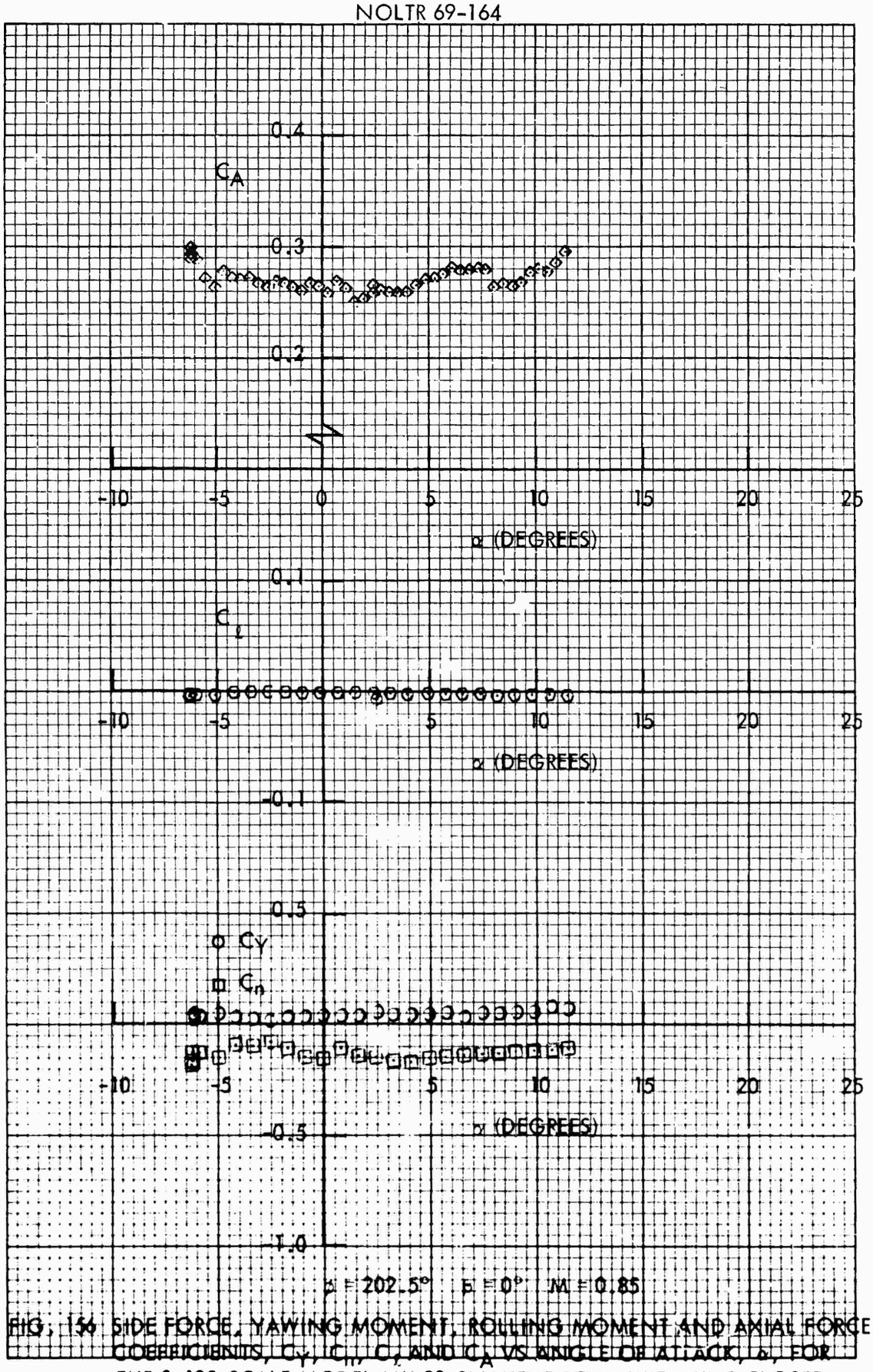

FIG. 156 SIDE FORCE, YAWING MOMENT, ROLLING MOMENT AND AXIAL FORCE COEFFICIENTS, C_Y, C_n, C_l AND C_A VS ANGLE OF ATTACK, α, FOR THE 0.125-SCALE MODEL MK 82-SNAKEYE BOMB WITH FINS CLOSED

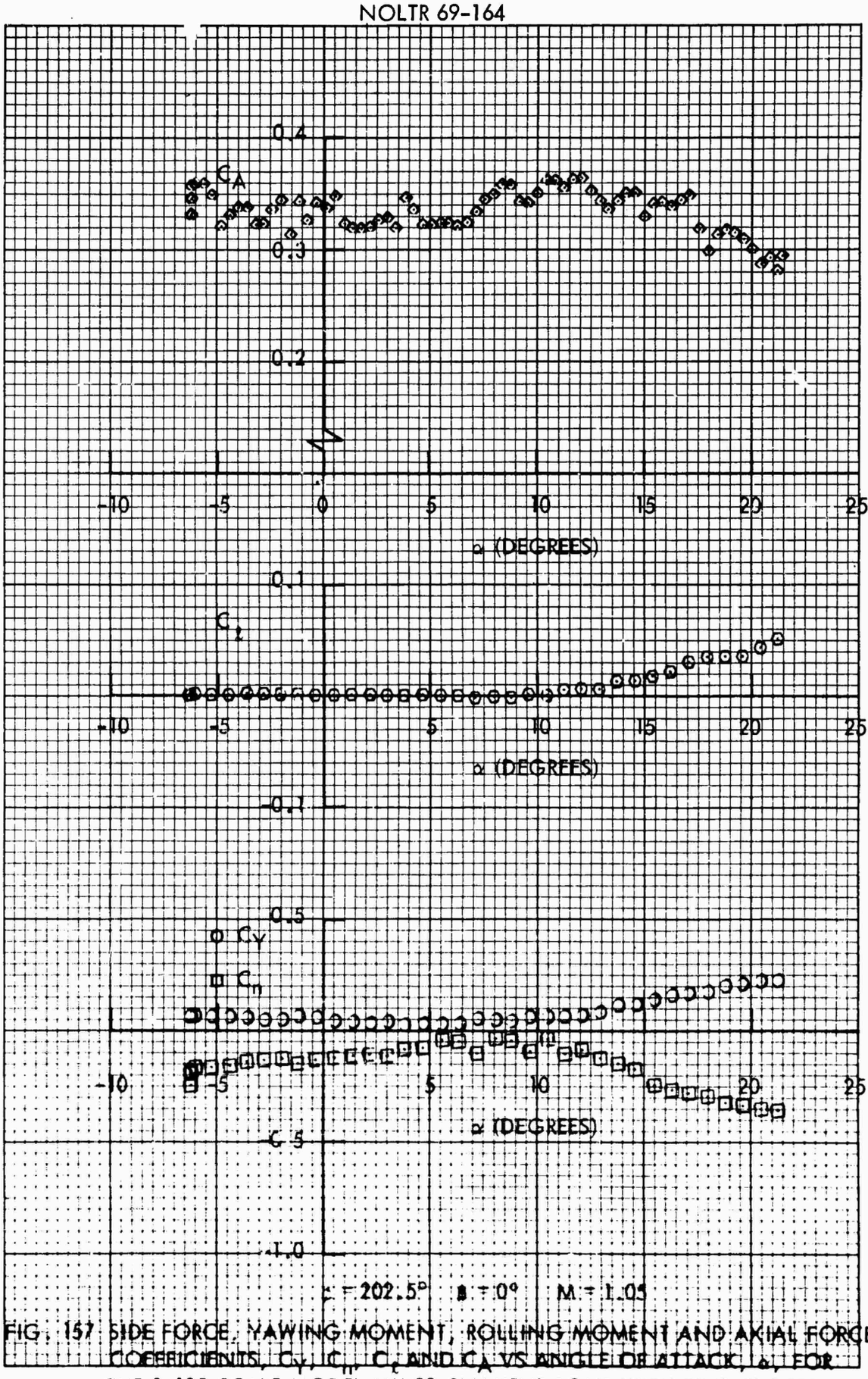

FIG. 157 SIDE FORCE, YAWING MOMENT, ROLLING MOMENT AND AXIAL FORCE COEFFICIENTS, C_Y, C_n, C_ℓ AND C_A VS ANGLE OF ATTACK, α, FOR THE 0.125-SCALE MODEL MK 82-SNAKEYE BOMB WITH FINS CLOSED

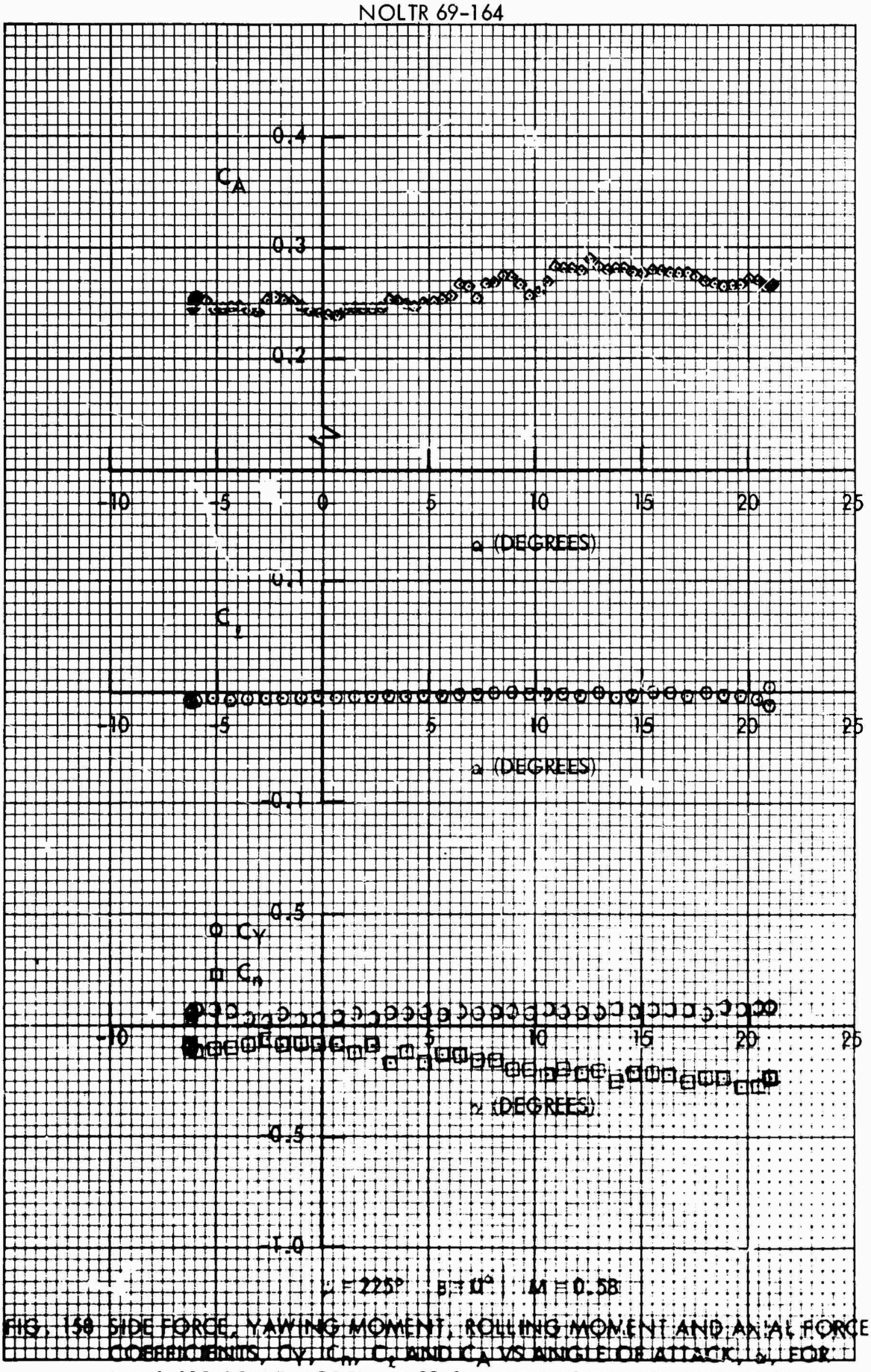

FIG. 158 SIDE FORCE, YAWING MOMENT, ROLLING MOMENT AND AXIAL FORCE COEFFICIENTS, C_Y, C_n, C_l AND C_A VS ANGLE OF ATTACK, α, FOR THE 0.125-SCALE MODEL MK 82-SNAKEYE BOMB WITH FINS CLOSED

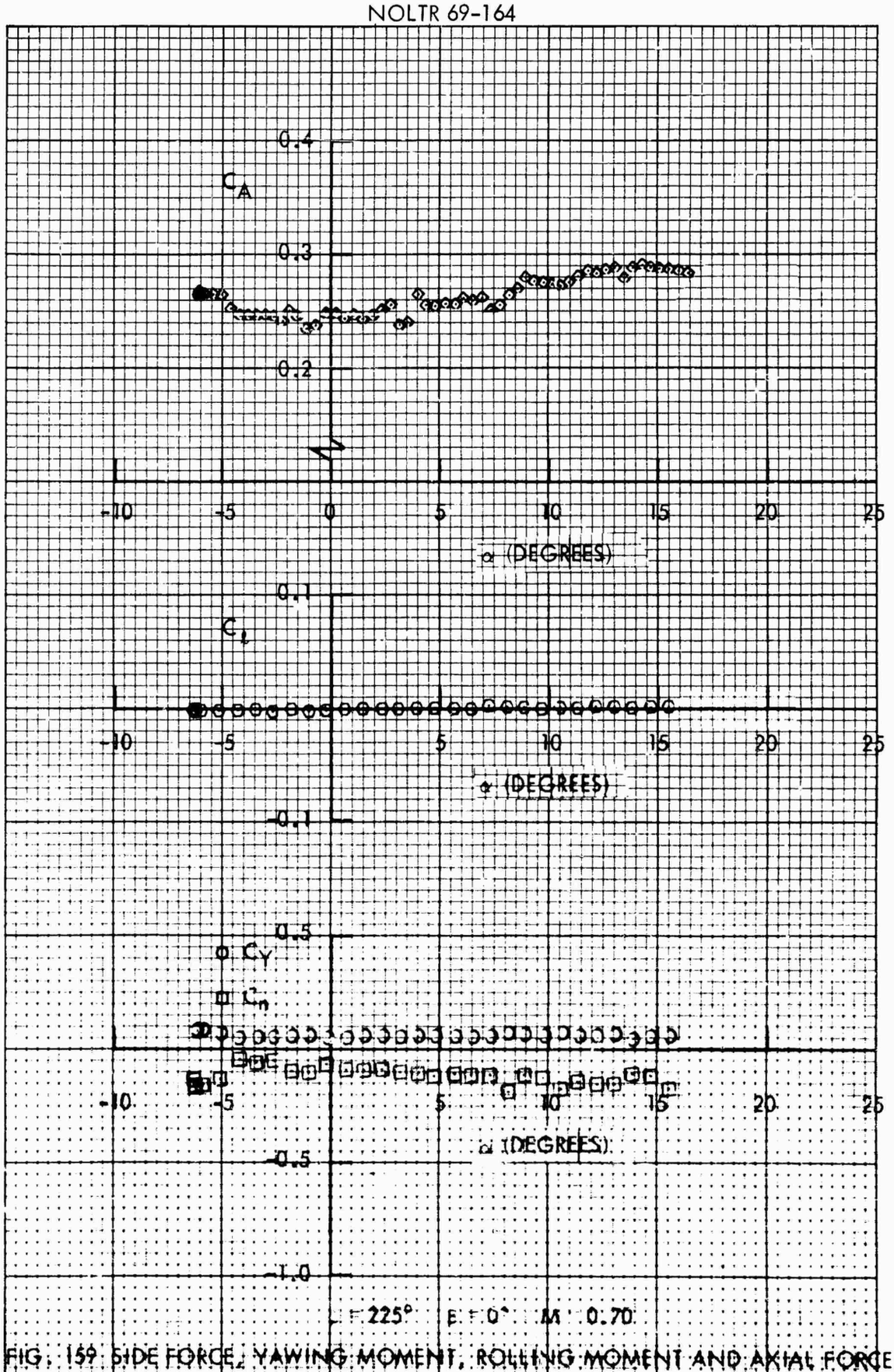

FIG. 159 SIDE FORCE, YAWING MOMENT, ROLLING MOMENT AND AXIAL FORCE COEFFICIENTS, C_Y, C_n, C_ℓ AND C_A VS ANGLE OF ATTACK, α, FOR THE 0.125-SCALE MODEL MK 82-SNAKEYE BOMB WITH FINS CLOSED

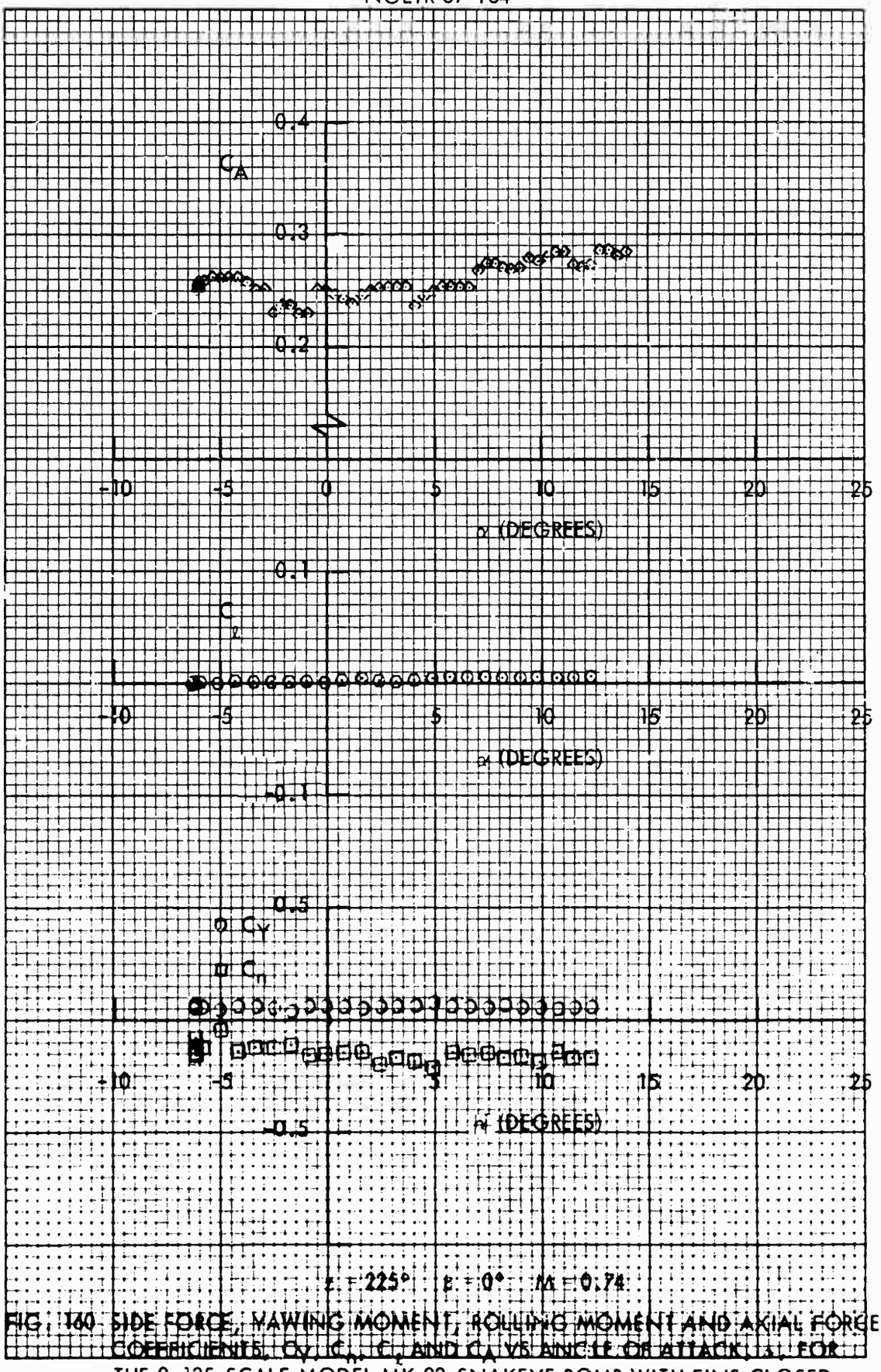

FIG. 140 SIDE FORCE, YAWING MOMENT, ROLLING MOMENT AND AXIAL FORCE COEFFICIENTS, C_Y, C_n, C_ℓ AND C_A VS ANGLE OF ATTACK, α, FOR THE 0.125-SCALE MODEL MK 82-SNAKEYE BOMB WITH FINS CLOSED

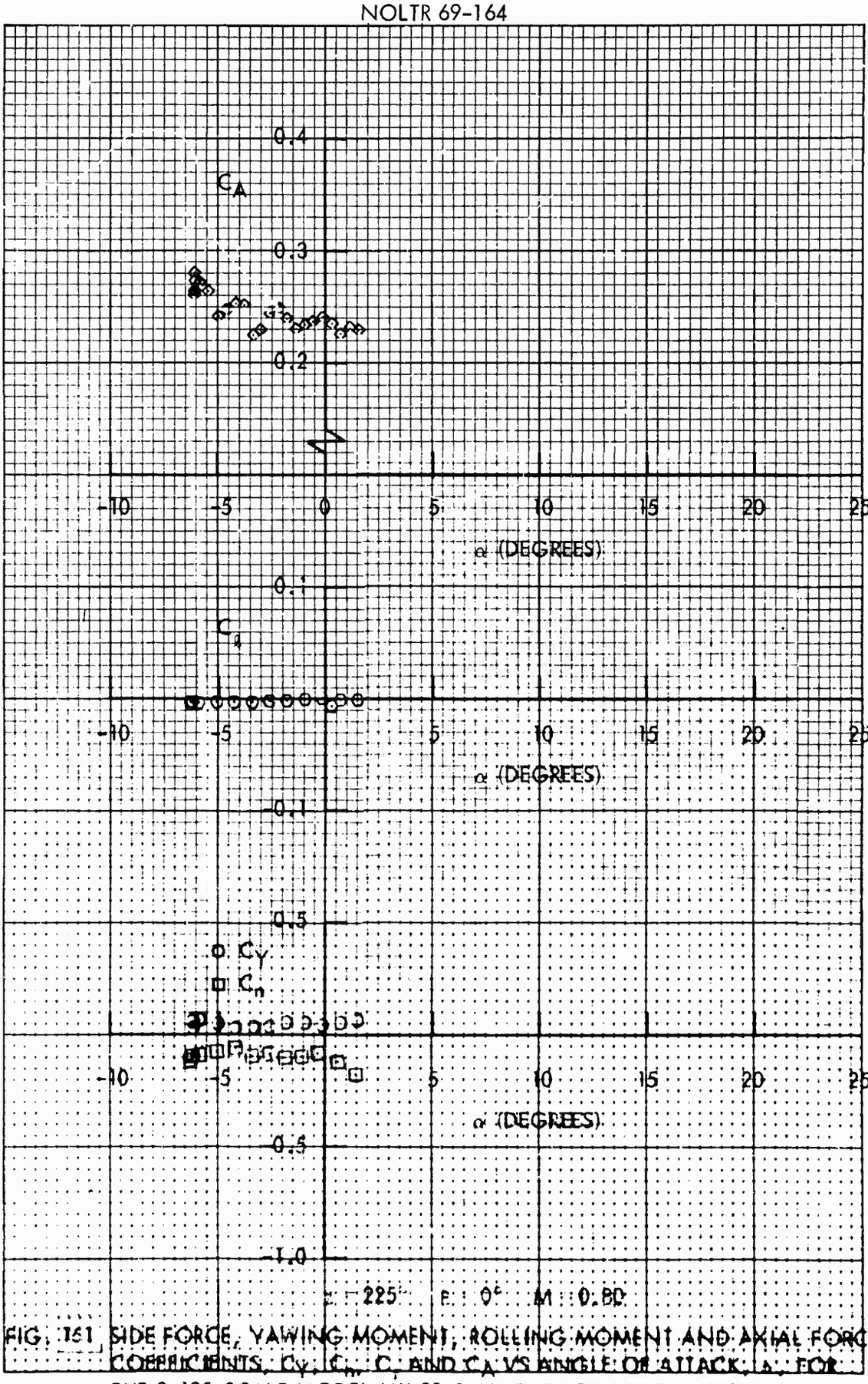

FIG. 161 SIDE FORCE, YAWING MOMENT, ROLLING MOMENT AND AXIAL FORCE COEFFICIENTS, C_Y, C_n, C_l AND C_A VS ANGLE OF ATTACK, α, FOR THE 0.125-SCALE MODEL MK 82-SNAKEYE BOMB WITH FINS CLOSED

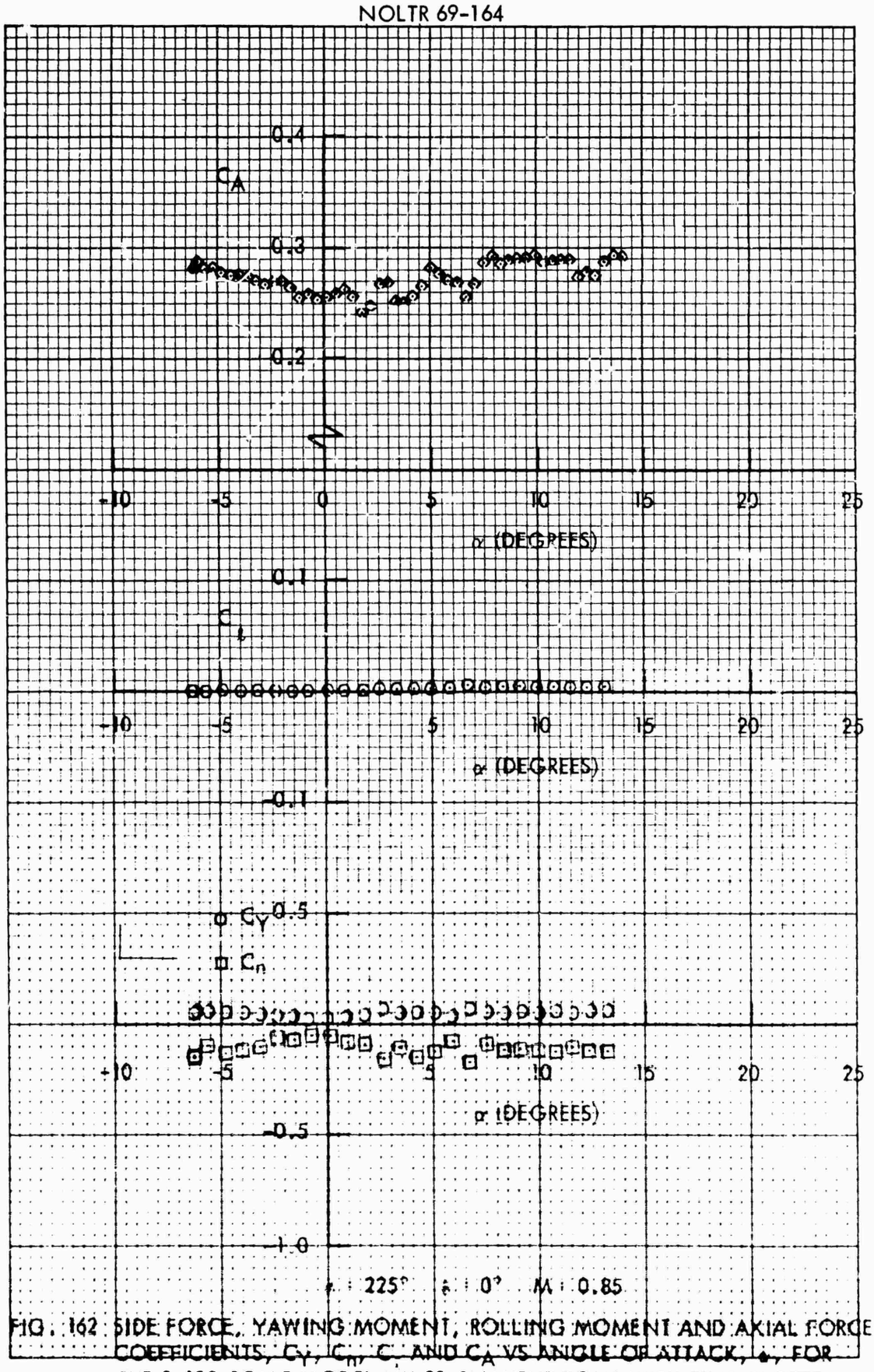

FIG. 162 SIDE FORCE, YAWING MOMENT, ROLLING MOMENT AND AXIAL FORCE COEFFICIENTS, C_Y, C_n, C_ℓ AND C_A VS ANGLE OF ATTACK, ϕ, FOR THE 0.125-SCALE MODEL MK 82-SNAKEYE BOMB WITH FINS CLOSED

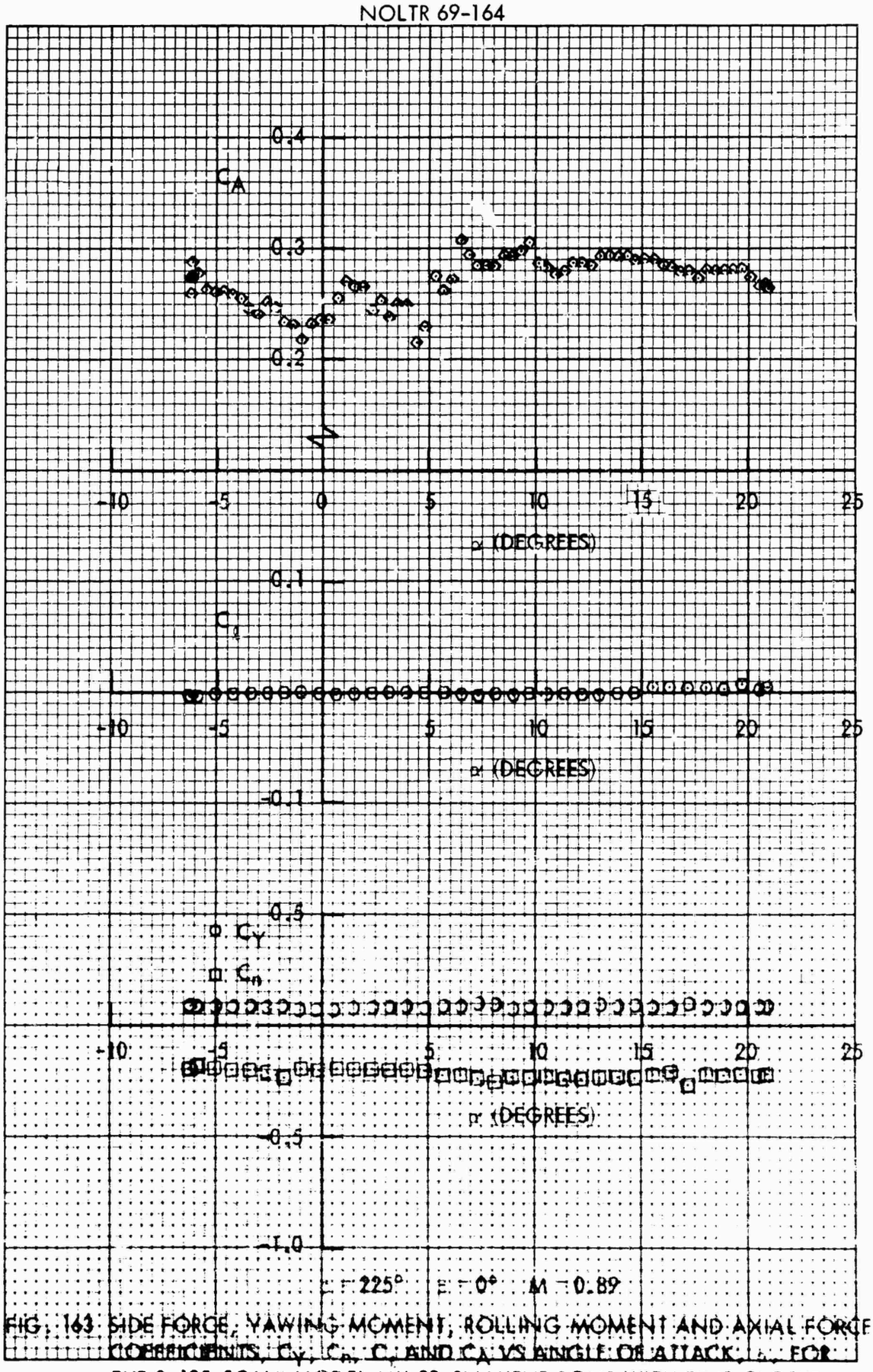

FIG. 163 SIDE FORCE, YAWING MOMENT, ROLLING MOMENT AND AXIAL FORCE COEFFICIENTS, C_Y, C_n, C_ℓ AND C_A VS ANGLE OF ATTACK, α, FOR THE 0.125-SCALE MODEL MK 82-SNAKEYE BOMB WITH FINS CLOSED

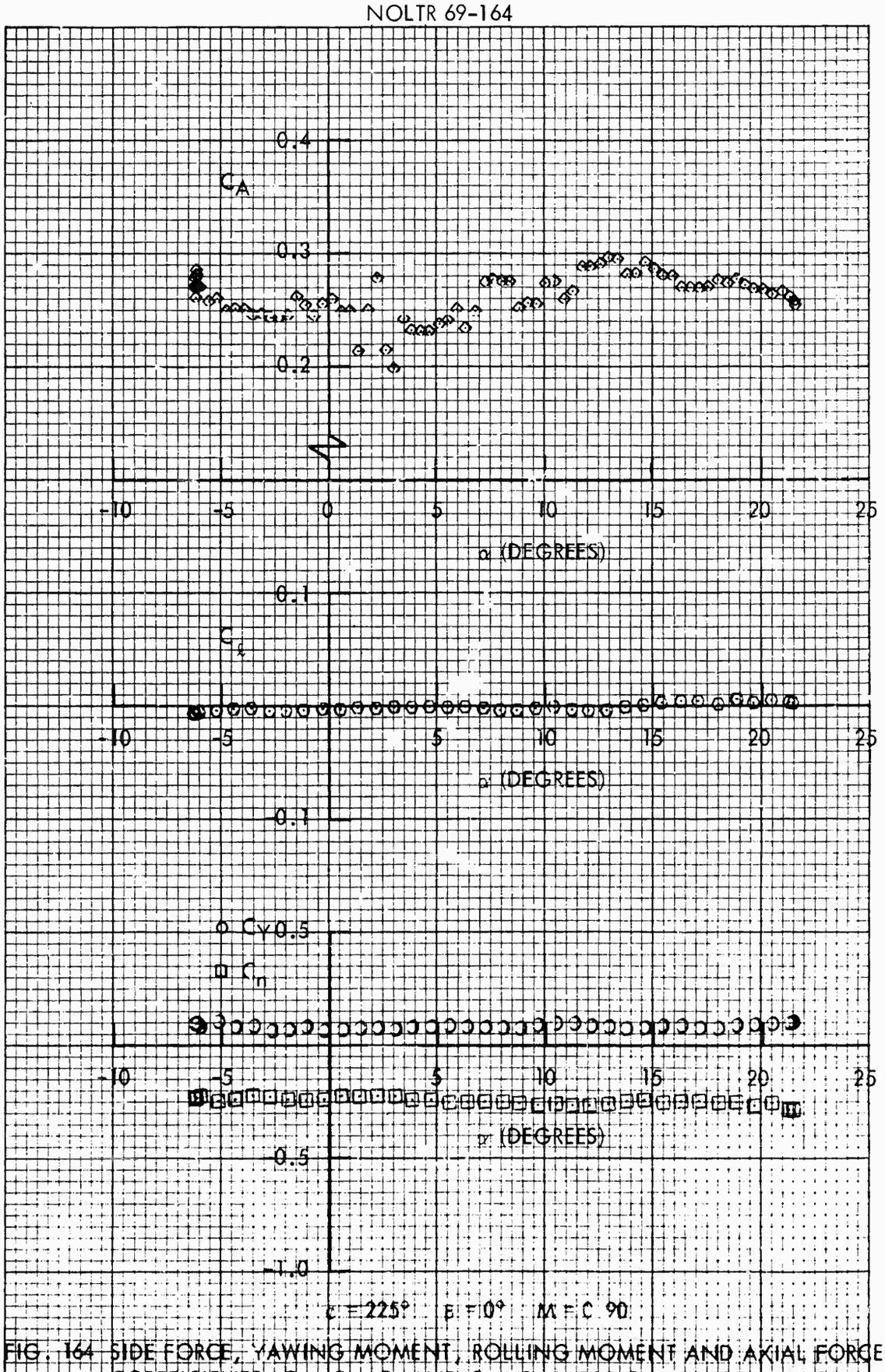

FIG. 164 SIDE FORCE, YAWING MOMENT, ROLLING MOMENT AND AXIAL FORCE COEFFICIENTS, C_Y, C_n, C_ℓ AND C_A VS ANGLE OF ATTACK, α, FOR THE 0.125-SCALE MODEL MK 82-SNAKEYE BOMB WITH FINS CLOSED

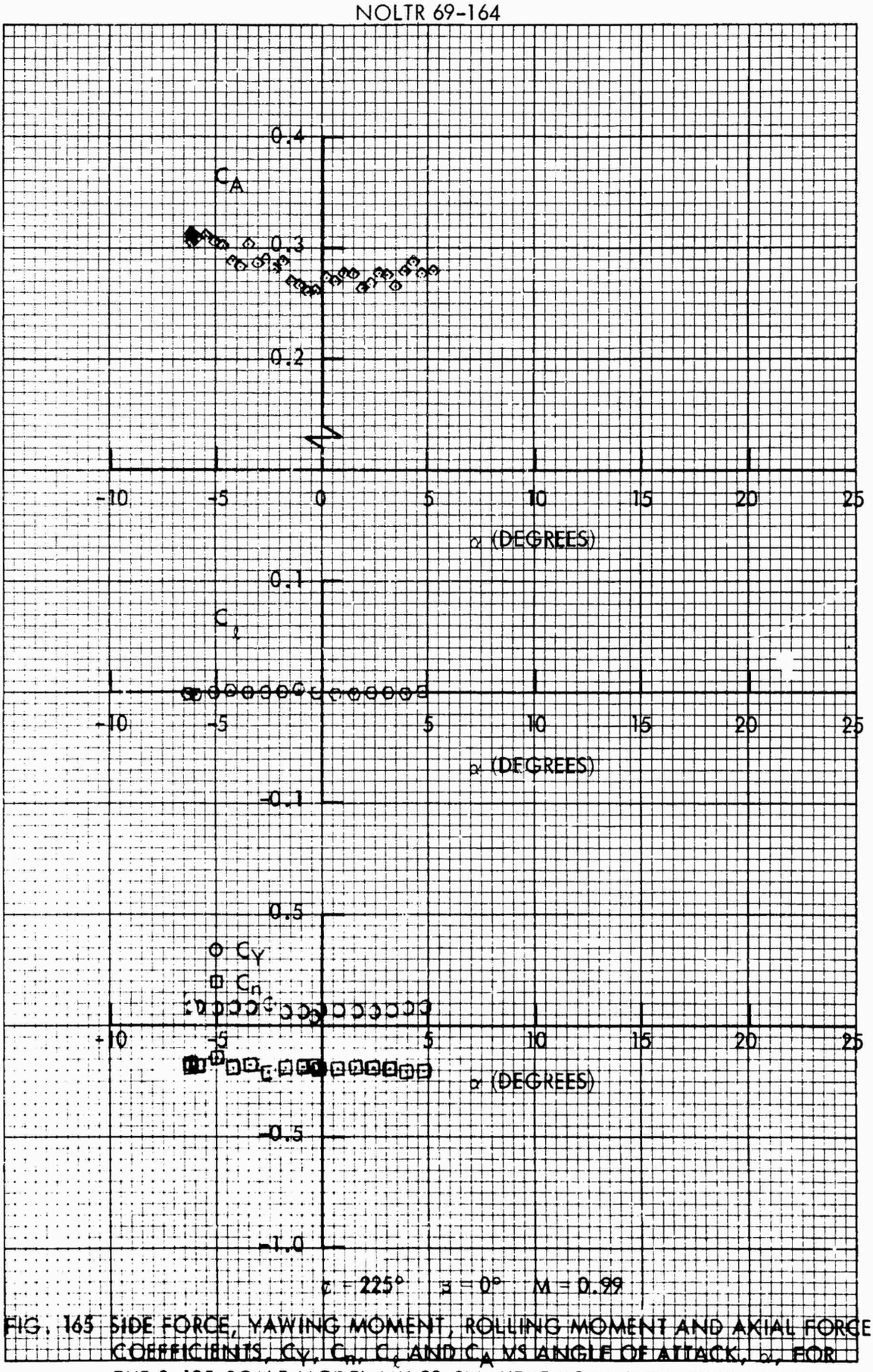

FIG. 165 SIDE FORCE, YAWING MOMENT, ROLLING MOMENT AND AXIAL FORCE COEFFICIENTS, C_Y, C_n, C_ℓ AND C_A VS ANGLE OF ATTACK, α, FOR THE 0.125-SCALE MODEL MK 82-SNAKEYE BOMB WITH FINS CLOSED

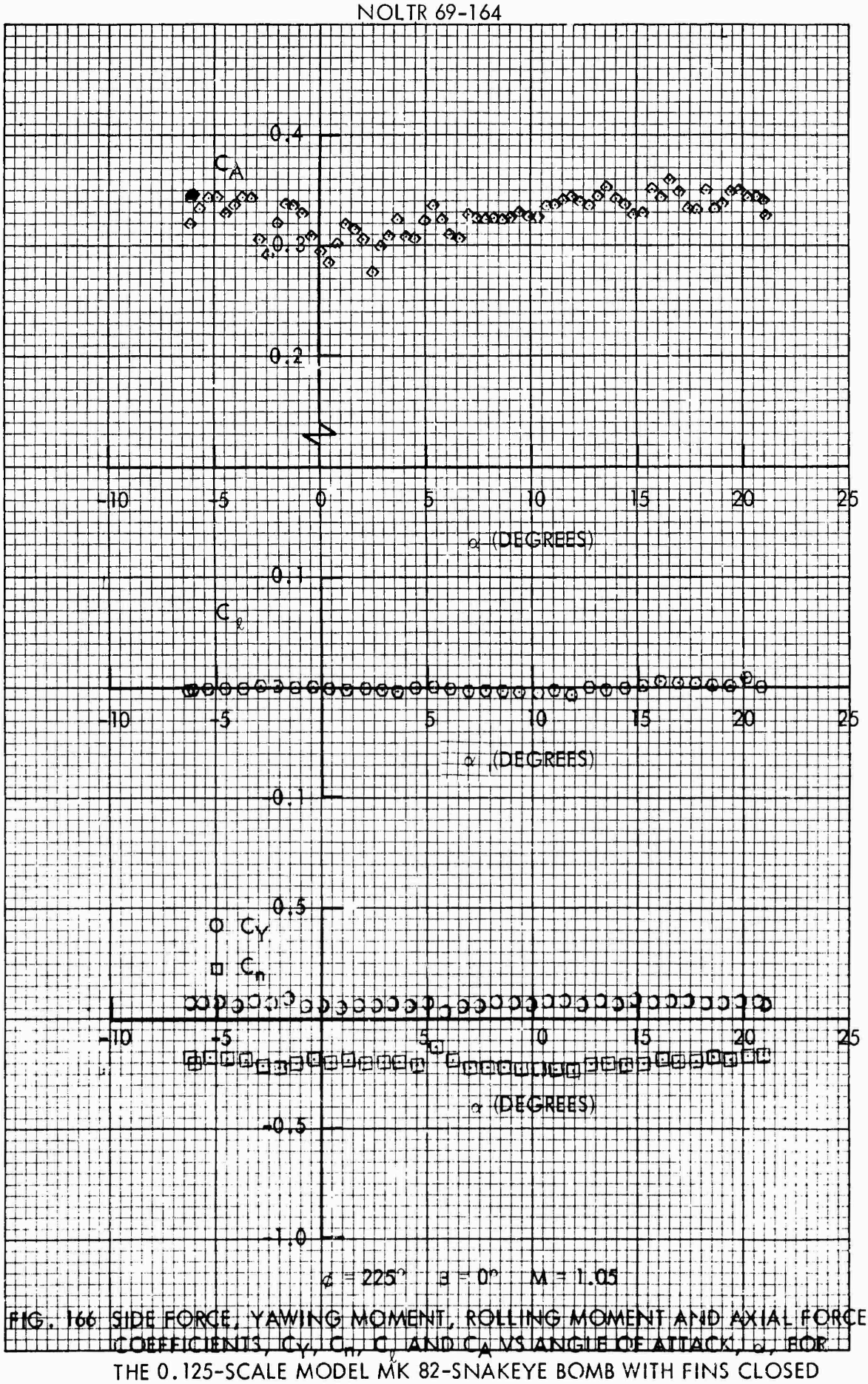

FIG. 166 SIDE FORCE, YAWING MOMENT, ROLLING MOMENT AND AXIAL FORCE COEFFICIENTS, C_Y, C_n, C_ℓ AND C_A VS ANGLE OF ATTACK, α, FOR THE 0.125-SCALE MODEL MK 82-SNAKEYE BOMB WITH FINS CLOSED

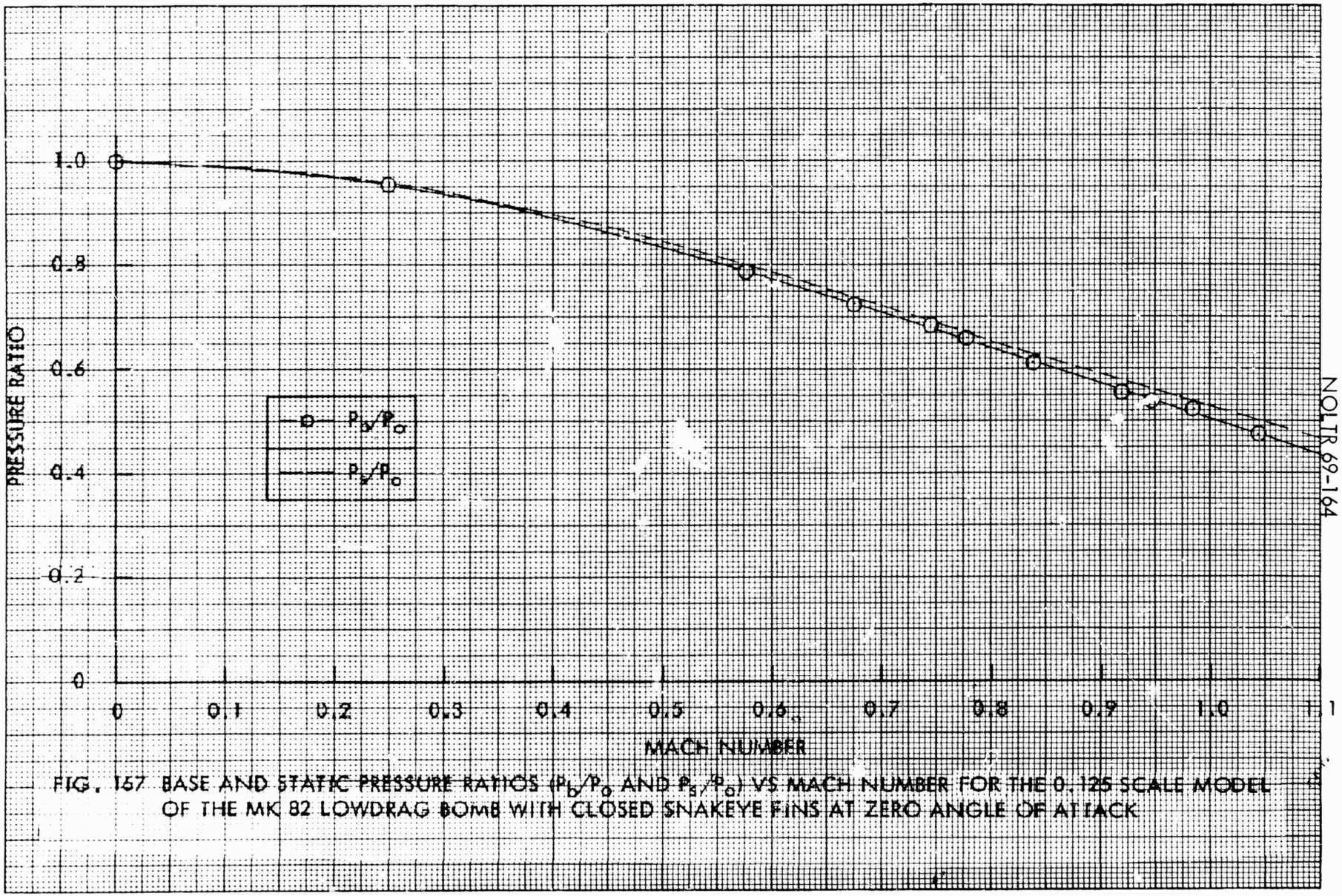

FIG. 167 BASE AND STATIC PRESSURE RATIOS (P_b/P_o AND P_s/P_o) VS MACH NUMBER FOR THE 0.125 SCALE MODEL OF THE MK 82 LOWDRAG BOMB WITH CLOSED SNAKEYE FINS AT ZERO ANGLE OF ATTACK

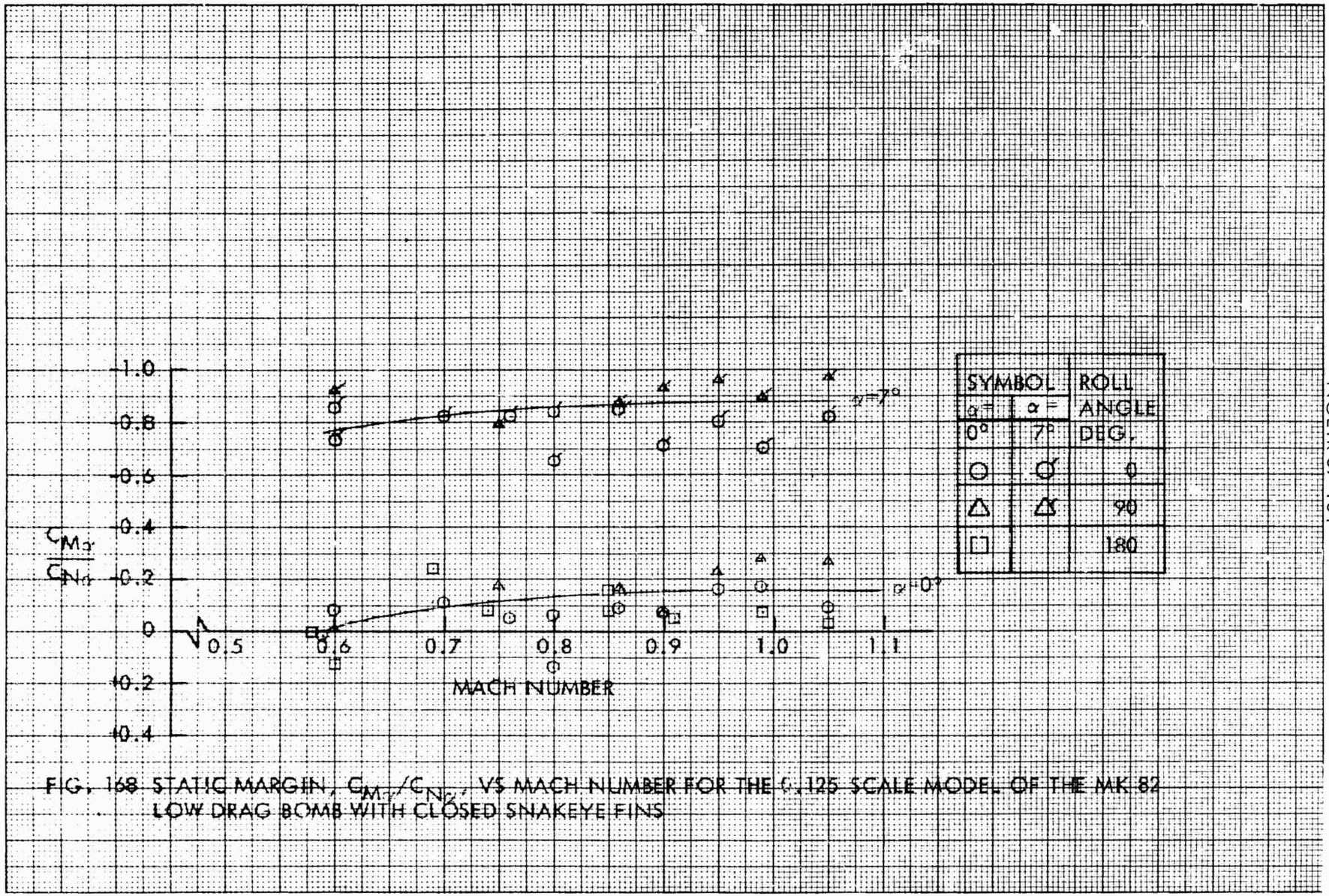

FIG. 168 STATIC MARGIN, $C_{M_\alpha}/C_{N_\alpha}$, VS MACH NUMBER FOR THE 0.125 SCALE MODEL OF THE MK 82 LOW DRAG BOMB WITH CLOSED SNAKEYE FINS

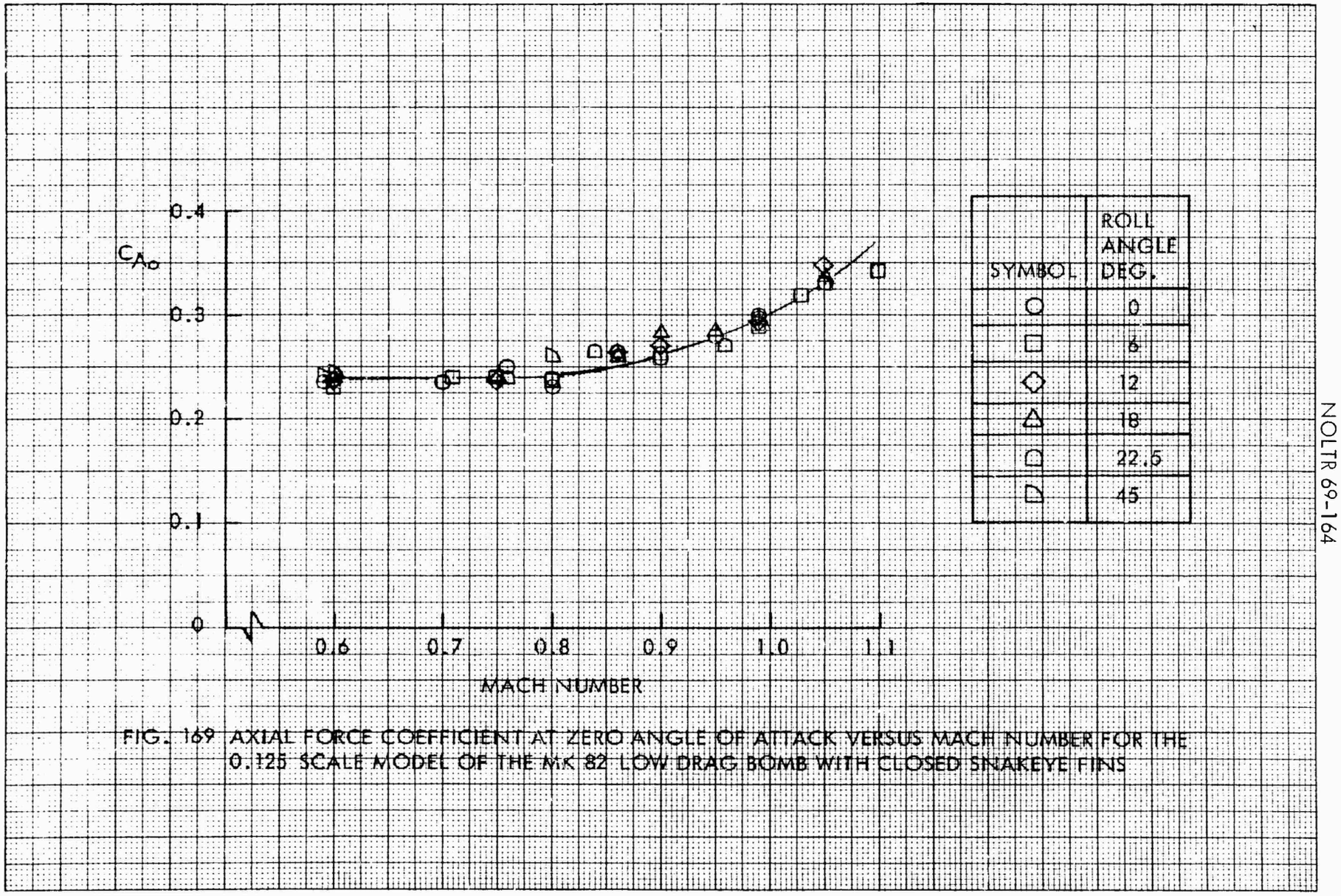

FIG. 169 AXIAL FORCE COEFFICIENT AT ZERO ANGLE OF ATTACK VERSUS MACH NUMBER FOR THE 0.125 SCALE MODEL OF THE MK 82 LOW DRAG BOMB WITH CLOSED SNAKEYE FINS

UNCLASSIFIED
Security Classification

DOCUMENT CONTROL DATA - R & D
(Security classification of title, body of abstract and indexing annotation must be entered when the overall report is classified)

1. ORIGINATING ACTIVITY *(Corporate author)*
U. S. Naval Ordnance Laboratory
White Oak, Silver Spring, Maryland

2a. REPORT SECURITY CLASSIFICATION
UNCLASSIFIED

2b. GROUP

3. REPORT TITLE
STATIC STABILITY AND AXIAL FORCE COEFFICIENTS FOR THE 0.125 SCALE MODEL MARK 82 LOW DRAG BOMB WITH CLOSED SNAKEYE I FINS AT SUBSONIC AND TRANSONIC SPEEDS

4. DESCRIPTIVE NOTES *(Type of report and inclusive dates)*

5. AUTHOR(S) *(First name, middle initial, last name)*
V. L. Schermerhorn

6. REPORT DATE	7a. TOTAL NO. OF PAGES	7b. NO. OF REFS
17 September 1969		none

8a. CONTRACT OR GRANT NO	9a. ORIGINATOR'S REPORT NUMBER(S)
b. PROJECT NO.	NOLTR 69-164
c. NOL 795/NWL	9b. OTHER REPORT NO(S) *(Any other numbers that may be assigned this report)*
d.	

10. DISTRIBUTION STATEMENT
Each transmittal of this document outside the agencies of the U. S. Government must have prior approval of NOL.

11. SUPPLEMENTARY NOTES	12. SPONSORING MILITARY ACTIVITY
	Naval Weapons Laboratories Dahlgren, Virginia

13. ABSTRACT

Static stability and axial force coefficients are presented as a function of angle of attack for the Mk 82 Low Drag Bomb with Snakeye Fins in the closed position. These data were obtained for a Mach number range from 0.6 to 1.1; an angle of attack range from -6 to +20 degrees; and, a roll angle range from 0 to 225 degrees in the NOL Supersonic Tunnel No. 1, using a subsonic nozzle.

DD FORM 1 NOV 65 1473 (PAGE 1)
S/N 0101-807-6801

UNCLASSIFIED
Security Classification

14 KEY WORDS	LINK A		LINK B		LINK C	
	ROLE	WT	ROLE	WT	ROLE	WT
force and moment coefficients						
low-drag bomb						
closed fins (unretarded mode)						